Terms and Conditions of Use of Digitised Theses from Trinity College Library Dublin

Copyright statement

All material supplied by Trinity College Library is protected by copyright (under the Copyright and Related Rights Act, 2000 as amended) and other relevant Intellectual Property Rights. By accessing and using a Digitised Thesis from Trinity College Library you acknowledge that all Intellectual Property Rights in any Works supplied are the sole and exclusive property of the copyright and/or other IPR holder. Specific copyright holders may not be explicitly identified. Use of materials from other sources within a thesis should not be construed as a claim over them.

A non-exclusive, non-transferable licence is hereby granted to those using or reproducing, in whole or in part, the material for valid purposes, providing the copyright owners are acknowledged using the normal conventions. Where specific permission to use material is required, this is identified and such permission must be sought from the copyright holder or agency cited.

Liability statement

By using a Digitised Thesis, I accept that Trinity College Dublin bears no legal responsibility for the accuracy, legality or comprehensiveness of materials contained within the thesis, and that Trinity College Dublin accepts no liability for indirect, consequential, or incidental, damages or losses arising from use of the thesis for whatever reason. Information located in a thesis may be subject to specific use constraints, details of which may not be explicitly described. It is the responsibility of potential and actual users to be aware of such constraints and to abide by them. By making use of material from a digitised thesis, you accept these copyright and disclaimer provisions. Where it is brought to the attention of Trinity College Library that there may be a breach of copyright or other restraint, it is the policy to withdraw or take down access to a thesis while the issue is being resolved.

Access Agreement

By using a Digitised Thesis from Trinity College Library you are bound by the following Terms & Conditions. Please read them carefully.

I have read and I understand the following statement: All material supplied via a Digitised Thesis from Trinity College Library is protected by copyright and other intellectual property rights, and duplication or sale of all or part of any of a thesis is not permitted, except that material may be duplicated by you for your research use or for educational purposes in electronic or print form providing the copyright owners are acknowledged using the normal conventions. You must obtain permission for any other use. Electronic or print copies may not be offered, whether for sale or otherwise to anyone. This copy has been supplied on the understanding that it is copyright material and that no quotation from the thesis may be published without proper acknowledgement.

Eamon John Sheehy, B.Eng., M.Sc.

Towards engineering whole bones through endochondral ossification

---

Trinity College Dublin, February 19, 2014

A thesis submitted to the University of Dublin in partial fulfilment of the requirements for the degree of

Doctor in Philosophy

Supervisor: Prof. Daniel J. Kelly
Internal examiner: Dr. Paula Murphy
External examiner: Prof. Robert E. Guldberg

Declaration

I declare that this thesis has not been submitted as an exercise for a degree at this or any other university and is entirely my own work. I agree to deposit this thesis in the University's open access institutional repository or allow the library to do so on my behalf, subject to Irish Copyright Legislation and Trinity College Library conditions of use and acknowledgement.

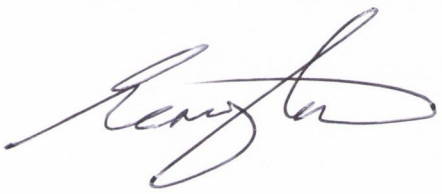

Eamon John Sheehy
Dublin, February 19, 2014

The geometry of innocence flesh on the bone
Causes Galileo's math book to get thrown
At Delilah who sits worthlessly alone
But the tears on her cheeks are from laughter

Bob Dylan

Summary

A number of clinical situations exist where bone regeneration is required in large quantities, such as for the treatment of critical size bone defects and for the replacement of whole bones lost due to trauma or disease. The current 'gold standard' treatment is implantation with an autologous bone graft, harvested from the patient's own body. Drawbacks of this approach include donor site morbidity, and a limitation on the quantity of tissue available for harvest, which have motivated the search for alternative novel strategies, aimed at bone regeneration. The field of tissue engineering aims to regenerate or replace damaged tissues through a combination of cells, three-dimensional scaffolds and signalling molecules. To date, bone tissue engineering applications have generally focussed on the direct osteogenic priming of mesenchymal stem cell (MSC) seeded scaffolds in a process resembling intramembranous ossification. Limitations associated with the traditional intramembranous approach have led to increased interest in the tissue engineering of hypertrophic cartilaginous constructs *in vitro* that remodel into bone *in vivo*, thereby recapitulating the process of endochondral ossification. This thesis set out to investigate: a) the optimum *in vitro* culture conditions required to tissue engineer hypertrophic cartilaginous grafts, and b) the appropriate biomaterial scaffold characteristics necessary to facilitate *in vivo* endochondral ossification of large anatomically accurate engineered constructs. The ultimate objective of the thesis was to tissue engineer a whole bone, containing a vasculature network, a marrow component, and an overlapping stable cartilage layer.

The thesis began by investigating the environmental conditions required to promote hypertrophy of MSC-based cartilaginous grafts. Oxygen tension was found to regulate the osteogenic, chondrogenic, and endochondral phenotype of MSCs. It was shown that, for the engineering of hypertrophic cartilaginous grafts, a low oxygen environment can be applied to enhance cartilaginous matrix production, and a normoxic enviroment can be utilised to promote hypertrophy.

A strategy to engineer large homogenous cartilaginous constructs, through a combination of channelled scaffold architecture and rotational culture, was then investigated. Chondrocytes and MSCs were found to respond differentially to rotational culture, with chondrogenesis being enhanced in chondrocyte-seeded agarose hydrogels, and suppressed in MSC-seeded agarose hydrogels. No beneficial effect of introducing channels into engineered cartilaginous constructs was demonstrated *in vitro*.

Subsequently, the capacity of channelled architectures to accelerate endochondral ossification of engineered hypertrophic cartilaginous grafts *in vivo* was examined. Channelled architectures were found to facilitate mineralisation and vascularisation of engineered grafts. Furthermore, the channels provided a milieu for endochondral bone and marrow formation.

As the thesis moved towards whole bone tissue engineering, a strategy was required to generate an osteochondral tissue. To that end, chondrogenically primed bi-layered agarose hydrogels, consisting of a top chondral layer seeded with chondrocytes and a bottom osseous layer seeded with MSCs, were implanted *in vivo*. The constructs were found to undergo spatially regulated endochondral ossification, leading to the development of an osteochondral construct consisting of a layer of stable cartilage on top of a layer of calcifying cartilage undergoing endochondral ossification.

The agarose hydrogels utilised in early chapters only partially supported progression of engineered tissues down the endochondral route *in vivo*. This sub-optimal performance motivated the search for alternative naturally-derived hydrogels more suitable for endochondral bone tissue engineering applications. MSC-seeded alginate, chitosan, and fibrin hydrogels were primed to undergo hypertrophic chondrogenesis *in vitro* prior to subcutaneous implantation. Both alginate and fibrin hydrogels supported vascularisation, marrow formation, and endochondral ossification, with alginate constructs generating the greater volume of endochondral bone.

Finally, the use of engineered anatomically shaped cartilaginous grafts for regenerating whole bones through endochondral ossification was investigated. An MSC-seeded alginate hydrogel in the shape of the distal phalanx acted as the osseous component, while a self-assembled chondrocyte construct served as the articulating surface or chondral layer. Following implantation, the osseous component underwent endochondral ossification leading to the development of an articular cartilage layer anchored to an anatomic bone tissue penetrated with vasculature.

To conclude, this thesis demonstrates a novel framework for the regeneration of whole bones by utilising tissue engineering methodologies directed at recapitulating developmental skeletal processes. This work provides an insight into the appropriate combinations of factors that can be leveraged to promote endochondral ossification of engineered hypertrophic cartilaginous grafts, the successful application of which will be crucial as tissue engineering strategies move towards whole bone regeneration.

Acknowledgements

I'd like to begin by thanking Danny for his supervision over the course of my PhD. He had this really fantastic ability to motivate and inspire, and I'd always leave the meetings we had with a positive outlook, even when things weren't going great in work. I genuinely couldn't have asked for a better mentor.

I'd like to acknowledge Conor, Tatiana, Mary, Tariq, and Lara for their contribution to the work presented in this thesis. I'd also like to acknowledge and thank all the postdocs and PIs in the lab (Gráinne, Paula, Yurong, Mark, Matt, Raja, Eric, Olivier and Binu) for their help and guidance. A big thank you must also go to the postgrads and lab members who supported me and helped make TCBE such a great place to work. So thank you Stephen, Eoghan, Thomas, Alanna, Darren, Andy S., Lu, Henrique, Simon, Adam, Alan, Rebecca, Katey, Masooma, Amy, Elly, Andy D., Susan, Rukmani, Tomy, Pedro, Paola, Mirka and Dinorath. Thank you also to everyone from the Neural, Cardiovascular, and Biomaterial groups, as well as to Melanie and June for all their assistance.

A very special thank you must go to all my friends in Dublin, London and Kilkenny (R.I.P. Harky).

Finally, I'd like to acknowledge the wonderful support of my family down throughout the years.

Contents

Table of Contents vii

List of Figures xii

List of Tables xv

Nomenclature xvi

Publications xix

1. Introduction 1
- 1.1. The clinical problem with bone defects . . . 1
- 1.2. Endochondral bone tissue engineering: A better route to bone regeneration? . . . 2
- 1.3. Objectives of this thesis . . . 4

2. Literature Review 9
- 2.1. Introduction . . . 9
- 2.2. Bone and cartilage development . . . 10
- 2.3. Bone tissue engineering . . . 19
- 2.4. Cartilage tissue engineering . . . 25
  - 2.4.1. Hydrogels for cartilage tissue engineering . . . 27
  - 2.4.2. MSCs for cartilage tissue engineering . . . 30
  - 2.4.3. Osteochondral tissue engineering . . . 33
- 2.5. Engineering anatomic constructs for whole joint and bone regeneration 35
- 2.6. The endochondral approach to bone tissue engineering . . . 38
- 2.7. Oxygen tension as a regulator of MSC differentiation . . . 45
- 2.8. Summary . . . 48

3. In vitro environmental conditions for engineering hypertrophic cartilage **51**
3.1. Introduction . . . 51
3.2. Materials and methods . . . 53
3.2.1. Experimental design . . . 53
3.2.2. Cell isolation and expansion . . . 54
3.2.3. CFU-f assay and proliferation kinetics . . . 54
3.2.4. Osteogenesis . . . 55
3.2.5. Chondrogenesis in pellets . . . 55
3.2.6. Chondrogenesis in agarose hydrogels . . . 55
3.2.7. Biochemical analysis . . . 56
3.2.8. Histology and Immunohistochemistry . . . 57
3.2.9. Statistical analysis . . . 58
3.3. Results . . . 58
3.3.1. Oxygen tension regulates the proliferation of MSCs . . . 58
3.3.2. Expansion in a low oxygen environment enhances the osteogenic potential of MSCs . . . 59
3.3.3. Oxygen tension differentially regulates collagen synthesis of MSCs during chondrogenesis in pellets and hydrogels . . . 60
3.3.4. Oxygen tension regulates the hypertrophic phenotype of chondrogenically primed MSCs . . . 61
3.4. Discussion . . . 62
3.5. Concluding remarks . . . 66

4. Strategies to engineer large cartilaginous tissues **69**
4.1. Introduction . . . 69
4.2. Materials and methods . . . 71
4.2.1. Experimental design . . . 71
4.2.2. Cell isolation and expansion . . . 72
4.2.3. Solid and channelled cell encapsulated hydrogel constructs . 73
4.2.4. Dynamic rotational culture . . . 74
4.2.5. Mechanical testing . . . 75
4.2.6. Biochemical analysis . . . 76
4.2.7. Histology and Immunohistochemistry . . . 76
4.2.8. Statistical analysis . . . 76
4.3. Results . . . 77
4.3.1. Experiment 1: Long-term free swelling culture . . . 77
4.3.2. Experiment 2: Influence of rotational culture . . . 79
4.3.3. Experiment 3: Delayed rotation of MSC- seeded constructs . 84
4.4. Discussion . . . 85
4.5. Concluding remarks . . . 90

5. Modifying architecture to accelerate vascularisation and ossification 93
5.1. Introduction . . . 93
5.2. Materials and methods . . . 96
5.2.1. Experimental design . . . 96
5.2.2. Cell isolation, expansion . . . 96
5.2.3. Cell encapsulation in solid and channelled agarose hydrogels 97
5.2.4. Chondrogenic and hypertrophic culture conditions . . . 97
5.2.5. In vivo subcutaneous transplantation . . . 98
5.2.6. Biochemical analysis . . . 98
5.2.7. Histology and Immunohistochemistry . . . 98
5.2.8. Micro-computed tomography . . . 99
5.2.9. Statistical analysis . . . 100
5.3. Results . . . 101
5.3.1. Chondrogenically primed MSCs can be stimulated in vitro to produce a calcified cartilaginous tissue within solid and channelled hydrogels . . . 101
5.3.2. Channelled architectures accelerate in vivo mineralisation of MSC-seeded hydrogels . . . 102
5.3.3. Channels act as conduits for vascularisation and provide a milieu for endochondral bone and marrow formation . . . 106
5.4. Discussion . . . 108
5.5. Concluding remarks . . . 113

6. Modulating endochondral ossification to engineer osteochondral constructs 115
6.1. Introduction . . . 115
6.2. Materials and methods . . . 117
6.2.1. Experimental design . . . 117
6.2.2. Cell isolation and expansion . . . 118
6.2.3. Cell encapsulation in agarose hydrogels . . . 118
6.2.4. In vivo subcutaneous transplantation . . . 120
6.2.5. Biochemical analysis . . . 120
6.2.6. Histology and Immunohistochemistry . . . 120
6.2.7. Micro-computed tomography . . . 121
6.2.8. Statistical analysis . . . 121
6.3. Results . . . 122
6.3.1. A structured bilayered co-culture enhances chondrogenesis in the chondral layer of engineered constructs and suppresses hypertrophy and mineralisation in the osseous layer . . . 122
6.3.2. A hypertrophic medium induces in vitro mineralisation of the osseous layer of bilayered constructs . . . 123

6.3.3. Endochondral ossification can be spatially regulated in vivo 124
6.4. Discussion . . . 127
6.5. Concluding remarks . . . 132

7. Natural hydrogels for endochondral bone tissue engineering 135
7.1. Introduction . . . 135
7.2. Materials and methods . . . 137
7.2.1. Cell isolation and expansion . . . 137
7.2.2. Cell encapsulation in alginate, chitosan, and fibrin hydrogels 137
7.2.3. Chondrogenic and hypertrophic culture conditions . . . 138
7.2.4. Experimental design . . . 138
7.2.5. In vivo subcutaneous implantation . . . 139
7.2.6. Biochemical analysis . . . 139
7.2.7. Histology and Immunohistochemistry . . . 140
7.2.8. Micro-computed tomography . . . 140
7.2.9. Statistical analysis . . . 141
7.3. Results . . . 141
7.3.1. The in vitro development of hypertrophic cartilaginous grafts engineered using either MSC-seeded alginate, chitosan or fibrin hydrogels . . . 141
7.3.2. Endochondral bone formation following subcutaneous implantation of MSC-seeded alginate, chitosan and fibrin hydrogels . . . 143
7.4. Discussion . . . 148
7.5. Concluding remarks . . . 152

8. Engineering whole bones through endochondral ossification 153
8.1. Introduction . . . 153
8.2. Materials and methods . . . 155
8.2.1. Experimental design . . . 155
8.2.2. Cell isolation and expansion . . . 156
8.2.3. Fabrication of anatomically shaped constructs . . . 156
8.2.4. In vitro culture conditions . . . 157
8.2.5. In vivo subcutaneous implantation . . . 158
8.2.6. Histology and Immunohistochemistry . . . 158
8.2.7. Micro-computed tomography . . . 159
8.3. Results . . . 160
8.3.1. Anatomic cartilaginous grafts for whole bone tissue engineering 160
8.3.2. Modifying scaffold architecture augments endochondral bone formation . . . 164
8.4. Discussion . . . 167

8.5. Concluding remarks 172

9. Discussion **173**
9.1. Summary 173
9.2. Conclusions 179
9.3. Limitations 180
9.4. Future work 184

References **187**

A. Appendix **223**

List of Figures

2.1. The structural types of bone 11
2.2. Bone remodelling via BMUs 12
2.3. Endochondral bone formation 14
2.4. Ihh-PTHrP negative feedback loop 15
2.5. Cartilage canals 17
2.6. Hierarchical zonal structure of articular cartilage 20
2.7. The Mesengenic Process 22
2.8. BM-MSCs/β-TCP repair of mandibular bone defects 23
2.9. Radiographs from the first clincal trial of bone tissue engineering . . 23
2.10. Autologous chondrocyte implantation 26
2.11. Idealised tissue engineering process for the regeneration of cartilage 27
2.12. Histological evaluation of ectopic cartilage-like transplants formed by articular chondrocytes and BM-MSCs 33
2.13. Osteochondral defect repair 34
2.14. Patellar osteochondral construct 36
2.15. In vivo endochondral bone formation throughout time 41
2.16. Low oxygen tension measurements in various stem cell compartments 45
2.17. Levels of oxygen in the surrounding tissues of joints 48
2.18. The influence of oxygen tension during bone-cartilage tissue formation 49

3.1. Oxygen tension regulates the proliferation of MSCs 59
3.2. Expansion in a low oxygen environment enhances the osteogenic potential of MSCs 60
3.3. Oxygen tension differentially regulates collagen synthesis of MSCs during chondrogenesis in pellets and hydrogels 61
3.4. Differentiation in a low oxygen environment enhances sGAG synthesis during chondrogenesis in pellets and hydrogels 62
3.5. Oxygen tension regulates the hypertrophic phenotype of chondrogenically primed MSCs 63
3.6. Oxygen tension regulates cell morphology in MSC pellets 64

4.1. PTFE mould system for creating microchannelled hydrogels 74
4.2. Rotational bioreactor system 75
4.3. Experiment 1: Mechanical properties of chondrocytes and BM-MSCs 78
4.4. Experiment 1: Biochemical analysis of chondrocytes and BM-MSCs 80
4.5. Experiment 2: Annulus−core biochemical analysis of chondrocytes and BM-MSCs 82
4.6. Experiment 2: Annulus/core biochemical analysis of chondrocytes and BM-MSCs 83
4.7. Experiment 2: Histology and Immunohistochemistry of chondrocytes and BM-MSCs 85
4.8. Experiment 3: Annulus-core biochemical analysis of chondrocytes and BM-MSCs 86

5.1. Biochemical analysis and μCT of solid and channelled constructs undergoing long-term in vitro hypertrophic chondrogenesis 102
5.2. Biochemical analysis of solid and channelled constructs post- implantation 104
5.3. Histology of solid and channelled constructs post-implantation . . . 105
5.4. μCT analysis of solid and channelled constructs post-implantation . 106
5.5. H and E staining of solid and channelled constructs post-implantation 107
5.6. Histology and immunohistochemistry of channelled constructs 4 weeks post-implantation 108
5.7. Extra-cellular matrix progression in channelled constructs post-implantation 109

6.1. Experimental design of osteochondral study 119
6.2. Biochemical analysis of single layer and bilayer constructs cultured in chondrogenic medium 123
6.3. Histology of single layer and bilayer constructs cultured in chondrogenic medium 124
6.4. Immunohistochemistry of single layer and bilayer constructs cultured in chondrogenic medium 125
6.5. Hisotology and biochemical analysis of single and bilayer constructs cultured in hypertrophic medium 126
6.6. Histology and μCT of single layer MSC and bilayer constructs post-implantation 127
6.7. Immunohistochemistry of single layer MSC and bilayer constructs post-implantation 128

7.1. Biochemical analysis of constructs following 8 weeks of in vitro culture 143
7.2. Mass and biochemical analysis of constructs in vitro 144

7.3. Histology of constructs in vitro 145
7.4. Histology of constructs post-implantation 145
7.5. μCT of constructs post-implantation 147
7.6. H and E staining of constructs post-implantation 148

8.1. Fabrication of anatomically shaped constructs 161
8.2. Histology of chondrogenically primed anatomically shaped constructs 161
8.3. Anatomically shaped TMJ constructs primed to undergo hypertrophy 162
8.4. Anatomic alginate phalanx constructs post-implantation 163
8.5. Channelled alginate phalanx constructs post-implantation 165
8.6. Channelled fibrin phalanx constructs post-implantation 166

A.1. Experiment 1: Annulus–core biochemical analysis of chondrocytes and BM-MSCs in FS at day 63 223
A.2. Experiment 2: Annulus–core biochemical analysis of BM-MSCs at 5 rpm 224
A.3. Macroscopic image of channelled constructs post-implantation . . . 224
A.4. Open surface agarose-based mould 225
A.5. Implantation and retrieval of anatomic constructs 225

List of Tables

4.1. Experiment 2: sGAG release to media 84

Nomenclature

%ww	% wet weight
ACI	Autologous chondrocyte implantation
ALP	Alkaline phosphatase
ANOVA	Analysis of variance
β-TCP	β-glycerophosphate
BM-MSC	Bone marrow derived mesenchymal stem cell
BMP	Bone morphogenetic protein
BMU	Basic multicellular unit
β-TCP	β-tri calcium phosphate
$CaCl_2$	Calcium chloride
CC	Chondrocyte
CD	Caudal
CFU-f	Colony forming units-fibroblastic
CM	Chondrogenic medium
CP	Cephalic
DMSO	Dimethyl sulphoxide
EDTA	Ethylenediaminetetraacetic acid
FBS	Fetal bovine serum
FGF	Fibroblastic growth factor

FS	Free swelling
GAG	Glycosaminoglycan
H and E	Haematoxylin and eosin
HA	Hydroxyapatite
HCL	Hydrochloric acid
HEC	Hydroxyethyl cellulose
HM	Hypertrophic medium
Ihh	Indian hedgehog
IL	Interleukin
MACI	Matrix-induced autologous chondrocyte implantation
MC	Micro-channel
MNC	Mononuclear cell
MSC	Mesenchymal stem cell
PBS	Phosphate buffered saline
PCL	Polycaprolactone
PDLD	Polyla(L-lactide-co-D,L-lactide)
PDMS	Polydimethylsiloxane
PEG	Polyethylene-glycol
PLGA	Poly(lactic-co-glycolic)
pO_2	Partial pressure oxygen
PRP	Platelet-rich plasma
PTFE	Polytetrafluroethylene
PTHrP	Parathyroid hormone-related protein
R	Rotation
RGD	Arginine-glycine-aspartic acid
sGAG	Sulphated glycosaminoglycan

SOL	Solid
TCP	Tricalcium phosphate
TdT	Terminal deoxynucleotidyl Transferase
TGF-β	Transforming growth factor-β
TMJ	Temporomandibular joint
μCT	Micro-computed tomography
VEGF	Vascular endothelial growth factor

Publications

This is a list of publications generated from the work presented in this thesis.

Journal articles

Sheehy E.J., Buckley C.T., Kelly D.J., 2011. Chondrocytes and bone marrow-derived mesenchymal stem cells undergoing chondrogenesis in agarose hydrogels of solid and channelled architectures respond differentially to dynamic culture conditions. Journal of Tissue Engineering and Regenerative Medicine 5 (9), 747-758.

Sheehy E.J., Buckley C.T., Kelly D.J., 2012. Oxygen tension regulates the osteogenic, chondrogenic and endochondral phenotype of bone marrow derived mesenchymal stem cells. Biochemical and Biophysical Research Communications 417 (1) 305-310.

Sheehy E.J., Vinardell T., Buckley C.T., Kelly D.J., 2013 Engineering osteochondral constructs through spatial regulation of endochondral ossification. Acta Biomaterialia 9 (3), 5484-5492.

Sheehy E.J., Vinardell T., Toner M.E.,Buckley C.T., Kelly D.J., Altering the architecture of tissue engineered hypertrophic cartilaginous grafts facilitates vascularisation and accelerates mineralisation. PLoS one (In Press)

Conference abstracts

Sheehy E.J., Buckley C.T., Kelly D.J. Rotational culture differentially regulates chondrogenesis of bone marrow derived MSCs and chondrocytes. Bioengineering.. in Ireland, 16th Annual Conference, January 22-24, 2010, Grand Hotel Malahide, Co. Dublin, Ireland

Sheehy E.J. Buckley C.T., Kelly D.J. Cartiliaginous tissues engineered using chondrocytes and bone marrow derived MSCs by a combination of rotational culture and modified scaffold architecture. Tissue Engineering and Regenerative Medicine International Society, June 13-17, 2010, Galway, Ireland.

Sheehy E.J., Buckley C.T., Kelly D.J. Rotational culture differentially regulates chondrogenesis of bone marrow derived MSCs and chondrocytes. 17th congress of the European Society of Biomechanics, July 5-8, 2010, Edinburgh, Scotland.

Sheehy E.J., Vinardell T., Meyer E., Buckley C.T., Kelly D.J. The oxygen environment regulates mesenchymal stem cell expansion and chondrogenic differentiation in an in vitro cartilage defect model. Orthopaedic Research Society, January 13-16, 2011, Long Beach Convention Center, Long Beach, California. Poster No. 1727.

Sheehy E.J., Buckley C.T., Kelly D.J. The role of oxygen tension in regulating the osteochondral potential of bone marrow derived mesenchymal stem cells. Bioengineering.. in Ireland, 17th Annual Conference, January 28-29, 2011, Ardilaun Hotel, Galway, Ireland.

Sheehy E.J., Buckley C.T., Kelly D.J. The oxygen environment regulates the chondrogenic and osteogenic potential of bone marrow derived mesenchymal stem cells. Tissue Engineering and Regenerative Medicine International Society, June 7-10, Granada, Spain. Histology and Histopathology, Cellular and Molecular Biology, Volume 26 (supplement 1), 2011, page 262-263 (paper 29.06).

Sheehy E.J., Vinardell T., Buckley C.T., Kelly D.J. Engineering osteochondral constructs through spatial regulation of endochondral ossification. Bioengineering.. in Ireland, 18th Annual Conference, January 27-28, 2012, Hilton Templepatrick Hotel, Belfast.

Sheehy E.J., Vinardell T., Buckley C.T., Kelly D.J. Engineering osteochondral constructs through spatial regulation of endochondral ossification. Orthopaedic Research Society, Febuary 4-7, 2012, Moscone West Convention Center, San Francisco, California. Paper No. 0206.

Sheehy E.J., Vinardell T., Buckley C.T., Kelly D.J. Modulating Endochondral Ossification to Engineer Osteochondral Constructs. 18th congress of the European Society of Biomechanics, July 1-4, 2012, Technical University of Lisbon, Portugal.

Sheehy E.J., Vinardell T., Buckley C.T., Kelly D.J. Channelled architectures accelerate in vivo mineralisation of engineered hypertrophic cartilaginous constructs. Tissue Engineering and Regenerative Medicine International Society, 3rd World Congress, September 5-8, 2012, Vienna, Austria.

Sheehy E.J., Vinardell T., Toner M.E., Buckley C.T., Kelly D.J. Channelled architectures accelerate mineralisation of engineered hypertrophic cartilaginous constructs. Bioengineering.. in Ireland, 19th Annual Conference, January 18-19, 2013, Johnstown House Hotel, Co. Meath, Ireland.

Sheehy E.J., Vinardell T., Buckley C.T., Kelly D.J. Towards engineering whole bones via endochondral ossification. ASME Summer Bioengineering Conference, June 26-29, 2013, Sunriver Resort, Sunriver, Oregon, USA.

Sheehy E.J., Mesallati T., Buckley C.T., Kelly D.J. Anatomic Hypertrophic Cartilaginous Grafts For Whole Bone Tissue Engineering. Orthopaedic Research Society, March 15-18, 2014, Hyatt Regency New Orleans, New Orleans, Louisiana, USA. Paper No. 0153.

1 Introduction

1.1. The clinical problem with bone defects

Bone is the second most implanted tissue in the body after blood (Nilsson et al., 2003). A highly dynamic material, bone possesses an intrinsic capacity for regeneration and constantly undergoes a remodelling process involving the resorption of old bone and deposition of new bone. However, clinical situations do exist where bone regeneration is required in large quantities, such as for reconstruction of large bone defects caused by trauma, infection, tumour resection and skeletal abnormalities, or in cases where the regenerative process is compromised, such as in avascular necrosis, atrophic non-unions and osteoporosis (Dimitriou et al., 2011).

A 'critical size' bone defect is one which the body cannot heal itself and can be defined as a gap beyond two a half times the radius of the bone (Schroeder and Mosheiff, 2011). The 'gold standard' treatment for such a defect is an autologous bone graft, or autograft. This therapy involves the harvesting of a patient's own bone, usually from the anterior or posterior illiac crest of the pelvis, and then implantation into the defect site. Since it is the patient's own tissue autologous bone is histocompatible and non-immunogenic. Furthermore the grafts contain the osteoconductive scaffolds and osteogenic cells to drive bone repair. However there are a number of drawbacks associated with the current 'gold standard'. Harvesting

of the bone, for example, requires an additional surgical procedure which can result in donor site morbidity, and there is a limitation on the quantity of bone available for harvest. Such limitations can be addressed through the use of an allogeneic bone graft, or allograft, which can be obtained from human cadavers or living donors. However, allografts are devitalised prior to implantation and therefore do not possess the same osteoinductive potential as autografts. There are also complications due to immunogenicity and infection (Donati et al., 2005).

Other approaches used in clinical practice to stimulate bone regeneration include distraction osteogenesis and bone transport using the Ilizarov technique. Such processes involve the induction of a fracture and then gradual distraction (1 mm per day) allowing new bone to form in the fracture gap. These methods are tedious however, and require lengthy treatment periods (Aronson, 1997). The implantation of a prosthesis is another well established treatment (Learmonth et al., 2007). However, the artificial metals and polymers used in these implants can loosen and fail over time. Furthermore the non-biological nature of these materials mean they do not undergo any growth or remodelling *in vivo*, making them unsuitable for use in children. There is therefore a need for the development of novel biological strategies for the treatment of critical size bone defects and for the replacement of whole bones lost due to trauma or disease.

1.2. Endochondral bone tissue engineering: A better route to bone regeneration?

Tissue engineering has emerged as a multidisciplinary field which utilises aspects of cell biology, materials science, and engineering in order to repair or regenerate damaged tissues through the combination of cells, three-dimensional scaffolds, and signalling molecules (Koh and Atala, 2004; Langer, 2000). Mesenchymal stem cells

(MSCs) have become an attractive cell source for tissue engineering applications due to their relative ease of isolation and expansion, and their ability to differentiate down a number of tissue specific lineages (Caplan, 1991). To date, bone tissue engineering applications have generally focussed on the direct osteogenic priming of MSC-based constructs in a process resembling intramembranous ossification (Meijer et al., 2007). However, this approach has been hampered by the lack of a functional vascular supply upon *in vivo* implantation, required for the necessary delivery oxygen and nutrients to ensure cell survival (Santos and Reis, 2010). Furthermore, *in vitro* osteogenic priming of an engineered tissue can inhibit vascularisation of the graft by sealing up the pores of a scaffold with calcified matrix, resulting in core degradation (Lyons et al., 2010). These issues have, to a large extent, hindered the translation of intramembranous bone tissue engineering strategies into the clinic.

Chondrocytes, the cells intrinsic to cartilage, reside in an avascular tissue and are equipped to survive a low oxygen environment. Interestingly, long bones in the axial skeleton develop by a process called endochondral ossification, where mesenchymal cells differentiate into chondrocytes, forming an initial cartilaginous template. The chondrocytes then undergo hypertrophic differentiation, releasing pro-angiogenic factors facilitating vascularisation and remodelling of the cartilaginous template into bone (Kronenberg, 2003). This has led to increased interest in endochondral bone tissue engineering strategies that recapitulate developmental processes as a means to drive bone regeneration (Jukes et al., 2008; Farrell et al., 2009; Scotti et al., 2010). This endochondral approach to bone tissue engineering may circumvent the hurdles associated with the traditional intramembranous approach; i.e. by implanting a tissue engineered hypertrophic cartilaginous graft capable of surviving the initial hypoxic conditions and possessing the neccessary bioactive signals for the conversion of avascular tissue into vascularised tissue. There are, however, a number of issues that must be addressed before endochondral bone tissue engineering could

be applied in a clinical setting to repair critical size bone defects or to replace whole bones. For example, the optimum *in vitro* culture conditions required to tissue engineer hypertrophic cartilaginous grafts are presently unclear, as are the appropriate biomaterial scaffold characteristics necessary to facilitate *in vivo* endochondral ossification of large anatomically accurate engineered constructs. Elucidation of these conditions may provide a novel framework for the tissue engineering of whole bones.

1.3. Objectives of this thesis

During embryonic bone development chondrocytes in the centre of the cartilage mould differentiate from a chondrogenic phenotype, rich in collagen type II and the proteoglycan aggrecan, to a hypertrophic phenotype synthesising type X collagen, which directs matrix digestion, mineralisation and vascularisation of the cartilaginous template (Kronenberg, 2003). It is clear therefore that the regulation of the *in vitro* hypertrophic phenotype of a cell seeded construct is an essential pre-requisite to achieve endochondral ossification of the construct *in vivo*. Chondrogenically primed MSCs have been shown to possess this hypertrophic potential, an undesirable attribute in MSC-based articular cartilage repair therapies (Williams et al., 2010), but one which could be harnessed for use in the engineering of endochondral bone. Understanding how environment factors regulate MSC differentiation down the endochondral pathway will be critical in developing this therapy for bone tissue repair. One such factor known to regulate the osteogenic and chondrogenic potential of MSCs is the local oxygen tension (Lennon et al., 2001; Merceron et al., 2010). This thesis will explore the hypothesis that the local oxygen tension regulates the hypertrophic phenotype of chondrogenically primed MSCs.

Utilising engineered constructs for the regeneration of large bone defects through endochondral ossification requires strategies to scale-up engineered cartilaginous tissues. A significant challenge with scaling-up tissue engineered constructs is the associated issue of core degradation and ensuring adequate nutrient supply and waste removal throughout the construct. Studies have demonstrated that the functional properties of engineered cartilaginous tissue can be enhanced by culture in a bioreactor. An alternative approach is modifying the architecture of a scaffold to incorporate channels for nutrient transport (Bian et al., 2009). This thesis will explore the hypothesis that large MSC- and chondrocyte- based cartilaginous tissues can be engineered through a combination of bioreactor culture and modified scaffold architecture.

Promoting vascularisation of tissue engineered constructs *in vivo* is essential to ensure long- term survival and maintenance of the construct. During embryonic bone development cartilage canals act as conduits for vessel invasion (Blumer et al., 2008), and the method of encorporating channelled condiuts into 3D scaffolds has shown potential in enhancing vascularisation of engineered adipose tissue (Stosich et al., 2007). This thesis will explore the hypothesis that modifying the architecture of hypertrophic cartilaginous constructs, by engineering channelled hydrogels, will accelerate vascularisation and endochondral ossification of the graft following *in vivo* implantation.

Successful modulation of MSCs for endochondral ossification would raise the possibility of engineering osteochondral constructs for articular joint regeneration. Osteochondral defects are often associated with mechanical instability, which can induce osteoarthritic degenerative changes (Martin et al., 2007), and chondral defects alone sometimes require an osteochondral implant to ensure integration with the surrounding tissue. This thesis will explore the hypothesis that by implanting chondrogenically primed bilayered constructs containing chondrocytes and MSCs,

it will be possible to spatially regulate endochondral ossification *in vivo* leading to the development of an osteochondral construct. As tissue engineering strategies move towards whole bone regeneration, such an approach could be leveraged to generate the articular cartilage layer of an engineered limb.

A key design criteria in a scaled-up endochondral bone tissue engineering strategy is the selection of an appropriate biomaterial, capable of supporting hypertrophic chondrogenesis of MSCs *in vitro*, and subsequently facilitating vascularisation and endochondral ossification of the graft *in vivo*. The use of a hydrogel may be a particularly powerful tool in scaling-up tissue engineered cartilaginous grafts. This thesis will compare the capacity of different naturally-derived MSC seeded hydrogels to generate endochondral bone *in vivo*.

Appropriate combinations of the factors under investigation (environmental conditions, culture conditions, scaffold architectures, cell sources, biomaterials) may facilitate the engineering of large anatomic tissues for the regeneration of whole bones and limbs. This thesis will investigate the possibility of engineering, *in vivo*, an anatomically accurate osteochondral graft in the shape of the distal phalanx as a paradigm for whole bone tissue engineering through endochondral ossification.

In summary, the objectives of this thesis are:

1. To investigate the appropriate environmental conditions to promote hypertrophy of MSC-based cartilaginous constructs.

2. To develop a strategy, combining modified scaffold architecture and rotational culture, for the engineering of large homogenous cartilaginous constructs.

3. To accelerate *in vivo* vascularisation and endochondral ossification of engineered hypertrophic cartilaginous grafts through the use of channelled hydrogels.

4. To engineer an osteochondral construct through spatial regulation of endochondral ossification.

5. To compare the capacity of different naturally derived MSC-seeded hydrogels to facilitate endochondral bone tissue formation *in vivo*

6. To tissue engineer an anatomically accurate bone through endochondral ossification as a paradigm for whole bone tissue engineering.

2 Literature Review

2.1. Introduction

The embryonic process of endochondral ossification involves the remodelling of a hypertrophic cartilaginous template into bone. This literature review will therefore begin by describing the regulatory mechanisms that govern bone and cartilage development during endochondral skeletogenesis, as well as describing the structure and function of the tissues. Furthermore, the respective regenerative capacities of the tissues will be investigated, in order to better understand the need for the development of tissue engineering therapies to stimulate bone and cartilage repair.

The traditional bone tissue engineering paradigm involves the direct osteogenic differentiation of MSCs in a process resembling intramembranous ossification and this review will examine both early and more recent work investigating this strategy for bone regeneration. The endochondral approach to bone tissue engineering however, involves the engineering of a hypertrophic cartilaginous construct *in vitro* that will undergo ossification *in vivo*. Therefore, this review will also describe the various cells, scaffolds, and signalling factors used in cartilage tissue engineering applications, both in the context of generating a stable articular cartilage construct for joint condyle repair, and in the context of engineering a hypertrophic cartilaginous graft for bone regeneration through endochondral ossification. Moreover,

strategies implemented to engineer osteochondral constructs; i.e. constructs that consist of both bone and cartilage tissue, will be reviewed as a tissue engineered long bone will require a layer of articular cartilage to ensure proper biomechanical function.

The field of tissue engineering may provide a novel biological therapy for the treatment of degenerative joint disease through the engineering of anatomically accurate constructs for the regeneration of whole bones. This review will examine previous work carried out investigating the engineering of such anatomically accurate tissues. This chapter will then end by reviewing the key papers which have led to recent advances in the field of endochondral bone tissue engineering, as well as examining the role played by oxygen tension in regulating the endochondral phenotype of MSCs.

2.2. Bone and cartilage development

Bone is a dense connective tissue which functions to produce blood cells, store minerals, and support and protect the vital organs of the body. Bone can be described as a composite material consisting of a mineral phase (65-70% of the total matrix) and an organic phase (25-30% of the total matrix), as well as cells (2-5% of the organic matrix) and water (5%) (Sommerfeldt and Rubin, 2001). The mineral phase of bone consists of hydroxyapatite, a hard brittle material which is strong in compression. The organic phase (or osteoid) consists primarily of collagen type I ($\approx$90%) along with glycoproteins, proteoglycans, sialoproteins and bone "gla" proteins (Mackie, 2003), and provides good bending flexibility and tensile properties. The interaction between these two constituents, in which a ceramic phase is reinforced by collagen fibers, results in a stiff but tough material.

The skeleton consists of two main types of structural bone, see Figure 2.1. Cortical

bone accounts for 80% of bone in the skeleton and consists of concentric lamellae of bone tissue surrounding a central canal containing blood vessels. Trabecular bone has a lower density and higher surface area compared to cortical bone and fills the centre of long bones, flat bones and vertebrae with an interconnecting meshwork of bony trabeculae, filled with bone marrow. Due to its higher surface area trabecular bone has an increased turnover rate during remodelling compared to cortical bone. In disease, where bone turnover is impaired, bone is lost more rapidly in the trabecular regions (Ralston, 2009).

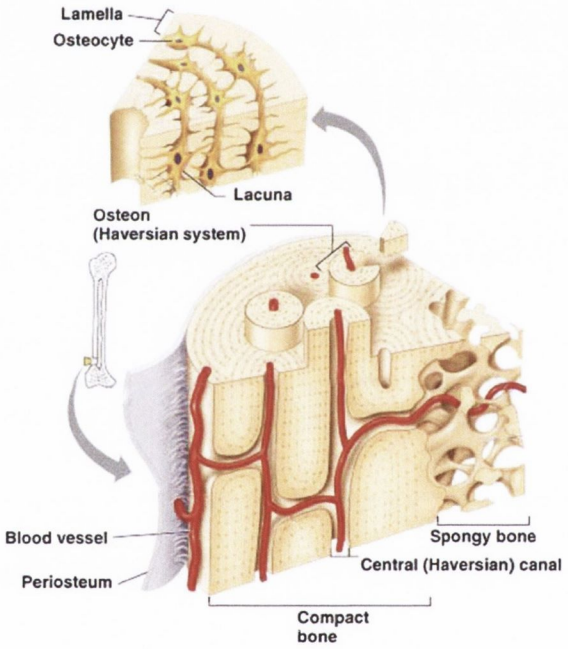

Figure 2.1.: *The structural types of bone. Compact (cortical) and spongy (trabecular) bone*

Bone in the adult skeleton is continuosly renewed in a process known as bone remodelling where old bone is resorbed by osteoclasts and new bone is deposited by osteoblasts, see Figure 2.2. Bone remodelling occurs via basic multicellular units (BMUs) which are headed by osteoclasts that act as cutting cones, removing trenches or tunnels of bone from the surfaces of the trabecular and cortical bone and a lining of osteoblasts follow filling in the trenches and laying down new bone

matrix (Little et al., 2011). This constant formation and resorption allows the renovation of 5-15% of total bone mass per year under normal conditions and in a healthy individual, under normal circumstances, bone formation matches bone resorption resulting in no net loss in bone mass (Perez-Sanchez et al., 2010).

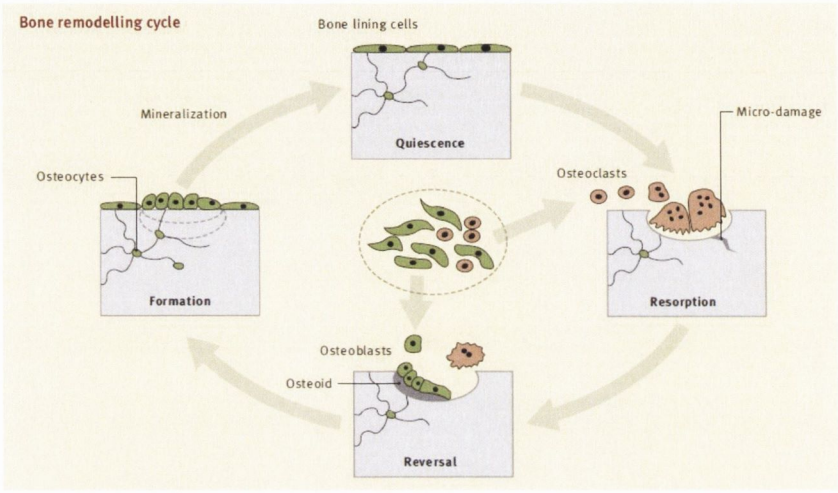

Figure 2.2.: *Bone remodelling via BMUs of osteoclasts, osteoblasts and osteocytes.* (Ralston, 2009)

Osteoblasts are derived from mesenchymal cells and are not only reponsible for the secretion of the organic components of the bone matrix but are also indirectly responsible for the mineralisation of osteoid through the production of phosphate containing proteins, such as bone sialoprotein, and through the provision of enzymes that regulate phosphoprotein phosphorylation, such as alkaline phosphatase (Mackie, 2003). While some osteoblasts undergo apoptosis others become embedded in the bone matrix to form osteocytes which continue to thrive but stop producing matrix proteins, though they do remain connected with similar cells and inactive osteoblasts at the bone's surface, creating an extensive network of intercellular communication (Sommerfeldt and Rubin, 2001). Unlike osteoblasts and osteocytes, osteoclasts are derived from mononuclear haematopoietic precursors. They are highly migratory, multinucleated, and polarised cells which carry lysosomal enzymes enabling them

to resorb fully mineralised bone (Sommerfeldt and Rubin, 2001).

Embryonic bone develops via two processes. The flat bones of the skull develop by intramembranous ossification, where mesenchymal cells form condensations and differentiate directlty into bone-forming osteoblasts, which lay down matrix. However, most bones, such as long bones and the axial skeleton, develop by endochondral ossification, which involves an intermediate cartilaginous stage (Ralston, 2009; Mackie et al., 2008; Kronenberg, 2003). The endochondral process also involves condensation of mesenchymal cells which then differentiate into chondrocytes, the primary cell type of cartilage. The resultant cartilaginous template enlarges as chondrocytes proliferate and lay down matrix. Central chondrocytes then halt their proliferation and undergo hypertrophy, in which the cells increase in volume and change their collagen production from type II to type X. Hypertrophic chondrocytes attract blood vessels through production of vascular endothelial growth factor (VEGF) and direct mineralisation and the formation of a bony collar. Hypertrophic chondrocytes then die leaving behind a cartilaginous scaffold for osteoblasts and blood vessels to invade and deposit bone. Chondrocyte proliferation continues causing lengthening of the bone and hematopoietic stem cells establish the site for hematopoietic marrow, (Kronenberg, 2003), see Figure 2.3 .

Chondrocyte differentiation during the endochondral ossification process has been shown to be regulated by the indian hedgehog (Ihh) - parathyroid hormone-related protein (PTHrP) signalling pathway (Karp et al., 2000). Ihh, described as "the master regulator" of bone development by Kronenberg (2003), is synthesised by pre-hypertrophic chondrocytes and hypertrophic chondrocytes leaving the proliferative pool which convert adjacent perichondral cells to osteoblasts of the bone collar. In response, chondrocytes at the ends of the bone synthesise PTHrP, which stimulates nearby chondrocytes exiting the proliferative pool to continue proliferating and delay hypertrophic differentiation (Kronenberg, 2006). When a sufficient distance

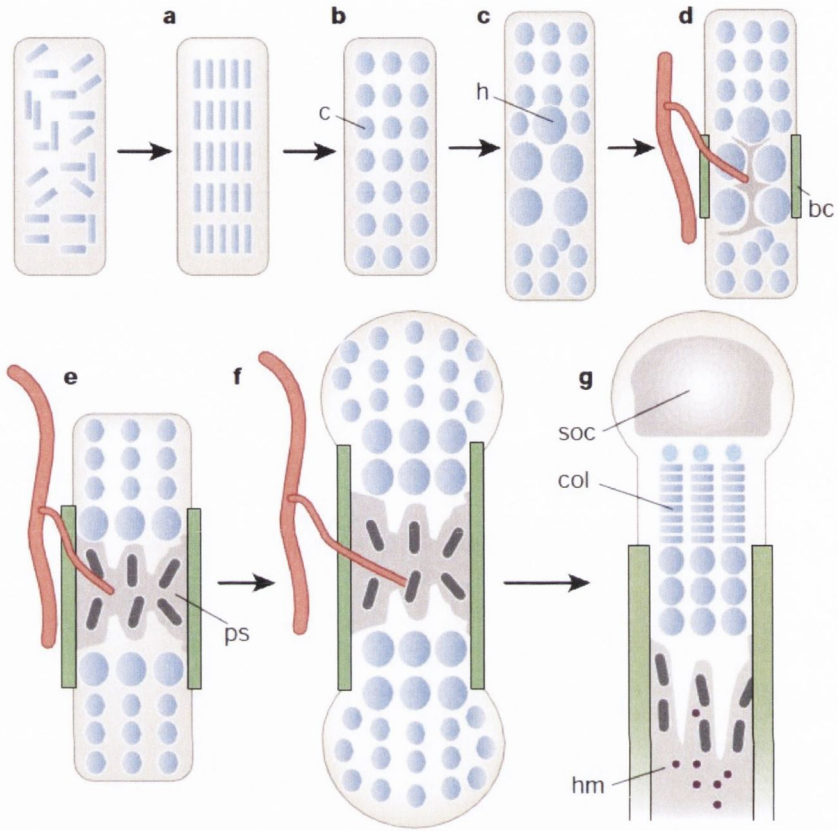

Figure 2.3.: *Endochondral bone formation.* **a**, *Mesenchymal cells condense.* **b**, *Cells of condensations become chondrocytes (c).* **c**, *Central chondrocytes stop proliferating and become hypertrophic (h).* **d**, *Perichondrial cells adjacent to hypertrophic chondrocytes become osteoblasts forming bone collar (bc). Hypertrophic chondrocytes direct the formation of mineralised matrix, attract blood vessels, and undergo apoptosis.* **e**, *Osteoblasts of primary spongiosa accompany vascular invasion, forming the primary spongiosa (ps).* **f**, *Chondrocytes continue to proliferate, lengthening the bone. Osteoblasts of primary spongiosa are precursors of eventual trabecular bone; osteoblasts of bone collar become cortical bone* **g**, *At the end of the bone, the secondary ossification centre (soc) forms through cycles of chondrocyte hypertrophy, vascular invasion and osteoblast activity. The growth plate below the secondary centre of ossification forms orderly columns of proliferating chondrocytes (col). Haematopoietic marrow (hm) expands in marrow space along with stromal cells.*

(Kronenberg, 2003)

from PTHrP production is reached, chondrocytes stop proliferating and Ihh is again up-regulated, which signals back to chondrocytes at the ends of the bone to stimulate the synthesis of more PTHrP. Ihh therefore directs the formation of the bony collar in endochondral ossification by regulating osteoblastic differentiation and the Ihh-PTHrP feedback loop determines the site at which chondrocytes stop proliferating and produce Ihh. This negative feedback loop is illustrated in Figure 2.4. A number of other pathways, such as fibroblast growth factor signalling and bone morphogenetic protein signalling, and transcription factors, such as SOX9 and Runx2, also play a role in regulating endochondral ossification (Kronenberg, 2006; Mackie et al., 2008).

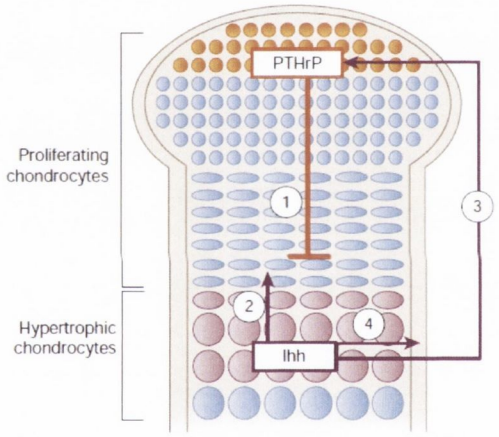

Figure 2.4.: *Indian hedgehog (Ihh)/parathyroid hormone-related protein (PTHrP) negative-feedback loop. PTHrP is secreted from perichondrial cells and chondrocytes at the ends of long bones (1). PTHrP acts on receptors on proliferating chondrocytes to keep the chondrocytes proliferating and, thereby, to delay the production of Ihh. When the source of PTHrP production is sufficiently distant, then Ihh is produced. The Ihh acts on its receptor on chondrocytes to increase the rate of proliferation (2) and, through a poorly understood mechanism, stimulates the production of PTHrP at the ends of bones (3). Ihh also acts on perichondrial cells to convert these cells into osteoblasts of the bone collar (4).*

(Kronenberg, 2003)

At the end of the bone the secondary ossification centre forms through cycles of chondrocyte hypertrophy and vascularisation, and a key feature in the formation of

the secondary ossification centre is the presence of cartilage canals, see Figure 2.5. These canals facilitate angiogenesis by acting as conduits for blood vessel migration into the epiphysis, and have been identified in mammals (Ganey et al., 1995; Ytrehus et al., 2004) and birds (Blumer et al., 2004, 2006). Cartilage canals function to serve three purposes. Firstly, they act to eliminate waste, and to nourish chondrocytes beyond the reach of diffusive nutrients from the synovial fluid (Ytrehus et al., 2004; Blumer et al., 2008). Secondly, they supply the cartilaginous template with progenitor cells of the osteogenic lineage which contribute to ossification within the epiphysis (Ytrehus et al., 2004; Blumer et al., 2008). Thirdly, the canals act as reservoirs for progenitor cells for the growth of the cartilage (Ytrehus et al., 2004; Blumer et al., 2008). In fully developed adult bone, the primary and secondary ossification centres are fused together and the only remaining cartilage left is the permanent articular cartilage at each end of the bone (Mackie et al., 2008).

Similar to embryonic bone development, bone repair also occurs by two mechanisms. If there is no movement between the fracture surfaces the bone heals via remodelling by BMUs, a process known as primary fracture healing. Secondary fracture healing occurs when there is movement between the fracture surfaces which results in the formation of a callus. This event can be described by the four stage model (Schindeler et al., 2008).

1. Stage 1: Inflammation.

   Damage to the vasculature and marrow leads to activation of wound healing pathways. The secretion of cytokines and growth factors, such as transforming growth factor-$\beta 3$ (TGF-$\beta 3$), VEGF, and interleukins (IL) 1 and 6 by inflammatory cells advance clotting into a fibrinous thrombus and promote migration and invasion of multipotent mesenchymal stem cells.

2. Stage 2: Soft callus formation.

   Chondrocytes derived from mesenchymal stem cells replace fibrous and gran-

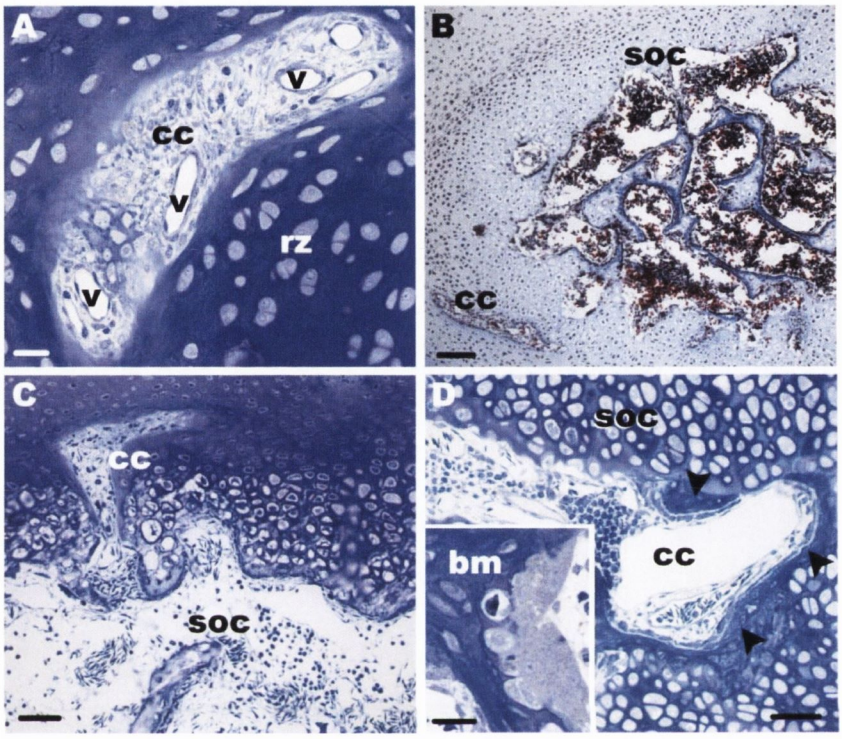

Figure 2.5.: *Light micrographs. (A) Semithin cross-section through a cartilage canal (cc). This canal is located within the reserve zone (rz) of the epiphysis of a 40-day-old chicken (D40). The canal contains several blood vessels (v) and mesenchymal cells which are embedded in the canal extracellular matrix. The canal matrix does not stain with toluidine blue. Scale bar, 20 μm. (B) This histological longitudinal section through the femur shows an overview of the epiphysis (D17). A secondary ossification centre (soc) is present and one cartilage canal (cc) lies outside this centre. Scale bar, 100 μm. (C) Semithin cross-section through the epiphysis (D15). A cartilage canal (cc) penetrates into the SOC and mesenchymal cells and blood vessels migrate into it. Scale bar, 50 μm. (D) Semithin longitudinal section through a cartilage canal which terminates blind within the SOC (D17). Around the end of the canal the bone matrix stains deeper with toluidine blue (arrowheads). The mesenchymal cells (= osteoblasts) of the canal border on this extracellular layer. Scale bar, 50 μm. Inset: an osteoclast which resorbs the newly formed bone matrix (bm). Scale bar, 20 μm.*

(Blumer et al., 2006)

ulation tissue with cartilage to produce a semi-rigid soft callus for mechanical stability. The chondrocytes then undergo hypertrophy, release pro-angiogenic factors, and mineralise the cartilaginous matrix.

3. Stage 3: Hard callus formation.
   As the soft callus is removed and revascularisation occurs a new hard callus forms to bridge the fracture surfaces. This woven bone is laid down by osteoblasts and is typically irregular and under-remodelled.

4. Stage 4: Bone remodelling.
   The final stage involves the remodelling of the woven bone hard callus into cortical and/or trabecular bone by BMUs.

Articular cartilage lines the ends of the diathrodial joints of the body and functions to dissipate large forces generated during walking and running as well as to provide a near frictionless surface allowing the joint to move with minimal wear occuring. Articular cartilage can be best described as bi-phasic material consisting of a solid matrix phase and an interstitial fluid phase. The solid matrix phase consists of proteoglycans and type II collagen. Sulphated glycosaminoglycans (sGAGs) in the proteoglycan are hydrophillic, negatively charged macromolecules, which attract water in to the tissue causing an osmotic swelling pressure, and also produce a repulsive force. These forces are balanced by a dense mesh of collagen fibers, constraining the proteoglycans. The collagen content of the tissue ranges from 10 to 30% wet weight and the proteoglycan content from 3 to 10% wet weight with the remaining 60 to 87% consisting of water and small amounts of inorganic salts and proteins.

Mature articular cartilage has a hierarchical zonal structure consisting of a superficial tangential, middle, and deep zone, see Figure 2.6. In the superficial tangential zone thin, densely packed, collagen fibrils are orientated parallel to the

articular surface. A low permeability to fluid flow is evident in this region. The middle zone consists of larger, more randomly orientated fibers and has a high proteoglycan content. In the deep zone the collagen fibrils are perpendicularly orientated and insert into calicified cartilage, anchoring the tissue to the bony interface.

Unlike bone, articular cartilage has a striking inability to heal even the most minor injury due to two of its structural features. Firstly, it is an avascular tissue. A vascular system delivers specific cells which remove necrotic material and synthesize new matrix, as well as creating the proper biochemical environment for healing (Newman, 1998). Secondly, chondrocytes in the neighbouring healthy cartilage are trapped in a mesh of collagen and proteoglycan, preventing cell migration to the damaged site. Surigical techniques for the treatment of chondral defects such as microfracture have resulted in decreased symptoms and improved function (Steadman et al., 2003), though a large percentage of the cartilage formed was reported to be fibrocartilage. Autograft techniques such as mosaicplasty are restricted due to issues associated with donor-site morbidity and limited quantity of harvestable tissue. The degenerative joint disease osteoarthritis is characterised by the degradation of cartilage. The ultimate therapy for this condition is total joint replacement.

2.3. Bone tissue engineering

As was highlighted in section 1.1, a number of clinical situations exist where bone regeneration is required in large quantities, and there is therefore an urgent need for alternatives to autografts in order to regenerate bone. One such alternative is the use of a biomaterial scaffold which once implanted *in vivo* would promote the migration, proliferation and differentiation of bone cells. Hydroxyapatite (HA),

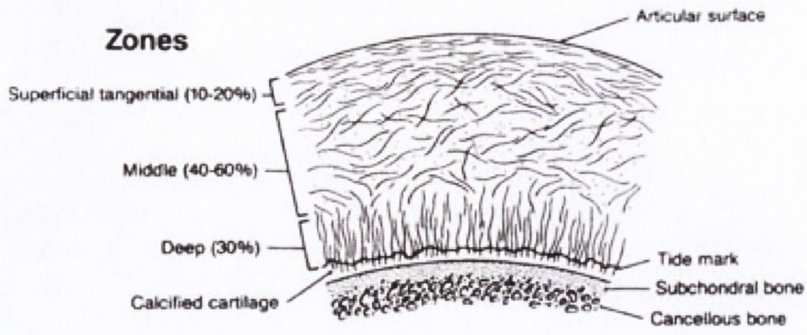

Figure 2.6.: *Hierarchical zonal structure of articular cartilage*

(Mow et al., 1980)

is the major inorganic constituent of bone and has garnered much attention in the field of bone tissue engineering. An early study by Yamasaki and Sakai (1992) implanted dense and porous HA ceramics subcutaneously in the abdomen of dogs and evaluated heterotopic bone formation after 1, 3 and 6 months. The authors found evidence of deposition of new bone via intramembranous ossification in the porous ceramics after 3 months but found no new bone in the dense ceramics even after 6 months. A later study by Klein et al. (1994) reported similar results for dense and porous HA ceramics implanted intramuscularly in dogs, with new bone being formed in the porous constructs only. These studies highlighted the importance of a porous network in order to provide the appropriate millieu for osteogenesis. Yuan et al. (2002) and Le Nihouannen et al. (2005) demonstrated that the osteoinductiveness of ceramics, implanted intramuscularly in goats and sheep respectively, could be enhanced through the combination of HA and β-Tri Calcium Phosphate (β-TCP) in a biphasic calcium phosphate ceramic. Whilst HA is the major inorganic constituent of bone, collagen is the major organic constituent and is also the most common protein in the body. Collagen can be combined with glycosaminoglycan and freeze-dried to produce a highly porous collagen-GAG scaffold (O'Brien et al., 2005). The addition of HA (200%wt) has been shown to

increase the mechanical stiffness of such scaffolds (Gleeson et al., 2010) and also enhance their *in vivo* bone healing potential (Lyons et al., 2010).

In order to improve the osteogenicity of such implants, scaffolds have been combined with osteogenic cells and signalling factors to produce tissue engineered constructs. Osteoblasts isolated from biopsies were the initial obvious cell choice. However, the relatively low numbers of cells obtained upon *in vitro* isolation and expansion were seen as a limitation (Salgado et al., 2004). The idea that an osteogenic precursor cell resided in the bone marrow started when Petrakova et al. (1963) obtained an osseous tissue by implanting bone marrow under the renal capsule. Friedenstein et al. (1974) later developed a method to isolate these cells which he defined as colony-forming units fibroblastic (CFU-f). Caplan (1991) named these cells mesenchymal stem cells and postulated that the isolation, expansion, and site directed delivery of MSCs could govern the repair of skeletal tissues, see Figure 2.7. The *in vitro* osteogenic differentiation of BM-MSCs has been demonstrated by stimulation with dexamethasone, β-glycerophosphate (β-GP) and ascorbic acid (Lennon et al., 2001; Farrell et al., 2006) in a process resembling intramembranous ossification.

A study by Kon et al. (2000) demonstrated the benefit of implanting a tissue engineered construct (ex vivo expanded BM-MSCs loaded onto a HA scaffold) as opposed to a biomaterial scaffold. This study, which examined critically sized long bone defects in sheep, found accelerated bone repair and more homogenous bone distribution with the tissue engineered construct compared to the cell-free scaffold. Osteogenically induced BM-MSCs loaded onto porous β-TCP and coralline scaffolds were shown to repair critically sized mandibular bone defects in canines whereas acelluar scaffolds formed soft tissue with no bone (Yuan et al., 2007, 2010), Figure 2.8. The first clinical case study involving the use of tissue engineered constructs for the treatment of long bone defects was performed by Quarto et al. (2001) and

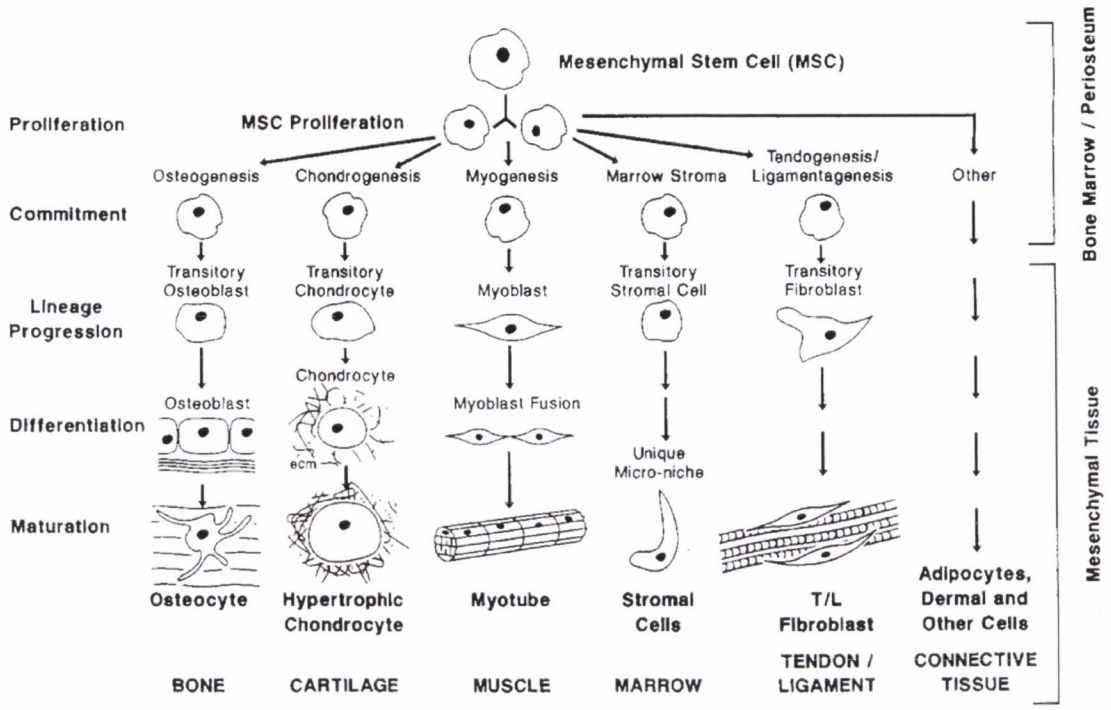

Figure 2.7.: *The Mesengenic Process*

(Caplan, 2005)

involved 3 patients implanted with macroporous HA scaffolds loaded with ex vivo expanded autologous BM-MSCs, see Figure 2.9. A follow up report by Marcacci et al. (2007) noted good osteointegration with no further complications 6-7 years after surgery but also highlighted limitations in the study, such as the lack of an acellular scaffold control group and lack of new bone quantification.

A major hurdle associated with *in vitro* bone tissue engineering is the lack of a functional vascular supply. When the engineered construct is implanted, due to the lack of vasculature, the seeded cells have a limited capacity to receive substrate molecules (oxygen, glucose, and amino acids) and to eliminate waste products thus threatening cell and construct viability (Santos and Reis, 2010). An additional limitation of the intramembranous ossification approach to bone tissue engineering is that the *in vitro* culture of a construct can lead to extensive

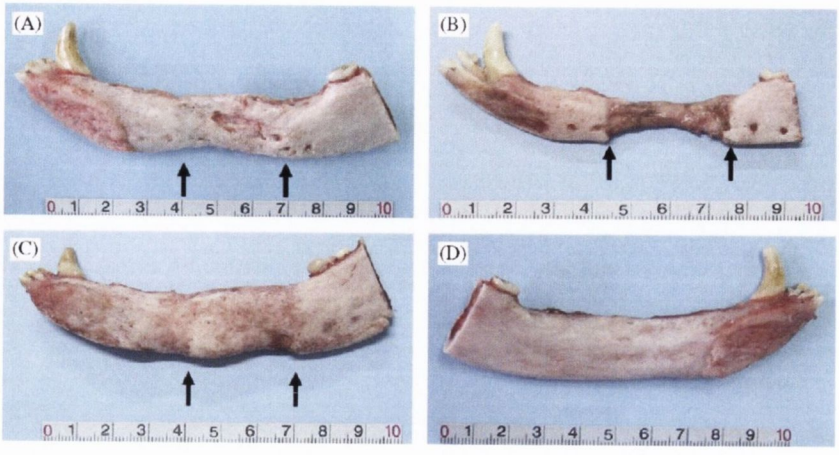

Figure 2.8.: *Gross view of repaired mandibles at 32 weeks post-operation. (A) BM-MSC seeded β-TCP scaffold (B) β-TCP scaffold (C) Autograft (D) Native mandible*

(Yuan et al., 2007)

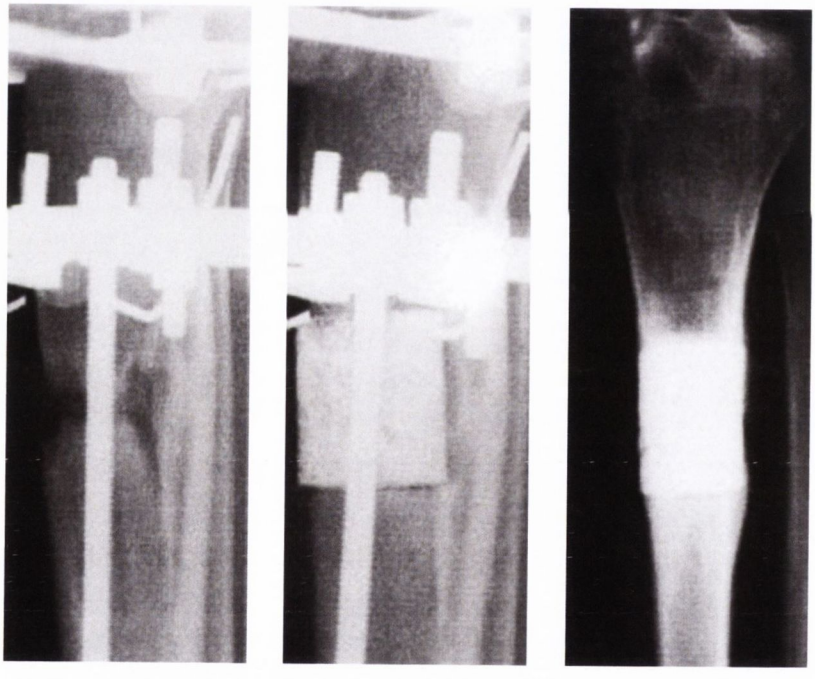

Figure 2.9.: *Radiographs Obtained before and after the Repair of Large Bone Defects. Panels A, B, and C show films obtained from Patient 1 before, immediately after, and 18 months after surgery, respectively.*

(Quarto et al., 2001)

matrix mineralisation, sealing the pores of the scaffold and further restricting *in vivo* vascularisation. Lyons et al. (2010) for example, found superior bone healing with the use of an acelluar collagen calcium phosphate scaffold in a rat cranial defect compared to a BM-MSC seeded scaffold. The authors postulated that the remodelling of the dense matrix of the tissue engineered construct slowed new host cell-mediated bone formation resulting in core degradation of the construct.

An alternative approach to implantation of an osteogenically primed cell-seeded scaffold is the implantation of a scaffold which is cell-free but loaded with growth factors and proteins capable of promoting osteogenesis of host cells (Guldberg et al., 2007). Bone morphogenetic proteins (BMPs) have been examined extensively in bone regeneration applications, with their potential being supported by a number of clinical trials (Friedlaender et al., 2001; Dimar et al., 2006). Indeed, two BMPs are presently applied in the clinc, recombinant human BMP-2 (InFUSE) and recombinant human BMP-7. Polyla(L-lactide-*co*-D,L-lactide) (PLDL) scaffolds loaded with TGF-β3 and BMP-2, and implanted into a rat segmental defect model, demonstrated enhanced bone regeneration compared to empty defects, and showed a trend towards enhancing bone formation compared to PLDL scaffolds not containing TGF-β3 and BMP-2 (Oest et al., 2007). Furthermore, polycaprolactone-tricalcium phosphate (PCL-TCP) scaffolds loaded with platelet-rich plasma (PRP) enhanced vascularisation and bone bridging in the same rat defect model, compared to scaffolds unloaded with PRP (Rai et al., 2007). However, the mechanical properties of the tissues generated by Oest et al. (2007) and Rai et al. (2007) in these polymer scaffolds remained an order of magnitude lower than those of age-matched intact femurs, with the slow resorption characteristics of the scaffolds postulated as one mechanism by which functional restoration is impeded.

Challenges associated with the slow resorption of these 'hard scaffolds' have led to an increased interest in 'soft scaffolds', the degradation rate of which can

be more efficiently controlled. For example, the degradation characteristics of alginate hydrogels (described further in section 2.4.1) can be modified by gamma-irradiating the alginate, which decreases the polymer chain size and increases the degradation rate *in vivo* (Alsberg et al., 2003). Such irradiated 'soft scaffold' alginate hydrogels, covalently coupled with the arginine-glycine-aspartic acid (RGD) peptide to facilitate cell adhesion and loaded with BMP-2, promoted the regeneration of bone with mechanical properties not significantly different to intact bone after 12 weeks when delivered within a perforated nanofiber mesh (Kolambkar et al., 2011b). In a follow-up study, this hybrid system also demonstrated enhanced bone defect repair when compared to the clinical standard collagen sponge (Kolambkar et al., 2011a).

In these studies by Kolambkar et al. (2011b,a), no cartilage formation was reported within bone defects, suggesting that bone formation occured by intramembranous ossification. In contrast, other studies using similar growth factor loaded hydrogels have demonstrated bone regeneration through endochondral ossification (Simmons et al., 2004; Boerckel et al., 2011). For example, earlier work by Simmons et al. (2004) demonstrated enhanced bone formation by BM-MSCs, which occurred by endochondral ossification, in a dual growth factor RGD modified alginate hydrogel which had been irradiated to accelerate *in vivo* degradation. Furthermore, a study by Alsberg et al. (2002) recapitulated the process of endochondral ossification by co-transplanting osteoblasts and chondrocytes into RGD modified alginate hydrogels thus engineering a growing cartilaginous tissue.

2.4. Cartilage tissue engineering

Autologous chondrocyte implantation (ACI) represents a first generation cell based therapy for the treatment of cartilage defects (Peterson et al., 2000; Brittberg et al.,

1994). This therapy involves taking a cartilage biopsy from a minor-load bearing region of the joint. Chondrocytes are then isolated from the tissue, expanded *in vitro*, and injected into the defect site sutured with a periosteal flap taken from the proximal medial tibia covering the defect, see Figure 2.10. Issues associated with hypertrophy of the periosteal patch led to the development of a second generation variation of this technique, which involves the use of a collagen membrane in place of the periosteal flap. The third generation matrix-induced autologous chondrocyte implantation (MACI) technique incorporates a three-dimensional scaffold, consisting of collagen types I and III, onto which cells are seeded. A study by Basad et al. (2010) highlighted advantages of MACI compared to ACI, describing the collagen I/III membrane as providing consistent quality, flexibility and easy handling.

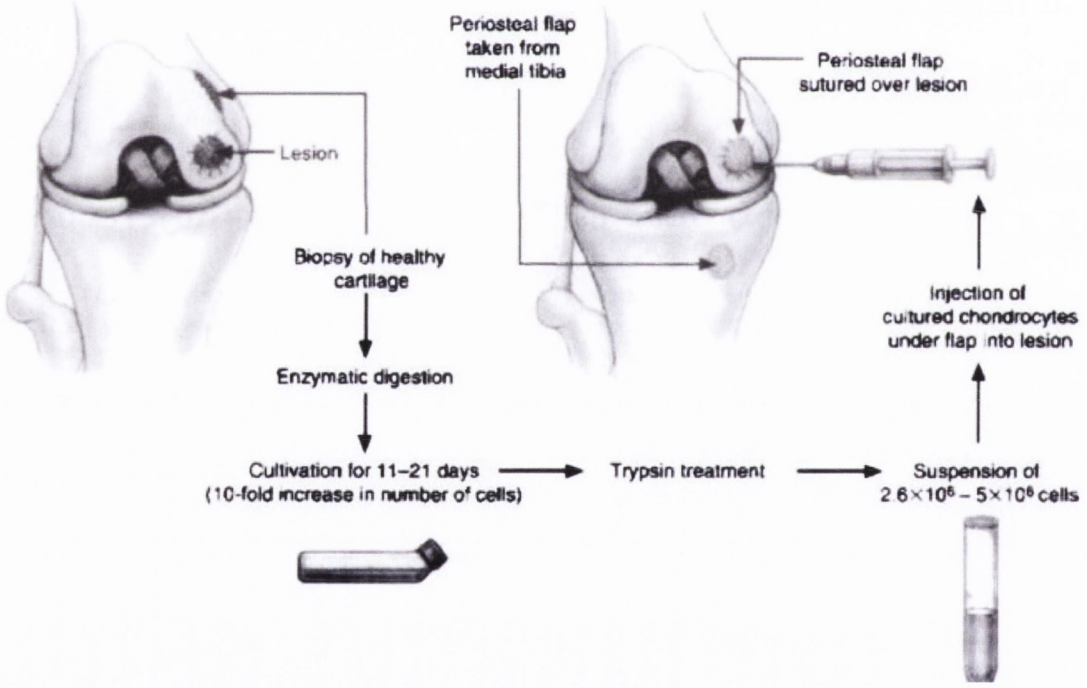

Figure 2.10.: *Autologous chondrocyte implantation*

(Mow and Huiskes, 2005)

An idealised tissue engineering process for the regeneration of cartilage is shown

in Figure 2.11. Isolated cells (chondrocytes or stem cells) can be expanded in monolayer culture until sufficient cell numbers are obtained. Cells can subsequently be seeded onto 3D scaffolds and cultured in the presence of chondrogenic growth factors and/or mechanically stimulated via a bioreactor in order to enhance matrix synthesis and maintain a chondrogenic phenotype. The neocartilage can then be implanted into the defect site, potentially with anti-inflammatory factors to prevent further degradation of the joint.

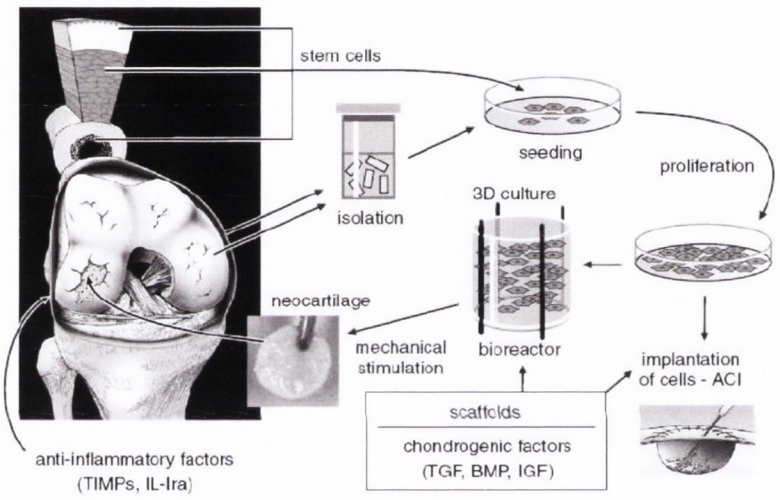

Figure 2.11.: *Idealised tissue engineering process for the regeneration of cartilage* (Nesic et al., 2006)

2.4.1. Hydrogels for cartilage tissue engineering

Identifying an appropriate scaffolding material is central to the successful development of tissue engineering therapy. Hydrogels are water swollen, cross-linked polymers which are suitable for use as scaffolds in cartilage tissue engineering applications for a number of reasons (Riley et al., 2001):

- The high water content and low coefficient of friction of a hydrogel is similar

to that of cartilage.

- A hydrogel may support chondrogenesis of a progenitor cell by promoting a spherical cell shape.
- A hydrogel may facilitate the seeding of different cell types into isolated regions of prefabricated scaffolds essentially creating multi-scaffold and multi-tissue composites.
- *In situ* cross-linking methods should facilitate the formation of large, abstract shaped constructs.
- Mechanical properties and degradation rates may be tailored to match the deposition of extra-cellular matrix by the embedded cells.
- *In situ* formation of the scaffolds allows for minimally-invasive delivery.

Naturally derived hydrogels are attractive materials for tissue engineering applications as they are either components of or have macro-molecular properties similar to native extra-cellular matrix (Drury and Mooney, 2003). For example, collagen is the most abudant protein in animals and the major component of connective tissue (Patino et al., 2002). Both type I and type II collagen hydrogels have been examined for MSC-based cartilage tissue engineering applications (Bosnakovski et al., 2006). Agarose, a naturally occuring polysaccharide that is extracted from marine red algae, is a thermosetting hydrogel that undergoes gelation in response to a reduction in temperature. Chondrocytes cultured in an agarose hydrogel have been shown to produce a mechanically functional matrix (Buschmann et al., 1992). Agarose has been used in animal models of cartilage defect repair (Weisser et al., 2001) and chondrocyte- seeded alginate-agarose hydrogels have been used for the treatment of chondral and osteochondral defects in humans (Selmi et al., 2008).

Alginate, a polysaccharide isolated from brown algae, is a copolymer that contains homopolymeric blocks of (1,4)-linked β-D-mannuronic acid (M) and its C-5 epimer α-L-guluronate (G) residues (Augst et al., 2006; Kharkar et al., 2013). Alginate hydrogels are formed when divalent cations such as Ca^{2+}, Ba^{2+} or Sr^{2+} interact with blocks of G monomers to form ionic bridges between polymer chains (Drury and Mooney, 2003). Ionically cross-linked alginate hydrogels undergo dissolution over time by losing the divalent cross-linking cations, though degradation rate can be accelerated through gamma-irradiation which cleaves M-G residues while leaving G-block length and G content constant (Alsberg et al., 2003; Augst et al., 2006).

Chitosan is a polysaccharide of β-(1-4)-linked D-glucosamine and *N*-acetyl-D-glucosamine residues, derived from chitin which is found in the exoskeletons of crustaceans (Drury and Mooney, 2003; Kharkar et al., 2013). Chitosan is soluble in water only up to pH 6.2, though the addition of polyol salts, such as β-glycerophosphate (β-GP), allows neutralisation of the pH while remaining in a liquid state at or below room temperature (Berger et al., 2004; Ruel-Gariepy and Leroux, 2004). Chitosan-β-GP hydrogels, supplemented with hydroxyethyl cellulose (HEC), have been used as injectable hydrogels seeded with chondrocytes for cartilage tissue engineering applications (Hoemann et al., 2005), and have also been encapsulated with intervertebral disc cells for the purpose of nucleus pulposus regeneration (Roughley et al., 2006). A follow-up study by Hoemann et al. (2007) elucidated that gelation in these chitosan-β-GP-HEC hydrogels is due to the presence of glyoxal in the commercial grade HEC which covalently cross-links the chitosan. Chitosan has been shown to be degraded by the human enzyme lysozyme (Hong et al., 2007).

Fibrin is a protein that forms a hydrogel through the thrombin mediated cleavage of fibrinogen, which exposes regions on fibrin molecules that interact allowing self-assembly of fibrils which aggregate and lengthen (Hunt and Grover, 2010). During

wound healing, fibrin is the first network that a cell encounters (Janmey et al., 2009). Ahmed et al. (2008) describes fibrin hydrogels as having three major disadvantages for use in tissue engineering applications; Gel shrinkage, low mechanical stiffness, and rapid gel degradation by cell-associated enzymatic activity. The low mechanical stiffness can be addressed by 'blending' fibrin with other hydrogels, such as alginate for example (Ma et al., 2012). Degradation rate can be altered using the proteinase inhibitor aprotinin (Kharkar et al., 2013).

2.4.2. MSCs for cartilage tissue engineering

Agarose, alginate, chitosan and fibrin hydrogels have all been shown to support chondrogenesis of chondrocytes. There are however, limitations to the use of chondrocytes for cartilage tissue engineering applications. When expanded in 2D chondrocytes can de-differentiate toward a fibroblastic phenotype expressing collagen type I as opposed to collagen type II (Temenoff and Mikos, 2000). An age-related loss of the chondrogenic capacity of chondrocytes, which may limit their use to younger patients with isolated chondral lesions, has also been reported (Barbero et al., 2004). Finally isolating chondrocytes requires a biopsy, which can result in donor site morbidity and also limits the quantity of harvestable tissue (Vinatier et al., 2009).

These limitations have led to the search for alternative cell sources for cartilage repair therapies with BM-MSCs being recognised as a particularly attractive cell source. Johnstone et al. (1998) developed the "pellet" culture system to facilitate the *in vitro* chondrogenic differentiation of rabbit BM-MSCs. In this study BM-MSCs were pelleted and cultured in the presence of dexamethasone and transforming growth factor-β1. Assessment of the pellets demonstrated the production of a cartilaginous matrix (proteoglycan and collagen II) as well as markers of hypertrophy (alkaline phosphatase and collagen X). The pellet model

has since become the standard paradigm for the assessment of chondrogenesis in MSCs (Murphy et al., 2002; Bosnakovski et al., 2004; Tropel et al., 2004).

In order for MSCs to be used as a cell source for tissue engineering of cartilage they must have the ability to produce a 3D construct with the mechanical properties similar to those produced using chondrocytes. Mauck et al. (2006) demonstrated that although MSC-seeded agarose hydrogels cultured in chondrogenic conditions accumulated significant cartilaginous matrix, the functional properties were still two- to three-fold lower than those produced by chondrocyte-seeded hydrogels. Erickson et al. (2009) and Vinardell et al. (2011) also demonstrated inferior mechanical properties of MSC-seeded agarose hydrogels compared to chondrocyte-seeded hydrogels. Some studies have focussed on the use of an *in vitro* bioreactor in order to increase the properties of cartilaginous tisses. For example, Mauck et al. (2000) demonstrated that physiological levels of dynamic compression increased matrix accumulation within chondrocyte-seeded agarose hydrogels. Overcoming nutrient transfer limitation is another well documented challenge in the field of cartilage tissue engineering. Strategies to increase nutrient delivery to constructs include the introduction of channels into a cell-seeded scaffold. Bian et al. (2009) found that the introduction of a single channel into the center of chondrocyte-seeded agarose constructs increased the mechanical properties of the engineered tissue. Buckley et al. (2009a) demonstrated that a superior and more homogenous chondrocyte-seeded construct could be engineered through the combination of a channelled architecture and dynamic rotational culture.

If MSC-based cartilage repair therapies are to be translated into clinical applications, a critical factor will be ensuring the development of a phenotypically stable cartilaginous tissue that is resistant to hypertrophy and endochondral ossification (Pelttari et al., 2006). In order to examine the phenotypic stability of tissue engineered cartilage an ectopic model is often used where MSCs (in pellet

form or seeded onto scaffolds) are implanted under the skin or into the muscles of severe combined immunodeficient (SCID) mice. De Bari et al. (2004) investigated the *in vitro* and *in vivo* cartilage forming capacity of synovium membrane derived MSCs compared to articular chondrocytes. The authors demonstrated that although chondrogenically differentiated MSCs expressed stable chondrogenic markers, comparable to those expressed by chondrocytes, *in vitro*, it was not sufficient to maintain the chondrogenic phenotype *in vivo* as the cells failed to form a cartilaginous matrix resistant to vascular invasion. Pelttari et al. (2006) demonstrated that chondrogenically primed human BM-MSC pellets followed an "unnatural" differentiation pathway with an initial induction of type X collagen preceding type II collagen production which was followed by an up-regulation in alkaline phosphatase activity *in vitro*. This correlated with *in vivo* calcification and vascularisation of MSC pellets which still contained proteoglycan and collagen type II. Therefore, the pathway followed by the chondrogenically primed BM-MSCs was thus related to endochondral ossification and not stable cartilage formation, see Figure 2.12. A study by Dickhut et al. (2009) examing the phenotypic stability of stem cells isolated from different sources also demonstrated that chondrogenically primed BM-MSCs developed along the endochondral bone pathway *in vivo*, whilst synovium derived MSCs showed reduced calcification but demonstrated a tendancy toward fibrous dedifferentiation. An alternative study by Dickhut et al. (2008) did show that with the use of an appropriate biomaterial, in this case Matrigel ™, it was possible to prevent hypertrophy and calcification of MSC-seeded cartilginous constructs though predominantly it would seem that MSCs undergoing chondrogenesis *in vitro* create transient rather than stable cartilage (Richter, 2009).

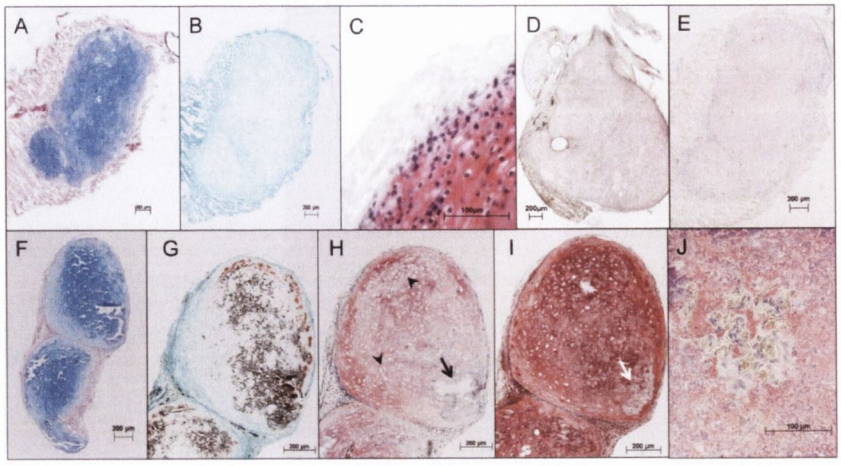

Figure 2.12.: *Histologic evaluation of ectopic cartilage-like transplants formed by articular chondrocytes (A-E) and BM-MSCs (F-G) cultured in vitro in the presence of TGFβ for 7 weeks and transplanted subcutaneously in SCID mice for 4 weeks. Proteoglycan accumulation (A,F), calcium deposition (B,G), type II collagen (C,H), type X collagen (D,I) and type I collagen (E,J).*

(Pelttari et al., 2006)

2.4.3. Osteochondral tissue engineering

Damage to the articular surface of a joint can penetrate to the subchondral bone. Such osteochondral defects are often associated with mechanical instability of the joint and warrant surgical intervention in order to prevent osteoarthritic degenerative changes (Martin et al., 2007). Even in cases where lesions do not penetrate to the subchondral bone an osteochondral construct may be a more desirable implant, as a bone to bone interface integrates better than a cartilage to cartilage interface (Schaefer et al., 2002). Autologous grafting procedures, such as mosaicplasty, are not ideal due to issues associated with topology conformity, donor site morbidity and tissue availability (Grayson et al., 2008). The field of tissue engineering may offer an alternative to autografts, through the engineering of osteochondral constructs, see Figure 2.13.

One strategy applied in osteochondral tissue engineering applications is biphasic scaffolding, which generally involves the attachment of a hard osseous

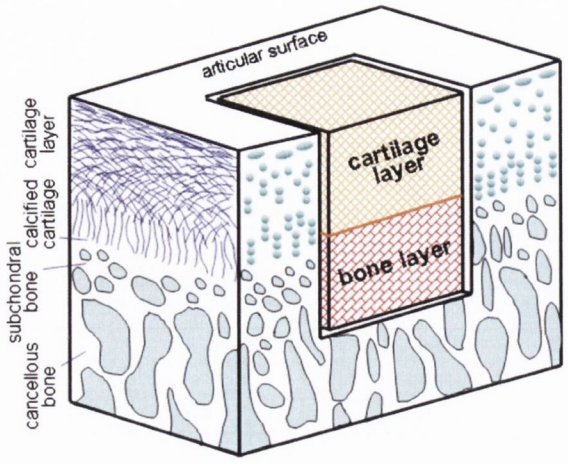

Figure 2.13.: *Schematic representation of a osteochondral defect showing the collagen fibres (left face) and the chondrocytes (right face) of the cartilage layer (upper side), the bone region (bottom), and the osteochondral implant*

(Mano and Reis, 2007)

phase to a softer chondral phase. Gao et al. (2001) for example, generated a bi-phasic scaffold for osteochondral defect repair by attaching, with a fibrin sealant, a porous calcium phosophate ceramic loaded with osteogenically primed MSCs to a hyaluronan sponge loaded with chondrogenically primed MSCs. Following subcutaneous implantation for a period of six weeks, the osteochondral graft remained structurally integrated and developed a fibrocartilaginous tissue in the hyaluronan sponge and bone in the calcium phosphate ceramic. In a follow-up study, an engineered osteochondral graft, this time fabricated using an injectable calcium phosphate for the osseous scaffold, stimulated osteochondral defect repair when implanted into the mechanically loaded environment of a rabbit femoral condyle (Gao et al., 2002). Khanarian et al. (2012) developed a bi-phasic scaffold consisting of hydroxyapatite and an alginate hydrogel and demonstrated that, when seeded with deep zone chondrocytes, the hydroxyapatite phase enhanced matrix accumulation and promoted the formation of a calcified cartilage interface. Zones of calcified cartilage have also been incorporated into bi-phasic osteochondral

constructs as a means of improving the mechanical properties and integration strength of the engineered tissues (St-Pierre et al., 2012).

2.5. Engineering anatomic constructs for whole joint and bone regeneration

No biological therapies currently exist for total joint condyle regeneration, with artificial prostheses still the 'gold standard' (Learmonth et al., 2007). Engineered anatomically accurate osteochondral grafts have been suggested as a potential biological treatment for conditions such as osteoarthritis (Alhadlaq et al., 2004, 2005). Using a computer-aided design model to drive a CNC milling machine, Hung et al. (2003) designed anatomic moulds capable of recapitulating osteochondral constructs in the shape of the patellofemoral joint. The anatomic constructs consisted of a chondrocyte-seeded agarose hydrogel attached to a devitalised trabecular bone disk, see Figure 2.14. Lee et al. (2009) fabricated a scaled-up proximal tibial joint condyle consisting of a poly-ϵ-caprolactone/hydroxyapatite osseous phase and a polyethylene-glycol (PEG) hydrogel chondral phase. To facilitate scaling-up of the graft, the osseous phase contained microchannels of diameter 400 μm which when seeded with MSCs underwent increased angiogenesis as compared to when seeded with MSC-derived osteoblasts.

An alternative to the bi-phasic approach for osteochondral tissue engineering is a single phase approach incorporating a structured co-culture of cells in a bi-layered construct. This strategy has advantages over the bi-phasic strategy in terms of ease of fabrication and integration. Alhadlaq et al. (2004) engineered a bi-layered PEG hydrogel, consisisting of a chondral layer seeded with MSC derived chondrocytes and an osseous layer seeded with MSC derived osteoblasts, in the shape of the mandibular condyle. When implanted into nude mice for a period of 12 weeks,

the chondral layer demonstrated sGAG and collagen type II accumulation and the osseous layer demonstrated trabecular bone structures, with the interface between the two layers showing evidence of collagen X deposition (Alhadlaq et al., 2005). The use of a hydrogel in these studies ensured homogenous encapsulation of cells, another advantage over the bi-phasic approach.

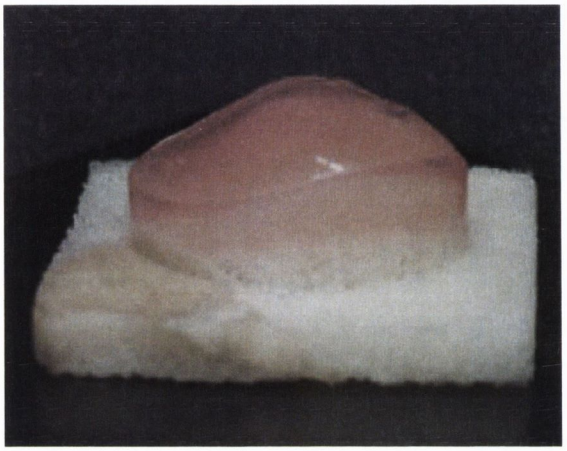

Figure 2.14.: *Patellar osteochondral construct*

(Hung et al., 2003)

Anatomically accurate constructs have also been examined for whole bone tissue engineering, with their potential for regenerating digits garnering particular attention (Komura et al., 2011). Vascularised autogenous joint transplantation from the foot to the hand is a clinical treatment which can provide a lifetime of proper hand function. This treatment is not without its drawbacks, however (Sedrakyan et al., 2006); Firstly, as with all autograft procedures, it is limited by the quantity of tissue available for harvest. Secondly, such an operation results in a significant, negative, aesthetic impact, rendering the treatment undesirable in many cases. Thirdly, the sacrifice of a toe can impair stability in the foot. These factors have led to a search for alternative strategies for digit regeneration.

Isogai et al. (1999) tissue engineered a distal interphalangeal joint consisting of distal and middle polymer phalanges, wrapped with periosteum and lined with

chondrocyte-based tissue engineered cartilage, joined together by a tissue engineered tendon. Following implantation into nude mice for up to 40 weeks, the retrieved constructs maintained their shape and developed bone, cartilage and tendon tissues with evidence of bone vascularisation. A follow-up study by Chubinskaya et al. (2004) used species-specific sequencing to examine the role of donor and host cells in the development of the new tissue and demonstrated that it was of donor origin with bone appearing to form through endochondral ossfication. Landis et al. (2009) sought to eludicate the role of the wrapped periosteum is this model and found that the periosteum directed the formation of a rudimentary growth plate within the phalanx and hypothesised that this was as result of secreted growth factors stimulating hypertrophy of neighbouring chondrocytes adjacent to the articular cartilage layer of the construct.

Vacanti et al. (2001) reported the replacement of a patient's partially avulsed thumb with a tissue engineered phalanx, consisting of a porous coral implant seeded with periosteal cells, which had been extracted from autologous pertiosteal tissue over a period of nine weeks. The cell-seeded scaffold was implanted directly into the defect site and twenty-eight months after the implantation the patient showed good pinch and grip strength, though dorsal sublaxation was also reported. Furthermore, Weinand et al. (2009) developed a methology for thumb regeneration which avoided the requirement for an *in vitro* expansion phase by loading CD 177^+ human BM-MSCs, a sub-population of MSCs which are part of periosteal cells, onto collagen based hydrogels and injecting the cell seeded hydrogel into an anatomically accurate β-TCP/PLGA scaffold. These studies demonstrate the potential of anatomically accurate engineered grafts for the regeneration of whole bones and limbs.

2.6. The endochondral approach to bone tissue engineering

As was highlighted in section 2.3, a signficant challenge with intramembranous bone tissue engineering applications is that it takes time for vasculature to invade a tissue engineered construct and provide cells with the necessary oxygen and nutrients required for survivial (Santos and Reis, 2010). Furthermore, osteogenically primed constructs can further inhibit *in vivo* vascularisation by sealing the pores of a scaffold with calcified matrx (Lyons et al., 2010). Farrell et al. (2011) described the rationales behind the hypothesis that the endochondral route to bone formation may be more successful than the traditional intramembranous approach:

1. Chondrocytes normally reside in an avascular tissue and as a result are designed to function in a low oxygen environment, similar to what they would encounter upon implantation into an unvascularised region.

2. MSCs under *in vitro* conditions become hypertrophic when cultured chondrogenically, the next step in the endochondral ossification pathway.

3. The release of factors from primed chondrogenic cells progressing along the endochondral route would be much more complex and controlled spatiotemporally than any growth factor combination one could devise in order to improve *in vivo* vascularisation and bone formation.

Bone defect repair with tissue-engineered cartilage was suggested as far back as 1994 by Vacanti et. al, who implanted articular chondrocyte-seeded polymer scaffolds into rat cranial defects. However, the neo-tissue formed in these engineered constructs was reported as stable cartilage, resistant to vascularisation and ossification. Indeed a follow-up study by Vacanti et al. (1995) compared the capacity of

periosteal cells and chondrocytes to induce tissue engineered bone defect repair in the same rat cranial model, and found that while chondrocytes again generated a stable cartilage resistant to ossification, periosteal cells generated a tissue which appeared to undergo morphogenesis from cartilage into bone, reminiscent of the process of endochondral ossification. A study by Case et al. (2003) did demonstrate that chondrocyte-based tissue engineered cartilaginous constructs, implanted into a bone chamber model in a rabbit femur, could support appositional bone formation and that this bone formation was enhanced by mechanical loading, suggesting that the capacity of chondrocyte-based tissue engineered constructs to promote bone repair may be dependent on the anatomical implantation site.

The afforementioned studies by Vacanti et al. (1995) and Case et al. (2003) utilised chondrocytes isolated from articular cartilage. Oliveira et al. (2009a) isolated cephalic (CP) and caudal (CD) sternal chondrocytes from 14-day chicken embryos, seeded them within chitosan sponges, and evaluated their capacity to undergo hypertrophic differentiation. The CD chondrocytes used in this study represented a permanent cartilage phenotype, comparable perhaps to articular chondrocytes, whereas the CP chondrocytes represented a transient cartilage phenotype. CP-seeded constructs expressed greater alkaline phosphatase activity and synthesised more collagen type X *in vitro* when compared to CD-seeded constructs (Oliveira et al., 2009a). Furthermore, when implanted *in vivo* CP-seeded constructs facilitated vascularisation and endochondral ossification, whereas CD-seeded constructs remained as stable cartilage (Oliveira et al., 2009b).

As was highlighted in section 2.4, MSCs provide an alternative to chondrocytes for tissue engineering applications. Muraglia et al. (2003) demonstrated that a chondro-osseous rudiment could be generated by culturing BM-MSC pellets in a chondrogenic medium for an initial three week period before switching to a β-GP loaded medium to induce mineralisation. The resultant tissue demonstrated a

hyaline cartilage-like core region surrounded by a peripheral calcified cartilage and bone-like outer layer, seemingly mimicking aspects of bony collar development during endochondral skeletogenesis. Huang et al. (2006) investigated if cartilaginous grafts, engineered using BM-MSCs, could be effective for carpal bone regeneration. To this end, autologous BM-MSCs were seeded within hyaluronic/gelatin sponge scaffolds, cultured in chondrogenic media for three weeks, and implanted into the excised lunate space of rabbits. After a 12 week *in vivo* period, the engineered cartilage had developed into an osteochondral tissue consisting of a peripheral cartilaginous layer surrounding a region of endochondral bone containing marrow space, which was mechanically functional for the duration of the experiment. This study emphasised the potential of utilising MSC-based cartilaginous grafts for the engineering of whole bones and joints.

Embryonic stem cell-based tissue engineering of bone through endochondral ossification was demonstrated by Jukes et al. (2008). In this study murine embryonic stem cells were seeded onto ceramic scaffolds and cultured chondrogenically for 21 days. Constructs were then implanted subcutaneously into immunodeficient mice and formed endochondral bone after 21 days *in vivo*. Figure 2.15 shows the time course of endochondral ossification where a cartilaginous template is gradually replaced by bone. Note evidence of cell viability after 2 days, hypertrophy after 7 days, and cartilage resorption/bone formation after 21 days. Another result of the study was that a cartilaginous template, and not just chondrogenically differentiated cells, was required for bone formation. Furthermore, articular chondrocytes cultured on ceramic particles and implanted *in vivo* were resistant to endochondral ossification.

Farrell et al. (2009) seeded human BM-MSCs onto collagen-gag scaffolds and primed them chondrogenically and osteogenically *in vitro* prior to subcutaneous implantation into nude mice. Osteogenically primed constructs showed increased

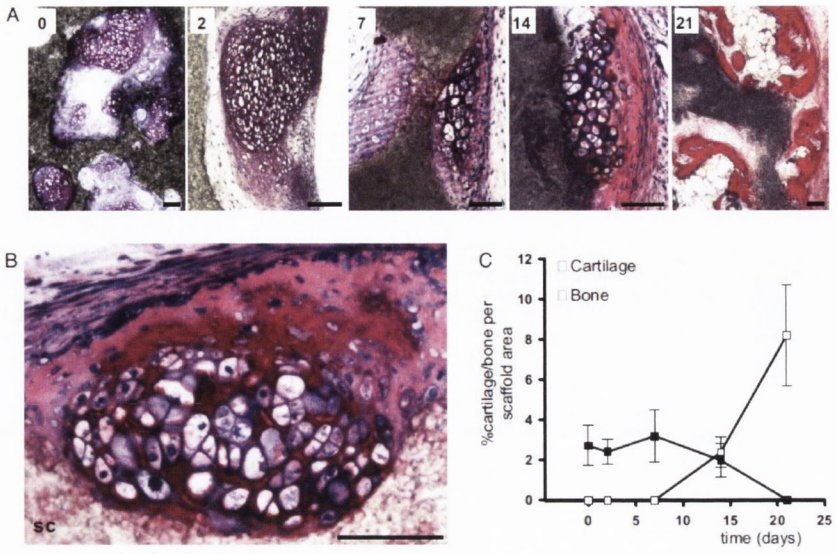

Figure 2.15.: *In vivo endochondral bone formation throughout time. (A) Histological sections of cartilaginous constructs 0, 2, 7, 14, and 21 days after implantation. Cartilage matrix is visualised by pink thionin staining of glycosaminglycans. Bone tissue is stained by methylene blue and basic fuchsin staining, which stains cells blue and bone tissue dark pink. (B) High magnification image after 14 days in vivo. (C) Histomorphometric analysis of the amount of cartilage and bone per available scaffold area in time*

(Jukes et al., 2008)

mineralisation, but poor cell viability with no vascularisation. Conversely, chondrogenically primed constructs did not mineralise, but had good cell viability with evidence of vascularisation. The authors postulated that the endochondral route was indeed being triggered in the chondrogenically primed constructs, but the *in vivo* time period (4 weeks) was not long enough for mineralisation to occur. A comparison of the angiogenic capacities of the two ossification mechanisms in a bone engineering context was also examined by Tortelli et al. (2010). Unprimed MSCs and osteoblasts were seeded onto ceramic scaffolds and implanted subcutaneously into nude mice. The results demonstrated that osteoblast-seeded constructs formed bone via intramembranous ossification whereas MSC-seeded constructs formed bone via endochondral ossification. Although bone was formed more rapidly through the intramembranous route, the endochondral route accelerated vascularisation and

recruitment of host endothelial cells.

The role of donor cells vs. host cells in endochondral bone tissue engineering is still unclear. It would be very attractive from a translational perspective to suggest that a hypertrophic cartilaginous template could recruit osteoprogenitor cells from the host to invade and mineralise the matrix, as this would open the possibility of a devitalised 'off the shelf' graft for implantation (Scotti et al., 2010). However, some studies have shown that donor cells do play a role in bone formation. Janicki et al. (2010) for example, demonstrated that chondrogenically primed human BM-MSCs seeded in fibrin/β-TCP scaffolds and implanted in nude mice formed bone of human origin with an organised haematopoietic environment. In generating tissue engineered bone *in vivo* through endochondral ossification, Farrell et al. (2011) noted that while osteoblasts in the deposited bone were almost entirely of host origin, osteocytes were of both donor and host origin, suggesting that donor cells do play a role in early bone formation. In the aforementioned study by Tortelli et al. (2010) tissue engineered constructs which underwent intramebranous ossification produced bone of donor origin whereas the constructs which underwent endochondral ossification produced bone of host origin, which may support the argument that a devitalised cartilaginous template could be used for bone repair. However, the authors also noted that the enhanced vascularisation in the endochondral constructs could be a result of the donor MSC mediated recruitment of host endothelial cells and blood vessels.

In vitro hypertrophic differentiation of chondrogenically primed MSCs can be stimulated by culture in the appropriate medium. Mueller and Tuan (2008) demonstrated that chondrogenically differentiated MSC pellets could be induced to undergo hypertrophy through the removal of TGF-β, the reduction of dexamethasone (from 100nM to 1nM), and the addition of triiodothyronine, with or without the addition of β-GP. This hypertrophic culture medium was utilised in a study by

Scotti et al. (2010) who cultured scaffold free human MSCs for 3 weeks in chondrogenic medium followed by 2 weeks in hypertrophic medium prior to subcutaneous implantation. These 'late hypertrophic' constructs formed tissue with a higher mineral volume and density compared to constructs which had not undergone an *in vitro* hypertrophic culture phase, and also displayed an interconnected network of trabeculae throughout the core of the construct. A number of the features typical of endochondral skeletogenesis, such as the formation of a bony collar surrounding trabecular bone and bone marrow foci, were recapitulated in this tissue engineering paradigm, though the scaffold-free tissues generated were quite small. Therefore, a follow-up study by Scotti et al. (2013) investigated the engineering of an up-scaled bone through endochondral ossification. To that end human BM-MSCs were seeded onto type I collagen meshes (⌀8 mm x 2 mm), cultured to undergo chondrogensis and subsequent hypertrophy, with additional supplementation of interleukin-1β to ensure efficient cartilage remodelling. The engineered tissues were then implanted into nude mice. Interestingly, the resultant engineered bone developed by two distinct mechanisms. The outer cortical-like bone developed by perichondral ossification, with host cells laying down bone over a pre-mineralised area. The inner trabecular-like bone developed by endochondral ossification, with donor cells forming bone over a cartilaginous template. Furthermore, the bone marrow generated in the up-scaled tissues reconstituted multilineage long-term hematopoiesis in lethally irradiated mice, thus demonstrating the functionality of the engineered organ. It should be noted however, that the central region of the *in vitro* engineered cartilage was devoid of cells and matrix, signifying the challenges in scaling-up engineered tissues to clinically relevant sizes, and highlighting the importance of utilising a suitable scaffold material when doing so.

An interesting approach to tissue engineering a 3D construct is utilising a biomaterial as an interim scaffolding system. Su et al. (2012) developed a 'living

hyaline cartilage graft' which was scaffold-free by culturing chondrocytes in an alginate hydrogel containing cavities for micro tissue nodule formation. Following extensive cartilaginous extra-cellular matrix formation, the alginate was removed by treatment with sodium citrate, with the 3D network anchored by neotissue formation within the original cavities remaining intact. This living cartilage graft was also evaluated *in vivo* as a template for bone formation, where osteogenesis was reported both with and without additional seeding with MSCs (Lau et al., 2012). Bone tissue engineering through endochondral ossification has also been demonstrated on MSC-seeded three dimensional electrospun fibers (Yang et al., 2013), and with the clonal murine cell line ATDC5 in conjunction with the bone void filler NuOss which validated the efficacy of the endochondral approach using a globally accessible, reproducible cell source (Weiss et al., 2012).

Recently, the capacity of adipose-derived stem cells, genetically modified to express either BMP-2 or TGF-β3, to promote calvarial bone defect repair when seeded within apatite-coated PLGA or gelatin scaffold were evaluated (Lin et al., 2013). Interestingly, though the BMP-2/PLGA and TGF-β3/gelatin combinations were initially selected due to their respective pro-osteogenic and pro-chondrogenic capabilities, the most effective bone healing occurred with BMP-2 expressing stem cells seeded within gelatin scaffolds, and this healing proceeded via endochondral ossification. Since most previous studies investigating MSCs for endochondral bone tissue engineering applications have used TGF-β3 to induce chondrogenesis (Scotti et al., 2010; Janicki et al., 2010; Farrell et al., 2011), this experiment highlighted the potential benefit of utilising BMP-2 in endochondral bone tissue engineering strategies.

2.7. Oxygen tension as a regulator of MSC differentiation

Oxygen is inhaled at an ambient tension of 20-21%. The partial pressure oxygen (pO_2) of the inhaled air then decreases successively as it enters the lungs and is distributed throughout the body via the blood, and by the time it has reached the organs and tissues of the body the levels have dropped to 2-9% pO_2 (Mohyeldin et al., 2010). Therefore, cells such as MSCs actually reside in stem cell niches of much lower oxygen levels than the normoxic levels in ambient air, see Figure 2.16. Despite this, most tissue engineering and regenerative medicine stratgies typically involve culturing MSCs at 20% pO_2, which places the cells in a non-physiological hyperoxygenated state.

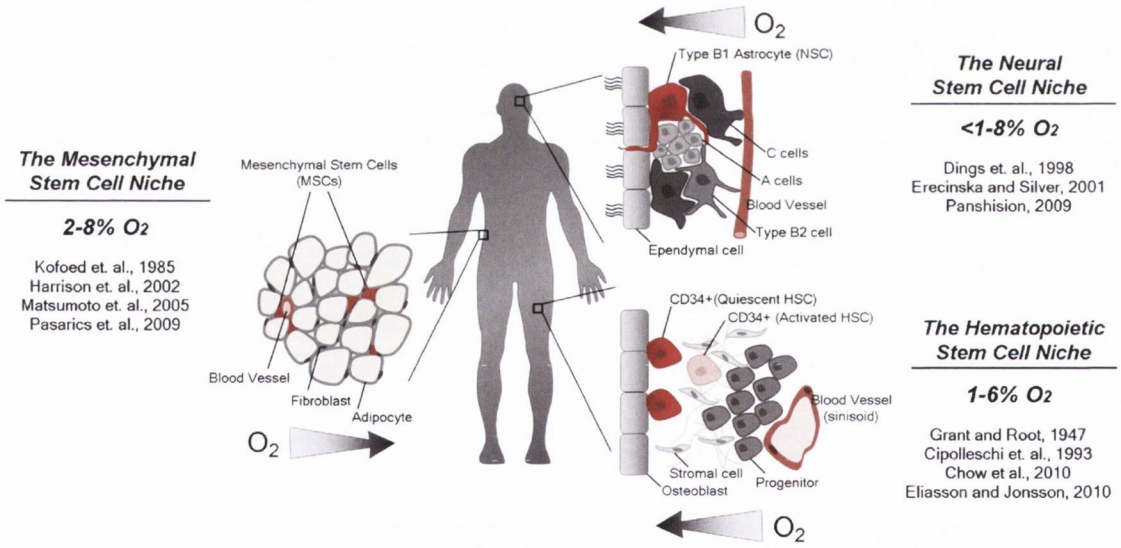

Figure 2.16.: *Low oxygen tension measurements in various stem cell compartments* (Mohyeldin et al., 2010)

Lennon et al. (2001) demonstrated that expanding rat BM-MSCs in low oxygen tension (5%pO_2) enhanced their proliferative capacity as well as their subsequent

in vitro osteogenesis and *in vivo* osteochondrogenesis. Other authors such as D'Ippolito et al. (2006) and Zscharnack et al. (2009) also reported increased MSC proliferation with expansion in a low oxygen environment, with Fehrer et al. (2007) demonstrating that MSCs expanded at 3% pO_2 had the ability to undergo 10 more population doublings, compared to MSCs cultured at 20% pO_2, prior to terminal growth arrest. The negative effect of culturing MSCs in normxic conditions has also been reported by Grayson et al. (2006) and D'Ippolito et al. (2006). Grayson et al. (2006) demonstrated that hypoxia maintained human MSCs in their stem cell niche with hypoxic cells expressing higher levels of stem cell genes compared to normoxic cells and also improved their subsequent differentiation potential. D'Ippolito et al. (2006) also demonstrated that low oxygen enhanced the stemness of MIAMI cells (a subpopulation of BM-MSCs), maintaining them in an undifferentiated state.

A number of studies have reported contrasting effects of low oxygen conditioning on the osteogenesis of MSCs. Hirao et al. (2006) and Fehrer et al. (2007) demonstrated that differentiation in a low oxygen environment, 5%pO_2 and 3%pO_2 respectively, inhibited osteogenesis in 2D culture. Volkmer et al. (2010) also found that differentiation in hypoxia inhibited osteogenesis, though this inhibition could be overcome by hypoxic pre-conditioning of MSCs during the expansion phase, highlighting that if tissue engineered constructs are to be subjected to hypoxic conditions *in vivo* it would be beneficial to first subject them to hypoxic conditions *in vitro*. The effect of differentiation in a low oxygen environment on the chondrogenesis of MSCs has been more conclusive, with increased chondrogenic capacity in low oxygen conditions reported in pellets (Khan et al., 2010; Ronzière et al., 2010), 2D culture (Hirao et al., 2006), and cell-seeded agarose constructs (Meyer et al., 2010; Buckley et al., 2010).

The effects of oxygen on the hypertrophic differentiation of MSCs has also been examined. Ronzière et al. (2010) demonstrated that differentiation of adipose

tissue derived MSCs in a low oxygen environment favoured a chondrogenic phenotype whereas cells differentiated at 20% pO_2 exhibited a hypertrophic phenotype. Hirao et al. (2006) showed that ALP activity was inhibited by low oxygen conditioning during the chondrogenic differention of the embryonic precursor cell line C3H10T1/2. Reactive oxygen species, which can be generated when cells are placed in a hyperoxygenated state, have also been shown to induce hypertrophy in chondrocytes (Morita et al., 2007).

From a tissue engineering perspective, the well documented increased proliferative effect of expansion in a low oxygen environment has obvious benefits as it could reduce the amount of time needed to obtain a clinically relevent number of cells. There are many contrasting results reported on the effect that low oxygen conditioning has on osteogenic differentiation, which can partially be explained by differences in cell isolation methods, oxygen levels applied (2%, 3%, 5%), growth factor combinations and cell sources used. Since bone is vascularised and cartilage is not, oxygen has been suggested as having a regulatory effect on the osteogenic and chondrogenic differentiation of MSCs, as higher levels of oxygen are present in bone, see Figure 2.17. The process of endochondral ossification is characterised by a gradient increase in oxygen (Ma et al., 2009), see Figure 2.18, and it has been suggested by Gawlitta et al. (2010), in a review examing the modulation of BM-MSCs for endochondral bone tissue engineering applications, that oxygen levels *in vitro* can be augmented to promote a suitable endochondral construct for implantation, i.e. hypoxia can be imposed to stimulate rapid formation of cartilaginous matrix, followed by normoxia to allow regular transition to hypertrophy.

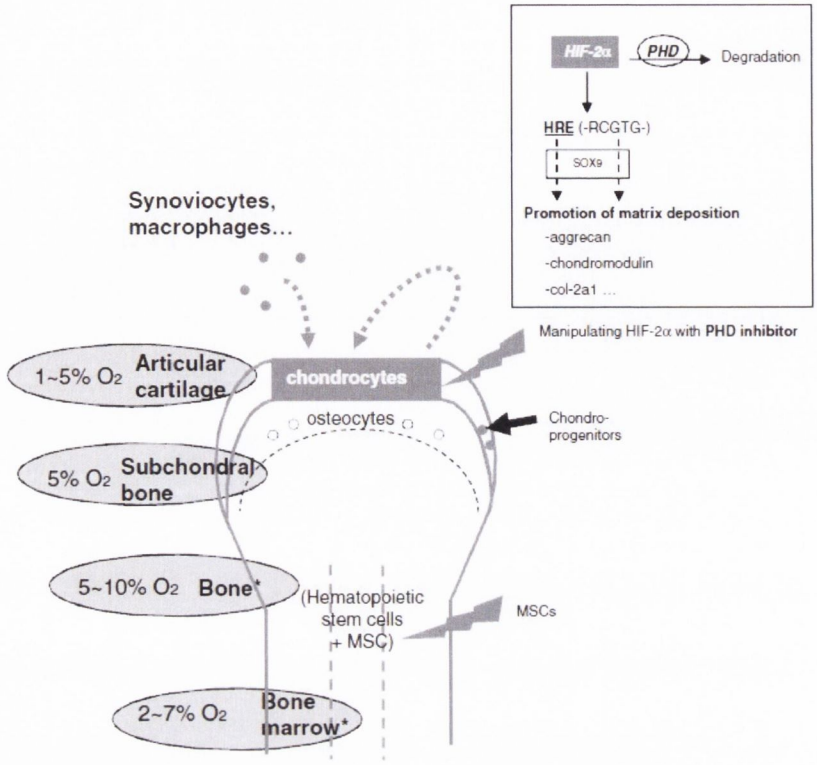

Figure 2.17.: *Levels of oxygen in the surrounding tissues of joints*

(Lafont, 2010)

2.8. Summary

This literature review has demonstrated that the traditional intramembranous approach to bone tissue engineering, involving the direct osteogenic priming of MSC-based constructs, suffers from certain limitations and may be unsuitable as a strategy to regenerate whole bones. It is also clear from the literature that chondrogenically primed MSCs to fail to generate a stable cartilage resistant to hypertrophy and endochondral ossification, and therefore do not currently present an alternative to chondrocytes for the engineering of articular cartilage. This apparent obstacle in MSC-based cartilage repair therapies has been realised as a potential advantage in bone regeneration strategies, with chondrogenically primed

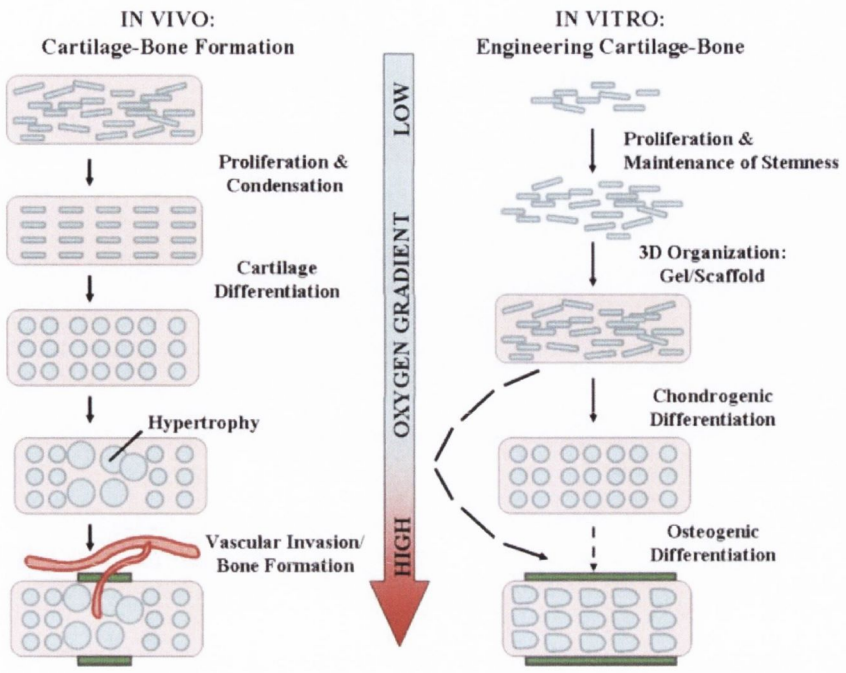

Figure 2.18.: *The influence of oxygen tension during bone-cartilage tissue formation* (Ma et al., 2009)

MSCs being utilised to engineer bone by recapitulating the process of endochondral ossification. Hydrogels have been identified as a suitable scaffolding material for endochondral bone regeneration strategies as they are capable of supporting chondrogenesis and hypertrophy of MSCs *in vitro*, and can facilitate bone formation *in vivo*. Moreover, they are an attractive scaffolding material for the scaling-up of engineered tissues to clinically relevant sizes, particularly when optimised with bioreactor culture or through modification of scaffold architecture. Hydrogels have also been shown capable of generating anatomically accurate osteochondral constructs in the shapes of different joints and bones. The literature would also suggest that it may be possible to regulate the phenotype of MSCs within such hydrogels by controlling the oxygen tension.

In light of this review on the appropriate literature, it is hypothesised that oxygen tension can regulate the phenotype of MSCs for use in endochondral bone regen-

eration strategies. It is further hypothesised that large homogenous cartilaginous tissue can be engineered through a combination of rotational culture and modified scaffold architecture *in vitro*, and that modifying the architecture of an engineered hypertrophic cartilaginous graft will accelerate vascularisation and endochondral ossification *in vivo*. It is also hypothesised that an osteochondral construct can be engineered by implanting chondrogenically primed by-layered hydrogels, containing chondrocytes and MSCs, and spatially regulating endochondral ossification *in vivo*. Finally, the capacity of various MSC-seeded hydrogels to generate endochondral bone will be compared and the most suitable hydrogel will be utilised in an attempt to generate an anatomically accurate bone through endochondral ossification, as a paradigm for whole bone tissue engineering.

3 In vitro environmental conditions for engineering hypertrophic cartilage

3.1. Introduction

Understanding how environmental factors regulate MSC fate during *in vitro* expansion and differentiation is critical for developing new therapies for tissue repair. The local oxygen environment has been shown to be a key modulator of MSC phenotype (Mohyeldin et al., 2010). Motivated by the fact that bone is vascularised and cartilage is not, oxygen tension has been proposed as a regulatory factor in determining osteogenic or chondrogenic differentiation (Merceron et al., 2010). In current tissue engineering or regenerative medicine strategies MSCs are typically expanded and differentiated in "normoxic" conditions (20% pO_2). However, *in vivo* MSCs reside in stem cell niches of lower oxygen levels (1-7% pO_2) (Grant and Smith, 1963; Kofoed et al., 1985; D'Ippolito et al., 2006) and therefore the normoxic conditions applied during *in vitro* expansion and differentiation place MSCs in a non-physiological hyperoxygenated state (Grayson et al., 2006). Physiological oxygen tensions in bone have been shown to be between 5-12.5% pO_2 but can

reduce to 1% pO_2 in a fracture hematoma (Brighton and Krebs, 1972; Heppenstall et al., 1975; Potier et al., 2007; Lafont, 2010) whereas physiological oxygen levels in articular cartilage are 1-5% pO_2 (Lafont, 2010). Previous studies have demonstrated that expansion at 5% pO_2 enhances subsequent osteogenesis (Lennon et al., 2001) and chondrogenesis (Zscharnack et al., 2009) of bone marrow derived MSCs. Furthermore, differentiation at 5% pO_2 has been shown to enhance chondrogenesis of MSCs (Kanichai et al., 2008; Robins et al., 2005) and the functional properties of cartilaginous tissues engineered using infrapatellar fat pad (Buckley et al., 2010), and bone marrow (Meyer et al., 2010), derived MSCs .

A major challenge in cartilage tissue engineering using MSCs is the prevention of hypertrophic and terminal differentiation (Gawlitta et al., 2010). When implanted subcutaneously in nude mice chondrogenically primed MSCs fail to produce stable cartilage resistant to vascularisation and calcification (Pelttari et al., 2006; Dickhut et al., 2009). Recently, this obstacle in cartilage tissue engineering has been realised as a potential benefit in bone tissue engineering with chondrogenically primed bone marrow derived MSCs being used to produce bone *in vivo* via endochondral ossification (Janicki et al., 2010; Scotti et al., 2010; Farrell et al., 2011). What is clear is that regulation of the hypertrophic phenotype of MSCs is critical when attempting to engineer cartilage or endochondral bone. The embryonic endochondral ossification process is characterised by blood vessels infiltrating cartilaginous martix thus increasing the oxygen levels in the tissue (Ma et al., 2009) and a low oxygen tension has previously been demonstrated to suppress hypertrophy of adipose tissue derived MSCs (Ronzière et al., 2010) and of the embryonic precursor cell line C3H10T1/2 (Hirao et al., 2006).

Clearly oxygen tension is a key regulator of stem cell fate, playing a key role not only in determining the initial differentiation pathway of the cell, but also possibly its terminal phenotype. In spite of the growing body of work demonstrating the

importance of this stimulus in regulating stem cell differentiation, it is still unclear if the local oxygen tension regulates plasticity during stem cell expansion and whether specific oxygen tensions preferentially support certain phenotypes during differentiation. The objective of this study is to explore the role of oxygen tension during both expansion and differentiation on the proliferation kinetics and the subsequent osteogenic and chondrogenic potential of bone marrow derived MSCs. It is first hypothesised that expanding MSCs in a physiological or low oxygen tension (5% pO_2) would improve their subsequent potential to differentiate along either the osteogenic or chondrogenic route compared to expansion in normoxic conditions (20% pO_2). It is further hypothesised that chondrogenic differentiation in a low oxygen environment would suppress hypertrophy of MSCs. As part of this study, MSCs will be directed along the chondrogenic pathway in both agarose hydrogels and using the traditional pellet culture system to investigate if the extracellular environment of the cell influences its response to altered oxygen tensions. If the local oxygen environment can be manipulated to regulate chondrogenesis and hypertrophy within MSC-seeded scaffolds or hydrogels, it may facilitate the engineering of functional cartilaginous grafts for both articular cartilage, and endochondral bone, regeneration strategies.

3.2. Materials and methods

3.2.1. Experimental design

Cells were expanded in expansion medium at either 20% or 5% pO_2 in order to investigate the effect of oxygen tension on the Colony Forming Unit - fibroblastic (CFU-f) potential and proliferation kinetics of MSCs. To examine osteogenesis, passage 2 (P2) MSCs were subsequently seeded in 6 well plates and cultured in osteogenic medium for 14 days at either 20% or 5% pO_2. To examine chondrogenesis,

P2 MSCs were pelleted and cultured in chondrogenic medium for 21 days at either 20% or 5% pO_2. Additionally P2 MSCs were encapsulated in 2% agarose hydrogels and cultured in chondrogenic medium for 42 days at either 20% or 5% pO_2.

3.2.2. Cell isolation and expansion

Bone marrow derived MSCs were isolated aseptically from the femoral shafts of four pigs and expanded according to a modified method developed for human MSCs (Lennon and Caplan, 2006) in DMEM GlutaMAX supplemented with 10% v/v fetal bovine serum (FBS) and 100 U/ml penicillin - 100 μg/ml streptomycin (Expansion Medium) (all Gibco, Biosciences, Dublin, Ireland) at either 20% or 5% pO_2. The media was replaced twice weekly. Following colony formation MSCs were trypsinised, counted, seeded at a density of 5 x 10^3 cells/cm^2 and expanded to P2 at either 20% or 5% pO_2. Cells from each donor were kept separate for all experiments.

3.2.3. CFU-f assay and proliferation kinetics

Freshly isolated porcine MSCs were seeded in 100 mm diameter petri dishes at a density of 50 x 10^3 mononuclear cells (MNCs)/cm^2 and maintained in expansion medium at either 20% or 5% pO_2. After 10 days expanded cells were fixed with 2% paraformaldehyde and stained with crystal violet. The number of colonies from each dish were counted in order to calculate the colony forming unit efficiency of the cells. In addition the diameter of the 10 largest colonies from each dish was calculated using ImageJ software (Rasband, W.S., Image J, U.S National Institutes of Health, Bethesda, Maryland, USA, http://imagej.nih.gov/ij/, 1997-2011).

To examine proliferation kinetics, freshly isolated MSCs were seeded in T-25 flasks at a density of 50 x 10^3 MNCs/cm^2 and expanded at either 20% or 5% pO_2. At days 7, 9, 12 and 14 of expansion, cells were trypsinised and counted using a

haemacytometer and 0.4% trypan blue. After colony formation (P0), cells were replated at a density of 5 x 10^3 MSCs/cm^2, expanded at either 20% or 5% pO_2 and counted at days 2, 4 and 7 of expansion.

3.2.4. Osteogenesis

P2 MSCs were seeded in 6 well plates at a density of 3 x 10^3 MSCs/cm^2 and maintained in expansion medium at either 20% or 5% pO_2. Cells were allowed to adhere for 24 hours, after which they were supplemented with β-Glycerophosphate (20 μg/ml), dexamethasone (100 nM) and L-ascorbic acid-2-phosphate. Negative controls were also maintained in parallel. The culture medium was replaced twice a week for a period of 14 days.

3.2.5. Chondrogenesis in pellets

250,000 P2 MSCs were pelleted by centrifugation at 650g. Pellets were maintained in a chondrogenic medium consisting of DMEM GlutaMax supplemented with penicillin (100 U/ml) - streptomycin (100 μg/ml) (both Gibco), 100 μg/ml sodium pyruvate, 40 μg/ml L-proline, 50 μg/ml L-ascorbic acid-2-phosphate, 1.5 mg/ml bovine serum albumin, 1 x insulin-transferrin-selenium, 100 nM dexamethasone, 2.5μg/ml amphotericin B (all from Sigma-Aldrich, Dublin, Ireland) and 10 ng/ml recombinant human transforming growth factor-β3 (TGF-β3; Prospec-Tany Techno-Gene Ltd, Israel) at either 20% or 5% pO_2. The culture medium was replaced twice weekly with discarded media stored at -80°C for further analysis.

3.2.6. Chondrogenesis in agarose hydrogels

MSCs (P2) were suspended in 2% agarose (type VII; Sigma-Aldrich) at a density of 15 x 10^6 MSCs/ml. The agarose cell suspension was cast in a stainless steel

mould and cored using a biopsy punch to produce construct cylinders (⌀5 x 3 mm). Constructs were maintained in chondrogenic medium at either 20% or 5% pO2 for a period of 42 days. The culture medium was replaced twice weekly with discarded media stored at -80°C for further analysis.

3.2.7. Biochemical analysis

Deposited matrix from osteogenically treated wells was digested in 1M hydrochloric acid at 60° C and 10 rpm for 18 hours. The calcium content was determined using a Sentinel Calcium kit (Alpha Laboratories Ltd, UK). Pellets and agarose constructs were digested with papain (125 μg/ml) in 0.1 M sodium acetate, 5mM L-cysteine-HCL, 0.05 M EDTA, pH 6.0 (all from Sigma-Aldrich) at 60°C and 10 rpm for 18 hours. DNA content was quantified using the Hoechst Bisbenzimide 33258 dye assay, with a calf thymus DNA standard. Proteoglycan content was estimated by quantifying the amount of sulphated glycosaminoglycan (sGAG) using the dimethylmethylene blue dye-binding assay (Blyscan, Biocolor Ltd., Northern Ireland), with a chondroitin sulphate standard. Total collagen content was determined by measuring the hydroxyproline content, using a hydroxyproline-to-collagen ratio of 1:7.69 (Ignat'eva et al., 2007). Briefly, samples were mixed with 38% hydrochloric acid (Sigma-Aldrich) and incubated at 110°C for 18 hours to allow hydrolysis to occur. Thereafter samples were dried in a fume hood overnight and the sediment re-suspended in ultra pure H_2O. Chloramine T and 4-(Dimethylamino)benzaldehyde (both Sigma-Aldrich) reagents were added and the hydroxyproline content quantified with a trans-4-Hydroxy-L-proline (Fluka analytical) standard using a Synergy HT (BioTek Instruments, Inc) multi-detection micro plate reader at a wavelength of 570 nm. Alkaline phosphatase (ALP) activity in the media (n=3) was measured using a Sensolyte pNPP Alkaline Phosphatase assay kit (Cambridge Biosciences, UK) with a calf intestine ALP standard.

3.2.8. Histology and Immunohistochemistry

At the final time point of experiments, samples were fixed in 4% paraformaldehyde overnight, dehydrated in a graded series of ethanols, embedded in paraffin wax, sectioned at 5 μm and affixed to microscope slides. The sections were stained with 1% alcian blue 8GX in 0.1 M HCL to assess sGAG content, picro-sirius red to assess collagen distribution, and 1% alizarin red to assess calcium accumulation (all Sigma-Aldrich). Sections stained with alcian blue were counter-stained with nuclear fast red to assess cellular distribution. Collagen types I, II and X were evaluated using a standard immunohistochemical technique; briefly, sections were treated with peroxidase, followed by treatment with chondroitinase ABC (Sigma-Aldrich) in a humidified environment at 37° C to enhance permeability of the extracellular matrix. Sections were incubated with goat serum to block non-specific sites and collagen type I (ab6308, 1:400; 1 mg/mL), collagen type II (ab3092, 1:100; 1 mg/mL) or collagen type X (ab49945, 1:200; 1.4 mg/mL) primary antibodies (mouse monoclonal, Abcam, Cambridge, UK) were applied for 1 hour at room temperature. Next, the secondary antibody (Anti-Mouse IgG biotin conjugate, 1:200; 2.1 mg/mL) (Sigma-Aldrich) was added for 1 hour followed by incubation with ABC reagent (Vectastain PK-400, Vector Labs, Peterborough, UK) for 45 min. Sections were rinsed in PBS for 5 min between each step. Finally sections were developed with DAB peroxidase (Vector Labs) for 5 min. Ligament, articular cartilage, and growth plate cartilage sections were included as postive controls for collagen type I, collagen type II, and collagen type X immunohistochemistry staining respectively. Articular cartilage, ligament, and articular cartilage sections were included as negative controls for collagen type I, collagen type II, and collagen type X immunohistochemistry staining respectively.

3.2.9. Statistical analysis

All statistical analyses were carried out using Minitab 15.1. Results are reported as mean ± standard deviation. Groups were analysed by a general linear model for analysis of variance with groups of factors. Tukey's test was used to compare conditions. Anderson-Darling normality tests were conducted on residuals to confirm a normal distribution. Nonnormal data was transformed using the Box-Cox procedure. Any nonnormal data which the Box-Cox procedure could not find a suitable tranformation for was transformed using the Johnson procedure. Significance was accepted at a level of $p<0.05$.

3.3. Results

3.3.1. Oxygen tension regulates the proliferation of MSCs

No statistical differences were found in the CFU-f of cells expanded at 5% or 20% pO_2, see Figure 3.1 (A,B). However expansion at 5% pO_2 significantly increased the colony diameter of cells compared to expansion at 20% pO_2 (4.69 ± 0.59 mm vs. 3.3 ± 0.46 mm; $p<0.001$), see Figure 3.1 (A,C). Expansion at 5% pO_2 significantly increased the cell yield obtained at days 7, 9 and 14 culminating in a total cell yield at day 14 of 2.05 ± 0.62 (x 10^6) cells for the 5% pO_2 group compared to 0.86 ± 0.36 (x 10^6) cells for the 20% pO_2 expansion group, see Figure 3.1 (D). When cells were replated after 1 passage no significant differences were found between oxygen groups, see Figure 3.1 (E).

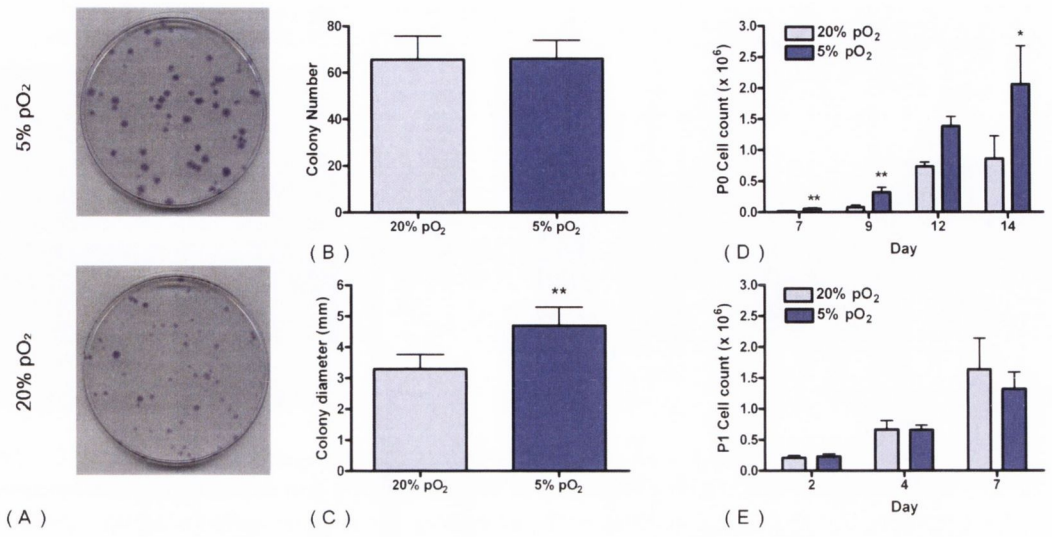

Figure 3.1.: *Oxygen tension regulates the proliferation of MSCs. (A) Images of CFU-f assays for MSCs expanded at 5% or 20% pO_2. (B) No. of colonies calculated from CFU-f assay. (C) Diameter of 10 largest colonies from CFU-f assay. (D) Cell yield of MSCs seeded fresh and expanded at 5% or 20% pO_2. (E) Cell yield of MSCs passaged once and expanded at 5% or 20% pO_2. *$p<0.05$, **$p<0.001$, vs. expansion at 20% pO_2*

3.3.2. Expansion in a low oxygen environment enhances the osteogenic potential of MSCs

For MSCs expanded at 20% pO_2, calcium accumulation was higher for cells subsequently differentiated at 5% pO_2 compared to 20% pO_2. Calcium accumulation was further increased, reaching 223.68 ± 81.47 μg, if MSCs were both expanded and differentiated at 5% pO_2, see Figure 3.2 (A). Of all groups, cells expanded and differentiated at 20% pO_2 accumulated the least amount of calcium, as also evidenced by alizarin red staining, see Figure 3.2 (B).

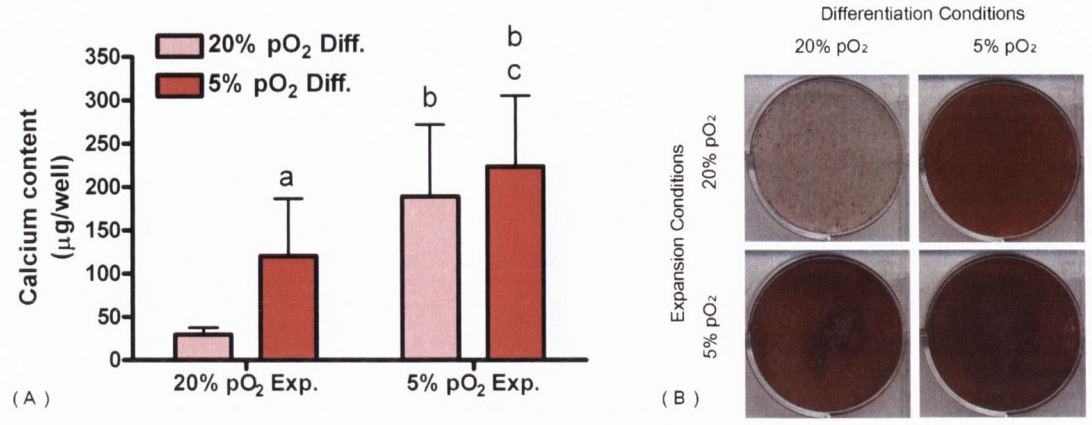

Figure 3.2.: *Expansion in a low oxygen environment enhances the osteogenic potential of MSCs. (A) Calcium deposition of MSCs expanded at 20% or 5% pO_2 and subsequently differentiated at 20% or 5% pO_2 (2 donors, n=3 per donor). (B) Alizarin Red staining. $p<0.05$, (a) compared to opposite differentiation condition (b) compared to opposite expansion condition (c) compared to opposite differentiation and opposite expansion condition.*

3.3.3. Oxygen tension differentially regulates collagen synthesis of MSCs during chondrogenesis in pellets and hydrogels

When MSCs were expanded at either 5% pO_2 or 20% pO_2, differentiation at 5% pO_2 significantly enhanced sGAG accumulation in both pellets (Figure 3.3(A)) and hydrogels (Figure 3.3(C)). In pellet culture, collagen accumulation following differentiation at 20% pO_2 was significantly higher than differentiation at 5% pO_2, see Figure 3.3(B). Expansion at a low oxygen tension had no significant effect on the biochemical content of pellets. In hydrogel culture, by day 42, collagen accumulation following differentiation at 5% pO_2 was significantly higher than differentiation at 20% pO_2, see Figure 3.3(D). Expansion at a low oxygen tension had no significant effect on collagen accumulation, with the exception of day 42, where expansion at 5% pO2 significantly increased collagen accumulation of constructs subsequently differentiated at 20% pO_2.

Pellets differentiated at 5% pO_2 appeared larger and stained strongly for alcian

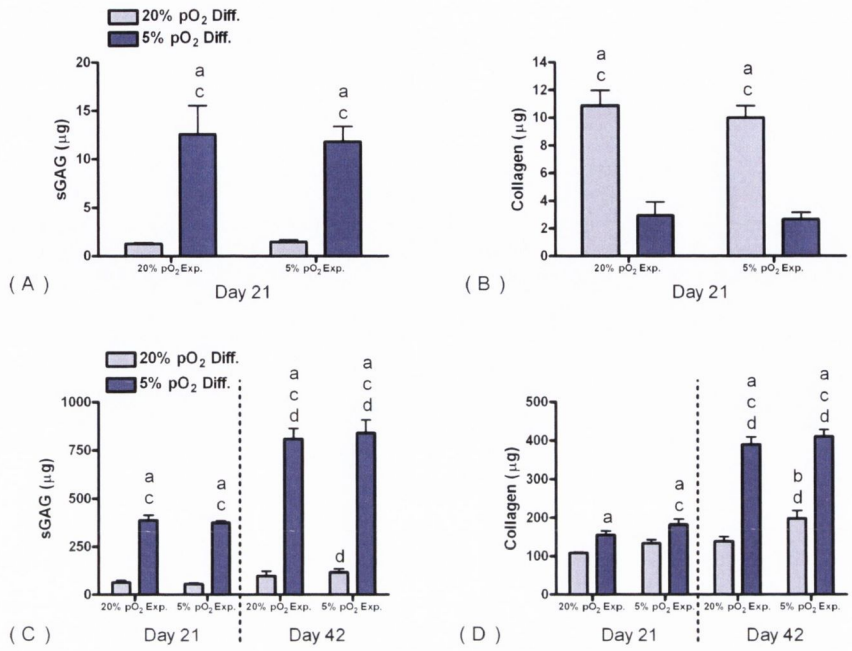

Figure 3.3.: *Oxygen tension differentially regulates collagen synthesis of MSCs during chondrogenesis in pellets and hydrogels. (A-D): sGAG and collagen accumulation in pellets (A,B) and hydrogels (C,D) for MSCs expanded (Exp.) at 20% or 5% and subsequently differentiated (Diff.) at 20% or 5% pO_2. n=3-4. $p<0.05$, (a) vs. opposite differentiation condition, (b) vs. opposite expansion condition, (c) vs. opposite differentiation and expansion condition, (d) vs. day 21.*

blue, whereas differentiation at 20% pO_2 resulted in smaller pellets that stained strongly for picro-sirius red, see Figure 3.4(A). Hydrogels differentiated at 5% pO_2 showed increased alcian blue and picro-sirius red staining compared to constructs differentiated at 20% pO_2, see Figure 3.4(B). Differentiation at 5% pO_2 also produced a more homogenous sGAG distribution in hydrogels.

3.3.4. Oxygen tension regulates the hypertrophic phenotype of chondrogenically primed MSCs

MSC pellets undergoing chondrogenic differentiation at 5% pO_2 demonstrated reduced alizarin red, collagen I and collagen X staining compared to pellets differen-

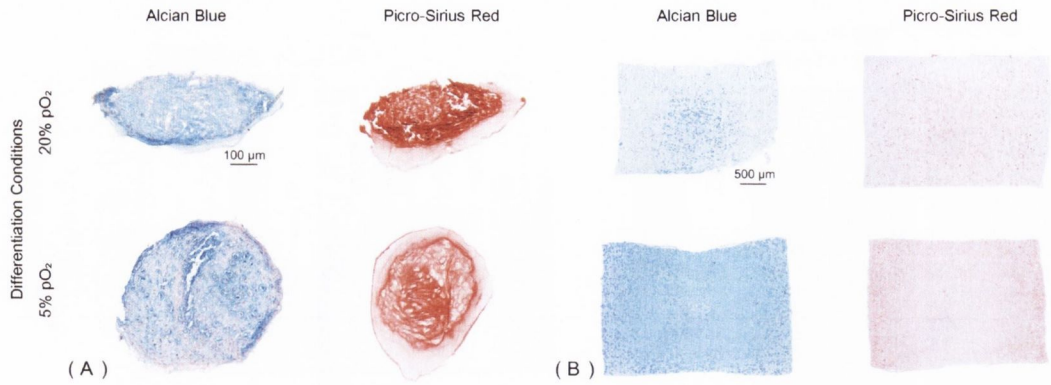

Figure 3.4.: *Alcian blue and picro-sirius red staining for MSC pellets (A) and hydrogels (B) differentiated at 20% or 5% pO_2 following expansion at 5% pO_2. n=1-2.*

tiated at 20% pO_2, see Figure 3.5 (A). Increased collagen II staining was observed in pellets differentiated at 5% pO_2. Cell-seeded agarose hydrogels maintained at 20% pO_2 stained homogenously for alizarin red, while staining was confined to the periphery of constructs maintained at 5% pO_2, see Figure 3.5 (B). Collagen type I and collagen type X staining was generally peri-cellular at both oxygen tensions, but appeared to co-localise to regions of greater alizarin red staining, i.e. confined to the periphery of constructs maintained at 5% pO_2. Furthermore, hydrogels maintained at 5% pO_2 demonstrated increased collagen II staining.

When MSCs were expanded at 20%pO_2, alkaline phosphatase actvity in the media during the first three weeks of culture was significantly higher for pellets (300.07 ± 16.1 ng vs. 65.68 ± 7.25 ng; $p<0.001$), and cell seeded hydrogels (817.48 ± 14.35 ng vs. 683.77 ± 18.81 ng; $p<0.01$), maintained at 20% pO_2 compared to 5% pO_2. Similar results were obtained when MSCs were expanded at 5%pO_2.

3.4. Discussion

This study demonstrates that oxygen tension plays a key role in regulating not only the proliferation kinetics of bone marrow derived MSCs, but also their subsequent

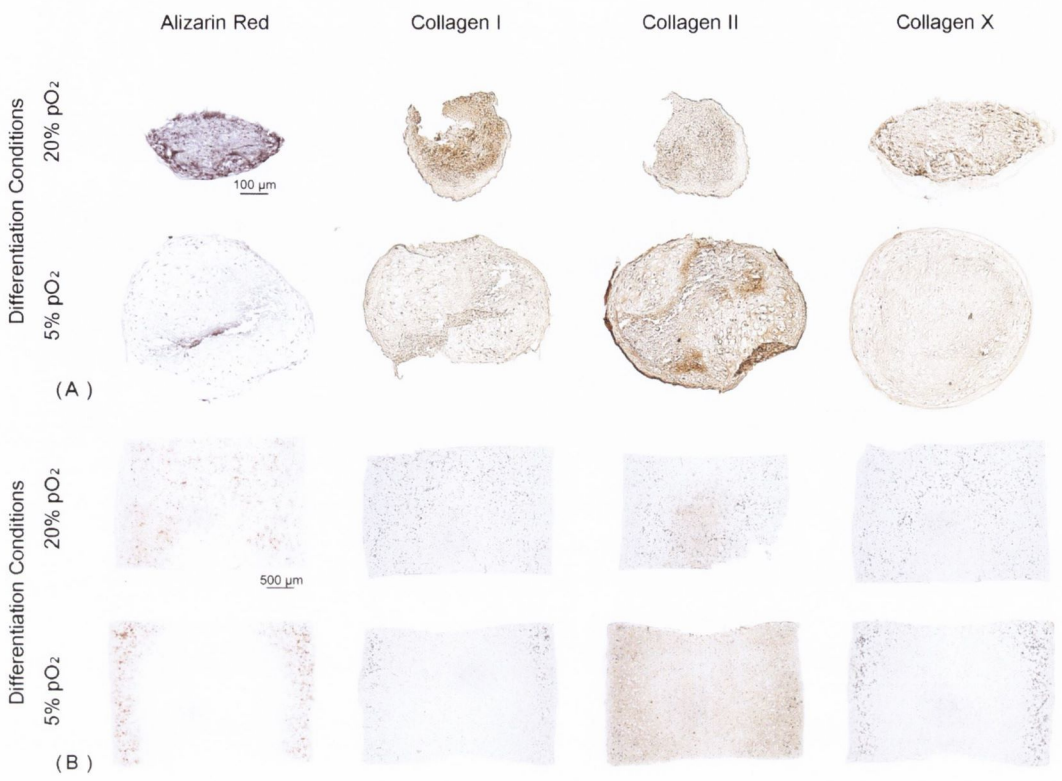

Figure 3.5.: *Oxygen tension regulates the hypertrophic phenotype of chondrogenically primed MSCs. (A-B): Alizarin Red and Collagen types I, II and X staining for MSC pellets (A) and hydrogels (B) differentiated at 20% or 5% pO_2 following expansion at 5% pO_2. n=1-2 for histology/immunohistochemistry*

osteogenic and chondrogenic potential as well as the inherent tendency of chondrogenically primed MSCs to proceed towards terminal differentiation. Expansion at a low oxygen tension was found to accelerate proliferation of freshly isolated MSCs, as demonstrated by the formation of larger colonies and the attainment of higher cell yields. Expansion at a low oxygen tension also enhanced the osteogenic capacity of MSCs, with cells expanded at 5% pO_2 accumulating significantly more calcium compared to cells expanded at 20% pO_2. Differentiation of MSCs at a low oxygen tension was found to be a more potent regulator of chondrogenesis than expansion at low oxygen tension. Pellets and cell seeded hydrogels maintained at 5% pO_2 accumulated significantly more sGAG, although the influence of oxygen tension on

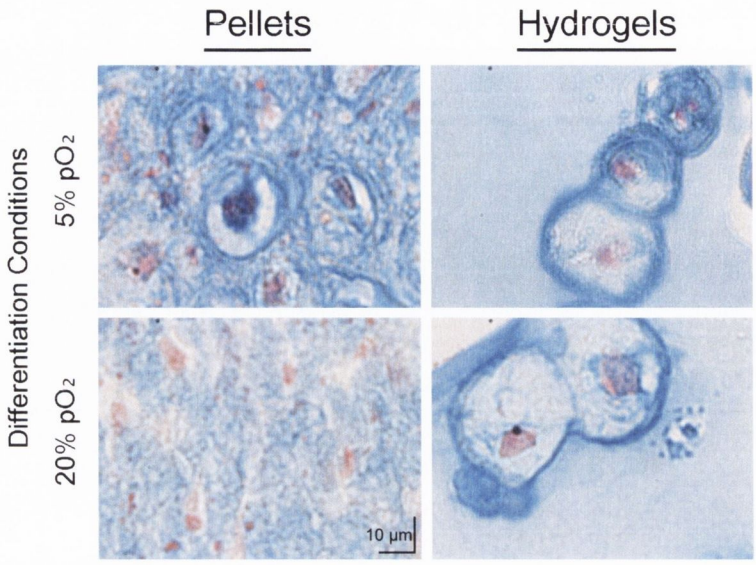

Figure 3.6.: *High magnification image of Alcian Blue staining for MSC pellets and hydrogels differentiated at 20% or 5% pO_2 following expansion at 5% pO_2.*

total collagen synthesis was dependant on whether MSCs were maintained in pellets or hydrogels. Differentiation at 5% pO_2 suppressed markers of fibroblastic (collagen type I straining) and hypertrophic differentiation (collagen type X staining, ALP activity), and reduced mineralisation (alizarin red staining) for both pellets and hydrogels and supported a more chondrogenic phenotype (collagen type II staining).

A number of studies reported in the literature have examined the effects of low oxygen conditioning on the proliferation of MSCs. The results of this study agree with the findings of Lennon et al. (2001) and D'Ippolito et al. (2006) which demonstrated an increased cell yield with low oxygen expansion using rat bone marrow derived MSCs and human MIAMI cells respectively. Zscharnack et al. (2009) also observed larger CFU-f colony diameters at low oxygen tensions, though the current study did not demonstrate increased colony numbers, as has been observed in other studies (Grayson et al., 2006) which may imply that during this study isolation and expansion at a low oxygen tension was not selecting for an alternative cell type.

There are a number of contrasting reports in the literature on the effect of oxygen tension during the *in vitro* osteogenic differentiation of MSCs, which can possibly be explained, at least in part, by the varying species, cell types and oxygen levels used in different studies. The results of this study agree with the findings of Lennon et al. (2001) that low oxygen conditioning (5% pO_2) during expansion and differentiation enhances osteogenesis of bone marrow derived MSCs. Of the studies which demonstrated that differentiation in a low oxygen environment inhibits osteogenesis of bone marrow derived MSCs (D'Ippolito et al., 2006; Fehrer et al., 2007) an oxygen tension of 3% pO_2 was used. Another study demonstrated that inhibition of osteogenic differentiation of MSCs occurs at 2% pO_2 unless cells are pre-conditioned to this oxygen level during the expansion phase (Volkmer et al., 2010). Since physiological oxygen levels in bone have been shown to be between 5 and 12.5% pO_2, a lower oxygen tension may be unable to facilitate direct osteoblastic differentiation. The hypoxic conditions experienced by MSCs *in vivo* during fracture repair and embryonic long bone development would appear to promote the formation of bone via endochondral rather that direct intramembranous ossification. The fact that 20% pO_2 is also outside these physiological levels may explain the reduced osteogenesis at this oxygen tension observed in the current study. Of the other studies which have demonstrated reduced osteogenic differentiation at 5% pO_2, adipose tissue derived MSCs (Merceron et al., 2010) and C3H10T1/2 cells (Hirao et al., 2006) were used, suggesting that the local oxygen tension has differential effects on MSCs from different sources.

Previous studies have also shown that maintenance in a low oxygen environment enhances chondrogenesis of bone marrow derived MSCs (Kanichai et al., 2008; Khan et al., 2010; Meyer et al., 2010), infra-patellar fat pad derived MSCs (Buckley et al., 2010), adipose tissue derived MSCs (Ronzière et al., 2010) and embryonic stem cells (Koay and Athanasiou, 2008). In the current study, it was observed

that oxygen tension differentially regulates collagen synthesis of MSCs undergoing chondrogenesis in pellets and hydrogels. This may be due to differences in cell morphology between the two different culture environments. MSCs encapsulated in hydrogels demonstrated a spherical morphology at both 20% and 5% pO_2, which is is known to support the chondrogenic phenotype. When MSCs were maintained in pellet culture, cells differentiated at 5% pO_2 appeared to be surrounded by a more spherical chondron, see Figure 3.6. A less spherical, more elongated, cellular morphology may be indicative of a more fibroblastic phenotype synthesising higher levels of type I collagen. The mechanism by which a lower oxygen tension ultimately leads to changes in cell shape is presently unclear.

The process of *in vivo* endochondral ossification is characterised intially by MSC condensation and chondrogenic differentiation at a low oxygen tension, followed by hypertrophic differentiation, vascularisation and mineralisation at a higher oxygen tension (Kronenberg, 2003; Ma et al., 2009). In this study it was demonstrated that differentiation in a low oxygen environment suppresses ALP activity and collagen X synthesis (both markers of hypertrophy) in pellets and hydrogels. Suppressing hypertrophy is a critical step in the successful development of stem cell based therapies for cartilage repair as maintenance of a chondrogenic phenotype must be achieved in order to ensure long-term *in vivo* stability (Pelttari et al., 2006). Further studies are required to better understand the molecular mechanisms by which a low oxygen microenvironment suppresses terminal differentiation of chondrogenically primed MSCs.

3.5. Concluding remarks

Bone marrow derived MSCs reside in stem cell niches of low oxygen and it has been previously demonstrated that *in vitro* expansion at a low oxygen tension

helps maintain their stemness (D'Ippolito et al., 2006; Grayson et al., 2006) and improve their subsequent differentiation potential (Lennon et al., 2001; Zscharnack et al., 2009). This chapter demonstrated that expansion at a low oxygen tension enhances subsequent osteogenesis of BM-MSCs, but has little effect on subsequent chondrogenesis. Therefore, expansion at a low oxygen tension will not be utilised in later chapters of this thesis. This chapter also showed that through manipulation of the *in vitro* oxygen environment of BM-MSCs during differentiation, it is possible to promote a chondrogenic phenotype for use in cartilage tissue engineering applications, or alternatively to promote a hypertrophic phenotype in order to repair bone via endochondral ossification. Chapters 5, 7 and 8 will utilise this switch in oxygen tension to promote chondrogenesis and then hypertrophy of cartilaginous grafts prior to implantation. Foremost however, strategies to scale-up these cartilaginous grafts will first be required. Chapter 4 will investigate if large, homogeneous, cartilaginous tissues can be engineered through a combination of modified scaffold architecture and rotational culture.

4 Strategies to engineer large cartilaginous tissues

4.1. Introduction

Articular cartilage has a limited capacity for repair. Cell-based therapies for cartilage regeneration, such as autologous chondrocyte implantation (ACI), provide a durable symptomatic relief and partial structural repair (Brittberg et al., 1994; Peterson et al., 2000). However, not all clinical data provide evidence that ACI is more effective than other conventional techniques, such as microfracture, in treating cartilage defects (Ruano-Ravina and Jato Diaz, 2006). Variations on ACI, such as matrix-assisted chondrocyte implantation (MACI), where cells are seeded or expanded on a scaffold prior to implantation, have also been in clinical use for a number of years. MRI assessment of cartilage repair has revealed a more hyaline-like zonal architecture following MACI compared to microfracture (Welsch et al., 2008) and recent studies have also highlighted advantages of MACI compared to ACI (Basad et al., 2010; Genovese et al., 2011). However, the repair tissue found with both procedures is still at best hyaline-like (Getgood et al., 2009b,a). In an effort to improve the outcomes of cartilage tissue engineering therapies, a number of investigators have attempted to engineer a more functional tissue *in*

vitro using novel combinations of cells, scaffolds, growth factors and bioreactor culture (Vunjak-Novakovic et al., 1999; Mauck et al., 2000, 2002, 2003b,a; Wendt et al., 2005; Buckley et al., 2009a; Daher et al., 2009; Stoddart et al., 2009; Vinatier et al., 2009). The use of serum-free culture conditions employing growth factor supplementation has also proved particularly beneficial (Wang et al., 2006; Lima et al., 2007; Byers et al., 2008). For example, chondrocyte-seeded agarose hydrogels receiving transient TGFβ3 exposure have been shown to reach native tissue levels of compressive modulus and proteoglycan content after less than 2 months of *in vitro* culture (Byers et al., 2008).

There are limitations to the use of chondrocytes for cell-based cartilage repair therapies. For example, an age-related loss of chondrogenic capacity of culture-expanded chondrocytes may limit their use to younger patients with isolated chondral lesions (Barbero et al., 2004). This has led to increased interest in the use of MSCs for cartilage repair (El Tamer and Reis, 2009). A number of studies report generating functional cartilaginous tissue using MSCs embedded in various types of hydrogels (Mauck et al., 2006; Huang et al., 2008, 2010; Kisiday et al., 2008; Thorpe et al., 2008; Erickson et al., 2009; Buckley et al., 2010); however, it is still unclear whether the quality of tissue generated using MSCs is comparable to that using chondrocytes (Mauck et al., 2006; Vinardell et al., 2009; Connelly et al., 2008). Regardless, an essential prerequisite to the utilisation of MSCs in cartilage tissue engineering is the identification of optimal culture conditions to generate a viable implantable tissue.

Whether engineering cartilaginous tissues using chondrocytes or mesenchymal stem cells, ensuring adequate nutrient supply and waste removal throughout the construct is critical to developing a viable implant. This is particularly the case when engineering large cartilaginous tissues for the treatment of large defects or potentially the entire articular surface of a joint, or when engineering cartilaginous

tissues for use in bone repair via endochondral ossification (Jukes et al., 2008; Farrell et al., 2009; Oliveira et al., 2009b,a). Incorporating channels into scaffolds is one approach that has been used to enhance nutrient transport and tissue formation (Silva et al., 2006; Bian et al., 2009; Buckley et al., 2009a). It has previously been demonstrated that the introduction of nutrient channels into chondrocyte-seeded agarose hydrogels results in the formation of a superior and more homogeneous cartilaginous tissue, but only if combined with forced convection of medium through these channels using a rotational bioreactor (Buckley et al., 2009a). The objective of this study was to investigate whether such an approach can be used to engineer large cartilaginous constructs using bone marrow (BM) derived MSCs and to compare the properties of these constructs to those derived using donor-matched chondrocytes. To this end, identical serum-free culture conditions employing TGFβ3 supplementation were used to engineer tissue using both cell types. The hypothesis was that the combination of nutrient channels and bioreactor culture would enhance the properties of relatively thick cartilaginous tissues engineered using both chondrocytes and MSCs.

4.2. Materials and methods

4.2.1. Experimental design

A 3 week time frame is commonly used in MSC pellet culture in order to assess chondrogenesis (Murphy et al., 2002; Bosnakovski et al., 2004; Tropel et al., 2004), so this study used 3 weeks as the minimum time interval. The study consisted of three separate experiments. In experiment 1, chondrocyte- and BM-MSC-seeded solid and microchannelled constructs were cultured in free swelling (FS) conditions for 9 weeks in order to investigate whether nutrient channels would be beneficial after significant extracellular matrix (ECM) accumulation and hence

reduced diffusion coeffients in the constructs. Constructs were evaluated at weeks 3, 6 and 9. In experiment 2, chondrocyte- and BM-MSC- seeded constructs were subjected to dynamic rotational culture (R) for a period of 3 weeks in order to assess chondrogenesis. Previous studies have demonstrated that dynamic culture conditions can inhibit chondrogenesis of MSC-seeded hydrogels, unless constructs are initially maintained in static conditions (Thorpe et al., 2008, 2010). Therefore, in experiment 3, BM-MSC-seeded constructs were subjected to delayed dynamic rotational culture (DR), in which the constructs were cultured for 3 weeks in free swelling conditions, followed by an additional 3 weeks in rotating conditions.

4.2.2. Cell isolation and expansion

Chondrocytes and BM-MSCs were harvested aseptically from 4 month old pigs. Chondrocytes were isolated from the articular cartilage of the femoropatellar joints. Cartilage slices were rinsed with phosphate-buffered saline (PBS) containing penicillin-streptomycin (200 U/ml) and digested by incubation with Dulbecco's modified Eagle's medium (DMEM)/F12 containing collagenase type II (0.5 mg/ml; Sigma-Aldrich, Dublin, Ireland) for 16-18 hours under constant rotation at 37°C. The resulting cell suspension was filtered through a 40 μm pore-size cell sieve (Falcon Ltd, Sarstedt, Ireland) and the filtrate centrifuged and rinsed twice with PBS. Cells were seeded at a density of 50 000 cells/cm^2 in 175 cm^2 T flasks and expanded to passage one (P1). Viable cells were counted using a haemocytometer and 0.4% trypan blue staining. Isolated chondrocytes from all donors were pooled and maintained in DMEM/F12 supplemented with 10% v/v fetal bovine serum (FBS) and 100 U/ml penicillin-streptomycin (Gibco, Biosciences, Dublin, Ireland) during the expansion phase. Porcine BM-MSCs were isolated from the femoral shaft and expanded according to a modified method developed for human MSCs (Lennon and Caplan, 2006) in DMEM GlutaMAX supplemented with 10% v/v

FBS and 100 U/ml penicillin/streptomycin. BM-MSCs were subcultured at a ratio of 1:3 following colony formation and expanded to passage three (P3)

4.2.3. Solid and channelled cell encapsulated hydrogel constructs

Expanded porcine chondrocytes (P1) and BM-MSCs (P3) were suspended in 2% agarose (Type VII, Sigma-Aldrich, Dublin, Ireland) at ≈40° C and a density of 15 x 10^6 cells/ml. The agarose cell suspension was cast in a stainless steel mould to produce regular solid (non-channelled) construct cylinders (⊘ 6 x 4 mm). Micro-channelled construct cylinders (⊘ 6 x 4 mm) were fabricated via a moulding process utilising a polydimethylsiloxane (PDMS) pillared array structure to produce a unidirectional channelled array in the transverse direction with diameters of 500 μm and a centre-centre spacing of 1 mm, see Figure 4.1. Chondrocyte-seeded and BM-MSC-seeded constucts were maintained in a chemically defined chondrogenic medium of DMEM supplemented with penicillin (100 U/ml)-streptomycin (100 μg/ml) (both GIBCO, Biosciences, Dublin, Ireland), 100 μg/ml sodium pyruvate, 40 μg/ml L-proline, 50 μg/ml L-ascorbic acid-2-phosphate, 1 mg/ml BSA, 1 x insulin-transferrin-selenium, 100 nM dexamethasone (all from Sigma-Aldrich, Dublin, Ireland) and 10 ng/ml recombinant human transforming growth factor-β3 (TGF-β3) (ProSpec-Tany TechnoGene Ltd., Israel). Constructs were allowed to equilibrate for 3 days before the addition of dexamethasone and TGF-β3, and the initiation of dynamic rotational culturing. Dexamethasone and TGF-β3 were removed from the medium after the first 3 weeks of culture. Culture medium was replaced twice a week.

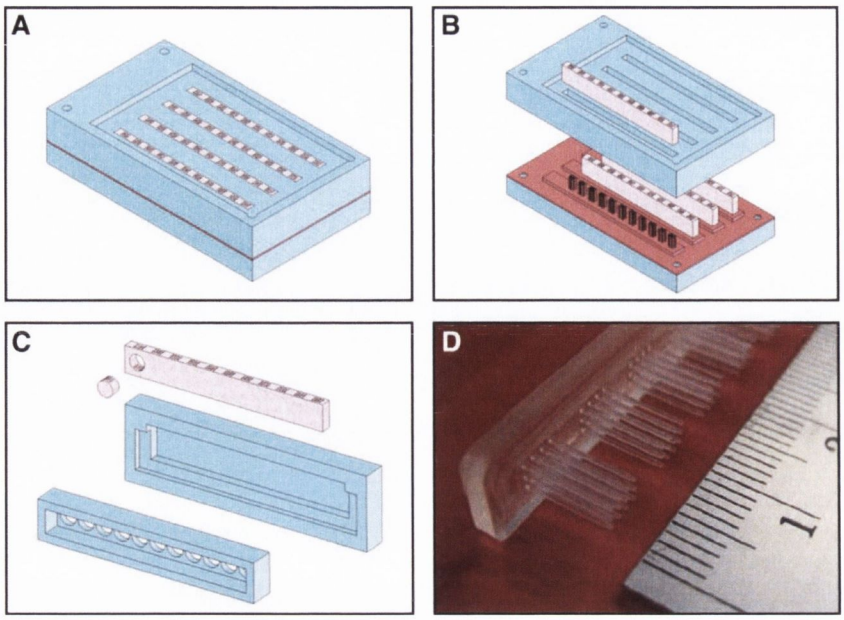

Figure 4.1.: *A) Assembled polytetrafluoroethylene (PTFE) mould system consisting of a polydimethylsiloxane (PDMS) array for creating microchannelled hydrogels. B) Once the cell-laden agarose (pink) is cast and allowed to set, the PDMS structure is removed to produce microchannelled agarose blocks. C) A 6 mm biopsy punch is used to core individual constructs. D) PDMS pillared mould.*

(Buckley et al., 2009a)

4.2.4. Dynamic rotational culture

Constructs were subjected to constant rotation in a rotational culture system or maintained in free swelling conditions. For application of dynamic rotational culture constructs were placed into the bottoms of 30 ml polypropylene tubes, of length 107 mm and diameter 25 mm (Sarstedt, Ireland) and capped with tissue flask filter caps. Each tube contained two or three constructs with 3 ml supplemented medium per construct. The tubes were placed into a rotator wheel (Stuart Rotator SB3, Lennox Laboratory Supplies Ltd, Ireland), and inclined at an angle of approximately 15°, and maintained in a humidified atmosphere at 37 °C, 5% CO_2, see Figure 4.2A. For experiment 2, rotational culturing was carried out at a rotational speed of 10 rpm and the experiment was then repeated at a speed of 5 rpm. For experiment 3,

rotational culturing was carried out at a rotational speed of 10 rpm.

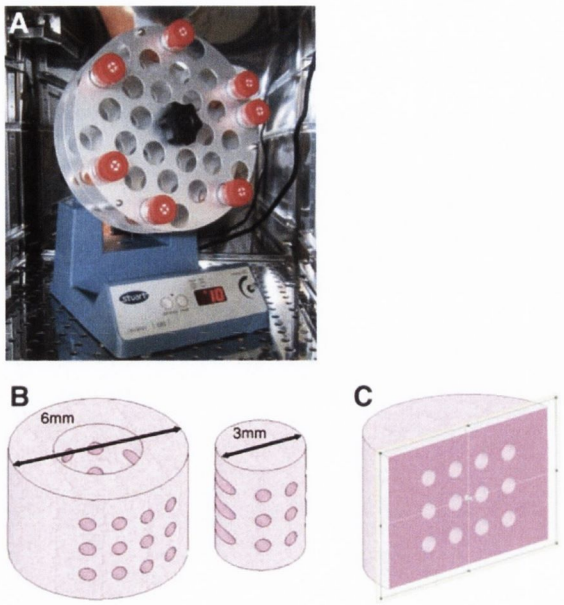

Figure 4.2.: *A) Rotational bioreactor system. Each tube contained two or three constructs. Rotation was performed at 10 rpm or 5 rpm. B) For biochemical analysis, constructs were separated into a core (⌀3 mm) and annulus. C) For histological analysis, constructs were sliced longitudinally.*

(Buckley et al., 2009a)

4.2.5. Mechanical testing

Constructs were removed from the culture medium and allowed to cool for 45 min in phosphate buffered saline at room temperature. The constructs were mechanically tested in unconfined compression between impermeable platens, using a standard materials testing machine (Zwick Z005, Roell, Germany) with a 5 N load cell. Agarose constructs were kept hydrated through immersion in a saline (0.9%) bath maintained at room temperature. Stress relaxation tests were performed, consisting of a ramp and hold cycle with a ramp displacement of 0.001 mm/s until 10% strain was obtained and maintained until equilibrium was reached (≈30 min). The compressive equilibrium modulus was calculated by application of the standard

uniaxial stress strain relationship, whereby the stress at full relaxation is divided by the applied strain. Dynamic tests were carried out immediately after the stress relaxation cycle. A cyclic strain amplitude of 1% superimposed upon the 10% strain was applied for 10 cycles at a frequency of 0.1 Hz, from which the dynamic modulus was determined. Following mechanical testing the constructs were cored, weighed, frozen and stored at -80° C.

4.2.6. Biochemical analysis

The biochemical content of constructs was assessed at each time point. The constructs were cored using a 3 mm biopsy punch and the wet mass of both annulus and core was recorded, see Figure 4.2B. Annuli and core samples were digested in papain and analysed for DNA, sGAG and collagen as described in section 3.2.7.

4.2.7. Histology and Immunohistochemistry

Samples were fixed in 4% paraformaldehyde overnight, dehydrated in a graded series of ethanols, embedded in paraffin wax, sectioned at 5 μm and affixed to microscope slides. Alcian blue and picro-sirius red histological stains, and collagen type II immunohistochemical stains, were carried out as described in section 3.2.8.

4.2.8. Statistical analysis

All statistical analyses were carried out using Minitab 15.1 with 3-4 samples analysed at each time point. Results are reported in the for mean $\pm$ standard deviation from the mean. Groups were analysed by one-way ANOVA or by a general linear model for analysis of variance with groups of factors, with time in culture, culture regime (free swelling or rotation) and architecture as the independent variables. Tukey's test was used to compare conditions. Anderson-Darling normality tests

were conducted on residuals to confirm a normal distribution. Significance was accepted at a level of $p<0.05$. Experiment 2 was replicated at rotational speeds of 5 and 10 rpm, with near identical results found for both speeds. Unless otherwise indicated, the results of the 10 rpm experiment are presented in this chapter.

4.3. Results

4.3.1. Experiment 1: Long-term free swelling culture

In the chondrocyte group, the DNA content at day 21 for both solid (496 ± 18 ng/mg) and microchannelled (495 ± 25 ng/mg) constructs was significantly greater compared to all other time points ($p < 0.001$) (Figure 4.3A). In the BM-MSC group no statistical differences in DNA content were found between construct architectures . DNA content was lower at day 63 than at day 21 for both cell types. sGAG accumulation (Figure 4.3B) in the chondrocyte group at days 42 (2.59 ± 0.14% ww for solid, 2.18 ± 0.14% ww for microchannel) and 63 (2.5 ± 0.13% ww for solid, 2.39 ± 0.03% ww for microchannel) was significantly greater than at day 21 (1.07 ± 0.07% ww for solid, 1.02 ± 0.06% ww for microchannel) ($p < 0.001$). The only significant difference between architectures was found at day 42, where sGAG accumulation in the solid group was greater than in the microchannelled group ($p < 0.01$). In the BM-MSC solid group, sGAG accumulation was also higher at days 42 (0.66 ± 0.07% ww) and 63 (0.65 ± 0.02% ww) compared to day 21 (0.45 ± 0.11% ww) ($p < 0.05$). In the microchannelled BM-MSC group, sGAG accumulation was greater at day 42 (0.65 ± 0.1% ww) than at day 21 (0.46 ± 0.09% ww)($p < 0.05$). Increases in collagen accumulation with time were also generally observed for chondrocyte- and MSC-seeded constructs (Figure 4.3C). Hydrogel architecture was not found to have a dramatic effect on the spatial accumulation (core vs. annulus) of biochemical constituents after 63 days in culture, see Figure

A.1.

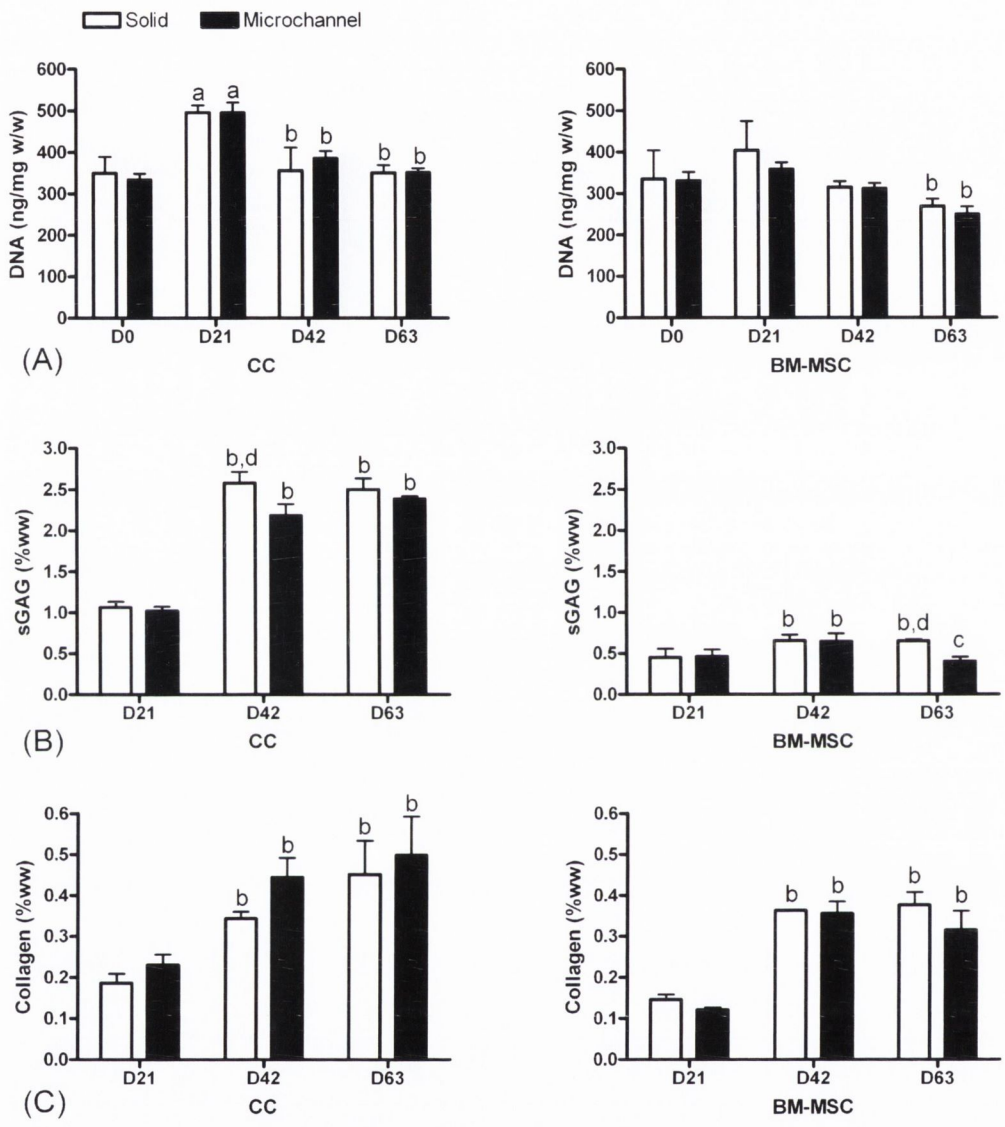

Figure 4.3.: *Experiment 1: Biochemical analysis of chondrocyte (CC) and BM-MSC, solid and microchannelled, constructs in free swelling culture conditions at days 21, 42 and 63. (A) DNA content (ng/mg w/w); (B) sGAG content (% ww); and (C) collagen content (% ww). Significance ($p < 0.05$): (a) compared to same group at day 0; (b) compared to same group at day 21; (c) compared to same group at day 42; (d) compared to microchannel at same time point; $n = 3–4$ for each group*

All mechanical properties were normalised to those obtained at day 0 to gain an

appreciation of their relative increases (Figure 4.4). At day 21 no statistical differences were observed between architectures (solid and microchannel) for equilibrium modulus (Figure 4.4A) or 0.1 Hz dynamic modulus (Figure 4.4B) for both cell types. In the chondrocyte group, at days 42 and 63, the normalised equilibrium moduli of the solid constructs were significantly greater than those of the microchannel constructs ($p < 0.01$). No statistical difference was found between architectures at day 63 for 0.1 Hz dynamic modulus. In the BM-MSC group the 0.1 Hz dynamic moduli of both architectures increased at days 42 and 63 compared to values at day 21 ($p < 0.01$) (Figure 4.4B). No statistical differences in dynamic modulus between architectures at any of the time points investigated were found for BM-MSC-seeded constructs.

4.3.2. Experiment 2: Influence of rotational culture

In the chondrocyte group, the DNA content in the annulus of both architectures was found to be significantly lower in the rotation (R) group (452 ± 18 ng/mg for solid, 418 ± 12 ng/mg for microchannel) compared to the free swelling (FS) group (551 ± 21 ng/mg for solid, 552 ± 37 ng/mg for microchannel) ($p < 0.05$). However, the DNA content in the core of the microchannel group increased due to rotation (337 ± 13 ng/mg) compared to free swelling conditions (269 ± 5 ng/mg). In the BM-MSC group, no statistical differences were found between FS and R constructs at day 21 when compared to their corresponding groups at day 0 (Figure 4.5A). In the chondrocyte group, rotation significantly increased sGAG accumulation in the core of constructs ($1.19 \pm 0.05\%$ ww for solid, $1.13 \pm 0.11\%$ ww for microchannel) compared to the core of free swelling constructs ($0.94 \pm 0.2\%$ ww for solid, $0.7 \pm 0.04\%$ ww for microchannel) ($p < 0.05$) (Figure 4.5B). In the BM-MSC group, rotation resulted in significantly lower amounts of sGAG accumulation compared to free swelling constructs ($p < 0.001$). Near-identical results were observed when

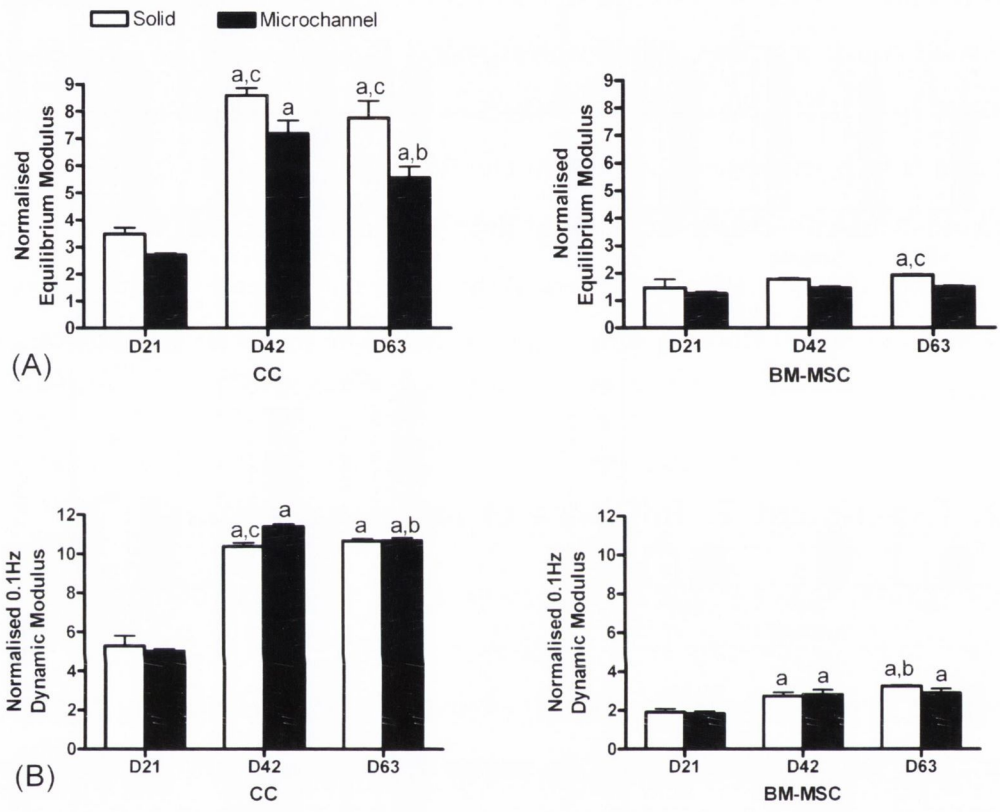

Figure 4.4.: *Experiment 1: Mechanical properties of chondrocyte (CC) and BM-MSC, solid and microchannelled constructs, subjected to free swelling culture conditions at days 21, 42 and 63. (A) Equilibrium modulus; (B) 0.1 Hz dynamic modulus. Significance ($p < 0.05$): (a) compared to same group at day 21; (b) compared to same group at day 42; (c) compared to microchannel at same time point; $n = 3$ for each group. Equilibrium and 0.1 Hz values of solid constructs at day 0 used for normalisation were 14.25 ± 0.22 and 40.6 ± 0.74 kPa for chondrocytes, and 15.84 ± 0.36 and 53.11 ± 1.31 kPa for BM-MSCs. Equilibrium and 0.1 Hz values of microchannel constructs at day 0 used for normalisation were 11.46 ± 0.54 and 30.71 ± 1.83 kPa for chondrocytes, and 12.79 ± 0.35 and 35.11 ± 1.21 kPa for MSCs*

the speed of rotational culture was reduced from 10 to 5 rpm, see Figure A.2 . In the chondrocyte group, collagen accumulation in the annulus of the FS group (0.21 ± 0.02% ww for solid, 0.28 ± 0.01% ww for microchannel) was significantly greater than in the core (0.12 ± 0.01% ww for solid, 0.1 ± 0.02% ww for microchannel) ($p < 0.05$) (Figure 4.5C). Rotation increased collagen accumulation in the core of the microchannelled group compared to the corresponding annulus ($p < 0.05$) and also compared to FS conditions ($p < 0.001$). The highest collagen accumulation in the BM-MSC groups was found in the annulus of the free swelling constructs (0.15 ± 0.01% ww for solid, 0.12 ± 0.01% ww for microchannel). Rotation significantly decreased collagen accumulation in BM-MSC constructs ($p < 0.001$).

Matrix accumulation in the annuli of constructs was normalised to matrix accumulation in the core in order to examine construct homogeneity. Rotational culture resulted in a more homogeneous accumulation (i.e. a value approaching 1) of sGAG compared to free swelling culture for both chondrocytes and BM-MSCs (Figure 4.6). A combination of a modified scaffold architecture and rotational culture promoted the formation of a more homogeneous collagen accumulation within the constructs.

sGAG release into the medium was also measured (Table 4.1). Rotational culture resulted in greater release of sGAG into the medium for the chondrocyte group ($p < 0.05$). Rotation did not increase sGAG loss to the medium in MSC-seeded constructs compared to free swelling conditions. When sGAG content retained in the chondrocyte constructs was combined with sGAG released to the medium, total sGAG synthesis values were higher in the rotational group compared to the free swelling group.

Chondrocyte-seeded constructs stained positive for Alcian blue for both free swelling and rotating conditions (Figure 4.7). BM-MSC-seeded constructs stained positive under free swelling conditions but not under dynamic rotating conditions. A

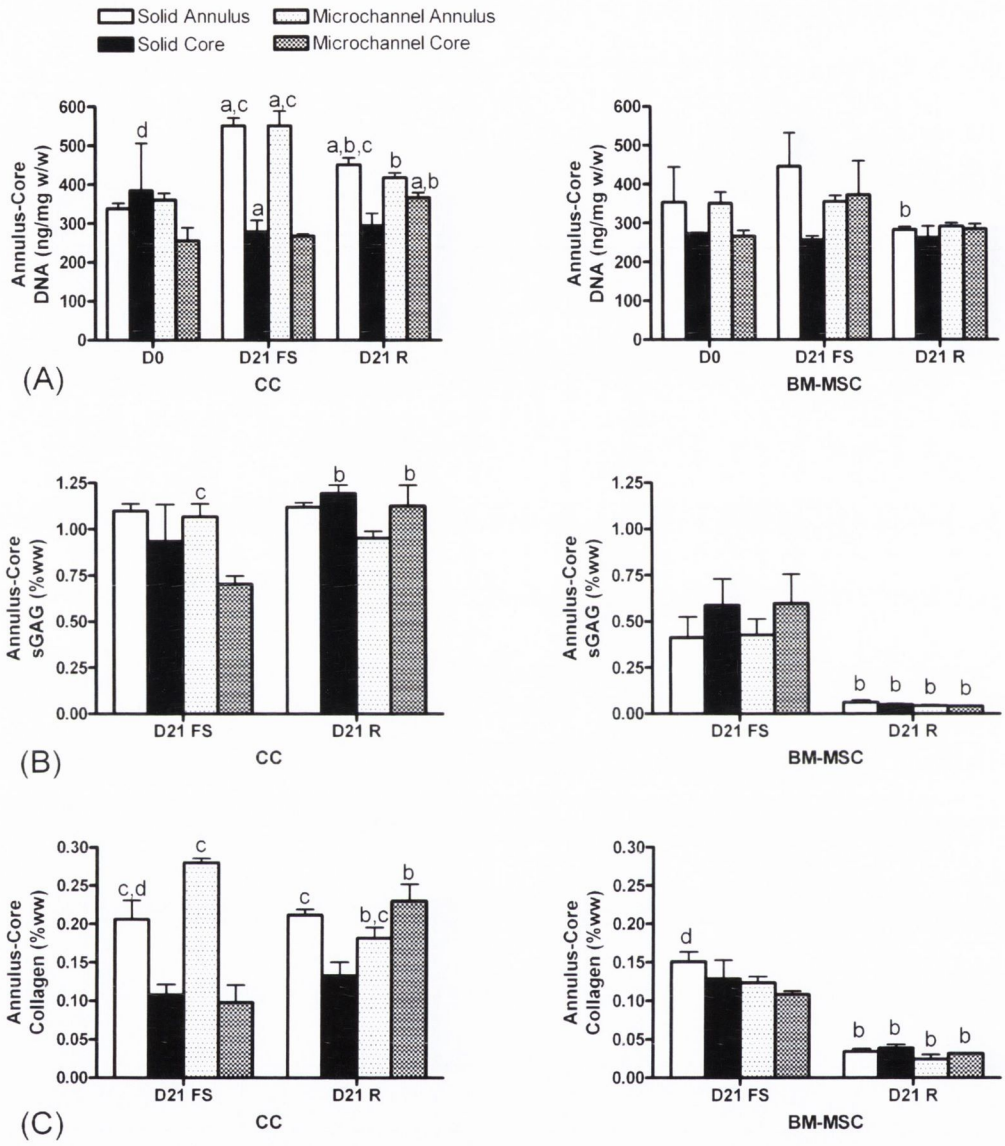

Figure 4.5.: *Experiment 2: Annulus–core biochemical analysis of chondrocyte (CC) and BM-MSC, solid and microchannelled constructs, subjected to free swelling (FS) or 10 rpm rotation (R) culture conditions at days 0 and 21. (A) DNA content (ng/mg w/w); (B) sGAG content (% ww); and (C) collagen content (% ww). Significance ($p < 0.05$): (a) compared to same group at day 0; (b) compared to same group at day 21 FS; (c) compared to corresponding core at the same time point and culture condition; (d) compared to same geometric region, alternative architecture, at same time point and culture condition; $n = 3–4$ samples for each group*

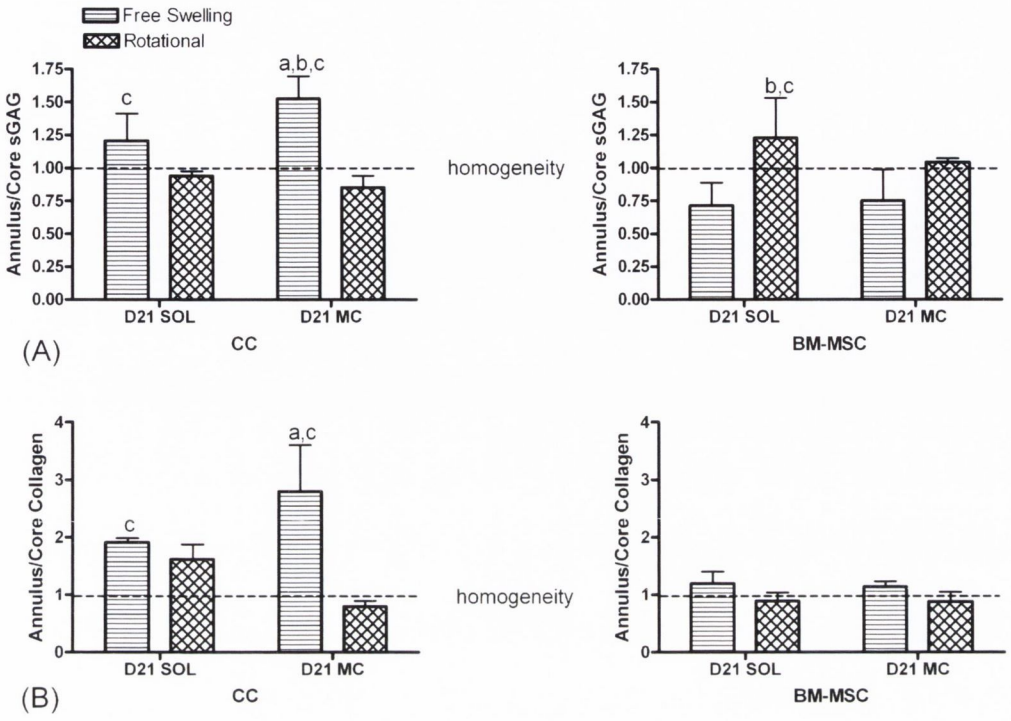

Figure 4.6.: *Experiment 2: Annulus/core biochemical analysis for homogeneity of chondrocyte (CC) and BM-MSCs, solid (SOL) and microchannelled (MC), constructs subjected to free swelling or 10 rpm rotation at day 21. (A) sGAG content; and (B) collagen content. Significance ($p < 0.05$): (a) compared to same architecture and alternative culture conditions; (b) compared to same culture conditions and alternative architecture; (c) compared to alternative culture conditions and alternative architecture; $n = 3–4$ for each group*

less intense alcian blue staining was observed in the core of free swelling chondrocyte-seeded constructs, while more intense staining was observed in the core of free swelling BM-MSC-seeded constructs, which correlates with the biochemical analysis. Immunohistochemistry revealed positive staining for type II collagen in free swelling BM-MSC-seeded constructs, with less staining around the construct periphery. All constructs stained weakly for collagen type I (data not shown). Free swelling chondrocyte constructs also showed evidence of the microchannels narrowing and being filled with matrix.

			Construct sGAG	Media sGAG	Total sGAG
CC	SOL	FS	1012±127.1[a]	90.4±9.5	1102.4±127.5
CC	SOL	R	880.8±113.4	423.6±8.2[b]	1304.4±113.7
CC	MC	FS	817.6±18.3[a]	230±25.7	1047.8±31.5
CC	MC	R	630.6±38.4	526±5.3[b]	1157.1±31.5
BM-MSC	SOL	FS	423.5±54.4[a]	23.7±1.2	456.3±54.4
BM-MSC	SOL	R	33.2±5.5[b]	32.2±19.4	65.3±20.1
BM-MSC	MC	FS	228.2±51.2[a]	60.5±11.7	288.7±52.6
BM-MSC	MC	R	12.8±0.8[b]	16.8±2.6	29.6±2.7

Table 4.1.: Experiment 2: sGAG retained in constructs vs. sGAG released into media for constructs subjected to free swelling (FS) or 5 rpm rotational (R) culture for 21 days. Data represents the mean ± SD for three or four samples for construct and two samples for media. Significance ($p<0.05$); [a] compared to corresponding media ; [b] compared to same group under free-swelling conditions

4.3.3. Experiment 3: Delayed rotation of MSC- seeded constructs

The application of delayed rotation to BM-MSC-seeded constructs significantly decreased DNA content in the annulus of the microchannelled group only (263.3 ± 19 ng/mg; $p < 0.05$) compared to free swelling conditions (307 ± 12 ng/mg) at day 42 (Figure 4.8A). No significant differences in sGAG accumulation (Figure 4.8B) were found between culture conditions. The free swelling group contained greater amounts of collagen in the core of microchannelled constructs compared to the delayed rotation group (0.48 ± 0.05% ww vs. 0.38 ± 0.02% ww; $p < 0.01$;

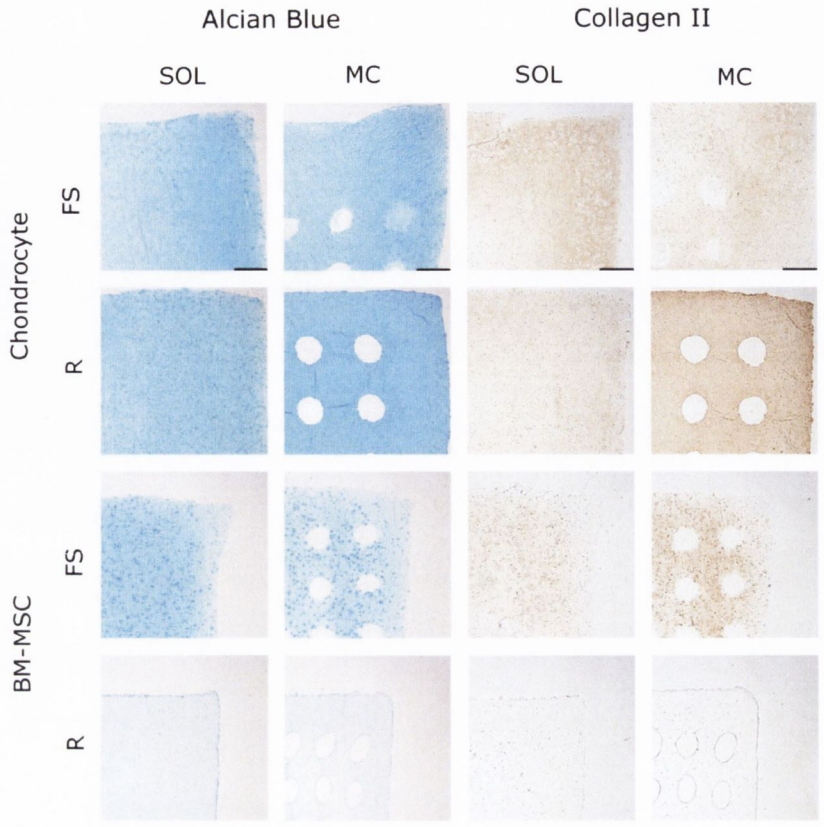

Figure 4.7.: *Experiment 2: Alcian blue staining and type II collagen staining of chondrocyte- and bone marrow derived mesenchymal stem cell- seeded solid (SOL) and microchannelled (MC) constructs subjected to free swelling (FS) and rotating (R) culture conditions at day 21. Scale bar is 500μm and is consistent across all images. Sections are representative of* $1/4$ *of a construct.*

Figure 4.8C).

4.4. Discussion

It has previously been demonstrated that a combination of forced convection and modified scaffold architecture can be used to engineer relatively homogeneous and thick cartilaginous tissues *in vitro* using chondrocytes embedded in agarose (Buckley et al., 2009a). The objective of this study was to investigate whether such an approach could also be used to generate large viable cartilaginous constructs using

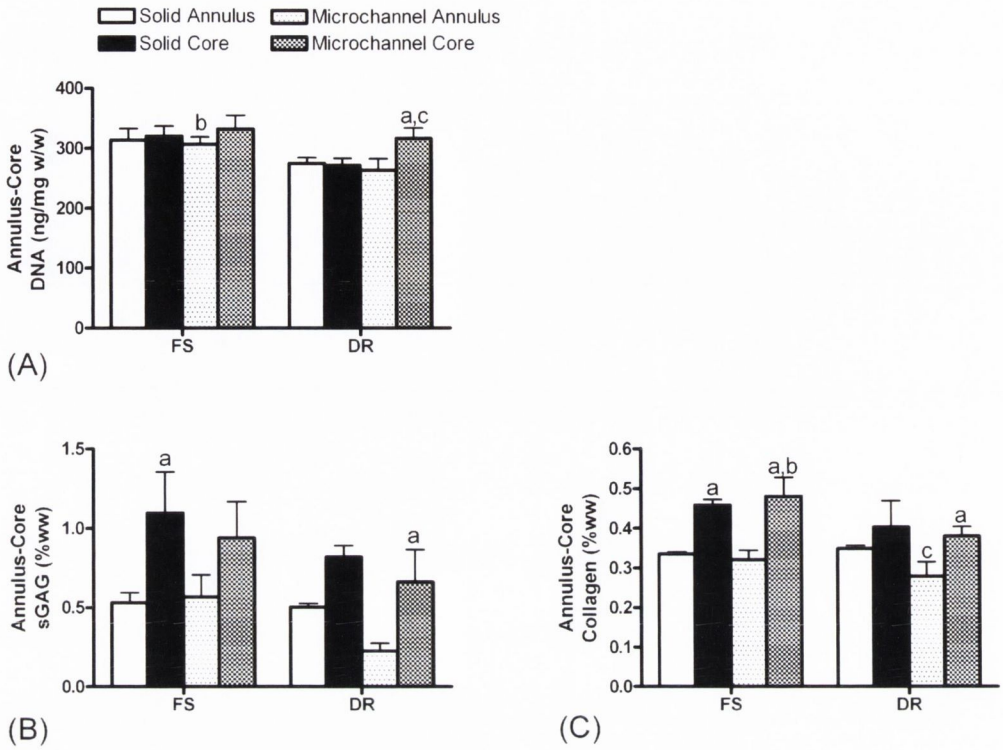

Figure 4.8.: *Experiment 3: Annulus-core biochemical analysis of bone marrow-derived mesenchymal stem cells (BM-MSCs), solid (SOL) and microchannelled (MC) constructs subjected to free swelling (FS) or 10 rpm delayed rotation (DR) culture conditions at day 42. (A) DNA content (ng/mg w/w); (B) sGAG content (% ww); (C) collagen content (% ww). Significance ($p < 0.05$): (a) compared to corresponding annulus; (b) compared to same group under DR conditions; (c) compared to same region and alternative architecture;*

BM-MSCs, and to compare the properties of these constructs to those generated using donor-matched chondrocytes. Donor-matched cells were used to ensure that differences in the response of both cell types to either hydrogel architecture or culture conditions could be attributed to general phenotypic differences between the cell types, and not due to inter-animal variation. The previous study utilised culture media supplemented with bovine serum (Buckley et al., 2009a), which may be preferentially supporting the formation of cartilaginous tissue in the peripheral regions of the construct. In the present study, which incorporated a chemically defined medium supplemented with TGF-β3, less dramatic differences

between matrix accumulation in the core and annulus of chondrocyte-seeded agarose constructs were observed (e.g. Figure 4.4). As was observed previously (Buckley et al., 2009a), the introduction of channels alone had little effect on either cell viability or the levels and spatial distributions of tissue accumulation, even after abundant matrix accumulation following 63 days of culture (Figure 4.3). Neither did the introduction of channels lead to increases in construct mechanical properties (Figure 4.5). This is in contrast to a recent study that demonstrated that the introduction of a single channel through the depth of a chondrocyte-seeded agarose hydrogel resulted in higher mechanical properties after 56 days of culture (Bian et al., 2009). The higher cell-seeding densities used in that study (Bian et al., 2009), and the greater levels of matrix accumulation, is one plausible explanation for this discrepancy in findings, as the introduction of nutrient channels in free swelling culture might be expected to be more beneficial for higher seeding densities.

Matrix accumulation was generally greater in the annulus of both solid and channelled chondrocyte-seeded constructs. Rotational culture increased sGAG accumulation in the core of both solid and channelled chondrocyte-seeded constructs, resulting in the formation of a more homogeneous engineered tissue (Figure 4.6). This may be due to forced convection of nutrients and other regulatory molecules into the centre of the construct, or perhaps the flow environment around the periphery of the construct in the rotational bioreactor alters the cellular consumption of such factors, allowing for enhanced transport to the core of the engineered tissue. Alternatively, the mechanical stimuli experienced by the chondrocytes due to rotational culture may be promoting matrix synthesis. A number of other studies have also reported that fluid perfusion or rotational culture enhances matrix production in chondrocyte-seeded constructs (Vunjak-Novakovic et al., 1999; Pazzano et al., 2000; Davisson et al., 2002; Raimondi et al., 2006, 2008; Wendt et al., 2006; Nagai et al., 2008).

In contrast, rotational culture inhibited chondrogenesis of BM-MSCs in both solid and channelled constructs (Figure 4.5B,C). This is in contrast to other studies demonstrating improved chondrogenesis of MSCs under dynamic culture conditions (Hannouche et al., 2007; Mahmoudifar and Doran, 2010). There was no evidence to suggest that this was due to a loss in cell viability, as comparable levels of DNA were observed in free swelling and rotational groups (Figure 4.5A). To determine whether this was purely due to secreted matrix components simply being flushed out of the construct in response to the rotational culture conditions, the sGAG content in the medium was analysed, which revealed that this was not the case (Table 4.1). The shear stresses exerted on the MSCs in rotational culture may also not support the chondrogenic phenotype, although this finding was observed at a rotational speed of both 5 and 10 rpm. It has been demonstrated that fluid flow can suppress *Sox9* mRNA expression in MSCs *in vitro* (McBride et al., 2008), while computational models have also suggested that high levels of fluid flow do not promote a chondrogenic phenotype (Prendergast et al., 1997; Lacroix and Prendergast, 2002; Kelly and Prendergast, 2005, 2006). Furthermore, under certain media supplementation conditions it has also been demonstrated that fluid perfusion can inhibit chondrogenesis of BM-MSCs embedded in agarose hydrogels used to engineer osteochondral tissues (Grayson et al., 2010). MSC-laden constructs may therefore require a period of free swelling pre-culture prior to exposure to mechanical forces. It has also been demonstrated that dynamic compression applied at the onset of TGF$-\beta$3-induced differentiation inhibited chondrogenesis of MSCs (Thorpe et al., 2008); however, this inhibition of chondrogenesis in response to dynamic compression is not observed if MSC-seeded constructs first undergo 21 days of chondrogenic differentiation in the presence of TGF-β3 (Thorpe et al., 2010). Enhanced oxygen transport throughout the construct due to rotational culture may also be inhibiting MSC chondrogenesis, as numerous studies have reported

more robust chondrogenesis of stem cells under low oxygen conditions (Lennon et al., 2001; Robins et al., 2005; Wang et al., 2005; Kanichai et al., 2008; Koay and Athanasiou, 2008; Buckley et al., 2010). The fact that sGAG accumulation in the core of free swelling MSC-laden constructs is significantly greater than the annulus may be due to cells on the periphery of the tissue consuming available oxygen, creating lower oxygen tensions in the core of the construct. Interestingly, rotational culture was not observed to significantly inhibit chondrogenesis of MSCs if the constructs were first maintained in free swelling culture for 3 weeks in the presence of TGF-β3 (Figure 4.8). This differential response to rotational culture with time may be due to the development of a pericellular matrix altering the mechanical stimulus experienced by the MSCs in the delayed rotation group. Furthermore, following 3 weeks of culture in free swelling culture conditions in the presence of TGF-β3 the MSC phenotype would have been altered, becoming more chondrogenic and perhaps more responsive to a high oxygen environment (Buckley et al., 2010).

As has been observed in a number of studies (Mauck et al., 2006; Connelly et al., 2008; Vinardell et al., 2009), chondrocytes generate a more functional cartilaginous tissue compared to MSCs. The culture conditions utilised in the long-term experiments reported in this study consist of a temporal exposure to TGF-β, which has previously been shown to be beneficial for developing functional cartilaginous tissue using chondrocytes (Byers et al., 2008). Such a temporal exposure to TGF-β has recently been shown to only be beneficial for MSC-laden constructs seeded at high cell densities (Huang et al., 2009). Future studies should investigate higher MSC-seeding densities, as matrix accumulation would be expected to significantly increase. As discussed previously, in such cases the use of channels may become beneficial to overcome nutrient supply limitations in these denser, more cellular tissues.

There was greater sGAG release into the medium in the chondrocyte rotational

group; however, levels of accumulation in the construct were not significantly lower than in free swelling constructs. It was also observed that the total sGAG release into the medium was greater in chondrocyte-seeded constructs than in MSC constructs, which may be due in part to larger repulsive forces generated by the greater amounts of sGAG accumulating within the chondrocyte constructs. Other studies have also reported high levels of sGAG release from hydrogels seeded with chondrocytes or MSCs (Babalola and Bonassar, 2010). While total sGAG levels (medium plus construct) were found to be higher in rotational groups for chondrocyte-seeded constructs, scaffold and bioreactor systems need to be carefully designed to retain the majority of secreted matrix components within the construct. In addition, promotion of a collagenous network to restrain the swelling and diffusion of sGAG out of the construct may lead to the formation of a more functional engineered tissue.

4.5. Concluding remarks

In a chemically defined medium, rotational culture leads to the formation of a more homogeneous cartilaginous tissue for both solid and channelled chondrocyte-seeded constructs. In contrast, rotational culture was observed to inhibit chondrogenesis of MSC-seeded constructs unless they were first maintained in free swelling conditions in the presence of TGF-β3. The results of this chapter demonstrate that bioreactor culture conditions that are beneficial for chondrocyte-based cartilage tissue engineering may be suboptimal for MSC-based cartilage tissue engineering. Rotational culture will therefore not be utilised in further chapters in this thesis.

The introduction of channels into engineered cartilaginous tissues did not enhance matrix deposition when cultured in free swelling conditions *in vitro*. It is possible that the benefit of such channels may only be seen *in vivo*. Chapter 5 will investigate

if the introduction of channels into engineered MSC-based hypetrophic cartilaginous grafts will accelerate vascularisation and mineralisation following subcutaneous implantation.

5 Modifying architecture to accelerate vascularisation and ossification

5.1. Introduction

The goal of tissue engineering is to replace or regenerate damaged tissues through the combination of cells, three-dimensional scaffolds, and signalling molecules (Koh and Atala, 2004; Langer, 2000). Bone tissue engineering has, thus far, generally focussed on the direct osteoblastic differentiation of mesenchymal stem cells (MSCs), in a process resembling intramembranous ossification (Meijer et al., 2007). However, the success of this approach to bone regeneration has been hampered by insufficient blood vessel infiltration, preventing the necessary delivery of oxygen and nutrients to the engineered graft (Lyons et al., 2010; Santos and Reis, 2010). Recently an endochondral approach to bone tissue engineering, which involves remodelling of an intermediate hypertrophic cartilaginous template (Farrell et al., 2011, 2009; Janicki et al., 2010; Jukes et al., 2008; Lau et al., 2012; Scotti et al., 2013, 2010; Sheehy et al., 2013; Tortelli et al., 2010), has been proposed as an alternative to direct intramembranous ossification for bone regeneration using MSCs. Chondrogenically

primed bone marrow derived MSCs have an inherent tendency to undergo hypertrophy (Pelttari et al., 2006), an undesirable attribute in MSC-based articular cartilage repair therapies, but one which may be harnessed for use in endochondral bone tissue engineering strategies. Hypertrophic chondrocytes are equipped to survive the hypoxic environment a tissue engineered graft will experience once implanted *in vivo* (Farrell et al., 2011). Furthermore, cells undergoing hypertrophy release pro-angiogenic factors, such as vascular endothelial growth factor, to facilitate the conversion of avascular tissue to vascularised tissue (Gerber et al., 1999). The endochondral approach to bone regeneration may therefore circumvent many of the issues associated with the traditional intramembranous method; however, in order to be used to repair large bone defects, this approach first requires strategies to engineer scaled-up hypertrophic cartilage. This may be challenging, as recent attempts to generate such hypertrophic constructs using MSC seeded collagen scaffolds have demonstrated the formation of a core region devoid of cells and matrix (Scotti et al., 2013).

Such scaling up of engineered grafts, and the associated issue of core degradation, is a well-documented challenge in the field of tissue engineering (Lee et al., 2009). Strategies to promote nutrient supply and waste removal include the use of bioreactors (Martin et al., 2004; Mauck et al., 2003b, 2000; Thorpe et al., 2010), modification of scaffold architectures (Bian et al., 2009; Zhang et al., 2012), or a combination of both (Buckley et al., 2009b; Mesallati et al., 2012; Sheehy et al., 2011). An alternative approach might be to recapitulate the mechanisms adopted during skeletogenesis to provide nutrients to the cartilaginous templates. During normal bone development, canals within the developing hypertrophic cartilage have been identified (Ganey et al., 1995; Ytrehus et al., 2004). These canals play an important role in supplying nutrients to the developing cartilage (Blumer et al., 2008). Furthermore, endochondral ossification is dependent on neo-vascularisation

of the cartilaginous template, with the in-growth of blood vessels via these cartilage canals identified as a key event during bone development (Blumer et al., 2008). Finally, these canals act as conduits for the migration of osteogenic cells into the cartilaginous template which in turn lay down new bone matrix (Blumer et al., 2006). Executing a developmental engineering paradigm (Lenas et al., 2009), directed at mimicking the structure and function of the cartilage canal network, may therefore be a powerful tool in endochondral bone tissue engineering strategies.

In this study it was hypothesised that recapitulating the cartilage canal network observed during endochondral skeletogenesis, by engineering channelled hypertrophic cartilaginous constructs, would firstly facilitate extracellular matrix synthesis and the *in vitro* development of the construct, and secondly would accelerate mineralisation and vascularisation of the graft once implanted *in vivo*. To assess the influence of scaffold architecture on *in vitro* graft development, bone marrow derived MSCs were encapsulated in agarose hydrogels either containing an array of micro-channels (termed channelled), or in non-channelled (termed solid) controls, and cultured long-term (up to 10 weeks) to undergo hypertrophic chondrogenic differentiation. Furthermore, to test the efficacy of channelled architectures to enhance mineralisation and vascularisation *in vivo*, channelled and solid constructs were also subjected to a shorter period of hypertrophic priming (6 weeks) prior to subcutaneous implantation in nude mice. Constructs were harvested at 4 and 8 weeks post-implantation to test the hypothesis that graft architecture would influence mineralisation and vascularisation of the engineered hypertrophic tissue.

5.2. Materials and methods

5.2.1. Experimental design

The first phase of this study investigated the *in vitro* development of engineered cartilaginous constructs undergoing long-term hypertrophic chondrogenesis. MSCs were encapsulated in solid and channelled hydrogels, cultured in chondrogenic conditions (further details below), for a period of 5 weeks. Thereafter constructs were switched to hypertrophic conditions for an additional 5 weeks, resulting in a total *in vitro* culture period of 10 weeks. The second phase of this study investigated the potential of engineered hypertrophic cartilaginous constructs to undergo mineralisation and vascularisation *in vivo*. MSCs were encapsulated in solid and channelled constructs and cultured in chondrogenic conditions for a period of 5 weeks, as per phase 1. Thereafter constructs received an additional week in hypertrophic conditions (6 weeks total in vitro priming) prior to subcutaneous implantation in nude mice. Constructs were harvested at 4 and 8 weeks post-implantation.

5.2.2. Cell isolation, expansion

Porcine bone marrow derived MSCs were isolated as describe in section 4.2.2. Following colony formation, MSCs were trypsinised, counted, seeded at density of 5 x 10^3 cells/cm^2, and expanded to passage 1 (P1).

5.2.3. Cell encapsulation in solid and channelled agarose hydrogels

At the end of P1 MSCs were suspended in 2% agarose at a density of 20 x 10^6 cells/mL. The agarose cell suspension was cast in a stainless steel mould to produce regular solid (non-channelled) cylindrical constructs (⌀5 mm x 3 mm). Channelled cylindrical constructs were fabricated utilising a pillared polydimethylsiloxane array structure (Buckley et al., 2009a) inserted into a cylindrical Teflon mould to produce a unidirectional 4 x 3 channelled array in the longitudinal direction with diameters of 500 μm and a centre-centre spacing of 1 mm.

5.2.4. Chondrogenic and hypertrophic culture conditions

The chondrogenic conditions applied in this study are defined as culture at 5% pO_2 in a chondrogenic medium consisting of high glucose DMEM GlutaMAX supplemented with 100 U/mL penicillin/streptomycin (both Gibco), 100 μg/mL sodium pyruvate, 40 μg/mL L-proline, 50 μg/mL L-ascorbic acid-2-phosphate, 4.7 μg/mL linoleic acid, 1.5 mg/mL bovine serum albumine, 1x insulin-transferrin-selenium, 100 nM dexamethasone (all from Sigma-Aldrich) and 10 ng/mL of human transforming growth factor-β3 (TGF-β3) (Prospec-Tany TechnoGene Ltd., Israel). The hypertrophic conditions applied are defined as culture at 20% pO_2 in a hypertrophic medium consisting of high glucose DMEM GlutaMAX supplemented 100 U/mL penicillin/streptomycin, 100 μg/mL sodium pyruvate, 40 μg/mL L-proline, 50 μg/mL L-ascorbic acid-2-phosphate, 4.7 μg/mL linoleic acid, 1.5 mg/mL bovine serum albumine, 1x insulin-transferrin-selenium, 1 nM dexamethasone, 1 nM L-thyroxine and 20 μg/mL β-glycerophosphate (both Sigma-Aldrich).

5.2.5. In vivo subcutaneous transplantation

In phase 2 of the study, following 6 weeks in vitro priming, MSC- seeded solid and channelled constructs (n=9 per group) were implanted subcutaneously into the back of nude mice (Balb/c; Harlan, UK). Briefly, two subcutaneous pockets were made along the central line of the spine, one at the shoulders and the other at the hips, and into each pocket three constructs were inserted. Nine constructs were implanted per each experimental group. Mice were sacrificed at 4 and 8 weeks post-implantation by CO_2 inhalation. The animal protocol was reviewed and approved by the ethics committee of Trinity College Dublin.

5.2.6. Biochemical analysis

The biochemical content of constructs was analysed at each time point. Prior to biochemical analysis, constructs were sliced in half, washed in PBS, weighed, and frozen for subsequent assessment. Half of each construct was digested with papain and analysed biochemically for DNA, sGAG and collagen content, as previously described in section 3.2.7. The other half was digested in 1 M hydrochloric acid (HCL) and 60° C and 10 rpm for 18 h. The calcium content was determined using a Sentinel Calcium kit (Alpha Laboratories Ltd, Uk). 3-4 samples were analysed for each *in vitro* experimental group. 4-6 samples were analysed for each *in vivo* experimental group. Alkaline phosphatase (ALP) activity in the media (n=3) at week 5 was measured using a Sensolyte pNPP Alkaline Phosphatase assay kit (Cambridge Biosciences, UK) with a calf intestine ALP standard.

5.2.7. Histology and Immunohistochemistry

At each time point samples were fixed in 4% paraformaldehyde overnight, dehydrated in a graded series of ethanols, embedded in paraffin wax, sectioned at 8

μm and affixed to microscope slides. Samples harvested at 8 weeks post- *in vivo* implantation were decalcified in EDTA for 3-4 days prior to wax embedding. The sections were stained with haematoxylin and eosin (H and E), 1% alcian blue 8GX in 0.1 M HCL to assess sGAG content with a counter stain of nuclear fast red to assess cellular distribution, picro-sirius red to assess collagen distribution, and 1% alizarin red to assess calcium accumulation. Collagens I, II and X were evaluated as described in section 3.2.8. Terminal deoxynucleotidyl Transferase (TdT+) cells were identified on the fully automated IHC Leica BOND-MAX (Leica biosystems). Briefly, sections were incubated with a mouse monoclonal TdT Clone SEN28 ready to use primary antibody (PA0339) (Leica biosystems). Heat mediated antigen retrieval was performed with epiptope retrieval solution 2 (AR9640) for 10 min (Leica biosystems). Thereafter, visualisation of the antibody was performed with the Bond Polymer Refine Detection kit (DS9800) (Leica biosystems). TdT staining was performed by Dr. Mary Toner. Heat mediated antigen retrieval was performed on sections, for detection of CD31 antigen, with sodium citrate solution (Sigma-Alrich) for 20 min. Thereafter, sections were incubated with goat serum, biotin and avidin, to block non-specific sites. The CD31 (ab28364, 1:50; 0.2 mg/mL) primary antibody (Rabbit polyclonal, Abcam, Cambridge, UK) was applied overnight at 4° C. Sections were treated with peroxidase followed by the secondary antibody (ab97051, goat polyclonal secondary antibody to Rabbit IgG, 1:200, 1mg/mL, Abcam, Cambridge, UK) for 1 h, ABC reagent for 45 min, and developed with DAB peroxidase for 5 min (both Vector Labs). Positive and negative controls were included.

5.2.8. Micro-computed tomography

Micro-computed tomography (μCT) scans were carried out using a Scanco Medical 40 μCT system (Scanco Medical, Bassersdorf, Switzerland) in order to quantify

mineral content and to assess mineral distribution in MSC-seeded hydrogels. In phase 1 of the experiment, constructs were scanned at the end of the 10 week *in vitro* culture period. In phase 2, constructs were scanned at 4 and 8 weeks post-implantation. Constructs were scanned in PBS, at a voxel resolution of 12 μm, a voltage of 70 kVp, and a current of 114 μA. Circular contours were drawn in an anit-clockwise direction around the periphery of the constructs. Additionally, circular contours were drawn in a clockwise direction around the perimeter of the channels, so as to exclude the area within the channels from the analysis. A Gaussian filter (sigma=0.8, support=1) was used to suppress noise and a global threshold of 129, corresponding to a density of 172.6 mg hydroxyapatite/cm^3, was applied. This threshold was selected by visual inspection of individual scan slices so as to include mineralised tissue and exclude non-mineralised tissue. 3D evaluation was carried out on the segmented images to determine mineral volume and to reconstruct a 3D image. 3 constructs were analysed per experimental group. The variance of mineralisation with depth through the construct was analysed qualitatively by examining sections $\approx$ 0.75 mm of depth from the top of the construct (quarter section), and $\approx$ 1.5 mm of depth from the top of the construct (centre section). 10 slices were compiled per section, resulting in a thickness of 120 μm

5.2.9. Statistical analysis

All statistical analyses were carried out using Minitab 15.1. Results are reported as mean $\pm$ standard deviation. Groups were analysed by a general linear model for analysis of variance with groups of factors. Tukey's test was used to compare conditions. Anderson-Darling normality tests were conducted on residuals to confirm a normal distribution. Nonnormal data was transformed using the Box-Cox procedure. Any nonnormal data which the Box-Cox procedure could not find a suitable tranformation for was transformed using the Johnson procedure.

Significance was accepted at a level of $p<0.05$.

5.3. Results

5.3.1. Chondrogenically primed MSCs can be stimulated in vitro to produce a calcified cartilaginous tissue within solid and channelled hydrogels

MSCs were encapsulated in solid and channelled hydrogels and were subjected to chondrogenic culture conditions for a period of 5 weeks, followed by an additional 5 weeks in hypertrophic culture conditions, resulting in a total *in vitro* culture period of 10 weeks. Solid MSC-seeded hydrogels accumulated significantly more sGAG compared to channelled MSC- seeded hydrogels after 5 weeks (1.31 ± 0.06 vs. 0.94 ± 0.08 %ww, $p<0.0001$) and 10 weeks (0.70 ± 0.01 vs. 0.58 ± 0.04 %ww, $p=0.0304$) of *in vitro* culture, see Figure 5.1(A). Both solid and channelled constructs show a significant reduction in sGAG after 10 weeks compared to their levels at 5 weeks. Both collagen and calcium accumulation increased with time in culture for both solid and channelled constructs, with greater levels of collagen observed in solid constructs after 10 weeks of culture (1.58 ± 0.09 vs. 1.27 ± 0.15 %ww, $p= 0.03$), see Figure 5.1(B). Channelled constructs accumulated significantly more calcium than solid constructs after 10 weeks *in vitro* culture (3.72 ± 0.61 vs. 2.58 ± 0.15 %ww, $p=0.0035$), see Figure 5.1(C). μCT analysis confirmed the enhancement of mineralisation in channelled constructs, see Figure 5.1(E). Both solid and channelled constructs mineralised preferentially around their periphery, with a reduction in mineralisation observed with depth through the constructs. ALP activity measured in the media at week 5 was 135.2 ± 10.9 ng for solid constructs and 155.3 ± 3.2 ng for channelled constructs.

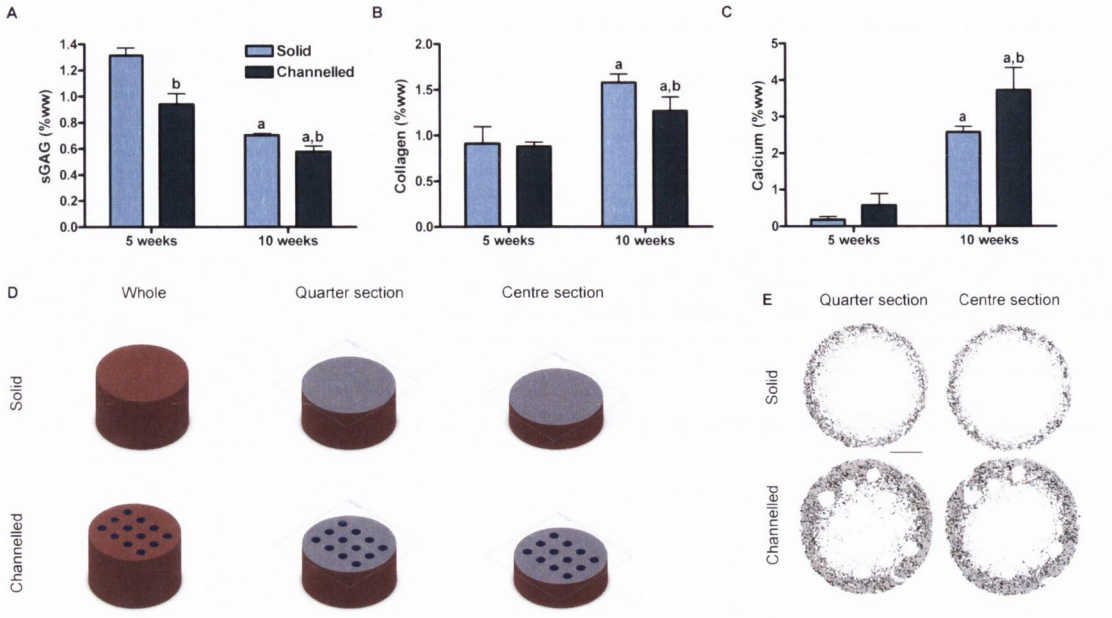

Figure 5.1.: *(A) sGAG, (B) collagen, (C) and calcium (% wet weight) accumulation of solid and channelled constructs after 5 and 10 weeks of in vitro culture (n=3-4). Significance $p<0.05$: a vs. 5 weeks, b vs. solid constructs (D) Illustration of spatial analysis of constructs, quarter section corresponds to a region $\approx$ 0.75 mm into the depth of the construct, centre section corresponds to a region $\approx$ 1.5 mm into the depth of the construct. (E) μCT analysis of solid and channelled constructs after 10 weeks in vitro culture, sections correspond to a thickness of 120 μm. Images are representative of three constructs analysed. Scale bar is 1 mm and is consistent across all images*

5.3.2. Channelled architectures accelerate in vivo mineralisation of MSC-seeded hydrogels

MSC-seeded solid and channelled hydrogels underwent 5 weeks of culture in chondrogenic conditions, followed by an additional week of culture in hypertrophic conditions, prior to subcutaneous implantation in nude mice. Constructs were harvested at 4 and 8 weeks post-implantation. The DNA content of solid constructs 4 and 8 weeks post-implantation were lower than pre- implantation levels, whereas the DNA content of channelled constructs was higher after 4 weeks *in vivo* compared to pre-implantation levels, and further increased after 8 weeks *in vivo*, see Figure 5.2(A). The sGAG content of both solid and channelled constructs

was lower 4 and 8 weeks post-implantation compared to pre-implantation levels, with solid constructs maintaining significantly higher levels of sGAG at both post-implantation time points compared to channelled constructs (0.34 ± 0.1 vs. 0.18 ± 0.07 %ww at 8 weeks post-implantation, p=0.0001), see Figure 5.2(B). Prior to implantation, collagen accumulation was similar in solid and channelled constructs. Collagen levels did not change in solid constructs post-implantation, whereas collagen accumulation was significantly higher in channelled constructs at 4 and 8 weeks post-implantation compared to pre-implantation levels (2.12 ± 0.53 vs. 1.2 ± 0.39 %ww, 8 weeks post-implantation vs. pre-implantation, p=0.0005), see Figure 5.2(C) . The calcium content of solid and channelled constructs increased at 4 weeks post-implantation compared to pre-implantation, with a further increase evident at 8 weeks post-implantation compared to 4 weeks post-implantation, see Figure 5.2(D) . Calcium accumulation in channelled constructs showed a trend towards a significant increase, as compared to solid constructs, at 4 weeks post-implantation (4.37 ± 0.61 vs. 3.27 ± 0.33 %ww, p=0.0593), with this difference becoming significant at 8 weeks post-implantation (7.97 ± 1.15 vs. 5.12 ± 0.53 %ww, p<0.0001).

Histological analysis of constructs, pre- and post- implantation, was carried out with constructs stained for alcian blue, picro-sirius red and alizarin red to assess the spatial distribution of sGAG, collagen, and calcium deposition respectively, see Figure 5.3. Prior to implantation, solid and channelled constructs stained positively and homogenously for alcian blue and picro- sirius red, whereas both constructs only stained positively for alizarin red around their periphery. At 4 weeks post-implantation, solid and channelled stained weakly for alcian blue with channels beginning to show positive staining for nuclear fast red. An increased number of channels stained positive for nuclear fast red at 8 weeks post-implantation. Tissue that had filled the channels also stained intensely for picro-sirius red at

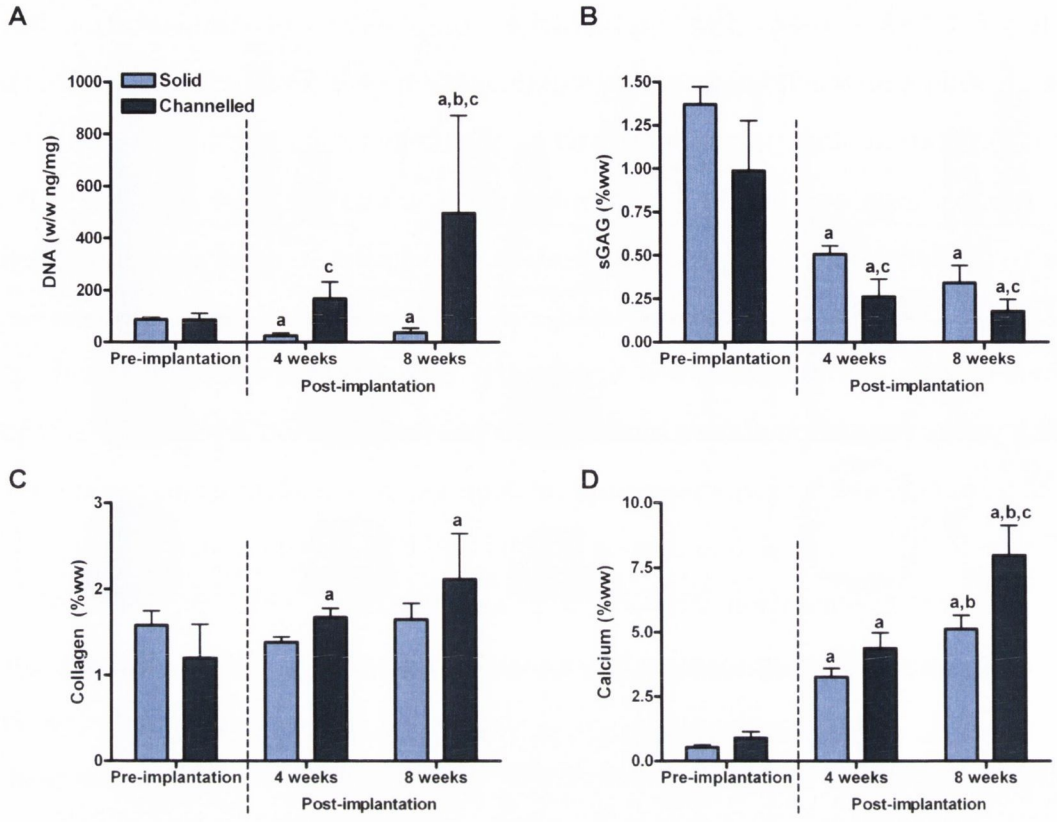

Figure 5.2.: *Biochemical analysis of constructs pre-implantation (n=3-4), and at 4 and 8 weeks post-implantation (n=4-6). (A) DNA content, normalised to mg wet weight. (B) sGAG, (C) collagen and (D) calcium content (% wet weight). Significance $p<0.05$: a vs pre-implantation, b vs. 4 weeks post-implantation, c vs. solid constructs.*

8 weeks post-implantation. At 4 weeks post-implantation, channelled constructs stained homogenously for alizarin red, whereas the staining in solid constructs was heterogeneous, with the core region of the engineered tissue staining negatively. H and E staining of acellular hydrogels 8 weeks post-implantation demonstrated no tissue formation in either solid or channelled constructs.

μCT analysis was performed on MSC- seeded hydrogels at 4 and 8 weeks post-implantation to assess the spatial distribution of mineral and its variance with depth through the construct, and also to quantify the volume of mineral in the construct. At 8 weeks post-implantation, at a depth of ≈ 0.75 mm from the tissue

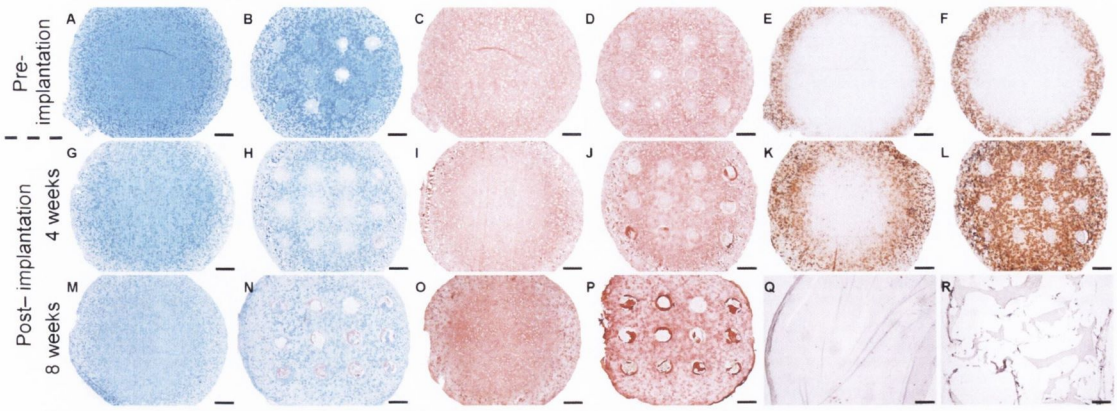

Figure 5.3.: *Histology of solid (A,C,E,G,I,K,M,O) and channelled (B,D,E,H,J,L,N,P) constructs pre-(A-F), 4 weeks post-implantation (G-L), and 8 weeks post-implantation (M-P). Alcian blue (A,B,G,H,M,N), picro-sirius red (C,D,I,J,O,P), alizarin red (E,F,K,L). H and E staining of acelluar solid (Q) and channelled (R) controls 8 weeks post-implantation. 8 week post-implantation samples were decalcified, hence no alizarin red staining was undertaken at this time point. Scale bars in A-P are 500 μm. Scale bars in Q-R are 250 μm*

surface, solid constructs had a core region devoid of mineral, whereas a homogenous deposition of mineral was observed in the channelled constructs, see Figure 5.5(A). At a depth of $\approx$ 1.5 mm from the surface, the core region devoid of mineral in solid constructs had increased in area. While there was also evidence of a non-mineralised core region developing in channelled constructs, this area appeared smaller than the corresponding region in the solid constructs. Mineral volume, as quantified by μCT, was significantly higher for channelled constructs as compared to solid constructs at both 4 and 8 weeks post-implantation (44.99 $\pm$ 6.54 vs. 28.54 $\pm$ 1.53 % $\text{Vol}_{mineral}/\text{Vol}_{total}$, channelled constructs vs. solid constructs at 8 weeks post-implantation, p=0.014), see Figure 5.5(B).

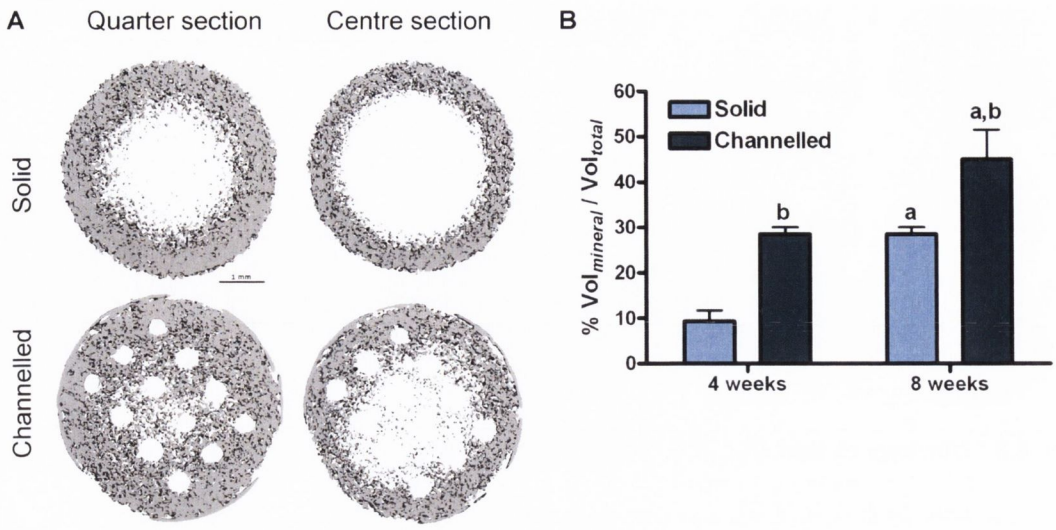

Figure 5.4.: *μCT analysis of solid and channelled constructs post-implantation. (A) μCT images of constructs 8 weeks post-implantation showing ppatial variance of mineralisation with depth through the construct. Quarter section corresponds to a region ≈ 0.75 mm into the depth of the construct, centre section corresponds to a region ≈ 1.5 mm into the depth of the construct. Sections correspond to a thickness of 120 μm. Images are representative of three constructs analysed. Scale bar is 1 mm and is consistent across all images (B) % volume of mineral per total volume of construct (n=3), significance p<0.05: a vs. 4 weeks, b vs solid constructs.*

5.3.3. Channels act as conduits for vascularisation and provide a milieu for endochondral bone and marrow formation

Histological and immunohistochemical analysis was carried out on constructs to investigate vascularisation and *de novo* tissue formation within the channels, and to determine the pathway through which this tissue formation occurs. H and E staining of solid constructs did not demonstrate bone formation 4 weeks post-implantation, see Figure 5.5(A). H and E staining of channelled constructs at 4 weeks post-implantation demonstrated woven bone formation within the channels, surrounding a marrow component consisting of a mixture of hematopoietic foci and marrow adipose tissue, see Figure 5.5(B). At 8 weeks post-implantation, no bone was evident in solid constructs, see Figure 5.5(C), whereas within the channels

of channelled constructs lamellar-like bone was evident, with the appearance of osteocyte-like cells embedded within the bone matrix, which again surrounded a marrow component, see Figure 5.5(D).

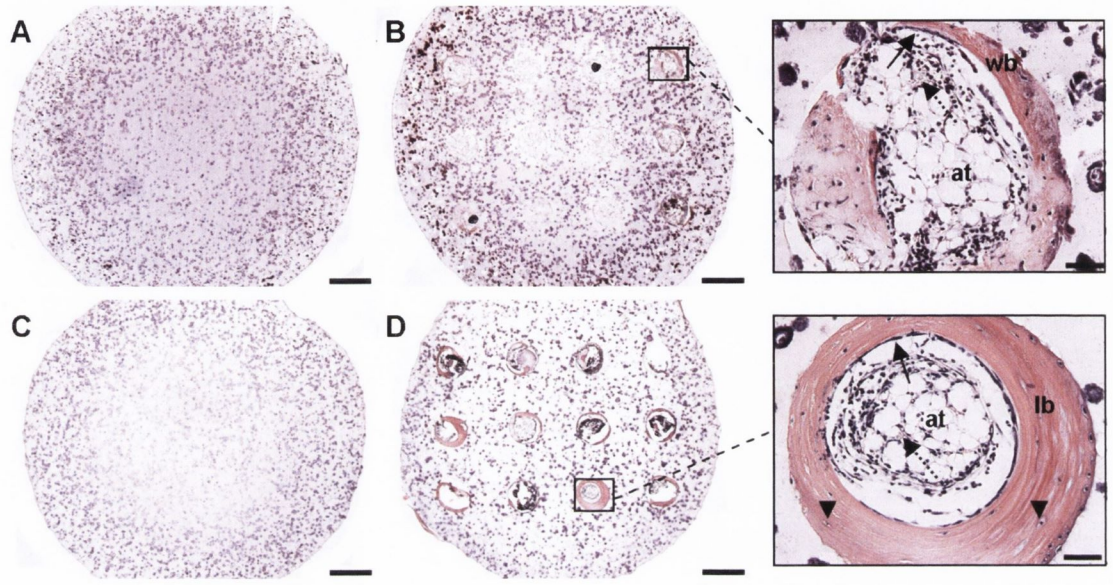

Figure 5.5.: *H and E staining of solid (A,C) and channelled (B,D) constructs 4 weeks post-implantation (A,B) and 8 weeks post-implantation (C,D). Arrows show lining of osteoblasts laying down new bone, arrowheads show osteocytes embedded within bone matrix, dotted arrows show hematopoietic elements. at - adipose tissue, wb - woven bone, lb - lamellar bone. Main image scale bars are 500 μm. Inset scale bars are 50 μm*

At 4 weeks post-implantation channels were stained for H and E and for CD31 to examine the presence of blood vessels and endothelial cells. TdT staining was also carried out to assess the proportion of lymphoid marrow cells in the cellular marrow. Blood vessel-like structures were identified by H and E staining and CD31 staining, see Figure 5.6(A,B). Vascularisation did not appear to progress significantly from the channels into the calcified cartilage within the hydrogel. TdT staining at 4 weeks post implantation indicated a scanty positive staining as expected for normal marrow, see Figure 5.6(C). Macroscopic examination also suggested the presence of hematopoietic elements within channels following implantation, see appendix Figure A.3.

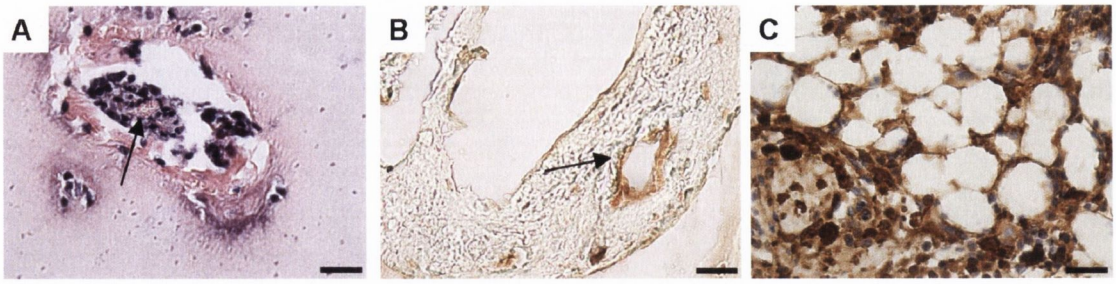

Figure 5.6.: *High magnificantion images of channels 4 weeks post-implantation stained with H and E (A), CD31 (B), and TdT (C). Arrows indicate vessel-like structures. Brown and blue staining in (C) indicate cells positive and negative for TdT respectively. Scale bars are 25 μm*

Prior to subcutaneous implantation (i.e. during the *in vitro* priming phase), channels had partially filled with a cartilaginous matrix containing MSCs which stained intensely for alcian blue and collagen type II and negatively for collagens type I and X, see Figure 5.7(A-D). At 4 weeks post-implantation channels stained very weakly for alcian blue, and very intensely for collagen type I, see Figure 5.7(E-F). At this time point a decrease in the intensity of staining for collagen type II, as well as an increase in the intensity of staining for collagen type X, was also observed within channels as compared to pre-implantation levels, see Figure 5.7(G-H). This suggests that the cartilage that had filled the channels *in vitro* supported endochondral bone formation *in vivo*.

5.4. Discussion

New vessel formation is critical for bone tissue regeneration. During long bone growth, canals within the developing hypertrophic cartilage facilitate vascular invasion and the migration of osteogenic cells, thus playing a key role in endochondral ossification. The aim of this study was to recapitulate this cartilage canal network in tissue engineered hypertrophic cartilaginous constructs. It was hypothesised that recapitulating this network by introducing an array of channels into MSC seeded

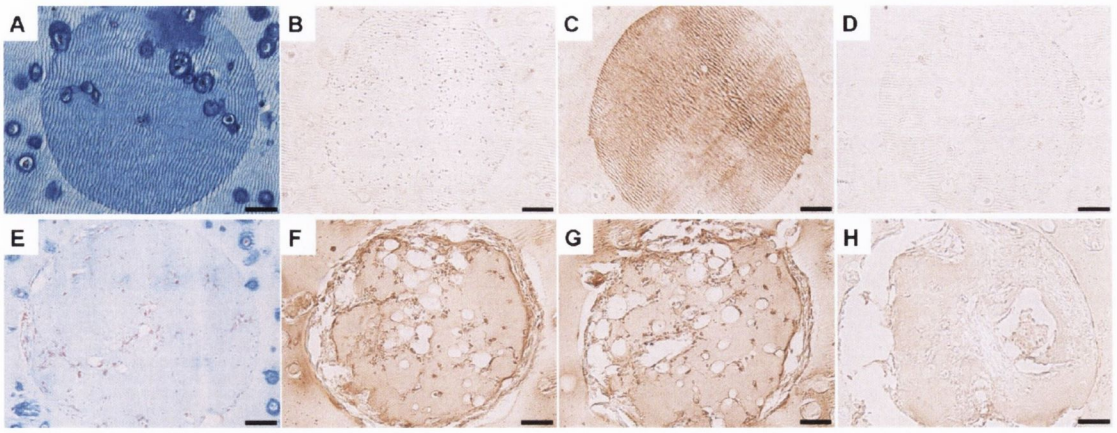

Figure 5.7.: *Alcian blue (A,E), collagen I (B,F), collagen II (C,G) and collagen X (D,H) staining of channels pre-implantation (A-D) and 4 weeks post-implantation (E-H). Scale bars are 50 μm*

constructs would firstly facilitate the *in vitro* engineering of scaled-up hypertrophic cartilaginous tissues, and secondly, would accelerate the vascularisation and mineralisation of the engineered graft following implantation *in vivo*. During long-term *in vitro* culture, the presence of this array of channels lead to a reduction in total sGAG and collagen accumulation, whereas calcium deposition was enhanced in channelled constructs. In support of the hypothesis, the channels acted as conduits for blood vessel infiltration and their presence accelerated mineralisation of the engineered tissue *in vivo*. Finally, channels themselves provided a milieu for bone and marrow formation, with *de novo* bone being generated via the endochondral pathway.

Previous studies have investigated introducing nutrient channels into cartilaginous constructs in order to enhance the matrix synthesis and the functional properties of tissue engineered cartilage (Buckley et al., 2009b). For example, the introduction of a single nutrient channel into chondrocyte seeded agarose hydrogels results in superior mechanical properties and the formation of a more uniform fibrillar network whilst maintaining similar levels of sGAG and collagen content (Bian et al., 2009). In the present study, scaffold architecture differentially regulated matrix

synthesis, with solid constructs accumulating significantly more sGAG and collagen, and channelled constructs accumulating significantly more calcium. It may be that the channels provide a pathway for the diffusion of sGAGs and collagen out of the engineered tissue and into the media, and that calcium deposition is less influenced by such phenomena. Alternatively, or perhaps in conjunction, it may be that the altered rates of sGAG, collagen and calcium deposition in solid and channelled constructs is due to differences in the spatial gradients in regulatory cues that develop in these tissues. In solid hydrogels, the cellular consumption of oxygen at the periphery of the construct will result in the development of a low oxygen microenvironment within the core (Buckley et al., 2012; Thorpe et al., 2013), which has been shown to enhance sGAG and collagen synthesis (Meyer et al., 2010; Sheehy et al., 2012). The introduction of channels into scaffolds may increase core oxygen levels (Buckley and O'Kelly, 2010), which has been shown to enhance hypertrophy and mineralisation of chondrogenically primed MSCs (Gawlitta et al., 2012; Sheehy et al., 2012).

Previous attempts to engineer scaled-up cartilaginous grafts for endochondral bone repair have reported the development of a core region devoid of cells and cartilaginous matrix (Scotti et al., 2013). This phenomenon was not observed in the present study. However, if the endochondral approach is to be implemented to treat critically sized bone defects further scaling-up of *in vitro* cartilaginous grafts will be required, and at these very large scales nutrient diffusion limitations are likely to develop within the construct. It is perhaps only at these dimensions, and where core degradation would otherwise occur, that the introduction of channels would benefit the *in vitro* development of an engineered cartilaginous tissue.

Following *in vivo* implantation, biochemical and histological analysis of MSC-seeded constructs revealed a reduction in sGAG content and an increase in calcium accumulation, indicating a loss of the chondrogenic phenotype and progression

down the endochondral route. Interestingly, while solid constructs maintained their pre-implantation collagen levels during the course of the *in vivo* implantation period, channelled constructs continued to accumulate collagen, which may be due in part to the formation of new tissue within the channels themselves. Both histological data and the DNA assay suggested that channels became highly cellularised once implanted *in vivo*. While we can not rule out a role played by donor cells, as there were MSCs present within channels pre-implantation, previous studies investigating bone tissue engineering via the endochondral pathway have highlighted an important role played by recruited host derived cells in endochondral ossification (Farrell et al., 2011; Tortelli et al., 2010). It would appear that the channels in the tissue engineered hypertrophic cartilaginous constructs may be acting as conduits for cellular infiltration from the host, which are then playing a role in laying down new tissue within the construct.

In bone tissue engineering strategies, the prevention of core necrosis during *in vitro* development and following *in vivo* implantation is a significant challenge (Lyons et al., 2010). In the present study, μCT was utilised to investigate the spatial variance of *in vivo* mineralisation with depth through the tissue and found that channelled architectures accelerated mineralisation promoting a more homogenous mineralised construct and limiting the development of a core region devoid of viable cells and mineral. In addition to the inherent increase in nutrients and oxygen due to presence of the channels, they also facilitate blood vessel infiltration as evident by staining for CD31+ endothelial cells, which in turn further increases oxygen levels and provides soluble factors and signals to promote osteogenesis (Brandi and Collin-Osdoby, 2006).

Subcutaneous implantation of chondrogenically primed MSCs has been shown to produce endochondral bone containing hematopoietic marrow at 8 weeks post-implantation (Janicki et al., 2010; Scotti et al., 2010). In the present study, high

magnification images of channels at 4 weeks post implantation demonstrated deposition of an immature woven bone, being laid down by osteoblasts, which at 8 weeks post-implantation had developed into lamellar bone with osteocyte-like cells evident within the bone matrix. Temporal analysis of chondrogenic extracellular matrix progression within channels indicated degradation of the sGAG/collagen type II rich-matrix following *in vivo* implantation, and a corresponding increase in the accumulation of collagen type I and collagen type X, signifying that *de novo* bone found in the channels was being generated via the endochondral pathway. Moreover, at both *in vivo* time points there was evidence of hematopoietic foci and marrow adipose tissue, enclosed within the developing bone matrix. Given that it has previously been demonstrated that endochondral ossification is required for hematopoietic stem cell niche formation (Chan et al., 2009), this provides further validation that the mechanism through which bone is formed is indeed endochondral.

In the current study cartilaginous tissues were engineered using 4 month old, skeletally immature, porcine MSCs. Skeletally immature MSC seeded hydrogels have been shown to generate cartilaginous tissues with superior matrix deposition and mechanical properties as compared to skeletally mature MSC seeded hydrogels (Erickson et al., 2011). Further studies are required to confirm if the beneficial effect of channels, as shown in this study, would occur with the use of engineered tissues generated from a skeletally mature donor where the inherent regenerative capacity is not as high.

Bone tissue engineering via endochondral ossification has recently been demonstrated with collagen mesh scaffolds (Scotti et al., 2013), on three-dimensional electrospun fibers (Yang et al., 2013), and with the bone void filler NuOss (Weiss et al., 2012). Utilising hydrogels as scaffolds for endochondral bone regeneration may be a particularly powerful tool in scaling up tissue engineered grafts in order to

treat defects of a clinically relevant size (Buckley et al., 2012). However, the chondrogenically primed MSC-seeded agarose hydrogels utilised in this study appeared to only partially support progression towards endochondral ossification, with the engineered tissue laid down in the main body of the hydrogel apparently locked within a hypertrophic, calcified cartilage state at 8 weeks post-implantation. Since the cartilaginous matrix within channels, which had filled up naturally *in vitro* with scaffold-free tissue, had the ability to undergo full endochondral ossification *in vivo* it would appear that the agarose hydrogel acted as a barrier for vascularisation and the transition from mineralised cartilage to endochondral bone. This may be due to the agarose hydrogel undergoing minimal degradation during the 8 week *in vivo* period. A previous study investigating alginate hydrogels as scaffolds for bone tissue engineering demonstrated enhanced bone formation by accelerating the degradation properties of the hydrogel (Simmons et al., 2004). Future chapters in this thesis will examine the capacity of different naturally derived biodegradable hydrogels to produce endochondral bone *in vivo*.

5.5. Concluding remarks

Recapitulating the cartilage canal network observed during endochondral skeletogenesis, through tissue engineering channelled hypertrophic cartilaginous constructs, accelerates mineralisation and vascularisation of the engineered graft and shows promise for use in future endochondral bone regeneration strategies. The chapter reinforces the importance of optimising the architecture of engineered constructs targeting bone tissue regeneration, even if this is achieved via an endochondral pathway as opposed to the traditional intramembranous route. Chapters 7 and 8 will utilise this approach when engineering endochondral bone.

To date, this thesis has either focussed on engineering cartilage *in vitro*, or

bone via endochondral ossification *in vivo*. However, if the endochondral approach is to be used to resurface an entire joint, or to engineer a whole bone, it must be capable of generating an ostechondral tissue; i.e. a structure two-part tissue containing both cartilage and bone within the same construct. Chapter 6 will investigate if osteochondral constructs can be engineered through spatial regulation of endochondral ossification.

6 Modulating endochondral ossification to engineer osteochondral constructs

6.1. Introduction

Articular cartilage has a limited capacity for self-renewal and repair. Damage to the articular surface can penetrate to the subchondral bone and such osteochondral defects are often associated with mechanical instability of the joint and warrant surgical intervention in order to prevent osteoarthritic degenerative changes (Martin et al., 2007). Even in cases where lesions do not penetrate to the subchondral bone an osteochondral construct may be a more desirable implant, as a bone to bone interface integrates better than a cartilage to cartilage interface (Schaefer et al., 2002). Autologous grafting procedures, such as mosaicplasty, are not ideal due to issues associated with topology conformity, donor site morbidity and tissue availability (Grayson et al., 2008). Tissue engineering applications aim to replace or regenerate damaged tissues through the combination of cells, three-dimensional scaffolds and signalling molecules (Langer, 2000; Koh and Atala, 2004). A number of strategies have been implemented to engineer osteochondral constructs, including

bi-phasic scaffolding (Gao et al., 2001; Oliveira et al., 2006; Mano and Reis, 2007; Khanarian et al., 2012; St-Pierre et al., 2012; Rodrigues et al., 2012; Theodoropoulos et al., 2011), bioreactor technologies (Wendt et al., 2005; Mahmoudifar and Doran, 2005; Grayson et al., 2010; Wang et al., 2004), and growth factor/gene delivery (Mason et al., 1998; Guo et al., 2009; Chen et al., 2011; Guo et al., 2010). Engineered anatomically accurate osteochondral grafts have also been suggested as a potential approach to joint condyle repair (Alhadlaq et al., 2004, 2005).

It is possible to engineer functional cartilaginous tissues by embedding chondrocytes in three-dimensional hydrogels (Mauck et al., 2000, 2002; Byers et al., 2008; Buckley et al., 2010; Vinardell et al., 2009). Well-documented limitations associated with chondrocytes (Barbero et al., 2004; Diaz-Romero et al., 2005) have led to increased interest in the use of mesenchymal stem cells (MSCs) for functional cartilage tissue engineering strategies (Vinardell et al., 2011; Sheehy et al., 2011; Erickson et al., 2009; Mauck et al., 2006; Thorpe et al., 2008, 2010). A major challenge in MSC-based cartilage repair therapies is the prevention of terminal differentiation, as maintenance of the chondrogenic phenotype is critical in order to ensure the long-term *in vivo* stability of a cartilaginous graft (Dickhut et al., 2009). When implanted subcutaneously in nude mice chondrogenically primed MSCs fail to produce cartilage resistant to hypertrophy and endochondral ossification, unlike fully differentiated chondrocytes, which are capable of producing stable cartilage *in vivo* (Pelttari et al., 2006; Vinardell et al., 2012b).

This apparent obstacle in MSC-based cartilage tissue engineering has recently been realised as a potential advantage in bone regeneration applications with chondrogenically primed bone marrow-derived MSCs being used to engineer bone *in vivo* via endochondral ossification (Scotti et al., 2010; Janicki et al., 2010; Farrell et al., 2011). One rationale as to why the endochondral route may be superior to the traditional intramembranous process for bone regeneration is that hypertrophic

chondrocytes are programmed to withstand the initial hypoxic conditions a tissue engineered graft will experience once implanted *in vivo* (Farrell et al., 2009). In contrast, osteogenically primed constructs often fail due to excessive *in vitro* mineralisation of the extracellular matrix inhibiting vascular invasion and the associated delivery of oxygen and nutrients into the engineered tissue (Lyons et al., 2010). Another inherent advantage of chondrogenically primed MSCs for bone regeneration is that they are programmed to release factors that drive the mineralisation and vascularisation of the engineered tissue (Farrell et al., 2009). Modulating the endochondral phenotype of chondrogenically primed bone marrow-derived MSCs may be an attractive approach to engineering the osseous phase of an osteochondral implant.

The objective of this study was to engineer an osteochondral tissue by promoting endochondral ossification in one layer of a chondrogenically primed bilayered hydrogel and stable cartilage in another. Bilayered hydrogels were fabricated by casting agarose seeded with chondrocytes (for the chondral layer) on top of agarose hydrogels seeded with MSCs (for the osseous layer). It was hypothesised that by seeding the top layer of agarose hydrogels with chondrocytes and the bottom layer with bone marrow-derived MSCs it would be possible to spatially restrict endochondral ossification to within the bottom layer both *in vitro* and *in vivo* following subcutaneous implantation in nude mice.

6.2. Materials and methods

6.2.1. Experimental design

This study consisted of three experiments. Experiment 1 investigated the synergistic effects of a structured co-culture of chondrocytes and bone marrow MSCs, comparing chondrogenesis and terminal differentiation in single layer chondrocyte- and MSC-

seeded agarose hydrogels with a bilayered agarose hydrogel where the top layer is seeded with chondrocytes and the bottom layer with MSCs. All constructs were maintained in chondrogenic medium (CM) supplemented with transforming growth factor-β3 (TGF-β3) for a period of 49 days. Experiment 2 investigated whether a hypertrophic medium could be used to engineer an osteochondral construct *in vitro* and involved culturing bilayered agarose hydrogels in CM for a period of 21 days after which the constructs were either maintained in CM for an additional 49 days, or transferred to a hypertrophic medium (HM) with (+) or without (-) β-glycerophosphate supplementation. Experiment 3 investigated the possibility of spatially regulating endochondral ossification *in vivo*. This involved culture of single layer MSC-seeded agarose hydrogels and bilayered agarose hydrogels in CM for a period of 21 days after which constructs were implanted subcutaneously in nude mice for an additional 28 days. The experimental design is illustrated in Figure 6.1.

6.2.2. Cell isolation and expansion

Chondrocytes and bone-marrow derived MSCs were isolated as described in section 4.2.2. Upon isolation chondrocytes and bone marrow derived MSCs were seeded at a density of 5 x 10^3 cells/cm^2 in 175 cm^2 T flasks, maintained in DMEM GlutaMax supplemented with 10% foetal bovine serum, 100 U/mL penicillin/streptomycin (both Gibco) and 5 ng/mL human fibroblast growth factor-2 (Prospec-Tany Techno-Gene Ltd., Israel), and expanded to passage two ($\approx$ 11 population doublings for chondrocytes and 14 population doublings for MSCs).

6.2.3. Cell encapsulation in agarose hydrogels

Expanded chondrocytes and MSCs were separately suspended in 2% agarose (type VII; Sigma-Aldrich) at $\approx$40° C and a density of 20 x 10^6 cells/mL and cast in a

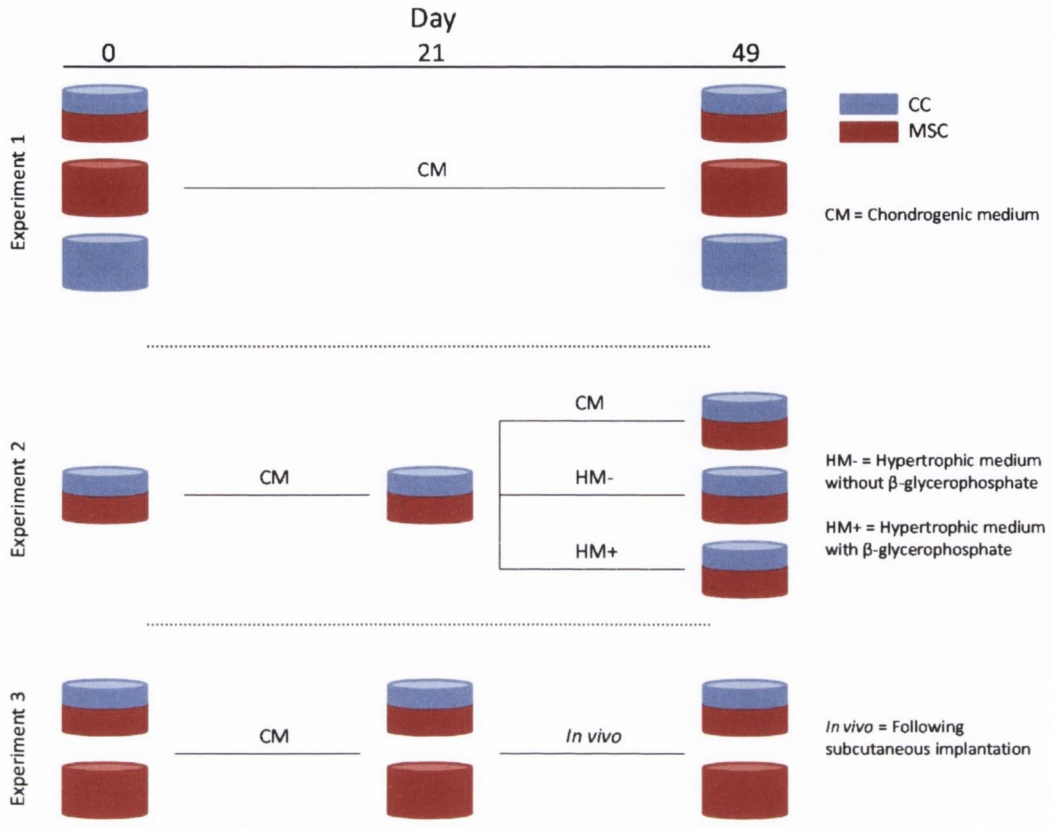

Figure 6.1.: *Schematic of experimental design. MSC, mesenchymal stem cell; CC, chondrocyte*

stainless steel mould to produce cylindrical (⊘ 5 x 3 mm) single-layered constructs. Bi-layered constructs (⊘ 5 x 3 mm) were fabricated by filling the bottom half (1.5 mm) of stainless steel moulds with MSC laden 2% agarose at ≈40° C and allowing the agarose cell suspension to set (termed osseous layer). Thereafter the top half of the mould was filled with chondrocyte laden 2% agarose at ≈40° C and left to set (termed chondral layer). The bottom surface of all bi-layered constructs were cast on a hatch patterned poly-dimethyl-siloxane (PDMS) sheet so that both layers of the construct could be identified. All constructs were maintained in a chemically defined CM consisting of DMEM GlutaMAX supplemented with 100 U/mL penicillin/streptomycin (both Gibco), 100 μg/mL sodium pyruvate, 40 μg/mL L-proline, 50 μg/mL L-ascorbic acid-2-phosphate, 4.7 μg/mL linoleic

acid, 1.5 mg/mL bovine serum albumine, 1x insulin-transferrin-selenium, 100 nM dexamethasone (all from Sigma-Aldrich) and 10 ng/mL of human transforming growth factor-β3 (TGF-β3) (Prospec-Tany TechnoGene Ltd., Israel) for 21 days. In experiment 1 all constructs were maintained in a CM for a further 28 days. In experiment 2, bi-layered constructs were either maintained in a CM or transferred to a hypertrophic medium, which constituted the removal of TGF-β3, the addition of 1 nM L-thyroxine (Sigma-Aldrich) and a reduction in the level of dexamethasone to 1 nM, either with (HM+) or without (HM-) the supplementation of 20 μg/ml β-glycerophosphate (Sigma-Aldrich), for a further 28 days.

6.2.4. In vivo subcutaneous transplantation

In experiment 3, following 21 days maintenance in a CM, single layer MSC- seeded constructs and bi-layered constructs were implanted subcutaneously into the back of nude mice (Balb/c; Harlan, Uk) as described in section 5.2.5. Mice were sacrificed 4 weeks post-implantation by CO_2 inhalation. The animal protocol was reviewed and approved by the ethics committee of Trinity College Dublin.

6.2.5. Biochemical analysis

Constructs were sliced in half transversely, digested in papain and analysed biochemically for DNA, sGAG and collagen content, as described in section 3.2.7. 3-4 samples were analysed per experimental group.

6.2.6. Histology and Immunohistochemistry

At each time point samples were fixed in 4% paraformaldehyde overnight, dehydrated in a graded series of ethanols, embedded in paraffin wax, sectioned at 5 μm and affixed to microscope slides. Alcian blue, picro-sirius red and alizarin red

histological stains, and collagen type I, II and X immunohistochemical stains, were carried out as described in section 3.2.8.

6.2.7. Micro-computed tomography

Micro-computed tomography (μCT) scans were carried out on the *in vivo* specimens using a Scanco Medical 40 μCT system (Scanco Medical, Bassersdorf, Switzerland), in order to quantify mineral content. Constructs were scanned in PBS, at a voxel resolution of 12 μm, a voltage of 70 kVp, and a current of 114 μA. Circular contours were drawn around the constructs. A Gaussian filter (sigma=0.8, support=1) was used to suppress noise and a global threshold of 105, corresponding to a density of 105.4 mg hydroxyapatite/cm^3, was applied. This threshold was selected by visual inspection of individual scan slices so as to include mineralised tissue and exclude non-mineralised tissue. 3D evaluation was carried out on the segmented images to determine mineral volume and to reconstruct a 3D image. 3 constructs were analysed per experimental group.

6.2.8. Statistical analysis

All statistical analyses were carried out using Minitab 15.1. Results are reported as mean $\pm$ standard deviation. Groups were analysed by a general linear model for analysis of variance with groups of factors. Tukey's test was used to compare conditions. Anderson-Darling normality tests were conducted on residuals to confirm a normal distribution. Significance was accepted at a level of $p<0.05$.

6.3. Results

6.3.1. A structured bilayered co-culture enhances chondrogenesis in the chondral layer of engineered constructs and suppresses hypertrophy and mineralisation in the osseous layer

Cartilage-specific matrix synthesis in constructs seeded only with chondrocytes or MSCs (termed single layer constructs) was compared with that in bilayered constructs where the top layer was seeded with chondrocytes (termed the chondral layer) and the bottom layer with MSCs (termed the osseous layer). Chondrocytes synthesised significantly more sGAG compared with MSCs in both single layer constructs and in bilayered constructs (Figure 6.2(a)). A structured co-culture of chondrocytes and MSCs significantly enhanced collagen synthesis in the top chondral layer of bilayered engineered constructs compared with single layer constructs that contained only chondrocytes (133.32 $\pm$ 21.8 vs. 72.45 $\pm$ 18.63 ng/ng, $p < 0.001$). In contrast, MSCs in single layer constructs accumulated significantly more collagen compared with MSCs in the bottom osseous layer of bilayered constructs (154.65 $\pm$ 14.53 vs. 83.57 $\pm$ 21.38 ng/ng, $p < 0.001$) (Figure 6.2(b)). No significant increases in DNA levels were observed in single layer or bilayered constructs over 49 days of *in vitro* chondrogenic culture (data not shown). All constructs stained positive for alcian blue (Figure 6.3). Single layer MSC constructs also stained positive for alizarin red, a marker of mineralisation, around the construct periphery. No alizarin red staining was observed in the osseous layer of bilayered constructs. In agreement with the biochemical analysis (Figure 6.2), the chondral layer of bilayered constructs stained more intensely for picro-sirius red compared with single layer chondrocyte constructs and the osseous layer stained weaker for picro-sirius

red compared with single layer MSC constructs. Immunohistochemical analysis demonstrated stronger staining for type II collagen in the chondral layer of the bilayered constructs compared with single layer chondrocyte constructs and weaker staining for type X collagen in the osseous layer compared with single layer MSC constructs (Figure 6.4). In general all constructs stained weakly for collagen type I accumulation.

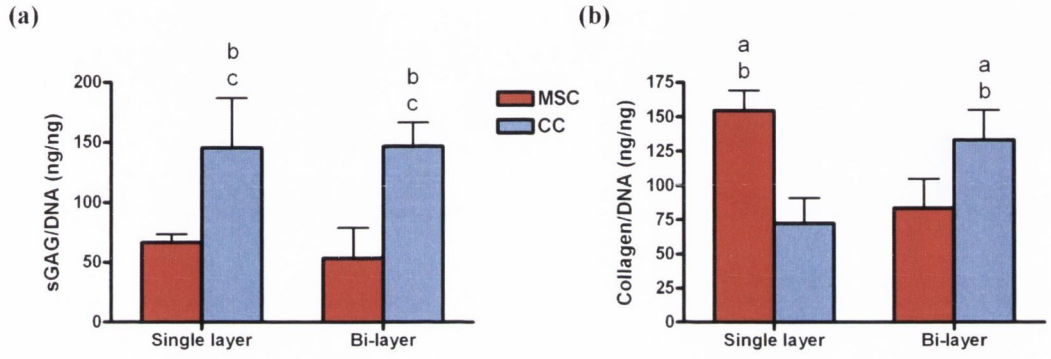

Figure 6.2.: *Experiment 1. (a) sGAG and (b) collagen content normalised to DNA for single layer and bilayer constructs cultured in chondrogenic medium for 49 days (n = 3-4). MSC, mesenchymal stem cell; CC, chondrocyte. Significance $P < 0.05$, a vs. single layer CC, b vs. single layer MSC, c vs. bilayer MSC.*

6.3.2. A hypertrophic medium induces in vitro mineralisation of the osseous layer of bilayered constructs

No evidence of mineralisation was observed in bilayered constructs maintained in hypertrophic medium without additional β-glycerophosphate supplementation (HM-). When β-glycerophosphate was added to the hypertophic medium (HM+) mineralisation of the osseous layer was observed, as demonstrated by intense alizarin red staining (Figure 6.5a). Both hypertrophic media formulations resulted in apparent elongation of the interface between the osseous and chondral layers of bilayered constructs. sGAG accumulation in the chondral layer of the engineered

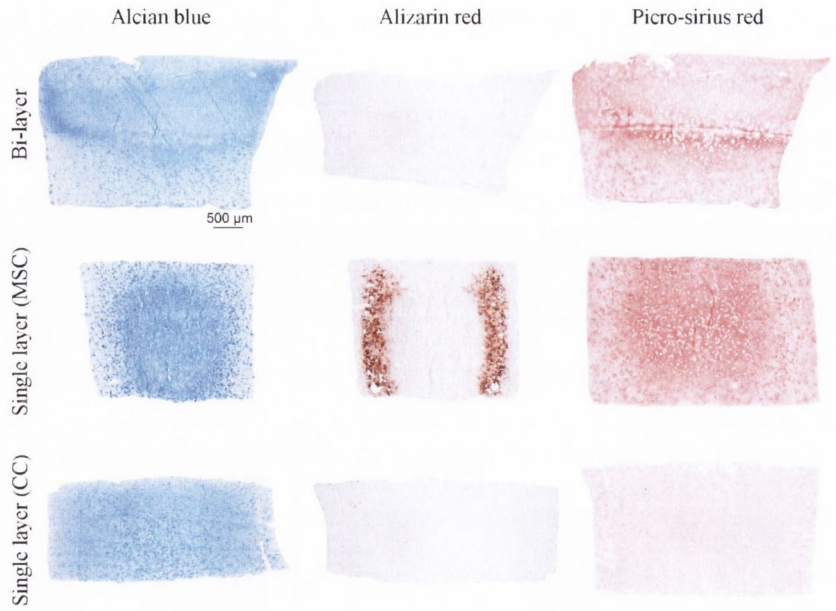

Figure 6.3.: *Experiment 1. Histology of single layer and bilayer constructs cultured in chondrogenic medium for 49 days. MSC, mesenchymal stem cell; CC, chondrocyte. One construct was sliced and stained per group.*

tissue was significantly reduced for constructs maintained in HM+ compared with CM (Figure 6.5b). No significant differences were observed in collagen accumulation between the CM, HM- and HM+ groups (Figure 6.5c). Mineralisation of the osseous layer correlated with significant cell death, as evident by a reduction in the DNA content in this layer of bilayered constructs when cultured in hypertrophic medium with additional β-glycerophosphate supplementation (HM+) (Figure 6.5d).

6.3.3. Endochondral ossification can be spatially regulated in vivo

Prior to subcutaneous implantation in nude mice both bilayered and single layer MSC constructs stained positively for alcian blue. No mineralisation of the osseous layer of bilayered constructs occurred prior to implantation, whereas evidence of mineralisation was observed around the periphery of single layer MSC constructs,

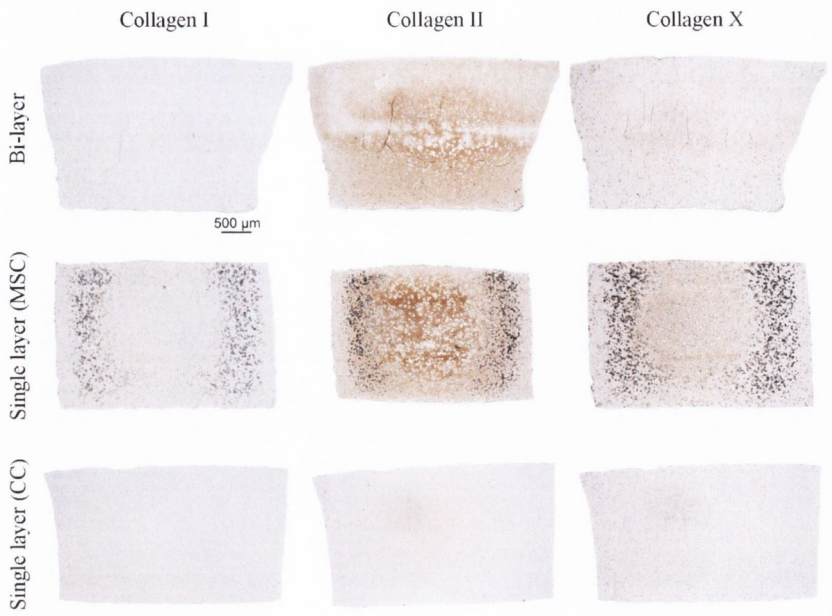

Figure 6.4.: *Experiment 1. Immunohistochemistry of single layer and bilayer constructs cultured in chondrogenic medium for 49 days. MSC, mesenchymal stem cell; CC, chondrocyte. Brown staining indicates positive immunostaining. Black staining indicates non-specific staining, thought to be mineralised regions of the tissue. One construct was sliced and stained per group.*

as demonstrated by alizarin red staining (Figure 6.6a). 4 weeks after subcutaneous implantation the chondral layer of bilayered constructs stained positive for alcian blue, with more intense staining observed in the deeper regions of this cartilage layer (Figure 6.6b). Endochondral ossification of the osseous layer had also commenced, as shown by strong alizarin red staining around the base of the construct with negligible staining observed at the interface with the chondral layer. Single layer MSC constructs continued to mineralise *in vivo*, with less intense alizarin red staining observed in the core of the constructs. Mineral volume, quantified via μCT (Figure 6.6b), was significantly greater for single layer MSC constructs compared with bilayered constructs (6.09 ± 0.59 vs. 1.36 ± 0.42 mm^3, $n = 3$, $p < 0.001$).

Bilayered constructs weakly stained for collagen types I and X prior to implantation (Figure 6.7a). Single layer MSC constructs were positively stained for

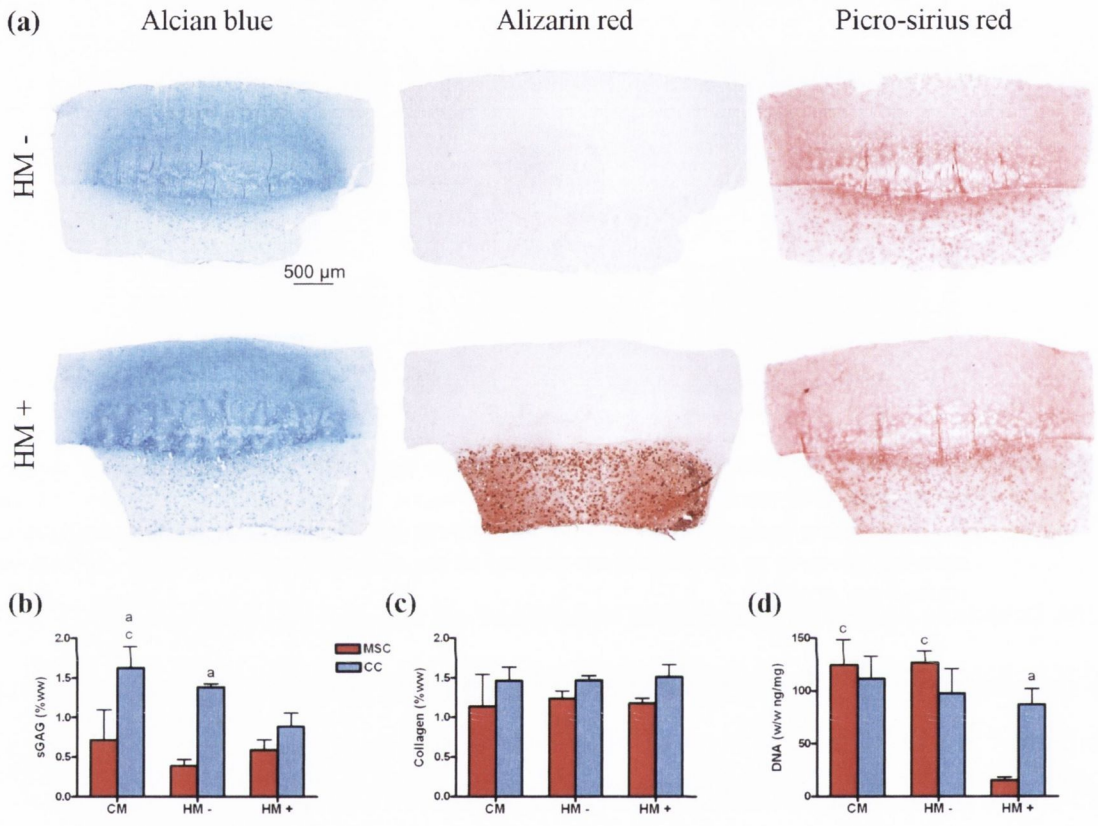

Figure 6.5.: *Experiment 2. (a) Histology of single layer and bilayer constructs cultured in chondrogenic medium for 21 days and then in hypertrophic medium either with (HM+) or without (HM-) β-glycerophosphate for an additional 28 days. One construct was sliced and stained per group. (b) sGAG and (c) collagen, normalised to percentage wet weight (% ww), and (d) DNA content for bilayer constructs cultured for 21 days in chondrogenic medium and then in chondrogenic medium (CM) or hypertrophic medium either with (HM+) or without (HM-) β-glycerophosphate for an additional 28 days (n = 3-4). Significance P < 0.05, a vs. MSC layer, b vs. HM-, c vs. HM+. MSC, mesenchymal stem cell; CC, chondrocyte.*

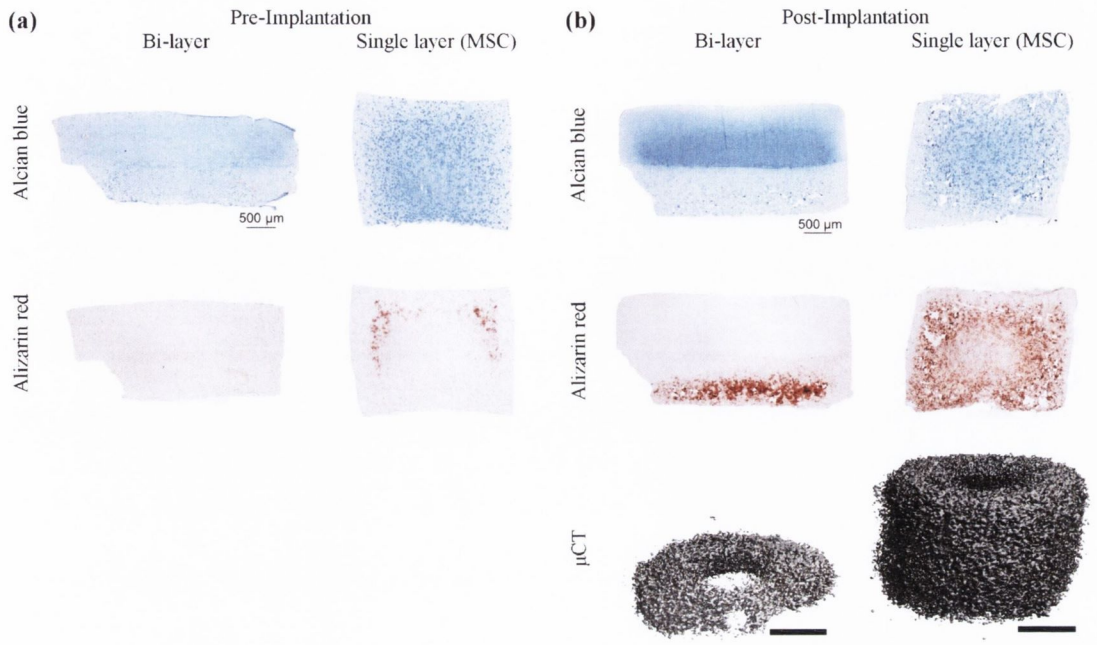

Figure 6.6.: *Experiment 3. (a) Histology of single layer MSC and bilayer constructs pre-implantation (day 21). (b) Histology and µCT analysis for single layer MSC and bilayer constructs post-implantation (day 49). µCT scale bar 1 mm. One construct was sliced and stained per group pre-implantation. Two constructs were sliced and stained per group post-implantation. Three constructs per group post-implantation were assessed by µCT.*

collagen type II but stained weakly for collagen types I and X prior to implantation. Post-implantation immunohistochemical analysis of the bilayered constructs demonstrated positive type II collagen staining in the chondral layer, with increased staining for collagen types I and X in the osseous layer compared with constructs pre-implantation (Figure 6.7b). Single layer MSC constructs demonstrated reduced collagen type II staining and increased collagen types I and X staining post implantation compared with pre-implantation.

6.4. Discussion

This study examined the effect of a structured bilayered co-culture on chondrogenesis of chondrocytes and bone marrow-derived MSCs seeded in agarose hydrogels and

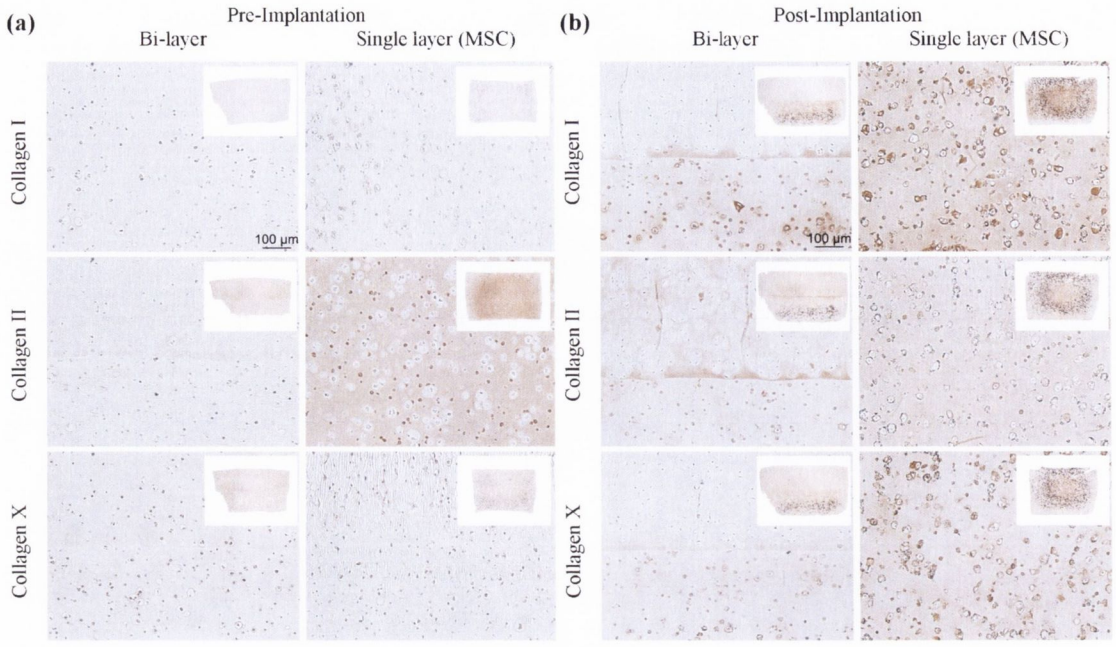

Figure 6.7.: *Experiment 3. Immunohistochemistry of single layer MSC and bilayer constructs (a) pre- and (b) post-implantation. The main images show high magnification images of the centres of the constructs. The inset images show the full constructs. Brown staining indicates positive immunostaining. Black staining indicates non-specific staining, thought to be mineralised regions of the tissue. One construct was sliced and stained per group pre-implantation. Two constructs were sliced and stained per group post-implantation.*

tested the hypothesis that it is possible to engineer an osteochondral construct *in vivo* through spatial regulation of endochondral ossification. *In vitro*, a structured bilayered co-culture enhanced type II collagen synthesis by chondrocytes seeded in the top chondral layer of the bilayered construct and reduced hypertrophy and mineralisation of MSCs in the bottom osseous layer. Mineralisation of the osseous layer of chondrogenically primed bilayered constructs could be achieved *in vitro* through culture in a hypertrophic medium supplemented with β-glycerophosphate. Perhaps more importantly, mineralisation of the osseous layer also occurred *in vivo*, resulting in the development of an osteochondral construct consisting of a layer of stable cartilage on top of a layer of calcifying cartilage undergoing endochondral ossification.

Previous studies have demonstrated that *in vitro* hypertrophy of MSCs is inhibited through co-culture with chondrocytes (Cooke et al., 2011; Bian et al., 2011), with parathyroid hormone-related protein secreted by chondrocytes proposed as one mechanism by which this suppression of terminal differentiation occurs (Fischer et al., 2010). In the present study a structured bilayered chondrogenic co-culture differentially regulated the synthesis of collagen by chondrocytes and MSCs within the construct. Immunohistochemical staining demonstrated reduced type X collagen accumulation in the osseous layer of bilayered constructs while type II collagen accumulation increased in the chondral layer. This suggests that a structured bilayered coculture suppresses hypertrophy of MSCs and enhances chondrogenesis of chondrocytes. Single layer chondrocyte-seeded constructs stained weakly for collagen type II, indicating that a certain degree of dedifferentiation had occurred prior to hydrogel encapsulation. Previous studies have demonstrated that chondrocytes lose their chondrogenic phenotype when expanded in monolayer (Diaz-Romero et al., 2005). Interestingly, a structured co-culture of chondrocytes and MSCs acted to help re-establish a chondrogenic phenotype in the expanded chondrocytes within the chondral layer of the bilayered constructs. It has been reported that chondrogenically primed MSCs release growth factors and cytokines such as TGF-β3, bone morphogenetic protein 2, insulin-like growth factor 1 and fibroblast growth factor 2 (Sekiya et al., 2002), and such soluble factors may play a role in enhancing chondrogenesis of chondrocytes co-cultured with MSCs (Wu et al., 2011; Tsuchiya et al., 2004). Co-culture of chondrocytes and MSCs has also been shown to enhance proliferation of chondrocytes (Wu et al., 2011; Acharya et al., 2012), although such a phenomenon was not observed in our bilayered co-culture system. Direct cell to cell interaction may be required to drive the enhanced proliferation of chondrocytes when co-cultured with MSCs (Acharya et al., 2012), which is absent in our culture model as cells are separately encapsulated in the

different regions of the hydrogel.

Single layer MSC seeded constructs tended to mineralise around their periphery, even in chondrogenic medium. Previous studies have demonstrated that a higher oxygen tension exists in this region (Buckley et al., 2012), and such high oxygen tensions are known to enhance mineralisation of engineered cartilaginous constructs (Sheehy et al., 2012). To accelerate such mineralisation hypertrophic cartilaginous templates can be supplemented with β-glycerophosphate (Mueller and Tuan, 2008). When bilayered constructs were transferred to hypertrophic medium supplemented with β-glycerophosphate mineralisation of the MSC layer occurred, whereas the chondrocyte-seeded layer remained resistant to mineralisation. In hypertrophic media formulations, both with and without β-glycerophosphate supplementation, elongation of the interface between the two cell types was observed, suggesting perhaps that aspects of long bone growth are being mimicked in this culture system. The large reduction in DNA content in the mineralised phase of bilayered constructs cultured in the presence of β-glycerophosphate is also representative of endochondral bone formation, in which hypertrophic chondrocytes undergo apoptotic cell death (Kronenberg, 2003).

Chondrogenically primed bone marrow-derived MSCs have been shown to produce bone *in vivo* via endochondral ossification (Scotti et al., 2010; Janicki et al., 2010; Farrell et al., 2011). When implanted subcutaneously into nude mice the MSC layer of bilayered constructs proceeded along the endochondral route with mineralisation progressing from the bottom of the construct. Previous studies exploring the fate of chondrogenically primed MSC pellets within a subcutaneous environment have observed a mineralised peripheral collar surrounding an inner cartilaginous region after 4 weeks *in vivo*, which became almost completely resorbed by bone after 8 weeks *in vivo* (Scotti et al., 2010). Therefore the 4 week *in vivo* time point in the current study may not have been sufficient to achieve complete endochondral

ossification of the ossesous layer of the bilayered constructs (see Figure 6.6). When mineralisation of the osseous layer occurred *in vivo* no significant drop in DNA content was observed compared with pre-implantation levels (data not shown), unlike that seen upon transfer of bilayered constructs to HM+ in the *in vitro* study. This may be indicative of host cells invading the implant, thus maintaining a high DNA content. Indeed, host cells have been shown to play a key role in the endochondral ossification of cartilaginous templates (Farrell et al., 2011). It would also appear that the chondrocyte layer suppresses mineralisation of the MSCs located adjacent to the interface of the tissue. As mentioned previously, this suppression may be a result of the secretion of anti-hypertrophic factors such as parathyroid hormone-related protein by chondrocytes in the chondral layer of the engineered construct. Further studies are required to determine whether this suppression of endochondral ossification occurs at the construct interface in the long term.

A critical question that remains to be answered is how this process of endochondral ossification would proceed within such a bilayered construct implanted into a defect in a load bearing joint. The subcutaneous environment differs in a number of notable ways to the orthotopic environment. Mechanical cues, absent in the subcutaneous environment, such as hydrostatic pressure (Steward et al., 2012; Vinardell et al., 2012a) and dynamic compression (Bian et al., 2012; Thorpe et al., 2012), have been shown to play a role in regulating the endochondral phenotype of MSCs, as well as matrix production (Delaine-Smith and Reilly, 2011). The evolving intrinsic properties of the extracellular matrix may also play a role in driving this differentiation pathway (Reilly and Engler, 2010). Furthermore, the subcutaneous environment is well vascularised, which differs from the low oxygen microenvironment of articular cartilage. A low oxygen environment has been shown to suppress hypertrophy and markers of endochondral ossification in

chondrogenically primed MSCs (Sheehy et al., 2012). How such cues are integrated to regulate cell fate is a key question that needs to be addressed to enable any putative MSC-based therapy to be successfully used in the treatment of damaged and diseased joints.

Scaling up of engineered grafts, and the associated nutrient diffusion and waste removal limitations, is a major challenge that will need to be overcome if the proposed engineered constructs are to be used in the treatment of large joint defects. Motivated by the fact that no biologically based therapies exist to treat patients with osteoarthritis a number of studies have investigated engineering anatomically accurate osteochondral grafts for joint condyle repair (Alhadlaq et al., 2004, 2005; Hung et al., 2003; Lee et al., 2009). The endochondral approach described in this study may be a powerful tool in scaling up the osseous phase of such grafts as it is possible to engineer large cartilaginous grafts *in vitro* using MSCs as the low oxygen conditions that develop within these constructs supports chondrogenic differentiation and the functional development of the engineered tissue (Buckley et al., 2012). Future studies should explore the potential of the proposed bilayered constructs to treat large scale osteochondral defects within the articular surface of load bearing joints.

6.5. Concluding remarks

In a structured bilayered chondrogenic co-culture of chondrocytes and MSCs, chondrogenesis is enhanced in the chondrocyte seeded layer while hypertrophy and mineralisation is inhibited in the MSC-seeded layer. Mineralisation of the osseous layer of such a bilayered construct can be induced *in vitro* through culture in a hypertrophic medium supplemented with β-glycerophosphate or *in vivo* following subcutaneous implantation. Implanting chondrogenically primed bilayered

constructs containing chondrocytes and MSCs and spatially regulating endochondral ossification *in vivo* represents a promising new strategy for the treatment of osteochondral defects.

This bilayered approach will again be applied in chapter 8, which will examine the use of anatomically accurate osteochondral constructs for whole bone tissue engineering. Such an application however will require the use of a hydrogel that supports robust endochondral bone formation and the agarose hydrogel utilised in this chapter appeared to only partially support progression down the endochondral route. Chapter 7 will therefore compare the capacity of different MSC-seeded hydrogels to support hypertrophic chondrogenesis *in vitro* and to facilitate vascularisation and endochondral bone formation *in vivo*.

7 Natural hydrogels for endochondral bone tissue engineering

7.1. Introduction

The need for alternative therapies to the autograft, in order to treat critically sized bone defects, has resulted in increased interest in the use of tissue engineered constructs for bone regeneration. The scaling up of tissue engineered grafts to clinically relevant sizes requires the use of a supporting scaffold or hydrogel, and understanding how cell-scaffold interactions will regulate the terminal phenotype of the cell is critical when developing novel tissue engineering strategies. Due to limitations associated with the traditional intramembranous approach to bone tissue engineering (Lyons et al., 2010), there has been a recent shift towards utilising engineered hypertrophic cartilaginous grafts to generate bone through endochondral ossification (Scotti et al., 2010; Farrell et al., 2009), thereby recapitulating the natural mechanism by which long bones are formed during skeletogenesis. Chondrogenically primed mesenchymal stem cells (MSCs) have been shown to undergo endochondral ossification *in vivo* when seeded onto various scaffolds (Janicki et al.,

2010; Yang et al., 2013; Farrell et al., 2011). However, challenges remain when scaling up such constructs and a recent attempt to engineer up-scaled endochondral bone using a collagen mesh scaffold reported the development of a core region devoid of cells and matrix (Scotti et al., 2013).

The use of a hydrogel may be a powerful tool in scaling-up tissue engineered cartilaginous grafts, as hydrogels exhibit a high water content which mimics the 3D environment of native cartilage and a number of naturally derived hydrogels have been shown to support chondrogenesis of MSCs *in vitro* (Erickson et al., 2009; Mauck et al., 2006; Sheehy et al., 2011; Ma et al., 2012; Erickson et al., 2012). Futhermore, the low oxygen conditions which develop in large MSC-seeded hydrogels promote the deposition of cartilage-specific matrix within the construct (Buckley et al., 2012). Previous studies have compared the chondrogenic capabilities of MSC-seeded hydrogels *in vitro* (Awad et al., 2004; Bosnakovski et al., 2006; Coleman et al., 2007), and also the potential of chondrogenically primed MSC-seeded hydrogels to maintain a stable chondrogenic phenotype *in vivo* (Dickhut et al., 2008). However, no studies have examined the suitability of different MSC-seeded hydrogels for endochondral bone tissue engineering applications.

The objective of this study was to compare the capacity of different naturally derived MSC-seeded hydrogels (alginate, chitosan and fibrin) to undergo hypertrophic chondrogenesis *in vitro*, and to determine the capacity of such constructs to subsequently support vascularisation and endochondral bone formation *in vivo*. In the first phase of the study MSCs were encapsulated in alginate, chitosan, and fibrin hydrogels and cultured in chondrogenic conditions (5 weeks) followed by hypertrophic conditions (3 weeks). In the second phase of the study MSCs were encapsulated in alginate, chitosan, and fibrin hydrogels and subjected to a shorter *in vitro* culture period (6 weeks) prior to subcutaneous implantation in nude mice, to be harvested 6 weeks post-implantation.

7.2. Materials and methods

7.2.1. Cell isolation and expansion

Bone marrow derived MSCs were isolated and expanded as described in section 4.2.2. Following colony formation, MSCs were trypsinised, counted, seeded at density of 5 x 10^3 cells/cm^2 in 500 cm^2 triple flasks (Thermo Fisher Scientific), supplemented with hgDMEM, 10% v/v FBS, 100 U/mL penicillin - 100 μg/mL streptomycin, 2.5 μg/mL amphotericin B, and 5 ng/mL human fibroblastic growth factor-2 (FGF-2; Prospec-Tany TechnoGene Ltd., Israel) and expanded to passage 2. At the end of passage 2, MSCs were either encapsulated in cylindrical alginate, chitosan, and fibrin hydrogels, or frozen in 90% v/v FBS and 10% dimethyl sulphoxide (DMSO; Sigma-Aldrich) and stored in liquid nitrogen, to be thawed and used in chapter 8.

7.2.2. Cell encapsulation in alginate, chitosan, and fibrin hydrogels

A custom-built tufset mould was used to create sterile agarose wells (Type VII; Sigma-Aldrich) of diameter 5 mm and thickness 3 mm, termed the 'open surface' mould, see Figure A.4. For the fabrication of alginate hydrogels, 8% agarose was mixed with 100 mM CaCl2 (Sigma-Aldrich) in a ratio of 1:1, to create a mould of final concentration 4% agarose/50 mM $CaCl_2$. 2% w/v alginate (Pronova, FMC BioPolymer, Norway) was dissolved overnight in PBS, sterile filtered, seeded with MSCs (20 x 10^6 cells/mL), pipetted into wells and allowed to gel for 30 min. For the fabrication of chitosan hydrogels, 3% w/v chitosan (Pronova) was dissolved overnight in ultra-pure water and sterilised by autoclave, 600 mg/mL β-glycerophosphate (β-GP; Sigma-Aldrich) was dissolved in ultra-pure water and sterile-filtered, 25 mg/mL hydroxyethylcellulose (HEC; Sigma-Aldrich) was dissolved in hgDMEM

and sterile-filtered, and 76 x 10^6 MSCs/mL were suspended in sterile chondrogenic medium. Under agitation, 1.5 mL chitosan was mixed with 350 μL β-GP, combined with 790 μL MSC cell suspension and 360 μL HEC, to give a final concentration of 1.5% w/v chitosan, 7% w/v β-GP, and 0.3% w/v HEC encapsulated with 20 x 10^6 MSCs/mL, which was pipetted into a 4% agarose mould and allowed to gel for 30 min at 37° C. For the fabrication of fibrin hydrogels, 100 mg/mL bovine fibrinogen (Sigma-Aldrich) was dissolved in 10,000 KIU/mL aprotinin solution (Nordic Pharma, UK) containing 19 mg/mL sodium chloride (Sigma-Aldrich) and sterilised by UV for 20 min. This fibrinogen/aprotinin solution was encapsulated with 40 x 10^6 MSCs/mL and combined with 5 U/mL thrombin in 40 mM $CaCl_2$ in the ratio 1:1, to give a final concentration of 50 mg/mL fibrinogen, 2.5 U/mL thrombin, 5,000 KIU/mL aprotinin, 17 mg/mL sodium chloride, 20 mM $CaCl_2$, encapsulated with 20 x 10^6 MSCs/mL, which was pipetted into a 4% agarose mould and allowed to gel for 30 min at 37° C.

7.2.3. Chondrogenic and hypertrophic culture conditions

The chondrogenic and hypertrophic conditions applied in this study are as described in section 5.2.4. Fibrin constructs were supplemented with 20 KIU/mL aprotinin for the first three weeks of culture. Additionally, alginate constructs were supplemented with 1 mM $CaCl_2$ for the final two weeks of the *in vitro* culture period, so as to avoid premature dissolution of the construct prior to implantation.

7.2.4. Experimental design

The first phase of this study investigated the *in vitro* development of engineered cartilaginous constructs generated by maintaining MSC-seeded hydrogels in culture conditions known to support chondrogenesis and subsequent hypertrophy. MSCs were encapsulated in alginate, chitosan, and fibrin hydrogels, and cultured in

chondrogenic conditions for a period of 5 weeks. Thereafter constructs were switched to hypertrophic conditions for an additional 3 weeks, resulting in a total *in vitro* culture period of 8 weeks. The second phase of this study investigated the capacity of these engineered hypertrophic cartilaginous constructs to undergo endochondral ossification *in vivo*. MSCs were encapsulated in alginate, chitosan, and fibrin hydrogels and cultured in chondrogenic conditions for a period of 5 weeks, as per phase 1. Thereafter, constructs received an additional week in hypertrophic conditions (6 weeks total *in vitro* priming). At the end of this 6 week culture period a 2 mm cylindrical core was removed from each construct using a biopsy punch (Hibernia Medical), the purpose of which was to better mimic long bone geometry and to provide a conduit for vascularisation. Constructs were implanted subcutaneously into nude mice and harvested 6 weeks post-implantation.

7.2.5. In vivo subcutaneous implantation

MSC-seeded alginate, chitosan, and fibrin hydrogels (n=9 per group) were implanted subcutaneously into the back of nude mice (Balb/c; Harlan, UK), as described in section 5.2.5. Mice were sacrificed 6 weeks post-implantation by CO_2 inhalation. The animal protocol was reviewed and approved by the ethics committee of Trinity College Dublin.

7.2.6. Biochemical analysis

The biochemical content of cylindrical alginate, chitosan and fibrin constructs was analysed at weeks 5 and 8 of *in vitro* culture. Prior to biochemical analysis, constructs were sliced in half, washed in PBS, weighed, and frozen for subsequent assessment. Upon thawing, chitosan constructs were homogenised using a pestle. Half of each construct was digested in papain and analysed biochemically for DNA, sGAG, and collagen content as described in section 3.2.7. The other half was

digested in 1 M hydrochloric acid at 60° and 10 rpm for 18 h.The calcium content was determined using a Sentinel Calcium kit (Alpha Laboratories Ltd, Uk). 3-4 samples per group were analysed by each biochemical assay.

7.2.7. Histology and Immunohistochemistry

At each time point chitosan and fibrin samples were fixed in 4% paraformaldehyde overnight. Alginate samples were fixed in 4% paraformaldehyde supplemented with barium chloride overnight to permanently crosslink the gels. Post-implantation samples were decalcified in EDTA for 3-4 days. Samples were dehydrated in a graded series of ethanols, embedded in paraffin wax, sectioned at 8 μm and affixed to microscope slides. The sections were stained with haematoxylin and eosin (H and E) and 1% alizarin red to assess calcium accumulation. An aldehyde fuschin - alcian blue composite stain was used to assess sGAG deposition due to the interaction, and subsequent background staining, of alginate with alcian blue. Immunohistochemical stains for collagen types I and II were performed as described in section 3.2.8.

7.2.8. Micro-computed tomography

Micro-computed tomography (μCT) scans were carried out on constructs post-implantation using a Scanco Medical 40 μCT system (Scanco Medical, Bassersdorf, Switzerland), in order to quantify mineral content. Constructs were scanned in deionized water, a voltage of 70 kVp, and a current of 114 μA. Alginate constructs required scanning in a larger chamber resulting in a voxel size of 16 μm. Chitosan and fibrin constructs were scanned in a smaller chamber at a voxel size of 12 μm. Circular contours were drawn around the constructs. A Gaussian filter (sigma=0.8, support=1) was used to suppress noise and a global threshold of 210, corresponding to a density of 399.5 mg hydroxyapatite/cm^3, was applied. This threshold was selected by visual inspection of individual scan slices so as to include mineralised

tissue and exclude non-mineralised tissue. 3D evaluation was carried out on the segmented images to determine mineral volume and to reconstruct a 3D image. 4 constructs were analysed per experimental group. The variance of mineralisation with depth through the construct was analysed qualitatively by examining sections at a depth of 25% from the top of construct (quarter section), and at a depth of 50% from the top of the construct (centre section). To correct for the different voxel sizes used during scanning, 6 slices per section were compiled for alginate constructs, and 8 slices per section were compiled for chitosan and fibrin constructs, resulting in a thickness of 96 μm for each section.

7.2.9. Statistical analysis

All statistical analyses were carried out using Minitab 15.1. Results are reported as mean $\pm$ standard deviation. Groups were analysed by a general linear model for analysis of variance with groups of factors. Tukey's test was used to compare conditions. Anderson-Darling normality tests were conducted on residuals to confirm a normal distribution. Where appropriate, Box-Cox transformations were applied. Significance was accepted at a level of $p<0.05$.

7.3. Results

7.3.1. The in vitro development of hypertrophic cartilaginous grafts engineered using either MSC-seeded alginate, chitosan or fibrin hydrogels

MSCs were encapsulated in alginate, chitosan, and fibrin hydrogels, and maintained in chondrogenic culture conditions for a period of 5 weeks, followed by an additional 3 weeks in hypertrophic culture conditions. After 5 weeks of chondrogenic culture,

sGAG accumulation was significantly higher within MSC-seeded alginate hydrogels (1.29 ± 0.07 mg) compared to chitosan and fibrin hydrogels ($p<0.05$), see Figure 7.1(A). sGAG released to the media was also lowest for alginate constructs during this culture period, see Figure 7.1(B). Collagen synthesis was significantly higher in chitosan constructs (620 ± 32 μg, $p<0.05$), see Figure 7.1(C).

The switch from chondrogenic to hypertrophic culture conditions at week 5 did not result in signficant changes in sGAG content within the engineered constructs by week 8, see Figure 7.1(A). However, sGAG release to the media from alginate constructs increased 125 fold at week 6 compared to week 4, with 2 fold increases measured for both chitosan and fibrin constructs, see Figure 7.1(B). Collagen synthesis continued to increase in both chitosan and fibrin constructs during the hypertrophic culture period, see Figure 7.1(C). Calcium accumulation also increased within all engineered tissues, with alginate and fibrin constructs accumulating signficantly more calcium compared to chitosan constructs ($p<0.01$), see Figure 7.1(D).

Alginate constructs had a signficantly higher wet weight at all time points, see Figure 7.2(A), and so when normalised to %wet weight, sGAG and collagen accumulation was highest in chitosan constructs, Figure 7.2(B and C), whereas calcium accumulation was highest in fibrin constructs, see Figure 7.2(D).

Histology and immunohistochemistry undertaken at week 8 indicated that all engineered constructs supported robust chondrogenesis, with aldehyde fuschin - alcian blue staining demonstrating the production of sGAG and immunohistochemical staining demonstrating the synthesis of collagen type II, see Figure 7.3. Fibrin constructs stained weakest for sGAG and alginate constructs stained strongest for collagen type II. Alizarin red staining demonstrated the deposition of a ring of calcium around the periphery of alginate and chitosan constructs, whereas fibrin supported homogenous calcium production throughout the engineered tissue.

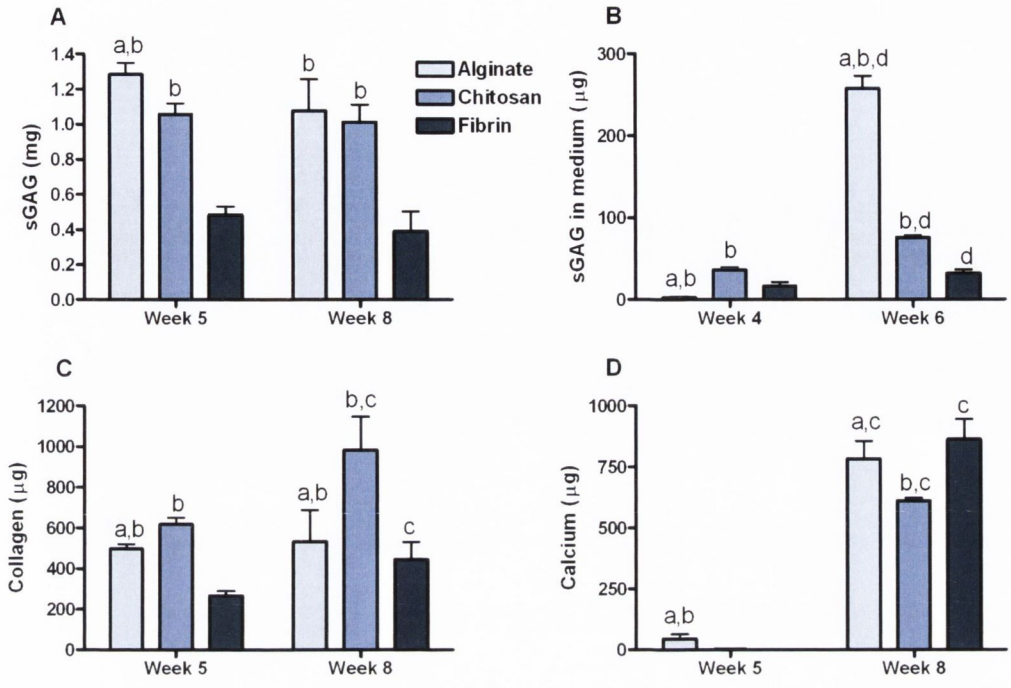

Figure 7.1.: *Biochemical analysis of alginate, chitosan, and fibrin constructs following 8 weeks of in vitro culture (n=3-4). (A) sGAG accumulation (mg), (B) sGAG measured in the medium (µg), (C) Collagen content (µg), and (D) Calcium accumulation (µg). Significance p<0.05: a vs. chitosan at same time point, b vs. fibrin at same time point, c vs. corresponding group at week 5, d vs. corresponding group at week 4.*

7.3.2. Endochondral bone formation following subcutaneous implantation of MSC-seeded alginate, chitosan and fibrin hydrogels

MSC- seeded alginate, chitosan and fibrin hydrogels were cultured for 5 weeks in chondrogenic conditions, followed by an additional week in hypertrophic conditions, prior to subcutaneous implantation in nude mice for an additional 6 weeks. A single channel was cored into these MSC-seeded cylinders immediately before implantation to better mimic the geometry of the mid-section of a long bone and

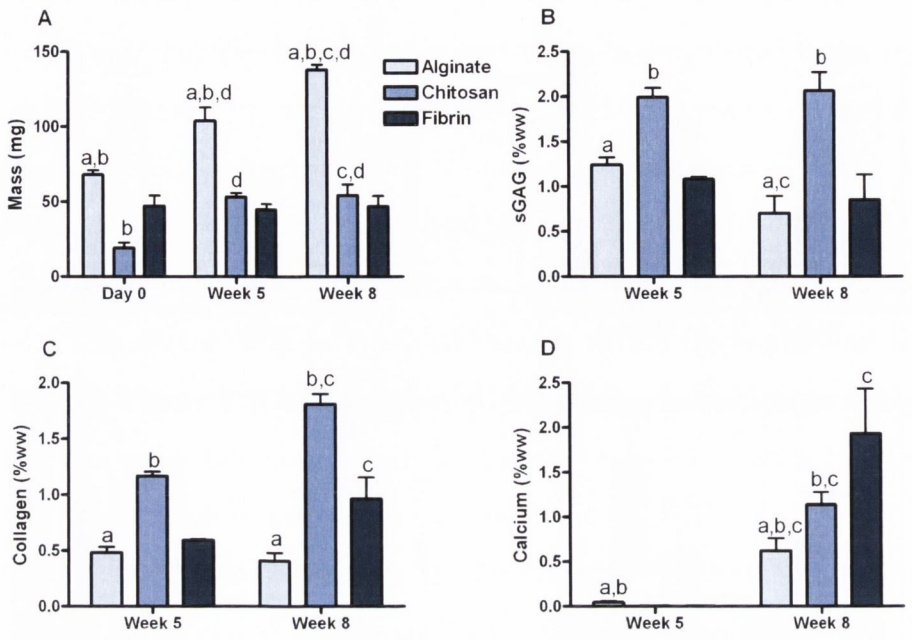

Figure 7.2.: *Mass and biochemical analysis of alginate, chitosan, and fibrin constructs following 8 weeks of in vitro culture (n=3-4). (A) Mass (mg). (B) sGAG, (C) collagen and (D) calcium accumulation, normalised to % wet weight (%ww). Significance p<0.05: a vs. chitosan at same time point, b vs. fibrin at same time point, c vs. corresponding group at week 5, d vs. corresponding group at day 0.*

to provide an additional conduit for vascularisation. Pre-implantation, alginate, chitosan and fibrin constructs stained positive for the cartilage markers collagen type II and aldehyde fuschin - alcian blue (sGAG), but weakly for collagen type I, see Figure 7.4. Post-implantation, a loss of the chondrogenic phenotype was observed in alginate and fibrin constructs, as evidenced by a dramatic increase in the intensity of collagen type I immunostaining and a decrease in aldehyde fuschin - alcian blue staining. Chitosan constructs appeared to better retain the chondrogenic phenotype *in vivo* as demonstrated by more intense staining for aldehyde fuschin - alcian blue post-implantation. It should be noted however there was also a dramatic reduction in type II collagen deposition in chitosan gels.

Prior to implantation, calcific deposits were confined to the periphery of alginate

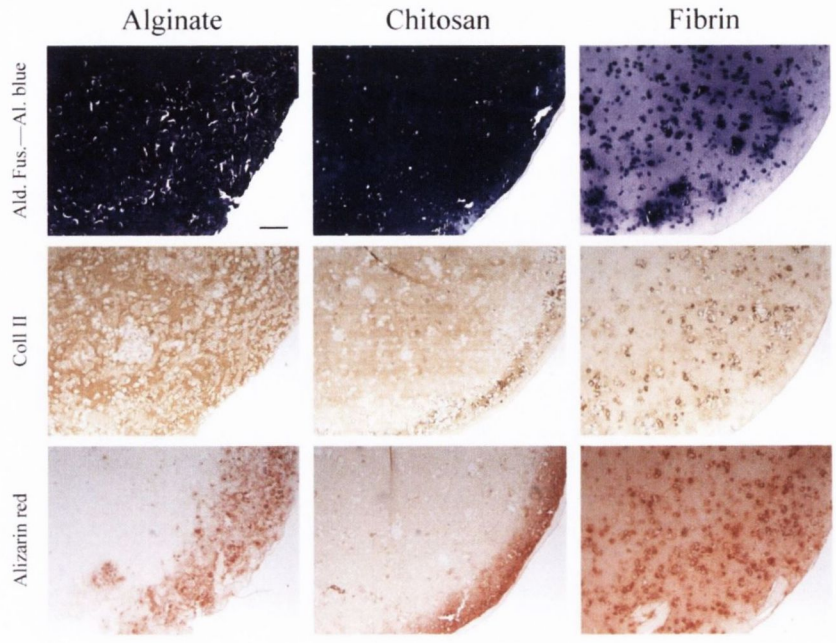

Figure 7.3.: *Histological and immunohistochemical analysis of constructs following 8 weeks of in vitro culture. Aldehyde fuschin-alcian blue (Ald. Fus.-Al. blue), collagen type II and alizarin red. Scale bar is 250 μm and is consistent across all images*

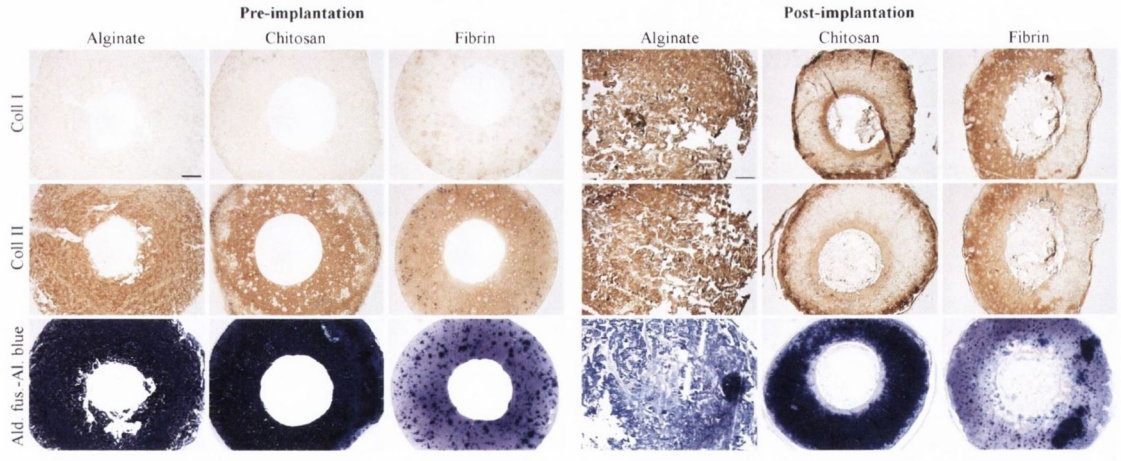

Figure 7.4.: *Histological and immunohistochemical analysis of constructs post-implantation. Collagen I, collagen II and aldehyde fuschin-alcian blue. Scale bar is 500 μm and is consistent across all images*

and chitosan constructs, but were more diffuse in fibrin constructs as evidenced by alizarin red staining, see Figure 7.5(A). μCT analysis of tissues post-implantation revealed extensive calcification occurred within all constructs *in vivo*, see Figure 7.5(B). μCT depth dependent analysis indicated that, for all constructs, mineralisation decreased with depth through the tissue. Chitosan and fibrin constructs better retained their *in vitro* shape, with the cylindrical core still evident throughout the depth of tissue, whereas in alginate constructs this core region was only partially retained with the overall shape of the engineered construct becoming more warped, see Figure 7.5(C). Alginate constructs appeared to support the greatest degree of mineralisation, which was confirmed by μCT quantification, with bone volume being significantly higher for alginate constructs as compared to chitosan and fibrin constructs, see Figure 7.5(D). The local density of the newly formed bone in alginate constructs (748.42 $\pm$ 42.26 mg HA/cm^3) was signficantly higher when compared to chitosan constructs (p=0.005), and showed a trend towards being significantly higher when compared to fibrin constructs (p=0.088), see Figure 7.5(E). The total bone density was significantly higher in alginate constructs, when compared to chitosan and fibrin constructs, see Figure 7.5(F).

Histological analysis (H and E staining) was used post-implantation to assess spatial tissue formation, see Figure 7.6. Alginate and fibrin constructs both supported bone formation at the top of the construct, with blood vessel infiltration apparent in fibrin constructs at this depth. Centre sections of fibrin constructs demonstrated the presence of a marrow component consisting of a mixture of hematopoietic foci and marrow adipose tissue, though less bone formation was observed at this depth. Alginate constructs appeared to support greater bone formation in the central region of the engineered construct, with evidence of trabecular struts as well as bone marrow foci and blood vessel infiltration. Chitosan hydrogels supported the development of a bony collar on the periphery of the

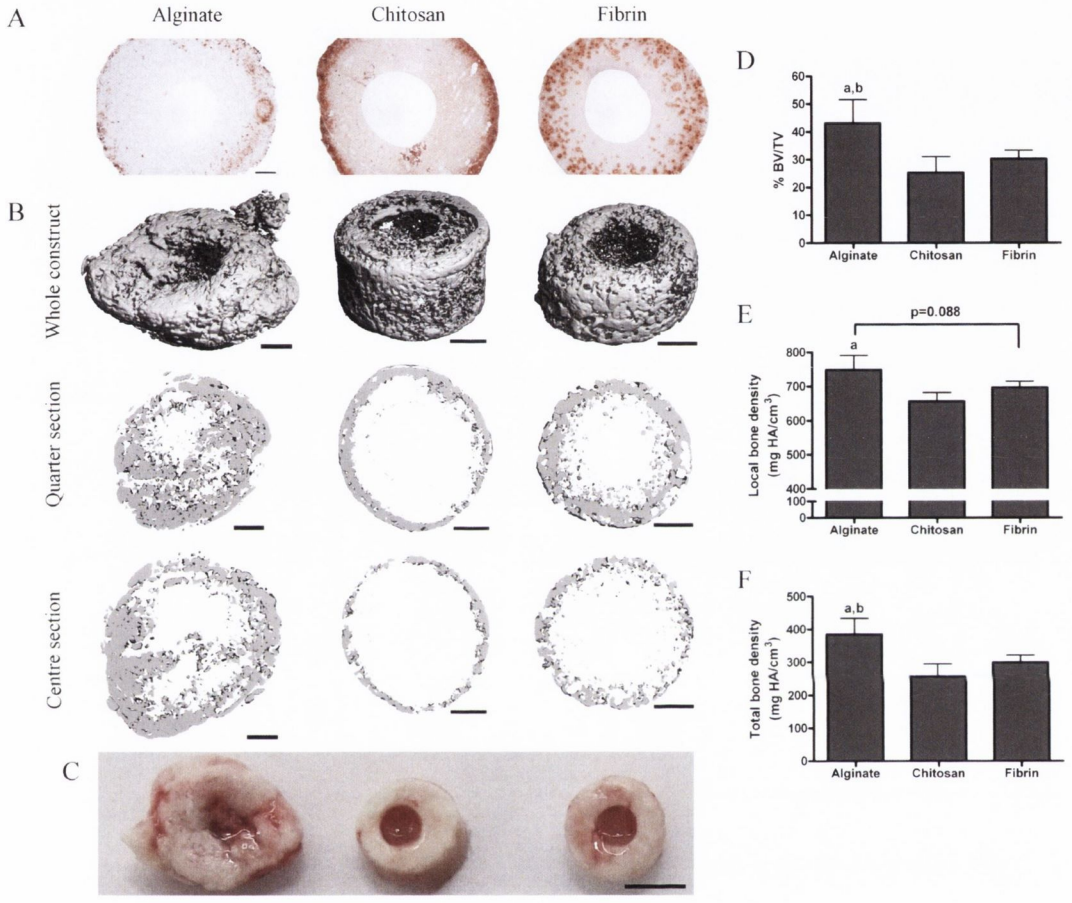

Figure 7.5.: *μCT analysis of constructs post-implantation. A) Alizarin staining of constructs pre-implantation. Scale bar is 500 μm and is consistent across the three images. B) Depth dependent μCT analysis of constructs post-implantation. Sections correspond to a thickness of 96 μm. Scale bars are 1 mm. C) Macroscopic image of alginate (left), chitosan (centre), and fibrin (right) constructs post-implantation. Scale bar is 3 mm. D) μCT quantification of mineralisation post-implantation. % Bone volume per total volume (BV/TV). E) Local bone density of constructs post-implantation. F) Total bone density of constructs post-implantation. 4 samples per group were analysed by μCT. Significance $p<0.05$; a vs chitosan, b vs. fibrin.*

construct, though there was no evidence of bone formation within the body of the hydrogel.

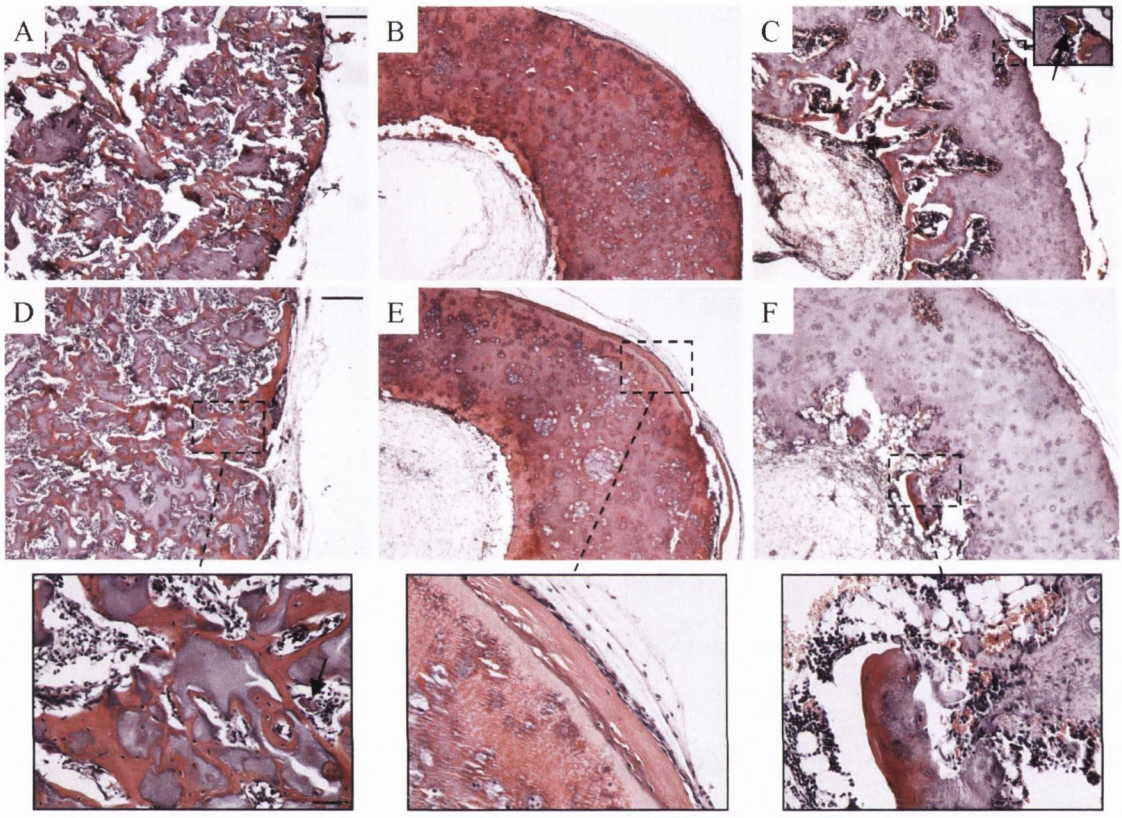

Figure 7.6.: *Depth dependent H and E staining of constructs post-implantation. Top (A-C) and centre (D-F) slices of alginate (A,D), chitosan (B,E) and fibrin (C,F) constructs. Arrows indicate blood vessel structures. Scale bar is 250 μm and is consistent across all images. Inset scale bar is 50 μm and is consistent. Note: the intense pink staining in (B) and (E) is due to the high eosinophilicity of chitosan.*

7.4. Discussion

The scaling-up of engineered hypertrophic cartilaginous grafts, to treat bone defects of a clincally relevant size, requires the use of a suitable scaffolding material tailored to facilitate vascularisation and the transition from engineered hypertrophic cartilage into bone. In this study, the effect of different naturally derived hydrogels

(alginate, chitosan, and fibrin) on the *in vitro* development of MSC-based engineered hypertrophic cartilaginous tissues, as well as the capacity of such hydrogels to generate *in vivo* endochondral bone, was investigated. *In vitro*, alginate and chitosan constructs accumulated the highest levels of sGAG, with chitosan constructs synthesising the highest levels of collagen. Alginate and fibrin constructs supported the greatest degree of calcium accumulation, though only fibrin constructs calcified homogenously. *In vivo*, both alginate and fibrin constructs facilitated vascularisation and endochondral bone formation as well as the development of a bone marrow environment, with alginate constructs accumulating significantly more mineral and supporting greater bone formation in central regions of the engineered tissue.

Understanding how cell-material interactions regulate stem cell fate is a key challenge in developing successful tissue engineering therapies. Cells encapsulated in alginate cannot directly adhere to the hydrogel and hence adopt a spherical morphology known to promote chondrogenesis, which coupled with the significant swelling and retention of matrix may explain the large accumulation in sGAG during culture in chondrogenic conditions. Unlike alginate, fibrin permits cell mediated integrin binding (Cheresh et al., 1989) with MSCs adopting a spread morphology in this hydrogel (Thorpe et al., 2012), and MSCs which adopt a spread morphology have been shown to support an osteogenic or myogenic phenotype (McBeath et al., 2004). In constrast to alginate and chitosan constructs, which calcified preferentially around their periphery upon culture in hypertrophic conditions, fibrin constructs facilitated a homogenous deposition of calcium *in vitro* while accumulating the highest levels of calcium when normalised by % wet weight. It has been suggested that the generation of a low oxygen micro-environment within core regions of MSC-seeded hydrogels undergoing hypertrophic chondrogenesis is generally thought to inhibit calcification in this region (Vinardell et al., 2012b). However, MSCs undergoing direct osteoblastic differentiation demonstrate enhanced

calcium deposition at an oxygen tension of 5% pO_2 compared to 20% pO_2 (Lennon et al., 2001; Sheehy et al., 2012). Due to their spread morphology the MSCs encapsulated in fibrin hydrogels may show a higher propensity towards direct osteoblastic differentiation in the presence of the β-GP (an osteogenic inducer) loaded hypertrophic medium. Interestingly, MSCs cultured in a chondrogenic medium containing β-GP accumulated more calcium in hypoxic conditions than in normoxic conditions when seeded onto an electrospun fibrous polymer scaffold (Meretoja et al., 2013), a scaffold which also promotes an elongated morphology in MSCs (Yang et al., 2011). Further work is required to determine the role of cell shape and oxygen tension in regulating the endochondral phenoype of MSCs.

Chitosan constructs appeared to generate the most stable cartilage-like tissue over the 8 week *in vitro* culture period, as demonstrated by the highest levels of collagen accumulation, lowest calcium accumulation, and comparable sGAG accumulation to alginate constructs which became significantly higher when the data was normalised to % wet weight. One mechanism which may support chondrogenesis within chitosan hydrogels is the polycation-polyanion structural relationship between the positively charged chitosan hydrogel and negatively charged sGAG polysaccharide (Wen et al., 2012), highlighted by the modest 2 fold increased in sGAG release by chitosan constructs to the culture media upon transition to hypertrophic conditions, as opposed to the dramatic 125 fold increase in sGAG release from alginate constructs during the same period.

To assess the capacity of the alginate, chitosan and fibrin hydrogels to generate endochondral bone *in vivo*, engineered hypertophic constructs were implanted subcutaneously. Both alginate and fibrin constructs supported endochondral bone formation, vascularisation, and the development of hematopoietic marrow component. Interestingly both these hydrogels demonstrated levels of dissolution/degradation following implantation with vascularisation and bone marrow formation apparently

localised to the regions of scaffold degradation. Of the two hydrogels, alginate underwent the greater remodelling and also the greater endochondral bone formation. Tailoring the degradations kinetics of a hydrogel may therefore be a critical strategy in promoting endochondral ossification of the engineered tissue (Simmons et al., 2004). Alternatively, or perhaps in conjunction, inflammatory cytokines may be leveraged to direct more efficient resorption of a large cartilaginous template (Mumme et al., 2012; Scotti et al., 2013).

Chitosan constructs did not undergo any degradation following *in vivo* implantation and only supported a collar of bone formation on the periphery of the hydrogel, nor was there any evidence of vascularisation or marrow formation. While chitosan appeared to best support the chondrogenic phenotype of MSCs *in vivo*, with retention of the sGAG matrix again perhaps occuring through the polycation-polyanion mechanism, a stable chondrogenic phenotype was not achieved as evident by a reduction in collagen type II and an increase in collagen type I production and matrix calcification. A previous study comparing the capacity of various hydrogels to support stable chondrogenesis of MSCs *in vivo* reported suppression of calcification by Matrigel (Dickhut et al., 2008). However, when the MSC source was changed from adipose tissue to bone marrow, as used in this study, Matrigel calcification was reported. Furthermore, cartilginous tissues engineered using stem cells isolated from different sources have been shown to be phenotypically different (Vinardell et al., 2012b). Therefore, MSC-based cartilage repair therapies would appear to depend greatly on the source from which the MSCs are isolated. The robust cartilaginous extra-cellular matrix production by chitosan, and the ability to retain sGAGs within the hydrogel, would suggest that, in conjunction with the appropriate stem cell source, chitosan may be an attractive material for the engineering of phenotypically stable functional articular cartilage.

7.5. Concluding remarks

This chapter examined the capacity of different naturally derived MSC-seeded hydrogels to support hypertrophic chondrogenesis *in vitro* and to generate endochondral bone *in vivo*. All hydrogels supported, to differing degrees, the development of mineralised cartilage *in vitro*, though only alginate and fibrin hydrogels facilitated endochondral bone formation *in vivo*, with alginate constructs accumulating signficantly more mineral and supporting bone formation in central regions of the engineered tissue. The superior performance of alginate in this study will motivate its use as the biomaterial for the osseous component of an anatomically shaped osteochondral construct, recapitulated in the shape of the distal phalanx, evaluated in chapter 8 as a paradigm for whole bone tissue engineering through endochondral ossification.

8 Engineering whole bones through endochondral ossification

8.1. Introduction

The digits perform critical functions for human beings. However, due to their frequent use, digits are particularly susceptible to traumatic injuries and degenerative joint diseases (Komura et al., 2011). Although stem cells residing in the nail matrix have been shown to play a role in digit tip regeneration, the region of repair is associated with the area beneath the nail only, and regeneration does not occur when amputation is proximal to the nail (Takeo et al., 2013). Therefore, full avulsion of a digit can result in extensive functional disability. Vascularised autogenous joint transfer is a well established clinical procedure capable of restoring hand function. This treatment is not without its limitations however (Sedrakyan et al., 2006); Firstly, as with all autograft procedures, it is limited by the quantity of tissue available for harvest. Secondly, such an operation results in a significant, negative, aesthetic impact, rendering the treatment undesirable in many cases. Thirdly, the procedure requires the sacrifice of a toe which can impair stability

in the foot. These factors have led to a search for alternative strategies for digit regeneration.

Since no biological therapies exist for whole bone regeneration, tissue engineered anatomically accurate bone grafts could theoretically be used as functional replacements for bones lost due to trauma and disease. A number of studies have investigated the use of engineered phalanx constructs for digit regeneration (Isogai et al., 1999; Vacanti et al., 2001; Weinand et al., 2009; Wang et al., 2009). Previous studies investigating the tissue engineering of phalanx constructs have utilised polymer scaffolds wrapped in periosteal tissue as their 'osseous' layer (Isogai et al., 1999; Chubinskaya et al., 2004; Landis et al., 2009). Such a model however, resulted in bone formation in peripheral regions of the scaffold only, even after 20 weeks *in vivo* (Isogai et al., 1999). A different study used a composite polymer/ceramic (PCL/TCP) scaffold loaded with an MSC-laden hydrogel (Weinand et al., 2009). Such scaffolds have slow degradation characteristics however, which may impair the biomechanical restoration of the engineered bone (Rai et al., 2007). Furthermore, none of these studies have reported the development of a functional marrow component. There is therefore a need for an alternative tissue engineering strategy to promote regeneration of digits.

It was previously demonstrated in chapter 6 of this thesis that it is possible to engineer osteochondral constructs by spatially regulating endochondral ossification within bi-layered cartilaginous grafts. In chapter 7 it was demonstrated that a chondrogenically primed MSC-seeded alginate hydrogel supports robust endochondral bone formation *in vivo*. Moreover, it was demonstrated in chapter 5 that endochondral ossification of an engineered construct can be accelerated by modifying the architecture of the scaffold. These advances pave the way for the scaling-up of endochondral bone tissue engineering strategies for repairing large bone defects or even regenerating whole bones.

This study investigated the possibility of tissue engineering a whole functional distal phalanx bone by recapitulating aspects of the developmental process of endochondral ossification. An MSC-seeded alginate hydrogel in the shape of the distal phalanx acted as the 'osseous component', while a self-assembled chondrocyte construct served as the articulating surface or 'chondral layer'. Constructs were chondrogenically primed *in vitro* for a period of 5 weeks, prior to subcutaneous implantation in nude mice for a period of 8 weeks.

8.2. Materials and methods

8.2.1. Experimental design

The first phase of this study investigated the possibility of tissue engineering bones of different shapes *in vitro*. To that end, anatomic moulds (more details below) were fabricated to generate MSC-seeded alginate hydrogels in the shape of the distal phalanx and temporomandibular joint (TMJ) condyle. Phalanx constructs were attached with a self-assembled chondrocyte layer. In the second phase of the study, chondrogenically primed alginate phalanx constructs were implanted subcutaneously into nude mice. In the third phase of the study, the architecture of the MSC-seeded alginate phalanx hydrogel was altered by inserting a channel into the longitudinal axis of the construct, in an attempt to generate a more homogenous osseous tissue *in vivo*. The fourth phase of the study investigated if the moulding system could be leveraged to fabricate anatomic constructs using different hydrogels. This involved tissue engineering channelled MSC-seeded fibrin phalanx constructs, and implanting the constructs subcutaneously into nude mice.

8.2.2. Cell isolation and expansion

Porcine chondrocytes were isolated as described in section 4.2.2, frozen in 90% v/v FBS and 10% dimethyl sulphoxide (DMSO; Sigma-Aldrich) and stored in liquid nitrogen. Donor matched chondrocytes and bone marrow derived MSCs were thawed and expanded for one additional passage (i.e. chondrocytes to passage 1, MSCs to passage 3) in hgDMEM supplemented 10% v/v FBS, 100 U/mL penicillin - 100 μg/mL streptomycin, 2.5 μg/mL amphotericin B, and 5 ng/mL human fibroblastic growth factor-2 (FGF-2; Prospec-Tany TechnoGene Ltd., Israel).

8.2.3. Fabrication of anatomically shaped constructs

The distal phalanx of the index finger of an adult skeleton model was scanned using a PICZA 3D Laser Scanner model LPX-250 and the program Pixform rendered and meshed the scans to reconstruct a 3D image which was exported to Meshlab. Meshlab catered for the reduction of the large file sizes to a size compatible with SolidWorks and also provided functions to clean and render the mesh. For fabrication of an anatomically accurate TMJ condyle a 3D mandible image was obtained from TURBOSQUID and, using Meshlab, was cut to produce a model of TMJ condyle, reduced in size, and exported to Solidworks. In Solidworks the 3D phalanx and TMJ images were cut in half and a two part reverse mould was created for each construct. This was exported as an STL file and rapid prototyped using a Stratasys dimension Fused Deposition Modeller to produce a two part acrylonitrile butadiene styrene (ABS) mould. This work was carried out in Trinity College by final year engineering student Lara Kelly.

The two part ABS mould was filled with a 4% agarose/50 mM $CaCl_2$ solution and allowed to set. The resultant two part 4% agarose/50 mM $CaCl_2$ mould was assembled to produce a 'closed-surface' mould, and MSC- laden (20 x 10^6

cells/mL) 2% alginate was injected using a hypodermic needle and syringe, through an infiltration extrusion included in the original mould design, and allowed to gel for 30 min. For fabrication of anatomic fibrin phalanx constructs, two part 4% agarose moulds were assembled and injected with a 50 mg/mL fibrinogen, 2.5 U/mL thrombin, 5,000 KIU/mL aprotinin, 17 mg/mL sodium chloride, 20 mM $CaCl_2$ solution encapsulated with 20 x 10^6 MSCs/mL and allowed to gel for 30 min at 37° C.

8.2.4. In vitro culture conditions

MSC- seeded alginate TMJ constructs were cultured in chondrogenic conditions for a period of 5 weeks. Thereafter constructs were switched to hypertrophic conditions for an additional 3 weeks, resulting in a total *in vitro* culture period of 8 weeks. The chondrogenic and hypertrophic conditions are as described in section 5.2.4. Anatomically accurate MSC-seeded alginate and fibrin phalanx constructs (osseous components) were cultured for 4 weeks in the chondrogenic conditions described in section 5.2.4. Alginate constructs were supplemented with 1 mM $CaCl_2$ from the onset of the experiment. Fibrin constructs were supplemented with 20 KIU/mL aprotinin for the first three weeks of culture. In parallel, self-assembled chondrocyte constructs were formed by suspending chondrocytes in hgDMEM supplemented with 10% v/v FBS, 100 U/mL penicillin - 100 μg/mL streptomycin and 2.5 μg/mL amphotericin B at a density of 100 x 10^6 cells/mL. 40 μL of this cell suspension was pipetted into 4% agarose cylindrical wells (⌀5 mm x 3 mm), to give a final concentration of 4 x 10^6 cells/construct, and allowed to self assemble for 12 h (Hu and Athanasiou, 2006; Mesallati et al., 2014). Self-assembled constructs (chondral layers) were cultured in a chondrogenic medium (CM) consisting of high glucose DMEM GlutaMAX supplemented with 100 U/mL penicillin/streptomycin (both Gibco), 100 μg/mL sodium pyruvate, 40 μg/mL L-proline, 50 μg/mL L-ascorbic

acid-2-phosphate, 4.7 μg/mL linoleic acid, 1.5 mg/mL bovine serum albumine, 1x insulin-transferrin-selenium, 100 nM dexamethasone (all from Sigma-Aldrich) and 10 ng/mL of human transforming growth factor-β3 (TGF-β3) (Prospec-Tany TechnoGene Ltd., Israel), at 20% pO_2 for 4 weeks. The osseous component and the chondral layer were attached using a fibrin sealant (same formulation as fibrin hydrogel) and cultured for an additional week in a CM at 20% pO_2, resulting in a total *in vitro* culture period of 5 weeks. In section 8.3.2, prior to the attachment of the osseous and chondral layers, a $\oslash$1.6 mm channel was inserted into the osseous layer using a hypodermic needle (Hibernia Medical). In total three engineered osteochondral phalanx groups were evaulated in vivo; 1) non-channelled alginate constructs, 2) channelled alginate constructs and 3) channelled fibrin constructs.

8.2.5. In vivo subcutaneous implantation

Anatomically accurate engineered phalanx constructs were implanted subcutaneously into the back of nude mice (Balb/c; Harlan, UK), see Figure A.5. Briefly, two subcutaneous pockets were made either side of the central line of the spine, and one construct was inserted per pocket. Four constructs were implanted per experimental group. Mice were sacrificed 8 weeks post-implantation by CO_2 inhalation. The animal protocol was reviewed and approved by the ethics committee of Trinity College Dublin.

8.2.6. Histology and Immunohistochemistry

At each time point alginate samples were fixed in 4% paraformaldehyde/barium chloride overnight. Fibrin samples were fixed 4% paraformaldehyde overnight. Post-implantation samples were decalcified in EDTA for up to 1 week. Samples were dehydrated in a graded series of ethanols, embedded in paraffin wax, sectioned

at 8 μm and affixed to microscope slides. A cross sectional slice of one post-implantation construct per group was embedded calcified. Constructs were stained with haematoxylin and eosin (H and E), picro-sirius red, alizarin red and aldehyde fuschin-alcian blue to assess bone formation, collagen accumulation, calcific deposits, and sGAG deposition respectively. Immunohistochemical stains for collagen types I and II were performed as described in section 3.2.8.

8.2.7. Micro-computed tomography

Micro-computed tomography (μCT) scans were carried out on phalanx constructs post-implantation using a Scanco Medical 40 μCT system (Scanco Medical, Bassersdorf, Switzerland), in order to quantify mineral content. Constructs were scanned in deionized water, at a voxel resolution of 30 μm, a voltage of 70 kVp, and a current of 114 μA. Contours were drawn around perimeter the constructs. A Gaussian filter (sigma=0.8, support=1) was used to suppress noise and a global threshold of 210, corresponding to a density of 399.5 mg hydroxyapatite/cm^3, was applied. This threshold was selected by visual inspection of individual scan slices so as to include mineralised tissue and exclude non-mineralised tissue. 3D evaluation was carried out on the segmented images to determine mineral volume and to reconstruct a 3D image. To qualitatively assess mineralisation in central regions of the construct, 10 slices (equivalent to a thickness of 300 μm) were taken from the centre of construct and compiled. 3-4 constructs were analysed per experimental group. A scan was also taken of one TMJ construct at week 8 of the *in vitro* culture period. This construct was scanned in deionized water at a voxel resolution of 20 μm, a voltage of 70 kVp, and a current of 114 μA. A contour was drawn around the construct and a Gaussian filter (sigma=0.8, support=1) was used to suppress noise. A global threshold of 132, corresponding to a density of 181.1 mg hydroxyapatite/cm^3, was applied. 3D evaluation was carried out to reconstruct a 3D image.

8.3. Results

8.3.1. Anatomic cartilaginous grafts for whole bone tissue engineering

This study explored the potential of MSC-seeded alginate hydrogels for the tissue engineering of scaled-up, anatomically accurate cartilaginous grafts for whole bone regeneration. Anatomically accurate distal phalanx and TMJ condyle constructs were recapitulated from 3D images by utilising a reverse two part ABS mould, loaded with a 4% agarose/50 mM $CaCl_2$ solution to produce a 'closed-surface' mould, and injected with MSC-laden 2% alginate, see Figure 8.1A. Engineered osteochondral phalanx and TMJ constructs were chondrogenically primed for 5 weeks *in vitro*, see Figure 8.1B. The engineered tissues generated a matrix rich in sGAG and collagen, as demonstrated by postive staining for aldehyde fuschin-alcian blue and picro-sirius red, see Figure 8.2. Constructs could be stimulated to produce a cartilaginous tissue surrounded by a calcified outer matrix through further culture in hypertrophic conditions, see Figure 8.3, demonstrating the ability of this approach to generate hypertrophic cartilaginous grafts mimicking the geometry of different bones.

Chondrogenically primed osteochondral phalanx constructs, consisting of an osseous component engineered using an MSC-laden alginate hydrogel and a chondral layer engineered using the chondrocyte self-assembly approach, were implanted subcutaneously for 8 weeks. The osseous component of the engineered phalanx was observed to undergo calcification *in vivo*. A clear vascular network developed within the osseous component, while the chondral layer remained intact and was not vascularised, see Figure 8.4A. Constructs stained intensely for picro-sirius red in the chondral layer, and also around the periphery of the osseous component,

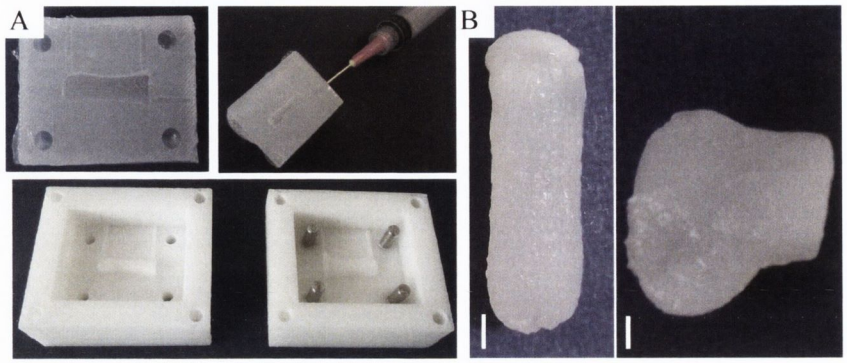

Figure 8.1.: *A) Fabrication of anatomically shaped constructs. B) Anatomically shaped osteochondral phalanx (left) and TMJ (right) constructs, chondrogenically primed for 5 weeks, scale bar 2 mm*

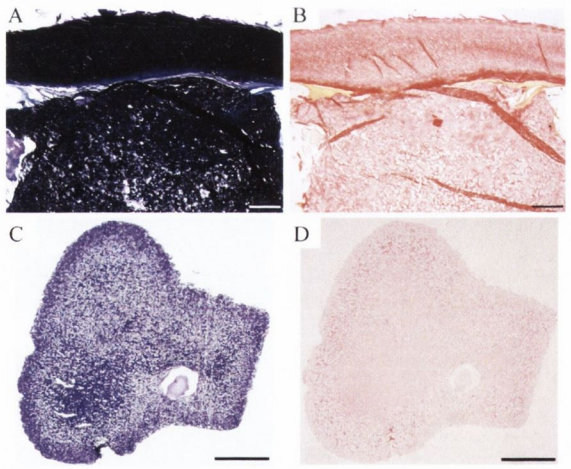

Figure 8.2.: *Histology of anatomically shaped constructs chondrogenically primed for 5 weeks. A) Aldehyde fuschin-alcian blue and B) picro-sirius red staining of osteochondral phalanx constructs, scale bar 500 μm. C) Aldehyde fuschin-alcian blue and D) picro-sirius red staining of TMJ constructs, scale bar 2 mm*

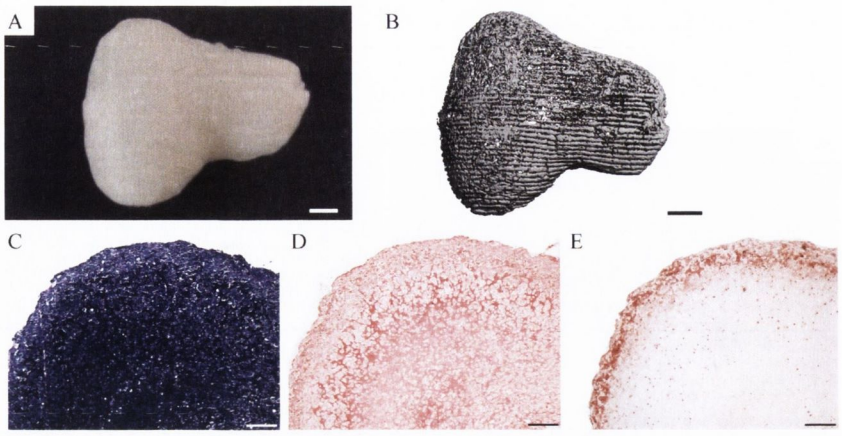

Figure 8.3.: *Anatomically shaped TMJ constructs primed to undergo hypertrophy. A) Macroscopic image and B) μCT image of constructs, scale bar 2 mm. C) Aldehyde fuschin-alcian blue, D) picro-sirius red and E) alizarin red staining of constructs, scale bar 500 μm*

see Figure 8.4B. The cartilage specific matrix molecules sGAG and collagen type II were identified in the chondral layer through aldehyde fuschin-alcian blue histology and collagen type II immunohistochemistry, see Figure 8.4C(top inset). Bone formation around the periphery of the osseous component was identified by collagen type I immunostaining and H and E staining, see Figures 8.4C(bottom inset) and 8.4D(bottom inset) respectively. Furthermore, a reduction in aldehyde fuschin-alcian blue staining was observed in this region, indicating the transition from cartilage into bone, which was followed by infiltration of blood vessel structures evidenced by H and E staining, see Figures 8.4D(top and middle insets). Central regions in the osseous component appeared to retain the morphological characteristics of cartilage, see Figure 8.4C(middle inset). μCT imaging confirmed the development of a heavily calcified outer matrix in the osseous component, see Figure 8.4E, with central regions of the construct remaining uncalcified, see Figure 8.4F. No evidence of calcification in the chondral layer was apparent.

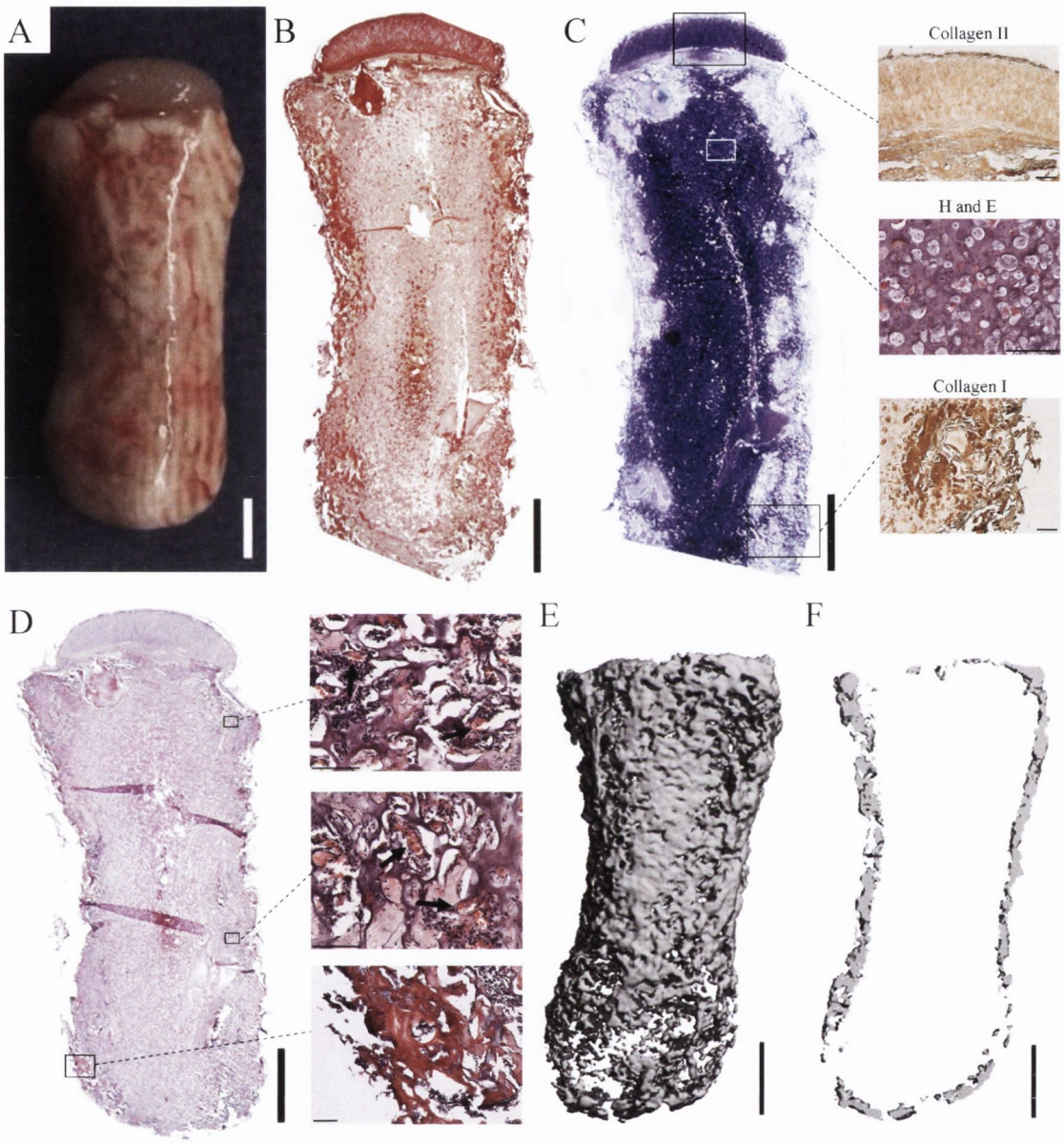

Figure 8.4.: *Anatomic alginate phalanx constructs post-implantation. A) Macroscopic image. B) Picro-sirius red staining. C) Aldehyde fuschin-alcian blue staining. Top inset shows immunhistochemical stain for collagen II, middle inset shows H and E stain, bottom inset shows immunhistochemical stain for collagen I, inset scale bars 250 μm. D) H and E staining, arrows indicate blood vessel structures, inset scale bars 100 μm. E) μCT image of whole construct. F) μCT image of the central region, corresponding to a thickness of 300 μm. Scale bars in main images are 2 mm*

8.3.2. Modifying scaffold architecture augments endochondral bone formation

In an effort to promote more homogenous bone formation throughout the engineered graft, a single cylindrical channel (⌀1.6 mm) was inserted into osseous component of anatomic alginate grafts prior to the attachment of the chondral layer, see Figure 8.5A. The channel remained partially patent for the duration of the *in vivo* study. H and E staining demonstrated bone formation around the periphery of the construct, see Figure 8.5B(inset, bottom), while central regions show a mixture of bone (inset, middle) and cartilage. Peripheral regions undergoing endochondral bone formation also demonstrated evidence of marrow adipose tissue, see Figure 8.5B(inset, top). μCT imaging demonstrated regions of bone formation in the centre of channelled construct, see Figure 8.5C. Cross sectional alizarin red staining confirmed the enhancement of calcification in central regions of channelled constructs (Figure 8.5D) as compared to regular non-channelled constructs (Figure 8.5E).

Due to the capacity of fibrin hydrogels to support endochondral bone formation in chapter 7, anatomic osteochondral fibrin phalanx constructs were also evaluated *in vivo*. A channel was inserted into the osseous component prior to the attachment of the chondral layer, see Figure 8.6A. Constructs harvested 8 weeks post-implantation showed evidence of a vascular network surrounding the osseous layer, while the chondral layer remained intact, see Figure 8.6B. H and E staining demonstrated bone formation around the periphery of the construct, see Figure 8.6C(middle inset), while the central region were devoid of bone, see Figure 8.6C(top inset). The mouth of the channel appeared closed and sealed off by a layer of bone, see Figure 8.6C(bottom inset). μCT imaging demonstrated dense cortical-like bone around the periphery of the construct, see Figure 8.6D, and confirmed a lack of bone formation in central regions, see Figure 8.6E. The osseous component calcified

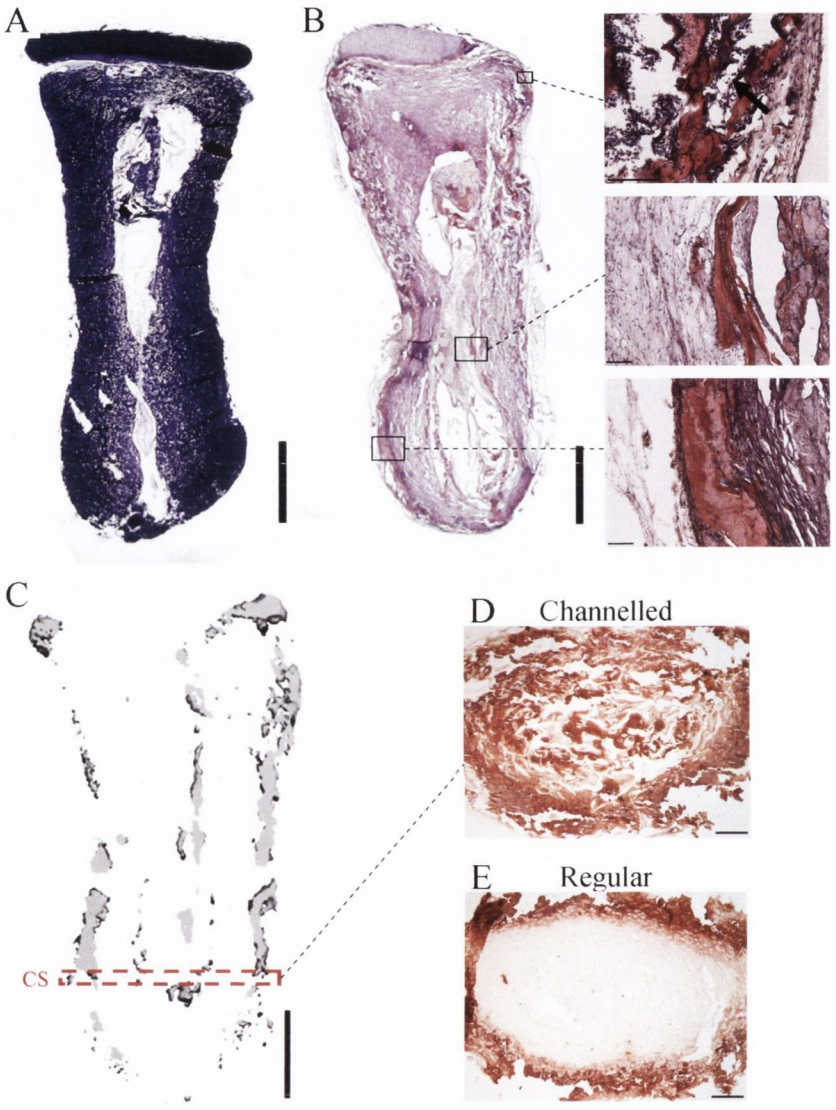

Figure 8.5.: *Channelled alginate phalanx constructs. A) Aldehyde fuschin-alcian blue staining pre-implantation. B) H and E staining post-implantation, arrow indicates marrow adipose tissue, inset scale bars 100 μm C) μCT image of the central region, corresponding to a thickness of 300 μm, post-implantation Scale bars in main images are 2 mm. D) Cross section of channelled construct, and E) cross section of non-channelled construct, post-implantation stained with alizarin red. Cross sections were taken at approximately 1/4 of the height from the distal end of the construct, see CS on D). Scale bars are 500 μm*

homogenously as demonstrated by alizarin staining, see Figure 8.6F, though H and E staining showed bone formation only around the periphery, suggesting that the tissue in the central section of the hydrogel was calcified cartilage, see Figure 8.6G.

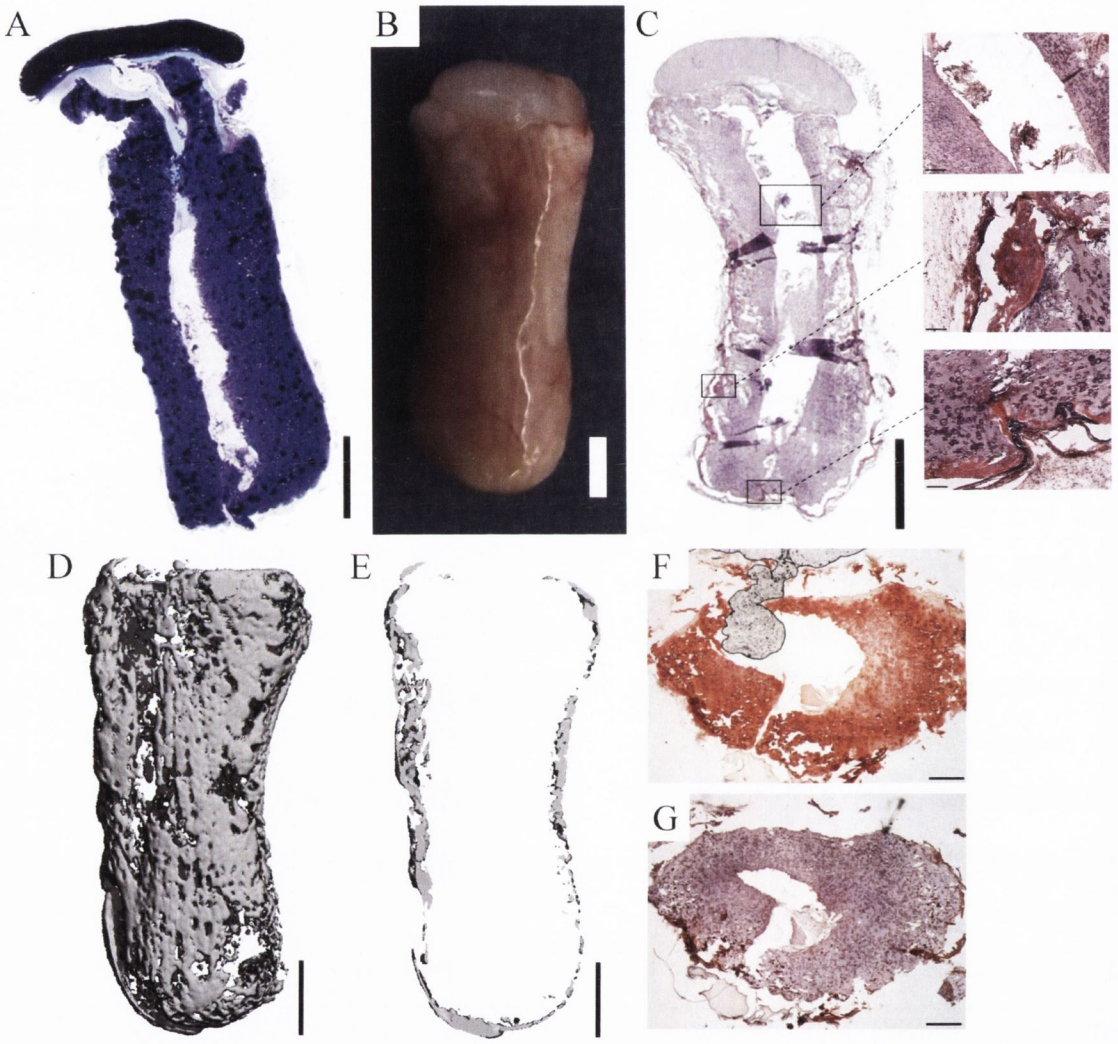

Figure 8.6.: *Channelled fibrin phalanx constructs. A) Aldehyde fuschin-alcian blue staining pre-implantation. B) Macroscopic image of construct post-implantation C) H and E staining post-implantation, top inset scale bar - 250 μm, middle and bottom inset scale bar - 100 μm. D) μCT image of whole construct post-implantation. E) μCT image of the central region, corresponding to a thickness of 300 μm, post-implantation. Scale bars in main images are 2 mm. F) Alizarin red and G) H and E staining of cross sections post-implantation. Cross sections were taken at approximately 1/4 of the height from the distal end of the construct. Scale bars are 500 μm*

8.4. Discussion

This study examined the use of engineered anatomically accurate cartilaginous grafts for regenerating whole bones through endochondral ossification. Using digitised images of a range of different bones it was possible to fabricate 'closed-surface' anatomic agarose moulds, which when injected with an MSC-laden hydrogel, recapitulated the shape of the human distal phalanx and TMJ condyle. MSC-seeded TMJ alginate constructs could be cultured *in vitro* to undergo hypertrophic chondrogenesis and generated a cartilaginous matrix consisting of a homogenous distribution of sGAG and collagen, surrounded by a peripheral layer of calcified tissue. Chondrogenically primed tissue engineered phalanx constructs, consisting of an MSC-laden alginate hydrogel with an overlapping articular cartilage layer generated by chondrocyte self-assembly, was found to undergo spatially regulated endochondral ossification *in vivo* with the chondral layer retaining its stable chondrogenic phenotype and the osseous component proceeding along the endochondral pathway and forming bone around its periphery. Modifying the architecture of anatomic constructs, by inserting a channel into the alginate hydrogel prior to implantation, augmented the spatial distribution of bone formation within the hydrogel, leading to the development of a more homogenous osseous component. Channelled fibrin phalanx constructs were also evaluated *in vivo* and developed a layer of dense cortical bone surrounding a inner region of calcified cartilage.

To test if anatomically accurate cartilaginous grafts could be engineered as a first step towards regenerating whole bones, 3D images of the distal phalanx and TMJ condyle were manipulated using 3D computer-aided design to create a two-part reverse mould for each construct, which was then fabricated by rapid prototyping. The resultant ABS mould was used to cast an agarose/$CaCl_2$ gel, which when assembled contained a conduit to allow injection of a MSC-laden alginate solution,

which upon $CaCl_2$ crosslinking, formed hydrogels in the shape of the desired bones. Other studies investigating the engineering of anatomically accurate grafts have also used anatomic moulds within which to cast cell-laden hydrogels (Hung et al., 2003; Alhadlaq et al., 2004, 2005). While this is a well established method for scaffold manufacturing, it does not allow for the fabrication of complex shapes with porous internal structures. An alternative approach is bioprinting, which can apply layers of computer-driven deposition of cell-laden gels to create more complex 3D geometries (Fedorovich et al., 2007).

A well documented challenge with the scaling-up of engineered tissues is the associated issue of nutrient limitation and waste removal. Recent work utilising MSC-seeded collagen scaffolds for endochondral bone tissue engineering reported the *in vitro* development of a core region devoid of cells and matrix (Scotti et al., 2013). A number of novel strategies have been implemented to ensure adequate nutrient delivery to and waste removal from engineered tissues, such as the application of dynamic culture conditions (Martin et al., 2004; Mauck et al., 2003b), as well as the modification of scaffold architures to include nutrient channels (Bian et al., 2009; Buckley et al., 2009b). However, the large phalanx and TMJ constructs engineered in this study showed homogenous cartilaginous matrix deposition after 5 weeks chondrogenic priming in free swelling conditions, demonstrating the benefit of utilising hydrogels when scaling-up cartilaginous constructs for endochondral bone tissue engineering appplications.

Hypertrophic priming of engineered cartilaginous tissues *in vitro* has been shown to enhance endochondral bone formation *in vivo* (Scotti et al., 2010). In the current study, after the initial 5 weeks culture in chondrogenic conditions, TMJ constructs were cultured in hypertrophic conditions for an additional 3 weeks and developed into a chondro-osseous tissue consisting of a central cartilaginous region rich in sGAG and collagen, surrounded by a peripheral layer of calcified tissue.

Further studies are required in order to evaluate the capacity of these hypertrophic cartilaginous TMJ constructs to generate endochondral bone *in vivo*.

As the osseous component of a bi-layered construct, the current study employed an alginate hydrogel, which undergoes dissolution over time (Drury and Mooney, 2003), encapsulated with chondrogenically primed bone marrow derived MSCs capable of surviving the initial hypoxic conditions experienced by large engineered tissues upon *in vivo* implantation (Scotti et al., 2013). The osseous component of this chondrogenically primed bi-layered tissue underwent endochondral ossification after 8 weeks *in vivo*, leading to the development of an articular cartilage layer anchored to a heavily calcified outer bony tissue penetrated with vasculature. However, tissue in central regions of the osseous component remained as cartilage. The lack of calcification in the centre may be explained, at least in part, by the large volumes of the constructs used in this endochondral strategy, calculated as 336.9 ± 38.7 mm^3. For comparison, a recent scaled-up endochondral bone tissue engineering study by Scotti et al. (2013) used cylindrical cartilaginous constructs of dimensions ⌀8 x 2 mm, equivalent to volumes of 100 mm^3, over 3 fold lower than those used in the current study. Another explanation for the inhibition of bone formation in the centre of the engineered tissue may be the slow degradation of the unmodified alginate hydrogel. Accelerating the degradation rate of alginate hydrogels through gamma-irradiation has been shown to enhance endochondral bone regeneration (Simmons et al., 2004), and the use of inflammatory cytokines to efficiently remodel engineered cartilaginous grafts have also shown to be beneficial for endochondral bone tissue engineering strategies (Mumme et al., 2012; Scotti et al., 2013).

An alternative method to enhance calcification in central regions of an engineered tissue is by modifying the architecture of the scaffold. Chapter 5 of this thesis demonstrated that the introduction of channels into MSC-seeded hydrogels

facilitated vascularisation, endochondral ossification and marrow formation in the engineered cartilaginous tissues. In the current study, it was hypothesised that the introduction of a single channel into the alginate hydrogel, prior to attachment of the osseous and chondral layers, would firstly enhance bone deposition in central sections of the tissue and secondly would provide a cavity for bone marrow formation. The first hypothesis was corroborated, with increased bone formation in the centre of the osseous component, as demonstrated by H and E staining, alizarin red staining and μCT imaging, resulting in the development of a more homogenous bone tissue in channelled constructs. The channel however, did not provide a cavity for bone marrow formation, though there were regions around the periphery of the engineered tissue; i.e. regions of endochondral bone formation and alginate hydrogel dissolution, where bone marrow formation was evident. The channels in chapter 5 ($\oslash$500 μm) were introduced at the begining of the *in vitro* culture and had filled up with scaffold free cartilaginous tissue prior to implantation. In the current study a larger channel ($\oslash$1.6 mm) was introduced 4 weeks into the *in vitro* culture period and only 1 week prior to implantation. It may therefore be that this large empty channel did not contain the neccessary endochondral cues for bone marrow formation. It would also appear that dissolution or degradation of a hydrogel is essential for bone marrow formation in large engineered tissues. During embryonic endochondral bone formation, the establishment of a hematopoietic marrow compartment occurs with elongation of the growth plate providing a space for marrow deposition, with hypertrophy and proliferation of growth plate chondrocytes being regulated by the Ihh-PTHrP negative feedback loop (Kronenberg, 2003). Recapitulation of these spatial and temporal cues would therefore appear to be critical when developing endochondral bone tissue engineering strategies for the regeneration of whole bones, as the bone marrow compartment is critical for maintaining normal bone homeostasis.

Due to their capacity to support endochondral bone formation, demonstrated in chapter 7, chondrogenically primed anatomically accurate channelled fibrin constructs were also evaluated *in vivo*. Alizarin red staining of constructs post-implantation demonstrated the formation of a homogenous calcified tissue, though H and E staining and μCT imaging demonstrated a lack of bone formation in central regions of the engineered construct. The channel introduced into fibrin constructs did therefore not have the same positive influence on the development of a more homogenous bone tissue as compared to the channel introduced into alginate constructs. H and E staining post-implantation demonstrated a peripheral layer of dense bone formation at the bottom of the construct, closing the mouth of the channel, which may have made eliminated any potential benefit of the nutrient channel. That the hydrogel could still support homogenous calcification may be as a result of a subset of the implanted MSCs retaining the ability to undergo direct osteogenic differention, due to the spread cell morphology promoted in fibrin hydrogels (McBeath et al., 2004; Thorpe et al., 2012).

This study employed a subcutaneous environment to facilitate the development of an engineered cartilaginous construct into an endochondral bone tissue. From a translational perspective, this approach may also be adopted in the clinic; i.e. using an ectopic environment as an *in vivo* bioreactor to allow maturation of an engineered tissue with functional vasculature, and possibly marrow, components which can then be implanted into an orthotopic defect site. The alternative would be to forsake the ectopic transplantation and implant the engineered cartilaginous construct directly into the defect site, allowing endochondral ossification to occur orthotopically. This approach has previously been demonstrated using a coral scaffold, which would have an inherent advantage over a hydrogel in terms of performing an immediate mechanical function, for the replacement of an avulsed phalanx (Vacanti et al., 2001). The non-load bearing environment of the upper

limbs may allow for direct implantation of an engineered cartilaginous construct into a bone defect, though it may be more challenging if applied in a mechanically loaded defect site in the lower limb, which would require the engineered tissue to perform a more demanding biomechanical function. It should be noted however, that when a cartilaginous graft engineered using MSCs was implanted into the excised lunar space of a rabbit, it performed a mechanical function for the 12-week duration of the experiment (Huang et al., 2006). Further studies using larger animal models are required to compare the efficacy of ectopic and orthotopic implantation strategies in endochondral bone tissue engineering applications.

8.5. Concluding remarks

This study investigated the use of chondrogenically primed anatomically shaped bi-layered constructs, consisting of a chondrocyte-based chondral layer attached to an MSC alginate hydrogel osseous component, as a paradigm for whole bone tissue engineering through endochondral ossification. These scaled-up constructs underwent chondrogenesis *in vitro* and spatially regulated endochondral ossification *in vivo* resulting in a stable articular cartilage layer anchored to a vascularised osseous tissue consisting of bone around the periphery and cartilage in the centre. More homogenous ossification of the osseous component was achieved by modifying the architecture of the alginate hydrogel. This work demonstrates the potential of utilising anatomically shaped grafts for the regeneraton of whole bones.

Many of the experimental parameters validated in earlier chapters of this thesis were leveraged in this study in order to better achieve the goal of engineering a whole bone through endochondral ossification. Chapter 9 will further describe, and elaborate on, the results presented in this thesis, relating the findings back to the intial objectives of the thesis.

9 Discussion

9.1. Summary

The objective of this thesis was to identify *in vitro* culture conditions appropriate for engineering anatomically accurate hypertrophic cartilaginous grafts, in order to generate endochondral bone *in vivo*, as a paradigm for whole bone tissue engineering through endochondral ossification. Oxygen tension was found to regulate the endochondral phenotype of MSCs, with a low oxygen tension ($5\%pO_2$) enhancing chondrogenesis and a normal oxygen tension ($20\%_2$) promoting hypertrophy. Rotational culture differentially regulated chondrogenesis of chondrocyte-seeded and MSC-seeded agarose hydrogels. Modifying the architecuture of hypertrophic cartilaginous grafts, by engineering channelled hydrogels, accelerated vascularisation and endochondral ossification when implanted *in vivo*. Chondrogenically primed bi-layered constructs, consisting of a top layer seeded with chondrocytes and a bottom layer seeded with MSCs, underwent spatially regulated endochondral ossification upon *in vivo* implantation resulting in the development of an engineered osteochondral tissue. The capacity of MSC-seeded alginate, chitosan, and fibrin hydrogels to undergo endochondral ossification *in vivo* was evaluated and alginate hydrogels were found to support the greatest degree of endochondral bone formation. Finally, cartilaginous grafts, recapitulated in the shape of the distal phalanx, were

implanted as a paradigm for whole bone tissue engineering through endochondral ossification.

The thesis began by investigating the appropriate environmental conditions to promote hypertrophy of MSC-based cartilaginous constructs (chapter 3). The embryonic process of endochondral ossification is characterised by blood vessels infiltrating a cartilaginous template thus increasing the oxygen levels in the tissue (Ma et al., 2009). The effect of oxygen tension during MSC expansion and susbsequent osteogenic and chondrogenic differentiation was therefore examined. Expansion in a low oxygen tension ($5\%pO_2$) enhanced proliferation and subsequent osteogenesis of MSCs. Chondrogenic differentiation in a low oxygen tension promoted markers of chondrogenesis such as sGAG accumulation and collagen type II synthesis, while differentiation in normoxic conditions ($20\%pO_2$) promoted markers of hypertrophy such as ALP activity and collagen type X synthesis. A number of other studies, published since commencement of the work undertaken in chapter 3, have also examined the role of oxygen tension in regulating hypertrophy of MSC-based cartilaginous constructs. Gawlitta et al. (2012) corroborated the results presented in chapter 3 by demonstrating that hypoxia impedes hypertrophic chondrogenesis of MSC pellets. Meretoja et al. (2013) however, reported increased calcification of chondrogenically primed MSC-seeded electrospun scaffolds in hypoxic conditions. This result may be explained by the use of a scaffold which promotes a spread morphology in MSCs (Yang et al., 2011), cultured in a medium supplemented with β-GP from the onset of the experiment, the combination of which may have promoted more direct osteogenic differention of the MSCs. The switch from $5\%pO_2$ to $20\%pO_2$ was utilised in later chapters in the thesis to promote initial chondrogenesis and subsequent hypertrophy of engineered cartilaginous constructs prior to implantation.

The objective of chapter 4 was to develop a strategy, combining modified scaffold

architecture and rotational culture, to facilitate the engineering of large homogenous cartilaginous constructs. Chondrocytes and MSCs were encapsulated in regular solid or channelled agarose hydrogels and cultured in free swelling conditions or in a rotational system. Rotational culture increased matrix accumulation in the core of chondrocyte-based constructs, leading to the development of a more homogenous cartilaginous tissue. Rotational culture, however, inhibited chondrogenesis of MSC-based constructs and there was no clear benefit of a channelled architecture in either cell type, when cultured in free swelling conditions or in a rotational system. However, a recent study by Mesallati et al. (2012) showed that, in chondrocyte-seeded channelled agarose hydrogels, collagen synthesis was enhanced in regions of elevated fluid flow induced by dynamic compression, demonstrating that combinations of modified scaffold architecture and dynamic culture conditions can be leveraged to direct spatial tissue deposition within engineered constructs. The sub-optimal effects on MSC chondrogenesis by rotational culture eliminated its potential application in later chapters of this thesis.

Though no clear positive effect of a channelled architecture was demonstrated in chapter 4, it was hypothesised that the benefit of channels might only become apparent following *in vivo* implantation. Inspired by the role played by cartilage canals during endochondral bone development, the objective of chapter 5 was to accelerate *in vivo* vascularisation and endochondral ossification of engineered hypertrophic cartilaginous grafts through the use of channelled hydrogels. MSCs were encapsulated in solid or channelled agarose hydrogels, maintained in culture conditions known to promote a hypertrophic cartilaginous phenotype and implanted subcutaneously in nude mice. Apparently mimicking the function of the cartilage canals, which facilitate angiogenesis and the migration of osteogenic cells, the channels acted as conduits for vascularisation and accelerated mineralisation of the graft, with cartilaginous tissue within the channels undergoing endochondral

ossification to produce lamellar bone surrounding a marrow component. This chapter highlighted the importance of optimising the architecture of a scaffold for use in endochondral bone tissue engineering applications, and this approach was therefore applied in later studies, in order to enhance endochondral bone formation in central regions of large engineered cartilaginous constructs.

As this thesis moved towards the ultimate goal of engineering a whole bone, it became clear a strategy was required to generate an osteochondral tissue, as a tissue engineered long bone would require an articular cartilage surface to ensure proper biomechanical function. The objective of Chapter 6 was therefore to engineer an osteochondral construct through spatial regulation of endochondral ossification. To that end, chondrocytes and MSCs were encapsulated in seperate layers of bi-layered agarose hydrogels. Constructs were maintained in a chondrogenic medium for 3 weeks and thereafter were either maintained in a chondrogenic medium, transferred to a hypertrophic medium, or implanted subcutaneously into nude mice, for an additional 4 weeks. A structured chondrogenic co-culture was found to enhance chondrogenesis in the chondrocyte 'chondral' layer, appearing to re-establish the chondrogenic phenotype lost during monolayer expansion, while suppressing mineralisation and hypertrophy in the MSC 'osseous' layer. Interestingly, transfer to a hypertrophic medium resulted in the formation of a rudimentary growth plate at the interface of the two layers. During endochondral skeletogenesis, growth plate development is regulated by the negative feedback loop between PTHrP-expressing articular chondrocytes and Ihh-expressing hypertrophic cells (Kronenberg, 2003). It was therefore likely that aspects of long bone growth were being recapitulated in this *in vitro* culture system. Future work could provide evidence in support this hypothesis by conducting immunohistochemical staining for Ihh. Following *in vivo* implantation, mineralisation of the osseous layer occurred resulting in the development of an osteochondral tissue consisting of a layer of stable cartilage on

top of a layer of calcifying cartilage undergoing endochondral ossification. This strategy of harnessing the endochondral phenotype of MSCs, in conjunction with the stable chondrogenic phenotype of chondrocytes, therefore presented a novel approach for the engineering of an osteochondral construct. However, the agarose hydrogel used in the study appeared to only partially support progression of the osseous layer down the endochondral route, with the tissue apparently locked in hypertrophic calcified cartilage state after 4 weeks *in vivo*. This may have been due to the non-biodegradable nature of the agarose hydrogel, with the ecapsulated or recruited cells lacking the neccesary enzymes to remodel the engineered cartilage within the hydrogel into bone. This led to the exploration of different hydrogels capable of facilitating endochondral ossification more effectively.

Chapter 7, therefore, compared the capacity of different naturally derived MSC-seeded hydrogels to generate endochondral bone *in vivo*. MSCs were encapsulated in alginate, chitosan and fibrin hydrogels and maintained in culture conditions to undergo hypertrophic chondrogenesis prior to subcutaneous implantation. Chitosan appeared to generate the most stable cartilage-like tissue both *in vitro* and following implantation. The ability of the positively charged chitosan hydrogel to retain negatively charged sGAG proteins may be a powerful tool in the engineering of functional articular cartilage. *In vivo*, both alginate and fibrin constructs supported vascularisation and endochondral bone formation as well as the development of a bone marrow environment. Alginate constructs generated the greatest volume of bone and facilitated ossification in central regions of the engineered tissue. Tailoring the degradation characteristics of a hydrogel for use in endochondral bone tissue engineering applications would therefore appear to be key, as alginate appeared to undergo the greatest degree of degradation/dissolution *in vivo*.

Chapters 3 through to 7 of this thesis were designed to elucidate the appropriate combinations of factors; i.e. environmental conditions, culture conditions, scaffold

architectures, cell sources, and biomaterials, to facilitate the engineering of an anatomically shaped cartilaginous graft for the regeneration of a whole bone through endochondral ossification, evaluated in Chapter 8. Motivated by the results of Chapter 7, this study utilised an MSC-encapsulated alginate hydrogel, recapitulated in the shape of the distal phalanx, as the 'osseous' component which was cultured *in vitro* using the switch in oxygen conditions outlined in chapter 3. An engineered self-assembled chondrocyte tissue acted as the articulating 'chondral' layer. Upon *in vivo* implantation the chondrogenically primed construct underwent spatially regulated endochondral ossification, as determined in Chapter 6, resulting in the development of a stable articular cartilage layer anchored to a vascularised bone layer. Future work might examine the mechanical strength of the interface between the chondral and osseous components through tensile testing. The engineered bone contained a large uncalcified central region, which retained the morphological features of cartilage. Therefore, adopting the approaches taken in Chapters 4 and 5, the architecture of the alginate hydrogel was modified prior to implantation, by inserting a channel into the longitudinal axis of the construct. This strategy promoted the development of a more homogenous osseous component.

In summary, this thesis demonstrates a novel framework for the regeneration of whole bones by utilising tissue engineering methodologies directed at recapitulating aspects of developmental skeletal processes. The emergence of developmental engineering strategies have resulted in a shift away from classical tissue engineering paradigms (Lenas et al., 2009). Accordingly, increased interest in endochondral approaches to bone tissue engineering may circumvent the hurdles that have hampered translation of traditional intramembranous approaches. This work provides an insight into the appropriate combinations of factors that can be leveraged to promote endochondral ossification of engineered hypertrophic cartilaginous grafts, the successful application of which will be crucial as tissue engineering strategies move

towards the repair of large bone defects and potentially whole bone regeneration.

9.2. Conclusions

- Oxygen tension regulates the osteogenic, chondrogenic, and endochondral phenotype of bone marrow derived MSCs. For the engineering of hypertrophic cartilaginous grafts, a low oxygen environment can be applied to enhance cartilaginous matrix production, and a normoxic enviroment can be utilised to promote hypertrophy.

- Chondrocytes and MSCs undergoing chondrogenesis respond differentially to rotational culture, demonstrating that the dynamic culture conditions beneficial for chondrocyte-based cartilaginous tissues may be sub-optimal for MSC-based constructs.

- Recapitulating the cartilage canal network observed during endochondral skeletogenesis, through tissue engineering channelled hypertrophic cartilaginous constructs, accelerates mineralisation and vascularisation of engineered grafts.

- By implanting chondrogenically primed bi-layered hydrogels containing chondrocytes and MSCs, it is possible to spatially regulate endochondral ossification *in vivo*, leading to the development of an osteochondral construct.

- MSC-seeded alginate hydrogels support more robust endochondral bone formation *in vivo* when compared to MSC-seeded chitosan and fibrin hydrogels.

- By recapitulating aspects of the developmental process of endochondral ossification it is possibile to engineer anatomically shaped tissues for the potential regeneration of whole bones.

9.3. Limitations

The early chapters of this thesis utilised agarose hydrogels as scaffolds for the engineering of 3D cartilaginous constructs. Previous work had demonstrated that agarose hydrogels could support chondrogenesis of MSCs *in vitro* (Awad et al., 2004; Mauck et al., 2006; Coleman et al., 2007; Thorpe et al., 2008), and indeed in Chapter 3 agarose hydrogels supported not only the initial chondrogenesis of MSCs but also subsequent hypertrophy and calcification, motivating its use as the biomaterial in later *in vivo* studies. However, following subcutaneous implantation, agarose appeared to only partially support progression down the endochondral route. In Chapter 6, chondrogenically primed MSC-seeded agarose hydrogels generated a hypertrophic, calcified cartilage after 4 weeks *in vivo*, while in chapter 5 no bone was generated in solid constructs after 8 weeks *in vivo* with endochondral bone forming in channelled constructs only in regions which had filled up *in vitro* with scaffold free cartilaginous tissue, suggesting that host cells lacked the neccessary enzymes to remodel the engineered cartilage within the body of agarose hydrogel into bone. As a result, the selection of agarose as the biomaterial for an endochondral bone tissue engineering application must be considered a significant limitation of this work.

Alternative hydrogels which undergo either dissolution (alginate) or degrade by cell-associated enzymatic activity (fibrin) were therefore investigated. Chitosan, a polysaccharide which has been shown to be degraded by the enzyme lysozyme (Hong et al., 2007), was also evaluated based on the principle that the material undergoes degradation *in vivo*. In chapter 7 however, this was found not to be the case, at least within the 6 week *in vivo* period, with chitosan hydrogels remaining stable following subcutaneous implantation and not supporting endochondral bone formation. The mechanism by which chitosan hydrogels undergo degradation after

implantation in a nude mouse model is therefore unclear. The MSC-seeded alginate hydrogels evaluated in chapter 7 appeared to support greater endochondral bone formation compared to the anatomic alginate-based constructs evaluated in Chapter 8. Though this in part may be explained by larger size of the anatomic constructs, another difference between the two chapters which may have had a significant effect on the degree of *in vivo* bone formation is the gel fabrication methods and subsequent cross-linking. Chapter 7 utilised an 'open surface' agarose/$CaCl_2$ mould allowing diffusion of calcium ions to occur from the bottom and radial surfaces only, whereas Chapter 8 utilised a 'closed surface' mould which facilitated calcium ion diffusion not only from the bottom and radial surfaces, but also from the top surface. Therefore the relatively weaker cross-links, and the associated quicker dissolution rates, of the alginate hydrogels formed in Chapter 7 may have facilitated greater endochondral bone formation, particularly in central regions of the construct. Regardless, work undertaken in this thesis suggests that more rapid degradation of engineered hypertrophic cartilaginous grafts accelerates endochondral ossification. That no additional strategies were utilised to accelerate degradation, either through scaffold modification (Simmons et al., 2004) or through supplementation with inflammatry cytokines (Mumme et al., 2012), may therefore be considered as a limitation of this thesis.

In Chapters 5, 7 and 8, neo-vascularisation of engineered constructs was assessed qualitatively through histology and/or immunohistochemistry. A more quantitative approach might have been taken, by examining a number of different slices at different depths of the same construct and counting the number of blood vessel structures. Furthermore, other groups have utilised μCT angiography to provide visualisation of the 3D vascular network, and to quantify vascular connectivity and thickness (Boerckel et al., 2011; Kolambkar et al., 2011b).

It is unclear whether the endochondral bone being formed *in vivo* is of donor

or host origin. Previous studies have used species-specific genomic sequences to determine the origin of the tissues present within their engineered constructs (Janicki et al., 2010; Scotti et al., 2013). If it had been applied in this thesis, such an analysis would have demonstrated whether the hypertrophic cells within the engineered constructs underwent osteogenic differentiation *in vivo* and began depositing new bone directly, or whether they contributed to bone formation indirectly by recruiting bone forming cells from the host. This work would also have benefit from an experiment comparing the capacity of non-primed MSCs, osteogenically primed MSCs, and chondrogenically primed MSCs, to generate bone *in vivo*.

Another key limitation of this thesis is the absence of a biomechanical characterisation assay, as is the lack of consideration of the effects a biomechanical environment would have on tissue engineered grafts. For example, dynamic compression has been shown to suppress hypertrophy of MSC-based cartilaginous constructs (Bian et al., 2012; Thorpe et al., 2012), and delayed mechanical loading has been shown to influence vascular remodelling in large bone defect regeneration (Boerckel et al., 2011). The anatomically shaped phalanx constructs in Chapter 8 would have benefitted from mechanical testing, and a comparison with the mechanical properties of intact bone.

All *in vivo* work carried out in this thesis involved the implantation of tissue engineered constructs into a subcutaneous, or ectopic, environment. This thesis did not investigate endochondral bone formation in an orthotopic environment. Since the repair of a critical size bone defect through endochondral ossification would ideally involve direct implantation of tissue engineered hypertrophic cartilage into a defect site, so as to reduce the need for multiple surgeries, that no orthotopic environments were evaluated may weaken the impact of this thesis. As does the lack of an experiment comparing the bone regeneration capacity of tissue engineered

hypertrophic cartilage to the clinical standard (INFUSE®) in an orthotopic model.

The MSCs and chondrocytes used in this thesis were isolated from skeletally immature, 3 to 4-month old, porcine donors. Since tissue engineering is an applied science that ultimately aims to implemented in a clinical setting, it should be noted that results generated using 'young' animal cells may differ from results generated using 'old' human cells. For example, Erickson et al. (2011) demonstrated that chondrogenesis of chondrocytes and MSCs was enhanced when cells were sourced from fetal and juvenile donors as compared to cells sourced from adult donors. Therefore, the use of mature human cells, as opposed to immature porcine cells, would have strengthened the impact of the results presented in this thesis.

This thesis utilised chondrocytes in order to engineer the chondral layer of an osteochondral construct (chapter 6) and a whole bone (chapter 8). While chondrocytes have been in clinical use for a number of years (Brittberg et al., 1994; Peterson et al., 2000), well documented issues may limit their application in cartilage tissue engineering strategies (Temenoff and Mikos, 2000; Barbero et al., 2004), particularly in the context of resurfacing a whole joint or bone where large cell numbers are required. While MSCs may offer an alternative as a cell source for cartilage repair therapies, MSC-based cartilaginous tissues do not retain a stable chondrogenic phenotype following implantation (Pelttari et al., 2006; Vinardell et al., 2012b). Another approach to cartilage repair, which was not explored in this thesis, is the use of a co-culture system incorporating both chondrocytes and MSCs in the same engineered tissue. Indeed, co-cultures of chondrocytes and MSCs have been shown to enhance chondrogenesis and reduce hypertrophy of cartilaginous constructs (Cooke et al., 2011; Bian et al., 2011). The co-culture approach to cartilage repair may therefore circumvent the issues associated with individual cell sources, as fewer numbers of chondrocytes would be required to generate a stable cartilaginous tissue, and warrants further investigation.

9.4. Future work

The fracture of a bone results in a signficant inflammatory response, resulting in the secretion of various growth factors and cytokines (Schindeler et al., 2008). Furthermore, the lower limbs of the body are subjected to mechanical forces, which have been shown to regulate hypertrophy of engineered cartilaginous constructs (Thorpe et al., 2012; Bian et al., 2012). Therefore, a key question that remains to be addressed is how endochondral ossification of an engineered hypertrophic cartilaginous graft will proceed in an orthopic enviroment, as opposed to the ectopic environment explored in this thesis. Future work should investigate the capacity of channelled MSC-seeded alginate hydrogels to generate endochondral bone when implanted into orthotopic site such as a femoral defect. Furthermore, implantation into cranial defects should also be investigated, to determine whether sites that develop through different ossification pathways (intramembranous or endochondral) are more suited to tissue engineering strategies that target those regeneration pathways.

As the endochondral approach moves towards regenerating large bones and joints, strategies will be required to ensure adequate nutrient delivery through scaled-up tissue engineered cartilaginous constructs during *in vitro* culture. Since Chapter 4 of this study demonstrated that dynamic flow conditions can inhibit chondrogenesis of MSCs, future work could investigate various flow rates so as to elucidate the appropriate bioreactor culture conditions to enhance nutrient transport without suppressing chondrogenesis.

Dissolution/degradation would appear to be a key parameter in the design of hydrogels and scaffolds for endochondral bone tissue engineering applications. Since alginate binds to dimethylmethylene blue, which is commonly used to measure sGAG accumulation, this assay could potentially be utilised to quantify alginate

dissolution *in vitro*. However, in the context of engineering anatomic tissues, maintenance of construct shape is also critical. Future work could explore the use of a bi-phasic scaffolding system, consisting of a porous scaffold or 'skeleton' to maintain the anatomic shape of the construct, and a gamma-irradiated alginate hydrogel to promote robust endochondral bone formation.

There are limitations to the use of chondrocytes in tissue engineering applications. Infrapatellar fat pad derived MSCs have been shown to generate functional cartilage *in vitro* (Vinardell et al., 2012b). Future studies could therefore investigate the capacity of co-cultures of chondrocytes and infrapatellar fat pad derived MSCs to form a stable chondral layer *in vivo*, with bone marrow MSCs acting as the osseous layer of the osteochondral construct.

The moulding methodologies used in this thesis to engineer phalanx and TMJ constructs can applied to bones and joints of different geometries. Future work will investigate the engineering of anatomically accurate constructs for total knee regeneration, consisting of chondral and osseous layers as outlined in this thesis, which could potentially serve as a biological joint prosthesis.

Bibliography

Acharya, C., Adesida, A., Zajac, P., Mumme, M., Riesle, J., Martin, I., Barbero, A., 2012. Enhanced chondrocyte proliferation and mesenchymal stromal cells chondrogenesis in coculture pellets mediate improved cartilage formation. Journal of Cellular Physiology 227 (1), 88–97.

Ahmed, T., Dare, E., Hincke, M., 2008. Fibrin: A versatile scaffold for tissue engineering applications. Tissue Engineering - Part B: Reviews 14 (2), 199–215.

Alhadlaq, A., Elisseeff, J., Hong, L., Williams, C., Caplan, A., Sharma, B., Kopher, R., Tomkoria, S., Lennon, D., Lopez, A., Mao, J., 2004. Adult stem cell driven genesis of human-shaped articular condyle. Annals of Biomedical Engineering 32 (7), 911–923.

Alhadlaq, A., Tang, M., Mao, J., 2005. Engineered adipose tissue from human mesenchymal stem cells maintains predefined shape and dimension: Implications in soft tissue augmentation and reconstruction. Tissue Engineering 11 (3-4), 556–566.

Alsberg, E., Anderson, K., Albeiruti, A., Rowley, J., Mooney, D., 2002. Engineering growing tissues. Proceedings of the National Academy of Sciences of the United States of America 99 (19), 12025–12030.

Alsberg, E., Kong, H., Hirano, Y., Smith, M., Albeiruti, A., Mooney, D., 2003. Regulating bone formation via controlled scaffold degradation. Journal of Dental Research 82 (11), 903–908.

Aronson, J., 1997. Limb-lengthening, skeletal reconstruction, and bone transport with the ilizarov method. The Journal of Bone and Joint Surgery 79-A (8), 1243–1258.

Augst, A., Kong, H., Mooney, D., 2006. Alginate hydrogels as biomaterials. Macromolecular Bioscience 6 (8), 623–633.

Awad, H. A., Wickham, M. Q., Leddy, H. A., Gimble, J. M., Guilak, F., 2004. Chondrogenic differentiation of adipose-derived adult stem cells in agarose, alginate, and gelatin scaffolds. Biomaterials 25 (16), 3211–3222.

Babalola, O., Bonassar, L., 2010. Effects of seeding density on proteoglycan assembly of passaged mesenchymal stem cells. Cellular and Molecular Bioengineering 3, 197–206.

Barbero, A., Grogan, S., Schäfer, D., Heberer, M., Mainil-Varlet, P., Martin, I., 2004. Age related changes in human articular chondrocyte yield, proliferation and post-expansion chondrogenic capacity. Osteoarthritis and Cartilage 12 (6), 476–484.

Basad, E., Ishaque, B., Bachmann, G., Sturz, H., Steinmeyer, J., 2010. Matrix-induced autologous chondrocyte implantation versus microfracture in the treatment of cartilage defects of the knee: A 2-year randomised study. Knee Surgery, Sports Traumatology, Arthroscopy 18 (4), 519–527.

Berger, J., Reist, M., Mayer, J., Felt, O., Peppas, N., Gurny, R., 2004. Structure and interactions in covalently and ionically crosslinked chitosan hydrogels for biomed-

ical applications. European Journal of Pharmaceutics and Biopharmaceutics 57 (1), 19–34.

Bian, L., Angione, S. L., Ng, K. W., Lima, E. G., Williams, D. Y., Mao, D. Q., Ateshian, G. A., Hung, C. T., 2009. Influence of decreasing nutrient path length on the development of engineered cartilage. Osteoarthritis Cartilage 17 (5), 677–85.

Bian, L., Zhai, D., Mauck, R., Burdick, J., 2011. Coculture of human mesenchymal stem cells and articular chondrocytes reduces hypertrophy and enhances functional properties of engineered cartilage. Tissue Engineering - Part A 17 (7-8), 1137–1145.

Bian, L., Zhai, D., Zhang, E., Mauck, R., Burdick, J., 2012. Dynamic compressive loading enhances cartilage matrix synthesis and distribution and suppresses hypertrophy in hmsc-laden hyaluronic acid hydrogels. Tissue Engineering - Part A 18 (7-8), 715–724.

Blumer, M., Longato, S., Fritsch, H., 2004. Cartilage canals in the chicken embryo are involved in the process of endochondral bone formation within the epiphyseal growth plate. Anatomical Record - Part A Discoveries in Molecular, Cellular, and Evolutionary Biology 279 (1), 692–700.

Blumer, M., Longato, S., Fritsch, H., 2008. Structure, formation and role of cartilage canals in the developing bone. Annals of Anatomy 190 (4), 305–315.

Blumer, M., Schwarzer, C., Perez, M., Konakci, K., Fritsch, H., 2006. Identification and location of bone-forming cells within cartilage canals on their course into the secondary ossification centre. Journal of Anatomy 208 (6), 695–707.

Boerckel, J., Uhrig, B., Willett, N., Huebsch, N., Guldberg, R., 2011. Mechanical regulation of vascular growth and tissue regeneration in vivo. Proceedings of

the National Academy of Sciences of the United States of America 108 (37), E674–E680.

Bosnakovski, D., Mizuno, M., Kim, G., Ishiguro, T., Okumura, M., Iwanaga, T., Kadosawa, T., Fujinaga, T., 2004. Chondrogenic differentiation of bovine bone marrow mesenchymal stem cells in pellet cultural system. Experimental Hematology 32 (5), 502–509.

Bosnakovski, D., Mizuno, M., Kim, G., Takagi, S., Okumura, M., Fujinaga, T., 2006. Chondrogenic differentiation of bovine bone marrow mesenchymal stem cells (mscs) in different hydrogels: influence of collagen type ii extracellular matrix on msc chondrogenesis. Biotechnol Bioeng 93 (6), 1152–63.

Brandi, M., Collin-Osdoby, P., 2006. Vascular biology and the skeleton. Journal of Bone and Mineral Research 21 (2), 183–192.

Brighton, C. T., Krebs, A. G., 1972. Oxygen tension of healing fractures in the rabbit. Journal of Bone and Joint Surgery - Series A 54 (2), 323–332.

Brittberg, M., Lindahl, A., Nilsson, A., Ohlsson, C., Isaksson, O., Peterson, L., 1994. Treatment of deep cartilage defects in the knee with autologous chondrocyte transplantation. New England Journal of Medicine 331 (14), 889–895.

Buckley, C., Meyer, E., Kelly, D., 2012. The influence of construct scale on the composition and functional properties of cartilaginous tissues engineered using bone marrow-derived mesenchymal stem cells. Tissue Engineering - Part A 18 (3-4), 382–396.

Buckley, C., O'Kelly, K., 2010. Fabrication and characterization of a porous multidomain hydroxyapatite scaffold for bone tissue engineering investigations. Journal of Biomedical Materials Research - Part B Applied Biomaterials 93 (2), 459–467.

Buckley, C. T., Thorpe, S. D., Kelly, D. J., 2009a. Engineering of large cartilaginous tissues through the use of microchanneled hydrogels and rotational culture. Tissue Engineering - Part A 15 (11), 3213–3220.

Buckley, C. T., Vinardell, T., Kelly, D. J., 2010. Oxygen tension differentially regulates the functional properties of cartilaginous tissues engineered from infrapatellar fat pad derived mscs and articular chondrocytes. Osteoarthritis and Cartilage 18 (10), 1345–1354.

Buckley, C. T., Vinardell, T., Thorpe, S. D., Haugh, M. G., Jones, E., McGonagle, D., Kelly, D. J., 2009b. Functional properties of cartilaginous tissues engineered from infrapatellar fat pad-derived mesenchymal stem cells. Journal of Biomechanics 43 (5), 920–926.

Buschmann, M. D., Gluzband, Y. A., Grodzinsky, A. J., Kimura, J. H., Hunziker, E. B., 1992. Chondrocytes in agarose culture synthesize a mechanically functional extracellular matrix. Journal of Orthopaedic Research 10 (6), 745–758.

Byers, B. A., Mauck, R. L., Chiang, I. E., Tuan, R. S., 2008. Transient exposure to transforming growth factor beta 3 under serum-free conditions enhances the biomechanical and biochemical maturation of tissue-engineered cartilage. Tissue Eng Part A 14 (11), 1821–34.

Caplan, A. I., 1991. Mesenchymal stem cells. Journal of Orthopaedic Research 9 (5), 641–650.

Caplan, A. I., 2005. Review: mesenchymal stem cells: cell-based reconstructive therapy in orthopedics. Tissue Eng 11 (7-8), 1198–211, caplan, Arnold I Research Support, Non-U.S. Gov't Review United States Tissue engineering Tissue Eng. 2005 Jul-Aug;11(7-8):1198-211.

Case, N., Duty, A., Ratcliffe, A., Muller, R., Guldberg, R., 2003. Bone formation on tissue-engineered cartilage constructs in vivo: Effects of chondrocyte viability and mechanical loading. Tissue Engineering 9 (4), 587–596.

Chan, C., Chen, C.-C., Luppen, C., Kim, J.-B., DeBoer, A., Wei, K., Helms, J., Kuo, C., Kraft, D., Weissman, I., 2009. Endochondral ossification is required for haematopoietic stem-cell niche formation. Nature 457 (7228), 490–494.

Chen, J., Chen, H., Li, P., Diao, H., Zhu, S., Dong, L., Wang, R., Guo, T., Zhao, J., Zhang, J., 2011. Simultaneous regeneration of articular cartilage and subchondral bone in vivo using mscs induced by a spatially controlled gene delivery system in bilayered integrated scaffolds. Biomaterials 32 (21), 4793–4805.

Cheresh, D., Berliner, S., Vicente, V., Ruggeri, Z., 1989. Recognition of distinct adhesive sites on fibrinogen by related integrins on platelets and endothelial cells. Cell 58 (5), 945–953.

Chubinskaya, S., Jacquet, R., Isogai, N., Asamura, S., Landis, W., 2004. Characterization of the cellular origin of a tissue-engineered human phalanx model by in situ hybridization. Tissue Engineering 10 (7-8), 1204–1213.

Coleman, R. M., Case, N. D., Guldberg, R. E., 2007. Hydrogel effects on bone marrow stromal cell response to chondrogenic growth factors. Biomaterials 28 (12), 2077–86.

Connelly, J., Wilson, C., Levenston, M., 2008. Characterization of proteoglycan production and processing by chondrocytes and bmscs in tissue engineered constructs. Osteoarthritis and Cartilage 16 (9), 1092 – 1100.

Cooke, M., Allon, A., Cheng, T., Kuo, A., Kim, H., Vail, T., Marcucio, R., Schneider, R., Lotz, J., Alliston, T., 2011. Structured three-dimensional co-culture of mesenchymal stem cells with chondrocytes promotes chondrogenic

differentiation without hypertrophy. Osteoarthritis and Cartilage 19 (10), 1210–1218.

Daher, R. J., Chahine, N. O., Greenberg, A. S., Sgaglione, N. A., Grande, D. A., 2009. New methods to diagnose and treat cartilage degeneration. Nature Reviews Rheumatology 5 (11), 599–607.

Davisson, T., Sah, R. L., Ratcliffe, A., 2002. Perfusion increases cell content and matrix synthesis in chondrocyte three-dimensional cultures. Tissue Engineering 8 (5), 807–816.

De Bari, C., Dell'Accio, F., Luyten, F. P., 2004. Failure of in vitro-differentiated mesenchymal stem cells from the synovial membrane to form ectopic stable cartilage in vivo. Arthritis and Rheumatism 50 (1), 142–150.

Delaine-Smith, R., Reilly, G., 2011. The effects of mechanical loading on mesenchymal stem cell differentiation and matrix production. Vitamins and Hormones 87, 417–480.

Diaz-Romero, J., Gaillard, J. P., Grogan, S. P., Nesic, D., Trub, T., Mainil-Varlet, P., 2005. Immunophenotypic analysis of human articular chondrocytes: changes in surface markers associated with cell expansion in monolayer culture. J Cell Physiol 202 (3), 731–42.

Dickhut, A., Gottwald, E., Steck, E., Heisel, C., Richter, W., 2008. Chondrogenesis of mesenchymal stem cells in gel-like biomaterials in vitro and in vivo. Frontiers in Bioscience 13 (12), 4517–4528.

Dickhut, A., Pelttari, K., Janicki, P., Wagner, W., Eckstein, V., Egermann, M., Richter, W., 2009. Calcification or dedifferentiation: Requirement to lock mesenchymal stem cells in a desired differentiation stage. Journal of Cellular Physiology 219 (1), 219–226.

Dimar, J., Glassman, S., Burkus, K., Carreon, L., 2006. Clinical outcomes and fusion success at 2 years of single-level instrumented posterolateral fusions with recombinant human bone morphogenetic protein-2/compression resistant matrix versus iliac crest bone graft. Spine 31 (22), 2534–2539.

Dimitriou, R., Jones, E., McGonagle, D., Giannoudis, P., 2011. Bone regeneration: Current concepts and future directions. BMC Medicine 9.

D'Ippolito, G., Diabira, S., Howard, G. A., Roos, B. A., Schiller, P. C., 2006. Low oxygen tension inhibits osteogenic differentiation and enhances stemness of human miami cells. Bone 39 (3), 513–522.

Donati, D., Bella, C. D., angeli, M. C., Bianchi, G., Mercuri, M., 2005. The use of massive bone allografts in bone tumour surgery of the limb. Current Orthopaedics 19 (5), 393 – 399.

Drury, J., Mooney, D., 2003. Hydrogels for tissue engineering: Scaffold design variables and applications. Biomaterials 24 (24), 4337–4351.

El Tamer, M. K., Reis, R. L., 2009. Progenitor and stem cells for bone and cartilage regeneration. Journal of tissue engineering and regenerative medicine 3 (5), 327–337.

Erickson, I., Kestle, S., Zellars, K., Farrell, M., Kim, M., Burdick, J., Mauck, R., 2012. High mesenchymal stem cell seeding densities in hyaluronic acid hydrogels produce engineered cartilage with native tissue properties. Acta Biomaterialia 8 (8), 3027–3034.

Erickson, I., Van Veen, S., Sengupta, S., Kestle, S., Mauck, R., 2011. Cartilage matrix formation by bovine mesenchymal stem cells in three-dimensional culture is age-dependent. Clinical Orthopaedics and Related Research 469 (10), 2744–2753.

Erickson, I. E., Huang, A. H., Chung, C., Li, R. T., Burdick, J. A., Mauck, R. L., 2009. Differential maturation and structure-function relationships in mesenchymal stem cell- and chondrocyte-seeded hydrogels. Tissue Eng Part A 15 (5), 1041–52.

Farrell, E., Both, S. K., Odorfer, K. I., Koevoet, W., Kops, N., O'Brien, F. J., De Jong, R. J. B., Verhaar, J. A., Cuijpers, V., Jansen, J., Erben, R. G., Van Osch, G. J. V. M., 2011. In-vivo generation of bone via endochondral ossification by in-vitro chondrogenic priming of adult human and rat mesenchymal stem cells. BMC Musculoskeletal Disorders 12.

Farrell, E., O'Brien, F., Doyle, P., Fischer, J., Yannas, I., Harley, B., O'Connell, B., Prendergast, P., Campbell, V., 2006. A collagen-glycosaminoglycan scaffold supports adult rat mesenchymal stem cell differentiation along osteogenic and chondrogenic routes. Tissue Engineering 12 (3), 459–468.

Farrell, E., Van Der Jagt, O. P., Koevoet, W., Kops, N., Van Manen, C. J., Hellingman, C. A., Jahr, H., O'Brien, F. J., Verhaar, J. A. N., Weinans, H., Van Osch, G. J. V. M., 2009. Chondrogenic priming of human bone marrow stromal cells: A better route to bone repair? Tissue Engineering - Part C: Methods 15 (2), 285–295.

Fedorovich, N., Alblas, J., De Wijn, J., Hennink, W., Verbout, A., Dhert, W., 2007. Hydrogels as extracellular matrices for skeletal tissue engineering: State-of-the-art and novel application in organ printing. Tissue Engineering 13 (8), 1905–1925.

Fehrer, C., Brunauer, R., Laschober, G., Unterluggauer, H., Reitinger, S., Kloss, F., Gully, C., Gabner, R., Lepperdinger, G., 2007. Reduced oxygen tension attenuates differentiation capacity of human mesenchymal stem cells and prolongs their lifespan. Aging Cell 6 (6), 745–757.

Fischer, J., Dickhut, A., Rickert, M., Richter, W., 2010. Human articular chondrocytes secrete parathyroid hormone-related protein and inhibit hypertrophy of mesenchymal stem cells in coculture during chondrogenesis. Arthritis and Rheumatism 62 (9), 2696–2706.

Friedenstein, A., Deriglasova, U., Kulagina, N., 1974. Precursors for fibroblasts in different populations of hematopoietic cells as detected by the in vitro colony assay method. Experimental Hematology 2 (2), 83–92.

Friedlaender, G., Perry, C., Cole, J., Cook, S., Cierny, G., Muschler, G., Zych, G., Calhoun, J., LaForte, A., Yin, S., 2001. Osteogenic protein-1 (bone morphogenetic protein-7) in the treatment of tibial nonunions. The Journal of bone and joint surgery. American volume 83 A Suppl 1 (Pt 2), S151–158.

Ganey, T., Ogden, J., Sasse, J., Neame, P., Hilbelink, D., 1995. Basement membrane composition of cartilage canals during development and ossification of the epiphysis. Anatomical Record 241 (3), 425–437.

Gao, J., Dennis, J., Solchaga, L., Awadallah, A., Goldberg, V., Caplan, A., 2001. Tissue-engineered fabrication of an osteochondral composite graft using rat bone marrow-derived mesenchymal stem cells. Tissue Engineering 7 (4), 363–371.

Gao, J., Dennis, J., Solchaga, L., Goldberg, V., Caplan, A., 2002. Repair of osteochondral defect with tissue-engineered two-phase composite material of injectable calcium phosphate and hyaluronan sponge. Tissue Engineering 8 (5), 827–837.

Gawlitta, D., Farrell, E., Malda, J., Creemers, L. B., Alblas, J., Dhert, W. J. A., 2010. Modulating endochondral ossification of multipotent stromal cells for bone regeneration. Tissue Engineering - Part B: Reviews 16 (4), 385–395.

Gawlitta, D., Van Rijen, M., Schrijver, E., Alblas, J., Dhert, W., 2012. Hypoxia impedes hypertrophic chondrogenesis of human multipotent stromal cells. Tissue Engineering - Part A 18 (19-20), 1957–1966.

Genovese, E., Ronga, M., Angeretti, M., Novario, R., Leonardi, A., Albrizio, M., Callegari, L., Fugazzola, C., 2011. Matrix-induced autologous chondrocyte implantation of the knee: mid-term and long-term follow-up by mr arthrography. Skeletal radiology 40 (1), 47–56.

Gerber, H.-P., Vu, T., Ryan, A., Kowalski, J., Werb, Z., Ferrara, N., 1999. Vegf couples hypertrophic cartilage remodeling, ossification and angiogenesis during endochondral bone formation. Nature Medicine 5 (6), 623–628.

Getgood, A., Bhullar, T. P. S., Rushton, N., 2009a. Current concepts in articular cartilage repair. Orthopaedics and Trauma 23 (3), 189–200.

Getgood, A., Brooks, R., Fortier, L., Rushton, N., 2009b. Articular cartilage tissue engineering: Today's research, tomorrow's practice? Journal of Bone and Joint Surgery - Series B 91 (5), 565–576.

Gleeson, J., Plunkett, N., O'Brien, F., 2010. Addition of hydroxyapatite improves stiffness, interconnectivity and osteogenic potential of a highly porous collagen-based scaffold for bone tissue regeneration. European cells & materials 20, 218–230.

Grant, J. L., Smith, B., 1963. Bone marrow gas tensions, bone marrow blood flow, and erythropoiesis in man. Annals of internal medicine 58, 801–809.

Grayson, W., Bhumiratana, S., Chao, P. G., Hung, C., Vunjak-Novakovic, G., 2010. Spatial regulation of human mesenchymal stem cell differentiation in engineered osteochondral constructs: effects of pre-differentiation, soluble factors and medium perfusion. Osteoarthritis and Cartilage 18 (5), 714 – 723.

Grayson, W. L., Chao, P. H., Marolt, D., Kaplan, D. L., Vunjak-Novakovic, G., 2008. Engineering custom-designed osteochondral tissue grafts. Trends Biotechnol 26 (4), 181–9.

Grayson, W. L., Zhao, F., Izadpanah, R., Bunnell, B., Ma, T., 2006. Effects of hypoxia on human mesenchymal stem cell expansion and plasticity in 3d constructs. Journal of Cellular Physiology 207 (2), 331–339.

Guldberg, R., Oest, M., Dupont, K., Peister, A., Deutsch, E., Kolambkar, Y., Mooney, D., 2007. Biologic augmentation of polymer scaffolds for bone repair. Journal of musculoskeletal & neuronal interactions 7 (4), 333–334.

Guo, X., Liao, J., Park, H., Saraf, A., Raphael, R., Tabata, Y., Kasper, F., Mikos, A., 2010. Effects of tgf-b3 and preculture period of osteogenic cells on the chondrogenic differentiation of rabbit marrow mesenchymal stem cells encapsulated in a bilayered hydrogel composite. Acta Biomaterialia 6 (8), 2920–2931.

Guo, X., Park, H., Liu, G., Liu, W., Cao, Y., Tabata, Y., Kasper, F., Mikos, A., 2009. In vitro generation of an osteochondral construct using injectable hydrogel composites encapsulating rabbit marrow mesenchymal stem cells. Biomaterials 30 (14), 2741–2752.

Hannouche, D., Terai, H., Fuchs, J. R., Terada, S., Zand, S., Nasseri, B. A., Petite, H., Sedel, L., Vacanti, J. P., 2007. Engineering of implantable cartilaginous structures from bone marrow-derived mesenchymal stem cells. Tissue Eng 13 (1), 87–99.

Heppenstall, R. B., Grislis, G., Hunt, T. K., 1975. Tissue gas tensions and oxygen consumption in healing bone defects. Clin Orthop Relat Res No. 106, 357–365.

Hirao, M., Tamai, N., Tsumaki, N., Yoshikawa, H., Myoui, A., 2006. Oxygen tension regulates chondrocyte differentiation and function during endochondral ossification. Journal of Biological Chemistry 281 (41), 31079–31092.

Hoemann, C., Chenite, A., Sun, J., Hurtig, M., Serreqi, A., Lu, Z., Rossomacha, E., Buschmann, M., 2007. Cytocompatible gel formation of chitosan-glycerol phosphate solutions supplemented with hydroxyl ethyl cellulose is due to the presence of glyoxal. Journal of Biomedical Materials Research - Part A 83 (2), 521–529.

Hoemann, C. D., Sun, J., Legare, A., McKee, M. D., Buschmann, M. D., 2005. Tissue engineering of cartilage using an injectable and adhesive chitosan-based cell-delivery vehicle. Osteoarthritis Cartilage 13 (4), 318–29.

Hong, Y., Song, H., Gong, Y., Mao, Z., Gao, C., Shen, J., 2007. Covalently crosslinked chitosan hydrogel: Properties of in vitro degradation and chondrocyte encapsulation. Acta Biomaterialia 3 (1), 23–31.

Hu, J., Athanasiou, K., 2006. A self-assembling process in articular cartilage tissue engineering. Tissue Engineering 12 (4), 969–979.

Huang, A., Farrell, M., Mauck, R., 2010. Mechanics and mechanobiology of mesenchymal stem cell-based engineered cartilage. Journal of Biomechanics 43 (1), 128–136.

Huang, A. H., Stein, A., Tuan, R. S., Mauck, R. L., 2009. Transient exposure to transforming growth factor beta 3 improves the mechanical properties of mesenchymal stem cell-laden cartilage constructs in a density-dependent manner. Tissue Engineering - Part A 15 (11), 3461–3472.

Huang, A. H., Yeger-McKeever, M., Stein, A., Mauck, R. L., 2008. Tensile properties of engineered cartilage formed from chondrocyte- and msc-laden hydrogels. Osteoarthritis and Cartilage 16 (9), 1074–1082.

Huang, J., Durbhakula, M., Angele, P., Johnstone, B., Yoo, J., 2006. Lunate arthroplasty with autologous mesenchymal stem cells in a rabbit model. Journal of Bone and Joint Surgery - Series A 88 (4), 744–752.

Hung, C. T., Lima, E. G., Mauck, R. L., Takai, E., LeRoux, M. A., Lu, H. H., Stark, R. G., Guo, X. E., Ateshian, G. A., 2003. Anatomically shaped osteochondral constructs for articular cartilage repair. J Biomech 36 (12), 1853–64.

Hunt, N., Grover, L., 2010. Cell encapsulation using biopolymer gels for regenerative medicine. Biotechnology Letters 32 (6), 733–742.

Ignat'eva, N. Y., Danilov, N. A., Averkiev, S. V., Obrezkova, M. V., Lunin, V. V., Sobol, E. N., 2007. Determination of hydroxyproline in tissues and the evaluation of the collagen content of the tissues. J Anal Chem 62 (1), 51–57.

Isogai, N., Landis, W., Kim, T., Gerstenfeld, L., Upton, J., Vacanti, J., 1999. Formation of phalanges and small joints by tissue-engineering. Journal of Bone and Joint Surgery - Series A 81 (3), 306–316.

Janicki, P., Kasten, P., Kleinschmidt, K., Luginbuehl, R., Richter, W., 2010. Chondrogenic pre-induction of human mesenchymal stem cells on beta-tcp: Enhanced bone quality by endochondral heterotopic bone formation. Acta Biomaterialia 6 (8), 3292–3301.

Janmey, P., Winer, J., Weisel, J., 2009. Fibrin gels and their clinical and bioengineering applications. Journal of the Royal Society Interface 6 (30), 1–10.

Johnstone, B., Hering, T. M., Caplan, A. I., Goldberg, V. M., Yoo, J. U., 1998. In vitro chondrogenesis of bone marrow-derived mesenchymal progenitor cells. Experimental Cell Research 238 (1), 265–272.

Jukes, J. M., Both, S. K., Leusink, A., Sterk, L. M. T., Van Blitterswijk, C. A., De Boer, J., 2008. Endochondral bone tissue engineering using embryonic stem cells. Proceedings of the National Academy of Sciences of the United States of America 105 (19), 6840–6845.

Kanichai, M., Ferguson, D., Prendergast, P. J., Campbell, V. A., 2008. Hypoxia promotes chondrogenesis in rat mesenchymal stem cells: A role for akt and hypoxia-inducible factor (hif)-1a. Journal of Cellular Physiology 216 (3), 708–715.

Karp, S., Schipani, E., St-Jacques, B., Hunzelman, J., Kronenberg, H., McMahon, A., 2000. Indian hedgehog coordinates endochondral bone growth and morphogenesis via parathyroid hormone related-protein-dependent and -independent pathways. Development 127 (3), 543–548.

Kelly, D. J., Prendergast, P. J., 2005. Mechano-regulation of stem cell differentiation and tissue regeneration in osteochondral defects. J Biomech 38 (7), 1413–22.

Kelly, D. J., Prendergast, P. J., 2006. Prediction of the optimal mechanical properties for a scaffold used in osteochondral defect repair. Tissue Eng 12 (9), 2509–19.

Khan, W. S., Adesida, A. B., Tew, S. R., Lowe, E. T., Hardingham, T. E., 2010. Bone marrow-derived mesenchymal stem cells express the pericyte marker 3g5 in culture and show enhanced chondrogenesis in hypoxic conditions. Journal of Orthopaedic Research 28 (6), 834–840.

Khanarian, N., Jiang, J., Wan, L., Mow, V., Lu, H., 2012. A hydrogel-mineral composite scaffold for osteochondral interface tissue engineering. Tissue Engineering - Part A 18 (5-6), 533–545.

Kharkar, P., Kiick, K., Kloxin, A., 2013. Designing degradable hydrogels for orthogonal control of cell microenvironments. Chemical Society Reviews 42 (17), 7335–7372.

Kim, W. S., Vacanti, C., Upton, J., Vacanti, J., 1994. Bone defect repair with tissue-engineered cartilage. Plastic and Reconstructive Surgery 94 (5), 580–584.

Kisiday, J. D., Kopesky, P. W., Evans, C. H., Grodzinsky, A. J., McIlwraith, C. W., Frisbie, D. D., 2008. Evaluation of adult equine bone marrow- and adipose-derived progenitor cell chondrogenesis in hydrogel cultures. J Orthop Res 26 (3), 322–31.

Klein, C., De Groot, K., Weiqun, C., Yubao, L., Xingdong, Z., 1994. Osseous substance formation induced in porous calcium phosphate ceramics in soft tissues. Biomaterials 15 (1), 31–34.

Koay, E. J., Athanasiou, K. A., 2008. Hypoxic chondrogenic differentiation of human embryonic stem cells enhances cartilage protein synthesis and biomechanical functionality. Osteoarthritis and Cartilage 16 (12), 1450–1456.

Kofoed, H., Sjontoft, E., Siemssen, S. O., Olesen, H. P., 1985. Bone marrow circulation after osteotomy. blood flow, po2, pco2, and pressure studied in dogs. Acta Orthopaedica Scandinavica 56 (5), 400–403.

Koh, C. J., Atala, A., 2004. Tissue engineering, stem cells, and cloning: Opportunities for regenerative medicine. Journal of the American Society of Nephrology 15 (5), 1113–1125.

Kolambkar, Y., Boerckel, J., Dupont, K., Bajin, M., Huebsch, N., Mooney, D., Hutmacher, D., Guldberg, R., 2011a. Spatiotemporal delivery of bone morphogenetic protein enhances functional repair of segmental bone defects. Bone 49 (3), 485–492.

Kolambkar, Y., Dupont, K., Boerckel, J., Huebsch, N., Mooney, D., Hutmacher, D., Guldberg, R., 2011b. An alginate-based hybrid system for growth factor delivery in the functional repair of large bone defects. Biomaterials 32 (1), 65–74.

Komura, M., Kim, J., Atala, A., Yoo, J., Lee, S., 2011. Priniciples of Regenerative Medicine. The Digit: Engineering of Phalanges and Small Joints. Elsevier Inc.

Kon, E., Muraglia, A., Corsi, A., Bianco, P., Marcacci, M., Martin, I., Boyde, A., Ruspantini, I., Chistolini, P., Rocca, M., Giardino, R., Cancedda, R., Quarto, R., 2000. Autologous bone marrow stromal cells loaded onto porous hydroxyapatite ceramic accelerate bone repair in critical-size defects of sheep long bones. Journal of Biomedical Materials Research 49 (3), 328–337.

Kronenberg, H., 2006. Pthrp and skeletal development. Annals of the New York Academy of Sciences 1068 (1), 1–13.

Kronenberg, H. M., 2003. Developmental regulation of the growth plate. Nature 423 (6937), 332–336.

Lacroix, D., Prendergast, P. J., 2002. A mechano-regulation model for tissue differentiation during fracture healing: Analysis of gap size and loading. Journal of Biomechanics 35 (9), 1163–1171.

Lafont, J. E., 2010. Lack of oxygen in articular cartilage: Consequences for chondrocyte biology. International Journal of Experimental Pathology 91 (2), 99–106.

Landis, W., Jacquet, R., Lowder, E., Enjo, M., Wada, Y., Isogai, N., 2009. Tissue engineering models of human digits: Effect of periosteum on growth plate cartilage development. Cells Tissues Organs 189 (1-4), 241–244.

Langer, R., 2000. Tissue engineering. Molecular Therapy 1 (1), 12–15.

Lau, T., Lee, L., Vo, B., Su, K., Wang, D.-A., 2012. Inducing ossification in an engineered 3d scaffold-free living cartilage template. Biomaterials 33 (33), 8406–8417.

Le Nihouannen, D., Daculsi, G., Saffarzadeh, A., Gauthier, O., Delplace, S., Pilet, P., Layrolle, P., 2005. Ectopic bone formation by microporous calcium phosphate ceramic particles in sheep muscles. Bone 36 (6), 1086–1093.

Learmonth, I., Young, C., Rorabeck, C., 2007. The operation of the century: total hip replacement. Lancet 370 (9597), 1508–1519.

Lee, H.-Y., Kopesky, P. W., Plaas, A. H. K., Diaz, M. A., Sandy, J. D., Kisiday, J. D., Frisbie, D. D., Ortiz, C., Grodzinsky, A. J., 2009. Adult equine mscs synthesize aggrecan having nanomechanical compressibility and biochemical composition characteristic of young growth cartilage. In: Transactions of the 55th Annual Orthopaedic Research Society. Las Vegas, NV, USA, p. PAPER 172.

Lenas, P., Moos, M., Luyten, F., 2009. Developmental engineering: A new paradigm for the design and manufacturing of cell-based products. part i: From three-dimensional cell growth to biomimetics of in vivo development. Tissue Engineering - Part B: Reviews 15 (4), 381–394.

Lennon, D. P., Caplan, A. I., 2006. Isolation of human marrow-derived mesenchymal stem cells. Exp Hematol 34 (11), 1604–5, lennon, Donald P Caplan, Arnold I Netherlands Experimental hematology Exp Hematol. 2006 Nov;34(11):1604-5.

Lennon, D. P., Edmison, J. M., Caplan, A. I., 2001. Cultivation of rat marrow-derived mesenchymal stem cells in reduced oxygen tension: Effects on in vitro and in vivo osteochondrogenesis. Journal of Cellular Physiology 187 (3), 345–355.

Lima, E. G., Bian, L., Ng, K. W., Mauck, R. L., Byers, B. A., Tuan, R. S., Ateshian, G. A., Hung, C. T., 2007. The beneficial effect of delayed compressive loading on tissue-engineered cartilage constructs cultured with tgf-beta 3. Osteoarthritis and Cartilage 15, 1025–1033.

Lin, C.-Y., Chang, Y.-H., Li, K.-C., Lu, C.-H., Sung, L.-Y., Yeh, C.-L., Lin, K.-J., Huang, S.-F., Yen, T.-C., Hu, Y.-C., 2013. The use of ascs engineered to express bmp2 or tgf-b3 within scaffold constructs to promote calvarial bone repair. Biomaterials 34 (37), 9401–9412.

Little, N., Rogers, B., Flannery, M., 2011. Bone formation, remodelling and healing. Surgery 29 (4), 141–145.

Lyons, F., Al-Munajjed, A., Kieran, S., Toner, M., Murphy, C., Duffy, G., O'Brien, F., 2010. The healing of bony defects by cell-free collagen-based scaffolds compared to stem cell-seeded tissue engineered constructs. Biomaterials 31 (35), 9232–9243.

Ma, K., Titan, A., Stafford, M., Zheng, C., Levenston, M., 2012. Variations in chondrogenesis of human bone marrow-derived mesenchymal stem cells in fibrin/alginate blended hydrogels. Acta Biomaterialia 8 (10), 3754–3764.

Ma, T., Grayson, W. L., Frohlich, M., Vunjak-Novakovic, G., 2009. Hypoxia and stem cell-based engineering of mesenchymal tissues. Biotechnology Progress 25 (1), 32–42.

Mackie, E., 2003. Osteoblasts: Novel roles in orchestration of skeletal architecture. International Journal of Biochemistry and Cell Biology 35 (9), 1301–1305.

Mackie, E., Ahmed, Y., Tatarczuch, L., Chen, K.-S., Mirams, M., 2008. Endochondral ossification: How cartilage is converted into bone in the developing skeleton. International Journal of Biochemistry and Cell Biology 40 (1), 46–62.

Mahmoudifar, N., Doran, P., 2005. Tissue engineering of human cartilage and osteochondral composites using recirculation bioreactors. Biomaterials 26 (34), 7012–7024.

Mahmoudifar, N., Doran, P. M., 2010. Chondrogenic differentiation of human adipose-derived stem cells in polyglycolic acid mesh scaffolds under dynamic culture conditions. Biomaterials 31 (14), 3858 – 3867.

Mano, J., Reis, R., 2007. Osteochondral defects: Present situation and tissue engineering approaches. Journal of Tissue Engineering and Regenerative Medicine 1 (4), 261–273.

Marcacci, M., Kon, E., Moukhachev, V., Lavroukov, A., Kutepov, S., Quarto, R., Mastrogiacomo, M., Cancedda, R., 2007. Stem cells associated with macroporous bioceramics for long bone repair: 6- to 7-year outcome of a pilot clinical study. Tissue Engineering 13 (5), 947–955.

Martin, I., Miot, S., Barbero, A., Jakob, M., Wendt, D., 2007. Osteochondral tissue engineering. Journal of Biomechanics 40 (4), 750–765.

Martin, I., Wendt, D., Heberer, M., 2004. The role of bioreactors in tissue engineering. Trends Biotechnol 22 (2), 80–6, 0167-7799 (Print) Journal Article Review.

Mason, J., Grande, D., Barcia, M., Grant, R., Pergolizzi, R., Breitbart, A., 1998. Expression of human bone morphogenic protein 7 in primary rabbit periosteal cells: Potential utility in gene therapy for osteochondral repair. Gene Therapy 5 (8), 1098–1104.

Mauck, R. L., Nicoll, S. B., Seyhan, S. L., Ateshian, G. A., Hung, C. T., 2003a. Synergistic action of growth factors and dynamic loading for articular cartilage tissue engineering. Tissue Eng 9 (4), 597–611.

Mauck, R. L., Seyhan, S. L., Ateshian, G. A., Hung, C. T., 2002. Influence of seeding density and dynamic deformational loading on the developing structure/function relationships of chondrocyte-seeded agarose hydrogels. Ann Biomed Eng 30 (8), 1046–56.

Mauck, R. L., Soltz, M. A., Wang, C. C. B., Wong, D. D., Chao, P. H. G., Valhmu, W. B., Hung, C. T., Ateshian, G. A., 2000. Functional tissue engineering of articular cartilage through dynamic loading of chondrocyte-seeded agarose gels. Journal of Biomechanical Engineering 122 (3), 252–260.

Mauck, R. L., Wang, C. C. B., Oswald, E. S., Ateshian, G. A., Hung, C. T., 2003b. The role of cell seeding density and nutrient supply for articular cartilage tissue engineering with deformational loading. Osteoarthritis and Cartilage 11 (12), 879–890.

Mauck, R. L., Yuan, X., Tuan, R. S., 2006. Chondrogenic differentiation and functional maturation of bovine mesenchymal stem cells in long-term agarose culture. Osteoarthritis Cartilage 14 (2), 179–89.

McBeath, R., Pirone, D. M., Nelson, C. M., Bhadriraju, K., Chen, C. S., 2004. Cell shape, cytoskeletal tension, and rhoa regulate stem cell lineage commitment. Dev Cell 6 (4), 483–95.

McBride, S. H., Falls, T., Knothe Tate, M. L., 2008. Modulation of stem cell shape and fate b: Mechanical modulation of cell shape and gene expression. Tissue Engineering - Part A. 14 (9), 1573–1580.

Meijer, G., De Bruijn, J., Koole, R., Van Blitterswijk, C., 2007. Cell-based bone tissue engineering. PLoS Medicine 4 (2), 0260–0264.

Merceron, C., Vinatier, C., Portron, S., Masson, M., Amiaud, J., Guigand, L., Cherel, Y., Weiss, P., Guicheux, J., 2010. Differential effects of hypoxia on osteochondrogenic potential of human adipose-derived stem cells. American Journal of Physiology - Cell Physiology 298 (2), C355–C364.

Meretoja, V., Dahlin, R., Wright, S., Kasper, F., Mikos, A., 2013. The effect of hypoxia on the chondrogenic differentiation of co-cultured articular chondrocytes and mesenchymal stem cells in scaffolds. Biomaterials 34 (17), 4266–4273.

Mesallati, T., Buckley, C., Kelly, D., 2014. A comparison of self-assembly and hydrogel encapsulation as a means to engineer functional cartilaginous grafts using culture expanded chondrocytes. Tissue Engineering - Part C: Methods 20 (1), 52–63.

Mesallati, T., Buckley, C., Nagel, T., Kelly, D., 2012. Scaffold architecture determines chondrocyte response to externally applied dynamic compression. Biomechanics and Modeling in Mechanobiology, 1–11.

Meyer, E. G., Buckley, C. T., Thorpe, S. D., Kelly, D. J., 2010. Low oxygen tension is a more potent promoter of chondrogenic differentiation than dynamic compression. Journal of Biomechanics 43 (13), 2516–2523.

Mohyeldin, A., Garzon-Muvdi, T., Quinones-Hinojosa, A., 2010. Oxygen in stem cell biology: A critical component of the stem cell niche. Cell Stem Cell 7 (2), 150–161.

Morita, K., Miyamoto, T., Fujita, N., Kubota, Y., Ito, K., Takubo, K., Miyamoto, K., Ninomiya, K., Suzuki, T., Iwasaki, R., Yagi, M., Takaishi, H., Toyama, Y.,

Suda, T., 2007. Reactive oxygen species induce chondrocyte hypertrophy in endochondral ossification. Journal of Experimental Medicine 204 (7), 1613–1623.

Mow, V. C., Huiskes, R., 2005. Basic Orthopaedic Biomechanics and Mechano-Biology, 3rd Edition. Lippincott Williams & Wilkins.

Mow, V. C., Kuei, S. C., Lai, W. M., Armstrong, C. G., 1980. Biphasic creep and stress relaxation of articular cartilage in compression: Theory and experiments. Journal of Biomechanical Engineering 102 (1), 73–84.

Mueller, M., Tuan, R., 2008. Functional characterization of hypertrophy in chondrogenesis of human mesenchymal stem cells. Arthritis and Rheumatism 58 (5), 1377–1388.

Mumme, M., Scotti, C., Papadimitropoulos, A., Todorov, A., Hoffmann, W., Bocelli-Tyndall, C., Jakob, M., Wendt, D., Martin, I., Barbero, A., 2012. Interleukin-1b modulates endochondral ossification by human adult bone marrow stromal cells. European Cells and Materials 24, 224–236.

Muraglia, A., Corsi, A., Riminucci, M., Mastrogiacomo, M., Cancedda, R., Bianco, P., Quarto, R., 2003. Formation of a chondro-osseous rudiment in micromass cultures of human bone-marrow stromal cells. Journal of Cell Science 116 (14), 2949–2955.

Murphy, J. M., Dixon, K., Beck, S., Fabian, D., Feldman, A., Barry, F., 2002. Reduced chondrogenic and adipogenic activity of mesenchymal stem cells from patients with advanced osteoarthritis. Arthritis and Rheumatism 46 (3), 704–713.

Nagai, T., Furukawa, K. S., Sato, M., Ushida, T., Mochida, J., 2008. Characteristics of a scaffold-free articular chondrocyte plate grown in rotational culture. Tissue Engineering - Part A. 14 (7), 1183–1193.

Nesic, D., Whiteside, R., Brittberg, M., Wendt, D., Martin, I., Mainil-Varlet, P., 2006. Cartilage tissue engineering for degenerative joint disease. Adv Drug Deliv Rev 58 (2), 300–22.

Newman, A., 1998. Articular cartilage repair. American Journal of Sports Medicine 26 (2), 309–324.

Nilsson, M., Fernandez, E., Planel, J., McCarthy, I., Lidgren, L., 2003. The effect of aging an injectable bone graft substitute in simulated body fluid. Key Engineering Materials 240-242, 403–406.

O'Brien, F. J., Harley, B. A., Yannas, I. V., Gibson, L. J., 2005. The effect of pore size on cell adhesion in collagen-gag scaffolds. Biomaterials 26 (4), 433–41.

Oest, M., Dupont, K., Kong, H.-J., Mooney, D., Guldberg, R., 2007. Quantitative assessment of scaffold and growth factor-mediated repair of critically sized bone defects. Journal of Orthopaedic Research 25 (7), 941–950.

Oliveira, J., Rodrigues, M., Silva, S., Malafaya, P., Gomes, M., Viegas, C., Dias, I., Azevedo, J., Mano, J., Reis, R., 2006. Novel hydroxyapatite/chitosan bilayered scaffold for osteochondral tissue-engineering applications: Scaffold design and its performance when seeded with goat bone marrow stromal cells. Biomaterials 27 (36), 6123–6137.

Oliveira, S. M., Amaral, I. F., Barbosa, M. A., Teixeira, C. C., 2009a. Engineering endochondral bone: In vitro studies. Tissue Engineering - Part A 15 (3), 625–634.

Oliveira, S. M., Mijares, D. Q., Turner, G., Amaral, I. F., Barbosa, M. A., Teixeira, C. C., 2009b. Engineering endochondral bone: In vivo studies. Tissue Engineering - Part A 15 (3), 635–643.

Patino, M., Neiders, M., Andreana, S., Noble, B., Cohen, R., 2002. Collagen as an implantable material in medicine and dentistry. The Journal of oral implantology 28 (5), 220–225.

Pazzano, D., Mercier, K. A., Moran, J. M., Fong, S. S., DiBiasio, D. D., Rulfs, J. X., Kohles, S. S., Bonassar, L. J., 2000. Comparison of chondrogensis in static and perfused bioreactor culture. Biotechnology Progress 16 (5), 893–896.

Pelttari, K., Winter, A., Steck, E., Goetzke, K., Hennig, T., Ochs, B. G., Aigner, T., Richter, W., 2006. Premature induction of hypertrophy during in vitro chondrogenesis of human mesenchymal stem cells correlates with calcification and vascular invasion after ectopic transplantation in scid mice. Arthritis and Rheumatism 54 (10), 3254–3266.

Perez-Sanchez, M.-J., Ramarez-Glindon, E., Lledo-Gil, M., Calvo-Guirado, J.-L., Perez-Sanchez, C., 2010. Biomaterials for bone regeneration. Medicina Oral, Patologia Oral y Cirugia Bucal 15 (3), e517–e522.

Peterson, L., Minas, T., Brittberg, M., Nilsson, A., Sjogren-Jansson, E., Lindahl, A., 2000. Two-to 9-year outcome after autologous chondrocyte transplantation of the knee. Clinical Orthopaedics and Related Research (374), 212–234.

Petrakova, K., Tolmacheva, A., Friedenstein, A., 1963. Bone formation occurring in bone marrow transplantation in diffusion. Bull. Exp. Bio. Med 56, 87–91.

Potier, E., Ferreira, E., Andriamanalijaona, R., Pujol, J. P., Oudina, K., Logeart-Avramoglou, D., Petite, H., 2007. Hypoxia affects mesenchymal stromal cell osteogenic differentiation and angiogenic factor expression. Bone 40 (4), 1078–1087.

Prendergast, P. J., Huiskes, R., Soballe, K., 1997. Biophysical stimuli on cells

during tissue differentiation at implant interfaces. Journal of Biomechanics 30 (6), 539–548.

Quarto, R., Mastrogiacomo, M., Cancedda, R., Kutepov, S., Mukhachev, V., Lavroukov, A., Kon, E., Marcacci, M., 2001. Repair of large bone defects with the use of autologous bone marrow stromal cells. New England Journal of Medicine 344 (5), 385–386.

Rai, B., Oest, M., Dupont, K., Ho, K., Teoh, S., Guldberg, R., 2007. Combination of platelet-rich plasma with polycaprolactone-tricalcium phosphate scaffolds for segmental bone defect repair. Journal of Biomedical Materials Research - Part A 81 (4), 888–899.

Raimondi, M. T., Candiani, G., Cabras, M., Cioffi, M., Laganà , K., Moretti, M., Pietrabissa, R., 2008. Engineered cartilage constructs subject to very low regimens of interstitial perfusion. Biorheology 45 (3-4), 471–478.

Raimondi, M. T., Moretti, M., Cioffi, M., Giordano, C., Boschetti, F., Laganà , K., Pietrabissa, R., 2006. The effect of hydrodynamic shear on 3d engineered chondrocyte systems subject to direct perfusion. Biorheology 43 (3-4), 215–222.

Ralston, S., 2009. Bone structure and metabolism. Medicine 37 (9), 469–474.

Reilly, G., Engler, A., 2010. Intrinsic extracellular matrix properties regulate stem cell differentiation. Journal of Biomechanics 43 (1), 55–62.

Richter, W., 2009. Mesenchymal stem cells and cartilage in situ regeneration. Journal of Internal Medicine 266 (4), 390–405.

Riley, S., Dutt, S., De la Torre, R., Chen, A., Sah, R., Ratcliffe, A., 2001. Formulation of peg-based hydrogels affects tissue-engineered cartilage construct

characteristics. Journal of Materials Science: Materials in Medicine 12 (10-12), 983–990.

Robins, J. C., Akeno, N., Mukherjee, A., Dalal, R. R., Aronow, B. J., Koopman, P., Clemens, T. L., 2005. Hypoxia induces chondrocyte-specific gene expression in mesenchymal cells in association with transcriptional activation of sox9. Bone 37 (3), 313–322.

Rodrigues, M., Lee, S., Gomes, M., Reis, R., Atala, A., Yoo, J., 2012. Bilayered constructs aimed at osteochondral strategies: The influence of medium supplements in the osteogenic and chondrogenic differentiation of amniotic fluid-derived stem cells. Acta Biomaterialia 8 (7), 2795–2806.

Ronzière, M. C., Perrier, E., Mallein-Gerin, F., Freyria, A. M., 2010. Chondrogenic potential of bone marrow- and adipose tissue-derived adult human mesenchymal stem cells. Bio-Medical Materials and Engineering 20 (3-4), 145–158.

Roughley, P., Hoemann, C., DesRosiers, E., Mwale, F., Antoniou, J., Alini, M., 2006. The potential of chitosan-based gels containing intervertebral disc cells for nucleus pulposus supplementation. Biomaterials 27 (3), 388–396.

Ruano-Ravina, A., Jato Diaz, M., 2006. Autologous chondrocyte implantation: a systematic review. Osteoarthritis Cartilage 14 (1), 47–51.

Ruel-Gariepy, E., Leroux, J.-C., 2004. In situ-forming hydrogels - review of temperature-sensitive systems. European Journal of Pharmaceutics and Biopharmaceutics 58 (2), 409–426.

Salgado, A., Coutinho, O., Reis, R., 2004. Bone tissue engineering: State of the art and future trends. Macromolecular Bioscience 4 (8), 743–765.

Santos, M., Reis, R., 2010. Vascularization in bone tissue engineering: Physiology, current strategies, major hurdles and future challenges. Macromolecular Bioscience 10 (1), 12–27.

Schaefer, D., Martin, I., Jundt, G., Seidel, J., Heberer, M., Grodzinsky, A., Bergin, I., Vunjak-Novakovic, G., Freed, L. E., 2002. Tissue-engineered composites for the repair of large osteochondral defects. Arthritis Rheum 46 (9), 2524–34.

Schindeler, A., McDonald, M., Bokko, P., Little, D., 2008. Bone remodeling during fracture repair: The cellular picture. Seminars in Cell and Developmental Biology 19 (5), 459–466.

Schroeder, J., Mosheiff, R., 2011. Tissue engineering approaches for bone repair: Concepts and evidence. Injury 42 (6), 609–613.

Scotti, C., Piccinini, E., Takizawa, H., Todorov, A., Bourgine, P., Papadimitropoulos, A., Barbero, A., Manz, M., Martin, I., 2013. Engineering of a functional bone organ through endochondral ossification. Proceedings of the National Academy of Sciences of the United States of America 110 (10), 3997–4002.

Scotti, C., Tonnarelli, B., Papadimitropoulos, A., Scherberich, A., Schaeren, S., Schauerte, A., Lopez-Rios, J., Zeller, R., Barbero, A., Martin, I., 2010. Recapitulation of endochondral bone formation using human adult mesenchymal stem cells as a paradigm for developmental engineering. Proceedings of the National Academy of Sciences of the United States of America 107 (16), 7251–7256.

Sedrakyan, S., Zhou, Z., Perin, L., Leach, K., Mooney, D., Kim, T., 2006. Tissue engineering of a small hand phalanx with a porously casted polylactic acid-polyglycolic acid copolymer. Tissue Engineering 12 (9), 2675–2683.

Sekiya, I., Vuoristo, J., Larson, B., Prockop, D., 2002. In vitro cartilage formation by human adult stem cells from bone marrow stroma defines the sequence of

cellular and molecular events during chondrogenesis. Proceedings of the National Academy of Sciences of the United States of America 99 (7), 4397–4402.

Selmi, T. A. S., Verdonk, P., Chambat, P., Dubrana, F., Potel, J. F., Barnouin, L., Neyret, P., 2008. Autologous chondrocyte implantation in a novel alginate-agarose hydrogel: Outcome at two years. Journal of Bone and Joint Surgery - Series B 90 (5), 597–604.

Sheehy, E., Buckley, C., Kelly, D., 2012. Oxygen tension regulates the osteogenic, chondrogenic and endochondral phenotype of bone marrow derived mesenchymal stem cells. Biochemical and Biophysical Research Communications 417 (1), 305–310.

Sheehy, E., Vinardell, T., Buckley, C., Kelly, D., 2013. Engineering osteochondral constructs through spatial regulation of endochondral ossification. Acta Biomaterialia 9 (3), 5484–5492.

Sheehy, E. J., Buckley, C. T., Kelly, D. J., 2011. Chondrocytes and bone marrow-derived mesenchymal stem cells undergoing chondrogenesis in agarose hydrogels of solid and channelled architectures respond differentially to dynamic culture conditions. Journal of Tissue Engineering and Regenerative Medicine 5 (9), 747–758.

Silva, M. M. C. G., Cyster, L. A., Barry, J. J. A., Yang, X. B., Oreffo, R. O. C., Grant, D. M., Scotchford, C. A., Howdle, S. M., Shakesheff, K. M., Rose, F. R. A. J., 2006. The effect of anisotropic architecture on cell and tissue infiltration into tissue engineering scaffolds. Biomaterials 27 (35), 5909–5917.

Simmons, C., Alsberg, E., Hsiong, S., Kim, W., Mooney, D., 2004. Dual growth factor delivery and controlled scaffold degradation enhance in vivo bone formation by transplanted bone marrow stromal cells. Bone 35 (2), 562–569.

Sommerfeldt, D., Rubin, C., 2001. Biology of bone and how it orchestrates the form and function of the skeleton. European Spine Journal 10 (SUPPL. 2), S86–S95.

St-Pierre, J.-P., Gan, L., Wang, J., Pilliar, R., Grynpas, M., Kandel, R., 2012. The incorporation of a zone of calcified cartilage improves the interfacial shear strength between in vitro-formed cartilage and the underlying substrate. Acta Biomaterialia 8 (4), 1603–1615.

Steadman, J., Briggs, K., Rodrigo, J., Kocher, M., Gill, T., Rodkey, W., 2003. Outcomes of microfracture for traumatic chondral defects of the knee: Average 11-year follow-up. Arthroscopy - Journal of Arthroscopic and Related Surgery 19 (5), 477–484.

Steward, A., Wagner, D., Kelly, D., 2012. The pericellular environment regulates cytoskeletal development and the differentiation of mesenchymal stem cells and determines their response to hydrostatic pressure. European Cells and Materials 25, 167–178.

Stoddart, M., Grad, S., Eglin, D., Alini, M., 2009. Cells and biomaterials in cartilage tissue engineering. Regenerative Medicine 4 (1), 81–98.

Stosich, M., Bastian, B., Marion, N., Clark, P., Reilly, G., Mao, J., 2007. Vascularized adipose tissue grafts from human mesenchymal stem cells with bioactive cues and microchannel conduits. Tissue Engineering 13 (12), 2881–2890.

Su, K., Lau, T., Leong, W., Gong, Y., Wang, D.-A., 2012. Creating a living hyaline cartilage graft free from non-cartilaginous constituents: An intermediate role of a biomaterial scaffold. Advanced Functional Materials 22 (5), 972–978.

Takeo, M., Chou, W., Sun, Q., Lee, W., Rabbani, P., Loomis, C., Mark Taketo, M., Ito, M., 2013. Wnt activation in nail epithelium couples nail growth to digit regeneration. Nature 499 (7457), 228–232.

Temenoff, J., Mikos, A., 2000. Review: Tissue engineering for regeneration of articular cartilage. Biomaterials 21 (5), 431–440.

Theodoropoulos, J., De Croos, J., Park, S., Pilliar, R., Kandel, R., 2011. Integration of tissue-engineered cartilage with host cartilage: An in vitro model. Clinical Orthopaedics and Related Research 469 (10), 2785–2795.

Thorpe, S., Buckley, C., Steward, A., Kelly, D., 2012. European society of biomechanics s.m. perren award 2012: The external mechanical environment can override the influence of local substrate in determining stem cell fate. Journal of Biomechanics 45 (15), 2483–2492.

Thorpe, S., Nagel, T., Carroll, S., Kelly, D., 2013. Modulating gradients in regulatory signals within mesenchymal stem cell seeded hydrogels: A novel strategy to engineer zonal articular cartilage. PLoS ONE 8 (4).

Thorpe, S. D., Buckley, C. T., Vinardell, T., O'Brien, F. J., Campbell, V. A., Kelly, D. J., 2008. Dynamic compression can inhibit chondrogenesis of mesenchymal stem cells. Biochemical and Biophysical Research Communications 377, 458–462.

Thorpe, S. D., Buckley, C. T., Vinardell, T., O'Brien, F. J., Campbell, V. A., Kelly, D. J., 2010. The response of bone marrow-derived mesenchymal stem cells to dynamic compression following tgf-b3 induced chondrogenic differentiation. Annals of Biomedical Engineering 38, 2896–2909.

Tortelli, F., Tasso, R., Loiacono, F., Cancedda, R., 2010. The development of tissue-engineered bone of different origin through endochondral and intramembranous ossification following the implantation of mesenchymal stem cells and osteoblasts in a murine model. Biomaterials 31 (2), 242–249.

Tropel, P., Noel, D., Platet, N., Legrand, P., Benabid, A.-L., Berger, F., 2004.

Isolation and characterisation of mesenchymal stem cells from adult mouse bone marrow. Experimental Cell Research 295 (2), 395–406.

Tsuchiya, K., Chen, G., Ushida, T., Matsuno, T., Tateishi, T., 2004. The effect of coculture of chondrocytes with mesenchymal stem cells on their cartilaginous phenotype in vitro. Materials Science and Engineering C 24 (3), 391–396.

Vacanti, C., Bonassar, L., Vacanti, M., Shufflebarger, J., 2001. Replacement of an avulsed phalanx with tissue-engineered bone. New England Journal of Medicine 344 (20), 1511–1514.

Vacanti, C., Kim, W., Upton, J., Mooney, D., Vacanti, J. P., 1995. The efficacy of periosteal cells compared to chondrocytes in the tissue engineered repair of bone defects. Tissue Engineering 1 (3), 301–308.

Vinardell, T., Buckley, C. T., Thorpe, S. D., Kelly, D. J., 2011. Composition-function relations of cartilaginous tissues engineered from chondrocytes and mesenchymal stem cells isolated from bone marrow and infrapatellar fat pad. Journal of Tissue Engineering and Regenerative Medicine 5 (9), 673–683.

Vinardell, T., Rolfe, R., Buckley, C., Meyer, E., Ahearne, M., Murphy, P., Kelly, D., 2012a. Hydrostatic pressure acts to stabilise a chondrogenic phenotype in porcine joint tissue derived stem cells. European Cells and Materials 23, 121–134.

Vinardell, T., Sheehy, E., Buckley, C., Kelly, D., 2012b. A comparison of the functionality and in vivo phenotypic stability of cartilaginous tissues engineered from different stem cell sources. Tissue Engineering - Part A 18 (11-12), 1161–1170.

Vinardell, T., Thorpe, S. D., Buckley, C. T., Kelly, D. J., 2009. Chondrogenesis and integration of mesenchymal stem cells within an in vitro cartilage defect repair model. Annals of Biomedical Engineering 37 (12), 2556–2565.

Vinatier, C., Mrugala, D., Jorgensen, C., Guicheux, J., Noel, D., 2009. Cartilage engineering: a crucial combination of cells, biomaterials and biofactors. Trends in Biotechnology 27 (5), 307–314.

Volkmer, E., Kallukalam, B., Maertz, J., Otto, S., Drosse, I., Polzer, H., Bocker, W., Stengele, M., Docheva, D., Mutschler, W., Schieker, M., 2010. Hypoxic preconditioning of human mesenchymal stem cells overcomes hypoxia-induced inhibition of osteogenic differentiation. Tissue Engineering - Part A 16 (1), 153–164.

Vunjak-Novakovic, G., Martin, I., Obradovic, B., Treppo, S., Grodzinsky, A. J., Langer, R., Freed, L. E., 1999. Bioreactor cultivation conditions modulate the composition and mechanical properties of tissue-engineered cartilage. J Orthop Res 17 (1), 130–8.

Wang, D. W., Fermor, B., Gimble, J. M., Awad, H. A., Guilak, F., 2005. Influence of oxygen on the proliferation and metabolism of adipose derived adult stem cells. Journal of Cellular Physiology 204 (1), 184–191.

Wang, J., Asou, Y., Sekiya, I., Sotome, S., Orii, H., Shinomiya, K., 2006. Enhancement of tissue engineered bone formation by a low pressure system improving cell seeding and medium perfusion into a porous scaffold. Biomaterials 27 (13), 2738–46.

Wang, P., Hu, J., Ma, P., 2009. The engineering of patient-specific, anatomically shaped, digits. Biomaterials 30 (14), 2735–2740.

Wang, X., Grogan, S., Rieser, F., Winkelmann, V., Maquet, V., La Berge, M., Mainil-Varlet, P., 2004. Tissue engineering of biphasic cartilage constructs using various biodegradable scaffolds: An in vitro study. Biomaterials 25 (17), 3681–3688.

Weinand, C., Gupta, R., Weinberg, E., Madisch, I., Neville, C., Jupiter, J., Vacanti, J., 2009. Toward regenerating a human thumb in situ. Tissue engineering. Part A 15 (9), 2605–2615.

Weiss, H., Roberts, S., Schrooten, J., Luyten, F., 2012. A semi-autonomous model of endochondral ossification for developmental tissue engineering. Tissue Engineering - Part A 18 (13-14), 1334–1343.

Weisser, J., Rahfoth, B., Timmermann, A., Aigner, T., Brauer, R., Von der Mark, K., 2001. Role of growth factors in rabbit articular cartilage repair by chondrocytes in agarose. Osteoarthritis and Cartilage 9 (SUPPL. A), S48–S54.

Welsch, G. H., Mamisch, T. C., Domayer, S. E., Dorotka, R., Kutscha-Lissberg, F., Marlovits, S., White, L. M., Trattnig, S., 2008. Cartilage t2 assessment at 3-t mr imaging: In vivo differentiation of normal hyaline cartilage from reparative tissue after two cartilage repair procedures - initial experience. Radiology 247 (1), 154–161.

Wen, Y., Grondahl, L., Gallego, M., Jorgensen, L., Moller, E., Nielsen, H., 2012. Delivery of dermatan sulfate from polyelectrolyte complex-containing alginate composite microspheres for tissue regeneration. Biomacromolecules 13 (3), 905–917.

Wendt, D., Jakob, M., Martin, I., 2005. Bioreactor-based engineering of osteochondral grafts: from model systems to tissue manufacturing. J Biosci Bioeng 100 (5), 489–94, 1389-1723 (Print) Journal Article Review.

Wendt, D., Stroebel, S., Jakob, M., John, G. T., Martin, I., 2006. Uniform tissues engineered by seeding and culturing cells in 3d scaffolds under perfusion at defined oxygen tensions. Biorheology 43 (3-4), 481–488.

Williams, R., Khan, I., Richardson, K., Nelson, L., McCarthy, H., Analbelsi, T., Singhrao, S., Dowthwaite, G., Jones, R., Baird, D., Lewis, H., Roberts, S., Shaw, H., Dudhia, J., Fairclough, J., Briggs, T., Archer, C., 2010. Identification and clonal characterisation of a progenitor cell sub-population in normal human articular cartilage. PLoS ONE 5 (10).

Wu, L., Leijten, J., Georgi, N., Post, J., Van Blitterswijk, C., Karperien, M., 2011. Trophic effects of mesenchymal stem cells increase chondrocyte proliferation and matrix formation. Tissue Engineering - Part A 17 (9-10), 1425–1436.

Yamasaki, H., Sakai, H., 1992. Osteogenic response to porous hydroxyapatite ceramics under the skin of dogs. Biomaterials 13 (5), 308–312.

Yang, W., Yang, F., Wang, Y., Both, S., Jansen, J., 2013. In vivo bone generation via the endochondral pathway on three-dimensional electrospun fibers. Acta Biomaterialia 9 (1), 4505–4512.

Yang, Y., Wimpenny, I., Ahearne, M., 2011. Portable nanofiber meshes dictate cell orientation throughout three-dimensional hydrogels. Nanomedicine: Nanotechnology, Biology, and Medicine 7 (2), 131–136.

Ytrehus, B., Carlson, C., Lundeheim, N., Mathisen, L., Reinholt, F., Teige, J., Ekman, S., 2004. Vascularisation and osteochondrosis of the epiphyseal growth cartilage of the distal femur in pigs - development with age, growth rate, weight and joint shape. Bone 34 (3), 454–465.

Yuan, H., Van Den Doel, M., Li, S., Van Blitterswijk, C., De Groot, K., De Bruijn, J., 2002. A comparison of the osteoinductive potential of two calcium phosphate ceramics implanted intramuscularly in goats. Journal of Materials Science: Materials in Medicine 13 (12), 1271–1275.

Yuan, J., Cui, L., Zhang, W., Liu, W., Cao, Y., 2007. Repair of canine mandibular bone defects with bone marrow stromal cells and porous beta-tricalcium phosphate. Biomaterials 28 (6), 1005–1013.

Yuan, J., Zhang, W., Liu, G., Wei, M., Qi, Z., Liu, W., Cui, L., Cao, Y., 2010. Repair of canine mandibular bone defects with bone marrow stromal cells and coral. Tissue Engineering - Part A 16 (4), 1385–1394.

Zhang, Y., Yang, F., Liu, K., Shen, H., Zhu, Y., Zhang, W., Liu, W., Wang, S., Cao, Y., Zhou, G., 2012. The impact of plga scaffold orientation on invitro cartilage regeneration. Biomaterials 33 (10), 2926–2935.

Zscharnack, M., Poesel, C., Galle, J., Bader, A., 2009. Low oxygen expansion improves subsequent chondrogenesis of ovine bone-marrow-derived mesenchymal stem cells in collagen type i hydrogel. Cells Tissues Organs 190 (2), 81–93.

A Appendix

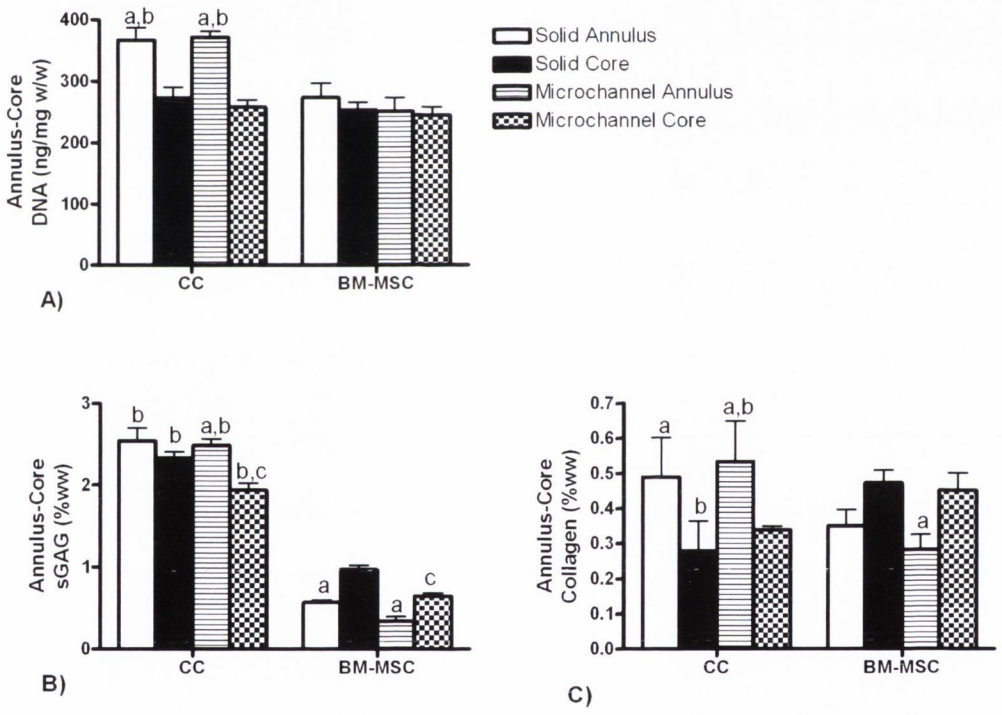

Figure A.1.: *Experiment 1: Annulus−core biochemical analysis of chondrocyte (CC) and BM-MSC, solid and microchannelled constructs, subjected to free swelling culture conditions at day 63. A) DNA content (ng/mg w/w); (B) sGAG content (% ww); and (C) collagen content (% ww). Significance ($p < 0.05$): (a) compared to corresponding core; (b) compared to MSC, same geometric region; (c) compared to solid construct, same cell type*

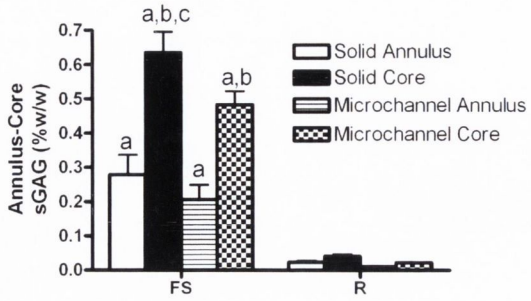

Figure A.2.: *Experiment 2: Annulus–core biochemical analysis of BM-MSC, solid and microchannelled constructs, subjected to free swelling (FS) or 5rpm rotation (R) culture conditions at day 21. sGAG content (% ww). Significance ($p < 0.05$): (a) compared to same group under rotational culture; (b) compared to corresponding annulus at the same culture condition; (c) compared to microchannel, same geometric region, same culture condition*

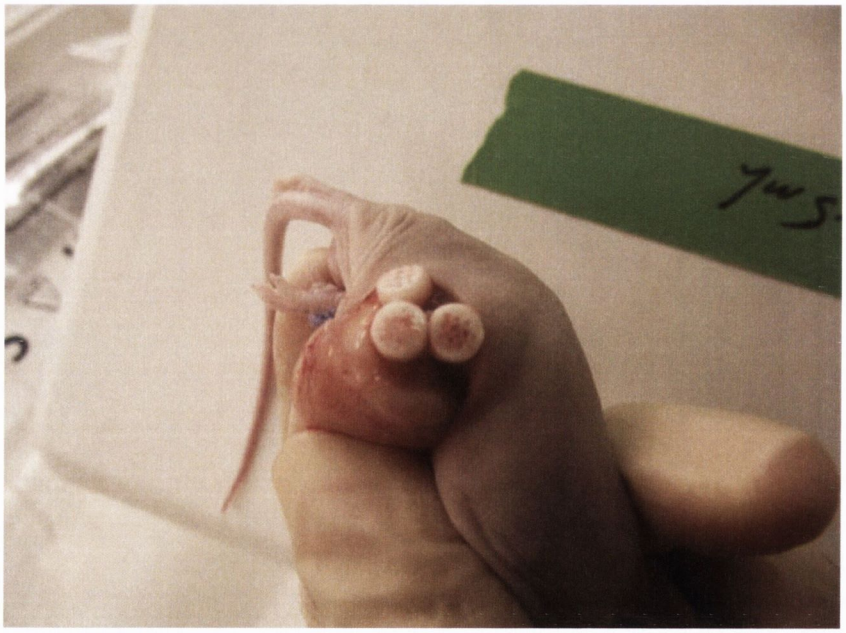

Figure A.3.: *Macroscopic image showing the retrieval of channelled constructs 8 weeks post-implantation. Red color within channels suggest the presence of hematopoietic elements*

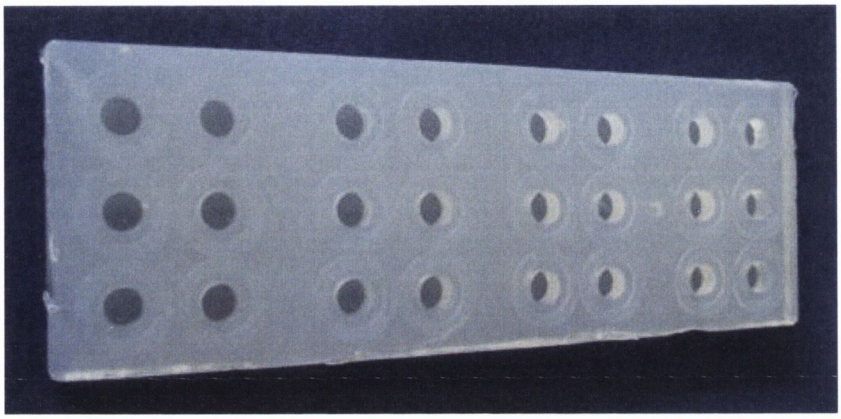

Figure A.4.: *The 'open surface' agarose-based mould used to cast cylindrical alginate, chitosan and fibrin hydrogels.*

Figure A.5.: *A) Two anatomic constructs were implanted either side of the spine. B) Visualisation of the construct before sacrifice. C) Harvesting of the anatomic construct 8 weeks post implantation.*